



WASHINGTON UNIVERSITY

SCHOOL OF
ENGINEERING
AND
APPLIED SCIENCE

THE EFFECTS OF YAWED FLOW

ON WIND TURBINE ROTORS

by

Andrew H. P. Swift, Jr.

DOCTORAL DISSERTATIONS

D

Referring to Instruction Sheet, enter information requested below:

PERSONAL DATA (Please type or print)

Do Not Write in This Space

1. Full Legal Name SWIFT (last name) ANDREW (first name) HOWARD POTTER, JR. (middle name)
2. Year of birth 1946 3. Country of citizenship USA
4. Present mailing address 2877 GILL AVE. MARYLAND HEIGHTS, MO. 63043
Future mailing address SAME
Effective date Immediately Telephone number 314-739-8238

Pub. No.
Vol./Issue
School Code
Subject Code
Copyright - Yes No Yr
Total Pages
Country Code
Sales Rest. Code
Advisor

DOCTORAL DEGREE DATA

5. Full name of University conferring degree WASHINGTON UNIVERSITY
6. Abbreviation for degree awarded D. Sc.
7. Date degree awarded MAY 22, 1981

Abstract length
TP Date
Bibliographic File

TITLE DATA

8. Title of dissertation exactly as it appears on title page and abstract.
9. Subject category for your dissertation. Choose from list on facing page.
Main Field MECHANICAL Sub Field Aero Nautical

COPYRIGHT DATA

10. If your dissertation has been previously published, please enter here the copyright notice as it appeared in the published edition.
11. Please file, on my behalf, an application for registration of a claim of U.S. copyright in my dissertation as outlined in the Copyright Authorization Section on the reverse side of the agreement form.
a. yes b. no (Circle one)
If you answer YES, please complete Items 12-14 and sign the authorization section on the reverse side of the agreement form.
12. Year dissertation was completed 1981
13. Has registration for your unpublished dissertation, or for an earlier version of the dissertation been made with the Copyright Office?
a. yes b. no (Circle one)
If yes, by whom?
Previous registration number Year

14. I authorize University Microfilms International to act on my behalf and grant to the Library of Congress nonexclusive permission to reproduce and distribute copies of my dissertation solely for the use of the blind and physically handicapped. (See Item 14 on Agreement form instructions.)
a. yes b. no (Circle one)
If yes, sign here Andrew H.P. Swift Jr.
Please check the method of reproduction you are authorizing.
Braille copies and phonorecords
Braille (or similar tactile symbols) copies only
Phonorecords only

REPRINTS

15. Please send me 0 reprints of my abstract. (Minimum order 100 copies.)
First set of 100 \$20.00
Additional sets of 100 @ \$5.00 each set \$
Enclosed please find my check for \$

PLEASE NOTE: Reprints are not mailed until the abstract appears in Dissertation Abstracts International, which is generally four months after we receive the material.

DISSERTATIONS AGREEMENT

Through my graduate school, I agree to supply you, University Microfilms International, with my dissertation and with an abstract of 600 words or less. The title of my dissertation is set forth on the accompanying information questionnaire.

I grant you the exclusive right to reproduce and distribute copies of the dissertation in and from microforms and the right to reproduce and distribute my abstract in any format. I represent to you that the dissertation and the abstract are my original work, do not infringe any rights of others, and that I have the right to make these grants.

You agree to offer copies of my dissertation for sale and to publish an abstract of my dissertation in *Dissertation Abstracts International*.

You also agree to pay me a royalty of ten percent, on sales of copies of my dissertation, for any calendar year when such sales equal \$100 or more. In order to be eligible for such royalties as to any calendar year, I agree that my obligation is to notify you of my current mailing address at least once during the subsequent two calendar years. Of course, I need send no address notice when my address remains the same as I have previously given you.

Andrew H. P. Supt.
(Author's Signature)

University Microfilms International
A Xerox Publishing Company
Ann Arbor, Michigan 48106

May 4, 1981
(Date)

AUTHORIZATION TO APPLY FOR REGISTRATION OF MY CLAIM TO COPYRIGHT

I authorize you, University Microfilms International, to file on my behalf, an application for registration of a claim of U.S. copyright, in my name, in my dissertation. You agree to complete the application form, and file it, together with the registration fee and required deposit copy(ies) of my dissertation, with the Copyright Office. I represent to you that the information I have provided you, on the accompanying information questionnaire, is accurate.

My certified check or money order to University Microfilms International (\$20) is enclosed unless I have paid the fee to my graduate school for forwarding to University Microfilms International.

Andrew H. P. Supt.
(Author's Signature)

May 4, 1981
(Date)

WASHINGTON UNIVERSITY
SEVER INSTITUTE OF TECHNOLOGY

ABSTRACT

THE EFFECTS OF YAWED FLOW
ON WIND TURBINE ROTORS

ADVISOR: Professor D. A. Peters

May, 1981

Saint Louis, Missouri

This dissertation examines the effect of yawed flow on wind turbine rotors. Results are obtained from two theoretical approaches, from experimental data for a wind tunnel model, and from atmospheric tests of a full scale wind turbine.

The first theoretical analysis involves the development and investigation of a simplified computer algorithm. The algorithm is derived from fundamental rotor equations and is used to study the effects of yawed flow on steady-state, average rotor performance. The second theoretical analysis is dynamic simulation of a rotor in yawed flow. The analysis is based on blade element theory and dynamic inflow

theory, and neglects stall effects. The analysis is designed to calculate local aerodynamic forces and moments, blade angle-of-attack profiles, induced flow profiles, and teeter or passive cyclic pitch deflections for rotors with a teetering axis or with cyclic pitch. A state-variable approach is used with a predictor-corrector solution to the system of first-order differential equations in order to obtain a time-history solution. Applications of the dynamic simulation model are used to investigate operating limits due to stall, gust response, and passive cyclic pitch response. Correlations are presented with the simplified theory and with experimental results, where applicable.

Experimental results are presented from wind tunnel tests in which a model rotor was operated in yawed flow. The results are compared with other wind tunnel test results and with some theoretical results. Experimental results are also presented from atmospheric tests of a 7.6 meter (25 ft.) diameter, two-bladed, yaw-controlled wind turbine with passive cyclic pitch.

Comparisons between the theoretical approaches and the experimental data show that both computer models are useful in analyzing the effects of yawed flow on wind turbine rotor performance.

WASHINGTON UNIVERSITY
SEVER INSTITUTE OF TECHNOLOGY

THE EFFECTS OF YAWED FLOW
ON WIND TURBINE ROTORS

by

Andrew H. P. Swift, Jr.

Prepared under the direction of Professor D. A. Peters

A dissertation presented to the Sever Institute of
Washington University in partial fulfillment
of the requirements for the degree of

DOCTOR OF SCIENCE

May, 1981

Saint Louis, Missouri

WASHINGTON UNIVERSITY
SEVER INSTITUTE OF TECHNOLOGY

ABSTRACT

THE EFFECTS OF YAWED FLOW
ON WIND TURBINE ROTORS

ADVISOR: Professor D. A. Peters

May, 1981

Saint Louis, Missouri

This dissertation examines the effect of yawed flow on wind turbine rotors. Results are obtained from two theoretical approaches, from experimental data for a wind tunnel model, and from atmospheric tests of a full scale wind turbine.

The first theoretical analysis involves the development and investigation of a simplified computer algorithm. The algorithm is derived from fundamental rotor equations and is used to study the effects of yawed flow on steady-state, average rotor performance. The second theoretical analysis is dynamic simulation of a rotor in yawed flow. The analysis is based on blade element theory and dynamic inflow

theory, and neglects stall effects. The analysis is designed to calculate local aerodynamic forces and moments, blade angle-of-attack profiles, induced flow profiles, and teeter or passive cyclic pitch deflections for rotors with a teetering axis or with cyclic pitch. A state-variable approach is used with a predictor-corrector solution to the system of first-order differential equations in order to obtain a time-history solution. Applications of the dynamic simulation model are used to investigate operating limits due to stall, gust response, and passive cyclic pitch response. Correlations are presented with the simplified theory and with experimental results, where applicable.

Experimental results are presented from wind tunnel tests in which a model rotor was operated in yawed flow. The results are compared with other wind tunnel test results and with some theoretical results. Experimental results are also presented from atmospheric tests of a 7.6 meter (25 ft.) diameter, two-bladed, yaw-controlled wind turbine with passive cyclic pitch.

Comparisons between the theoretical approaches and the experimental data show that both computer models are useful in analyzing the effects of yawed flow on wind turbine rotor performance.

TABLE OF CONTENTS

No.		Page
1.	Introduction.....	1
1.1	The Significance of Wind Power.....	1
1.2	The Importance of Yawed Flow Effects on Horizontal Axis Wind Machines.....	4
1.3	Previous Work.....	6
1.3.1	Other Computer Algorithms.....	6
1.3.2	Rotorcraft Experience.....	10
1.3.3	Test Results.....	11
1.3.4	Analytical Results.....	11
2.	Theoretical Developments.....	12
2.1	Simplified Yawed Flow Performance Theory....	12
2.1.1	General Equations.....	12
2.1.2	Computer Algorithm.....	13
2.1.3	Computer Algorithm, Results and Analysis.....	17
2.2	Dynamic Yawed Flow Rotor Simulation Model.....	34
2.2.1	Objectives.....	34
2.2.2	Simulation Model Algorithm Overview..	37
2.2.3	Derivations.....	40
2.2.3.1	Aerodynamic Equations.....	41
2.2.3.2	State Variable Equations for Yaw Angle and Cyclic Pitch Deflection About the Prelag Axis.....	48

TABLE OF CONTENTS

(continued)

No.		Page
	2.2.3.3 State Variable Equations for Flapping Angle.....	49
	2.2.3.4 State Variable Equation for Dynamic Induced Flow...	52
	2.2.3.5 State Variable Equation for Rotor Speed.....	56
	2.2.4 Dynamic Yawed Flow Computer Simulation Example Application.....	57
	2.2.4.1 Example Model Description..	58
	2.2.4.2 Running the Simulation and Error Analysis.....	70
	2.2.4.3 Comparison With Other Theoretical Results.....	72
3.	Experimental Testing.....	81
3.1	Wind Tunnel Testing.....	81
3.1.1	Wind Tunnel Model Description.....	81
3.1.2	Test Procedures and Results.....	84
3.1.3	Qualitative Comparison With Other Wind Tunnel Test Results.....	95
3.2	Full Scale, Atmospheric Testing.....	99
3.2.1	Experimental Wind Turbine Description.....	99
3.2.2	Instrumentation.....	108
3.2.2.1	Wind Speed.....	111
3.2.2.2	Rotor Speed.....	114
3.2.2.3	Furl and Yaw Post Position.....	115

TABLE OF CONTENTS
(continued)

No.		Page
	3.2.2.4 Load Voltage.....	117
	3.2.2.5 Strain Gauge Circuits.....	120
	3.2.2.6 Microcomputer System.....	121
	3.2.2.7 Lightning Protection.....	125
3.2.3	Data Acquisition and Processing Methods.....	129
	3.2.3.1 Analog Data.....	129
	3.2.3.2 Statistical Data Processing.....	131
3.2.4	Full Scale Test Results.....	140
	3.2.4.1 Power-Off Analog Data.....	140
	3.2.4.2 Power-Off Digital Data.....	144
	3.2.4.3 Power-On Analog Data.....	149
	3.2.4.4 Power-On Digital Data.....	153
	3.2.4.5 Steady-State Loads Survey..	169
	3.2.4.6 Transients Loads Survey....	174
	3.2.4.7 Overspeed Conditions Loads Survey.....	175
3.2.5	Correlation of Theoretical Results With Full Scale Experimental Results.....	177
	3.2.5.1 Correlation of Auto- rotational Data.....	178
	3.2.5.2 Correlation of Power-On Data.....	180

TABLE OF CONTENTS

(continued)

No.		Page
	3.2.5.3 Correlations of Cyclic Pitch Deflections.....	182
	3.2.5.4 Correlations of the Effects of Yaw Angle on C_T/σ and C_Q/σ	186
	3.2.6 Applications of the Theoretical Models.....	188
	3.2.6.1 Prediction of Stall Limits.	190
	3.2.6.2 Loss of Load, Overspeed Simulation.....	193
	3.2.6.3 Gust Response.....	194
	3.2.6.4 The Effects of Passive Cyclic Pitch on Aerodynamic Blade Forces in Yawed Flow Conditions.....	197
	3.2.6.5 Dynamic Loads.....	202
4.	Concluding Remarks.....	204
5.	Acknowledgements.....	212
6.	Appendices.....	213
	Appendix 6.1 Nomenclature.....	214
	Appendix 6.2 Documentation for the "Yawflow" and "Yawplot" Programs.....	219
	Appendix 6.3 Derivation of Rotor Equations.....	228
	Appendix 6.4 Documentation for "Constant Yaw Dynamics" and "Revplot Programs"...	240
	Appendix 6.5 Data Analysis Software.....	256
7.	Bibliography.....	326
8.	Vita.....	329

LIST OF TABLES

No.		Page
1.	Comparison of Dynamic Simulation With Simplified Theory for Two-bladed Experimental Turbine Parameters.....	73
2.	Wind Tunnel Data Fixed Yaw Angle.....	89
3.	Wind Tunnel Data Free Yawing Configuration.....	90
4.	Wind Tunnel Data Constant RPM Test - 1800 RPM...	91
5.	Full Scale Machine Data.....	107
6.	Instrument Gains.....	122
7.	Maximum Loads for Steady States Unfurled (15°).....	172
8.	Effect of Furl Angles on Loads.....	173
9.	Maximum Stresses.....	176
10.	Overspeed Loads.....	176
11.	Effect of Yaw Rate and Direction on τ	182
12.	Effect of RPM on τ	186
13.	C_T/σ Comparison for $C_Q/\sigma = 0.008$	187
14.	Gust Response.....	196
15.	1 P Aerodynamic Forces and Moments per Blade for Rigid Blade Rotor and Passive Cyclic Pitch Rotor	202

LIST OF FIGURES

No.		Page
1.	Example Blade Element Section Used In Wilson-Lissaman Axial Flow Computer Program (3).....	7
2.	Illustration of Dynamic Stall for An Oscillating Airfoil. Measured Force Coefficient vs. Angle-of-attack From (6) and Estimated Steady Airfoil Data.....	9
3.	Plot of Axial Tip Speed Ratio vs. Induced Flow Normalized on $(\frac{1}{2} C_T)^{\frac{1}{2}}$ Showing Three Operating States (14).....	14
4.	Typical Blade Element Operating at Radial Station, r.....	16
5a.	Graph of C_T/σ vs. Yaw Angle for $\sigma = 0.075$, A C_{do} Multiplier of 3, and $\theta = 0$ with v , C_Q/σ , and the Maximum Power Points Plotted as Parameters.....	19
5b.	Graph of C_T/σ vs. Yaw Angle for $\sigma = 0.032$ and $\theta = -0.5^\circ$ With v and C_Q/σ Plotted as Parameters.....	20
5c.	Graph of C_T/σ vs. Yaw Angle for $\sigma = 0.032$ and $\theta = -3^\circ$ With v and C_Q/σ Plotted as Parameters.....	21
6.	Nondimensional Velocities Acting on the Rotor Disk at Yaw Angle, χ	26
7.	Graph of C_P vs. Speed Ratio $\Omega R/V$ for $\sigma = 0.032$ and $\theta = -0.5^\circ$ With χ and C_Q/σ Plotted as Parameters. Data is the Same as That Plotted in Figure 5b.....	29
8.	Optimum Operating Conditions for a Wind Turbine Rotor.....	32
9.	Figure 5b Replotted With Lines of Constant Induced Velocity Added.....	33
10.	Rotor Coordinates.....	38

LIST OF FIGURES
(continued)

No.		Page
11.	Blade Element, dr , Operating at Radial Station r	42
12.	Rigid Blade Flapping Geometry and Definitions.....	50
13.	Induced Flow Pattern for Yawed Flow Proposed by Glauert (19).....	54
14.	Test Rotor Blade.....	62
15.	τ Response to $+10^\circ$ Deflection.....	79
16.	Model Rotor in Wind Tunnel.....	82
17.	Model Rotor Blade.....	83
18.	Hub and Cyclic Pitch Hinge for Wind Tunnel Model Rotor.....	85
19a.	Free Yaw Mode, Top View.....	86
19b.	Free Yaw Mode, Side View.....	86
19c.	Fixed Yaw Mode, Side View.....	86
20.	Photograph of Wind Tunnel Model, Fixed Yaw Mode.....	87
21.	Photograph of Wind Tunnel Model, Free Yaw Mode.....	88
22.	Effect of Reynolds Number on Airfoil Performance (25).....	93
23.	Effect of Rotor Speed or Reynolds Number on Tip Speed Ratio.....	93
24.	Speed Ratio $V/\Omega R$ vs. Yaw Angle for Various Wind Tunnel Tests (10), (11) and for Simplified Theory.....	94
25.	Wind Tunnel Tests for Windcharger 200 (9).....	98

LIST OF FIGURES
(continued)

No.		Page
26a.	Photograph of Experimental Wind Turbine at Test Site Showing Tower and Instrument Shed.....	100
26b.	Photograph of Wind Turbine, Side View.....	101
26c.	Photograph of Wind Turbine, Front View.....	102
26d.	Photograph of Wind Turbine, Furled.....	103
26e.	Photograph of Tower Operation.....	104
26f.	Photograph of Experimental Wind Turbine Nacelle Detail Showing Slip Rings, Gear Box, Main Bearings, Furl Actuator and Instrument Boxes.....	105
27.	Site Contour Map.....	106
28.	Wind Speed Signal Conditioning Circuit.....	113
29.	Rotor Speed Signal Conditioning Circuit.....	113
30.	Furl and Yaw Post Position Signal Conditioning Circuit.....	118
31.	Load Voltage Signal Conditioning Circuit.....	118
32.	Steady State Autorotation Test Results for Model and Full Scale Machine.....	141
33.	Power-off Automatic Furling Response to Strong Wind Gusts; Rotor Speed, Wind Speed and Furl Angle vs. Time.....	141
34a-1.	Power-off Run, Sample Distribution, Log (N) Samples vs. Wind Speed for 15 Degree Furl Angle.....	145
34a-2.	Power-off Run, RPM vs. Wind Speed for 15 Degree Furl Angle.....	145
34a-3.	Power-off Run, Cyclic Pitch Amplitude vs. Wind Speed for 15 Degree Furl Angle.....	146

LIST OF FIGURES

(continued)

No.		Page
34b-2.	Power-off Run, RPM vs. Wind Speed for 45 Degree Furl Angle.....	147
34b-3.	Power-off Run, Rotor Power vs. Wind Speed for 45 Degree Furl Angle.....	147
35.	Rotor Power vs. Rotor Speed; 25/1 Gear Ratio.....	150
36.	Power-on Automatic Furling Response to Wind Gusts; Rotor Speed, Wind Speed and Furl Angle vs. Time.....	152
37.	Power-on Rotor RPM Response to Wind Gust and Delayed Furling; Rotor Speed, Wind Speed and Furl Angle vs. Time.....	152
38a.	Power-on Run, Sample Distribution, Log (N) Samples vs. Wind Speed for 15 Degree Furl Angle.....	154
38b.	Power-on Run, RPM vs. Wind Speed for 15 Degree Furl Angle.....	154
38c.	Power-on Run, Rotor Power vs. Wind Speed for 15 Degree Furl Angle.....	155
38d.	Power-on Run, Generator to Rotor Efficiency vs. Wind Speed for 15 Degree Furl Angle.....	155
38e.	Power-on Run, Thrust vs. Wind Speed for 15 Degree Furl Angle.....	156
38f.	Power-on Run, Power Coefficient vs. Wind Speed for 15 Degree Furl Angle.....	156
39a.	Power-on Run, Sample Distribution, Log (N) Samples vs. Wind Speed for 45 Degree Furl Angle..	157
39b.	Power-on Run, RPM vs. Wind Speed for 45 Degree Furl Angle.....	157
39c.	Power-on Run, Rotor Power vs. Wind Speed for 45 Degree Furl Angle.....	158

LIST OF FIGURES

(continued)

No.		Page
39d.	Power-on Run, Power Coefficient vs. Wind Speed for 45 Degree Furl Angle.....	158
40a-1.	Sample Distribution, Log (N) Samples vs. Yaw Rate; Motion in Furl Direction.....	163
40a-2.	Cyclic Pitch Amplitude vs. Yaw Rate; Motion in Furl Direction.....	163
40b-1.	Sample Distribution, Log (N) Samples vs. Yaw Rate; Motion in Unfurl Direction.....	164
40b-2.	Cyclic Pitch Amplitude vs. Yaw Rate; Motion in Unfurl Direction.....	164
41a.	Sample Distribution, Log (N) Samples vs. RPM for 30 Degree Furl Angle.....	166
41b.	Mean Flap Bending vs. RPM for 30 Degree Furl Angle.....	166
41c.	Flap Bending Amplitude vs. RPM for 30 Degree Furl Angle.....	167
41d.	In-Plane Bending Amplitude vs. RPM for 30 Degree Furl Angle.....	167
41e.	Vertical Boom Bending Amplitude vs. RPM for 30 Degree Furl Angle.....	168
41f.	Cyclic Pitch Amplitude vs. RPM for 30 Degree Furl Angle.....	168
42.	Dynamic Loads vs. Rotor RPM for 15 Degree Furl Angle.....	170
43.	Autorotation Data Correlation for the Full Scale Experimental Wind Turbine.....	179
44.	Power-on Data Correlation for the Full Scale Experimental Wind Turbine.....	181

LIST OF FIGURES
(continued)

No.		Page
45a.	Correlation of Cyclic Pitch Deflection, Furl Direction.....	184
45b.	Correlation of Cyclic Pitch Deflection, Unfurl Direction.....	184
46.	Mean Flap Bending vs. RPM for 15 Degree Furl Angle.....	189
47a.	Angle-of-attack Profile, Yaw = 60 ^o , Rated Power, Wind Speed = 18.4 m/s.....	191
47b.	Angle-of-attack Profile, Yaw = 80 ^o , Auto- rotation, 230 RPM, Wind Speed = 25 m/s.....	192
48.	Simulated Overspeed With Power Loss.....	195
49.	Simulated Wind Speed Gust.....	195
50a.	Angle-of-attack Profile Yaw = 60 ^o , Rated Power, Steady State.....	198
50b.	Induced Velocity Profile, Yaw = 60 ^o , Rated Power, Steady State.....	199
50c.	Angle-of-attack Profile, Yaw = 55 ^o to 60 ^o Rated Power, Yaw Transient, 20 ^o per second.....	200
50d.	Induced Velocity Profile, Yaw = 55 ^o to 60 ^o , Rated Power, Yaw Transient, 20 ^o per second.....	201
Appendices:		
6.5.1.	Collect 5 Subroutine Flow Chart.....	268

THE EFFECTS OF YAWED FLOW ON WIND TURBINE ROTORS

1. INTRODUCTION

1.1 THE SIGNIFICANCE OF WIND POWER

At the time of writing this dissertation the United States and most industrialized and developing countries face an uncertain future in regard to conventional energy supply and demand. Many well researched studies (e.g. (1)*) indicate that short term future energy supplies, especially oil, will be unable to meet worldwide demand, even if that demand is sharply curtailed through conservation efforts.

It is within this climate and with a certain sense of urgency that many nations are intently seeking to; (a) increase the production of conventional energy sources, (i.e., oil, gas, coal and nuclear power); (b) reduce energy demand through improvements in energy utilization efficiency and conservation efforts; and (c) investigate alternative energy sources that may have the potential to displace conventional energy supplies.

*The numbers in parentheses in the text indicate references in the Bibliography.

Wind power utilization, and especially the conversion of wind energy to electricity, is considered by many to be an alternative that may have significant near term potential as an alternative and/or supplement to the conventional production of electrical power. This interest has manifested itself in both the public and private sectors, both domestically and outside the United States. To illustrate this point, the current U.S. Federal Wind Energy Program Budget has grown from \$59.6 million dollars in FY 1979, to \$63.4 million in FY 1980. The program has funded the design and construction of wind turbines from small 8 kW prototype machines up to 2500 kW utility connected machines in the MOD series. Furthermore, the program has funded research and development efforts, marketing studies, siting studies and various design alternatives. In addition to the Federal effort, according to the American Wind Energy Association, about 32 private U.S. companies are presently manufacturing and selling wind turbines. Efforts underway in other countries are similar.

The concept of using wind energy for electrical power production is not new. In the 1930's an established industry existed in the United States that produced and sold wind machines, mostly in rural areas, for the production of electrical power. The Rural Electrification Program essentially put these companies out of business by making inexpensive, central station, electrical power available to

rural customers. In 1941 a large, utility connected, wind turbine, rated at 1250 kW, was constructed in Vermont by Palmer Putnam and the S. Morgan Smith Company. Although the machine operated satisfactorily over three and one-half years, the project was discontinued after a blade failure in March 1943.

Although the technical feasibility of generating electrical power from the wind has been previously established, it appears doubtful that the technology, as it existed forty years ago, can be directly applied today. The primary impediments to the direct utilization of previous wind power plant designs are; (a) high first costs; (b) safety issues; (c) reliability; (d) maintenance issues; and (e) storm survivability. Until these issues are resolved it appears doubtful that wind energy conversion systems will displace a significant fraction of electrical power from conventional sources.

Since the construction of the Putnam Wind Turbine in 1941 there have been numerous technological developments that relate directly to the design, development and understanding of wind machines. These include the helicopter and associated rotorcraft technology, improved material and fabrication techniques, and the development of the high speed computer and microprocessor. Application of these technologies to wind turbine development could assist in resolving the impediments listed above.

In summary, present efforts in wind turbine development would best not be aimed at demonstrating the technical feasibility of generating electricity from the wind, this has been shown. Rather, they should be directed at applying recent technological advancements to the development, design, analysis and understanding of these machines so that their true potential as an alternative energy source might be evaluated. It is hoped that this dissertation is a modest contribution in that direction.

1.2 THE IMPORTANCE OF YAWED FLOW EFFECTS ON HORIZONTAL AXIS WIND MACHINES

At the present time there are two types of wind machine vying for a place in wind turbine development; namely the vertical axis and the horizontal axis wind turbine. The most common of the two is presently the horizontal axis machine. (Yaw effects are not applicable to vertical axis machines since wind direction changes have little effect on their performance, which is a point often considered in their favor. Other problems, however, such as wake induced vibrations on the downwind blade and aeroelastic problems still hamper the development of these machines.)

Since the wind is a continually varying phenomenon in both speed and direction, all horizontal axis wind turbines are subjected to unsteady yawed flow conditions (i.e., a crosswind component across the rotor disk) and respond accordingly. The response of a wind turbine to unsteady yawed flow conditions is a major factor in turbine design

and performance. Poor wind-direction following can lead to decreased performance and unsteady, periodic aerodynamic blade loading while rapid wind-direction following can lead to possible instabilities and high gyroscopic forces on the blades and tower.

Secondly, several recent wind turbine designs utilize yaw control methods to limit the power output of the machine at wind speeds in excess of rated speed or in storm conditions. Among these are the Hummingbird (manufactured by Power Group International Corporation), the Variable Axis Rotor Control System (manufactured by North Wind Power Company) and the design described herein, (used to study yawed flow effects). This method of power control is discussed fully by Hohenemser (2). In light of these comments, it is evident that a rather detailed understanding of wind turbine response to yawed flow, or crosswind conditions, is both desirable and necessary to the understanding and engineering design of horizontal axis wind turbines.

This dissertation develops two theoretical approaches. A simplified theory for steady state performance evaluation and a more complex, dynamic yawed flow rotor simulation model. Computer algorithms for both approaches are developed for compatibility with small, microcomputer systems, which should enhance the practicality of these developments and provide a larger user base. In addition, experimental work with wind tunnel model rotors and a full

scale, experimental, yaw controlled wind turbine is presented.

1.3 PREVIOUS WORK

1.3.1 Other Computer Algorithms

Wilson and Lissaman (3) present an axial flow rotor performance algorithm using a finite blade element method that combines blade element and momentum theory. Induced flow is calculated for each blade element using local momentum theory; and then blade element theory, which can account for twist and radially variable blade geometry, is used to calculate resulting aerodynamic forces. These forces are summed along the blade and multiplied by the number of blades to give aerodynamic forces, moments and performance. The method is able to take into account the following parameters for more refined results. See Figure 1. Wake rotation is accounted for by modification of the in-plane velocity component. Reynolds number effects can be included by varying lift and drag coefficients for the proper Reynolds number, (if the effects are quantitatively known). Tip losses can be accounted for; and, finally, steady state stall effects can be included if the data are known for the respective airfoil sections. Wilson and Patton have expanded the methodology to include yawed flow effects (i.e., crosswind effects) by including azimuth position variation in the calculation of axial, tangential, and induced velocity and then integrating both over the blade radius and around the rotor disk (4).

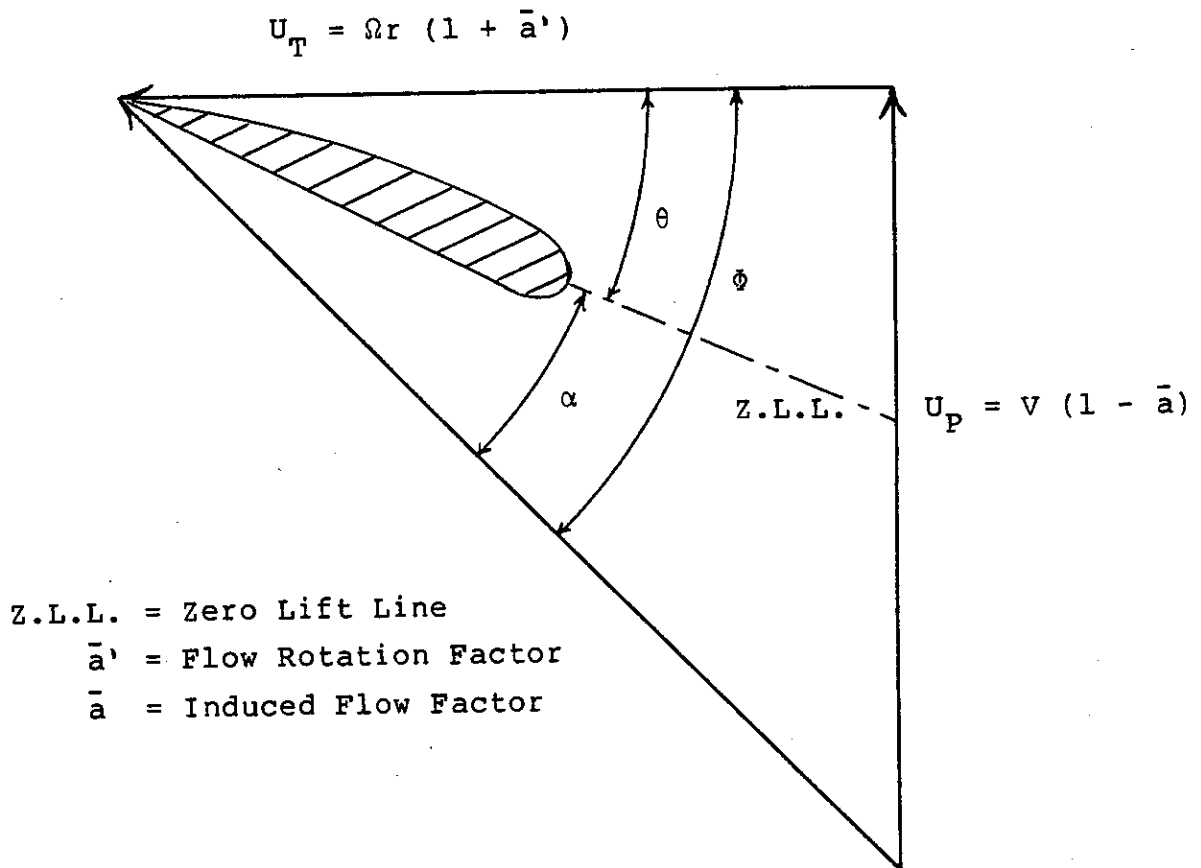


Figure 1. EXAMPLE BLADE ELEMENT SECTION USED IN WILSON-LISSAMAN AXIAL FLOW COMPUTER PROGRAM (3)

There are numerous difficulties with this extrapolation to yawed flow conditions that render the approach less desirable than for the axial flow case. First, studies of induced flow patterns over the rotor disk for rotorcraft operating at advance ratios > 0 (yawed flow) show that the induced flow at a given radial and azimuth position is a function of the induced flow at other portions of the disk and thus cannot be accurately determined using isolated local momentum theory (5). Second, steady state lift and drag coefficients based on local angle of attack become inaccurate in yawed flow conditions due to dynamic stall effects. For rotors operating at advance ratios > 0 the angle of attack at a given radial station oscillates once per revolution for steady operating conditions. It has been demonstrated (e.g. (6)) that steady state lift and drag coefficients of an oscillating airfoil are altered dramatically from their static values in a steady flow field. For example, angles of attack well beyond the static stall limit continue to produce increasing lift as shown in Figure 2. The Wilson-Patton program could account for these effects if they were known quantitatively, although standard methodology usually involves using static lift and drag coefficient values. Also, since local angle of attack values are determined by local induced flow velocities, angle of attack values calculated by the Wilson-Patton method will be in error since induced flow patterns are also

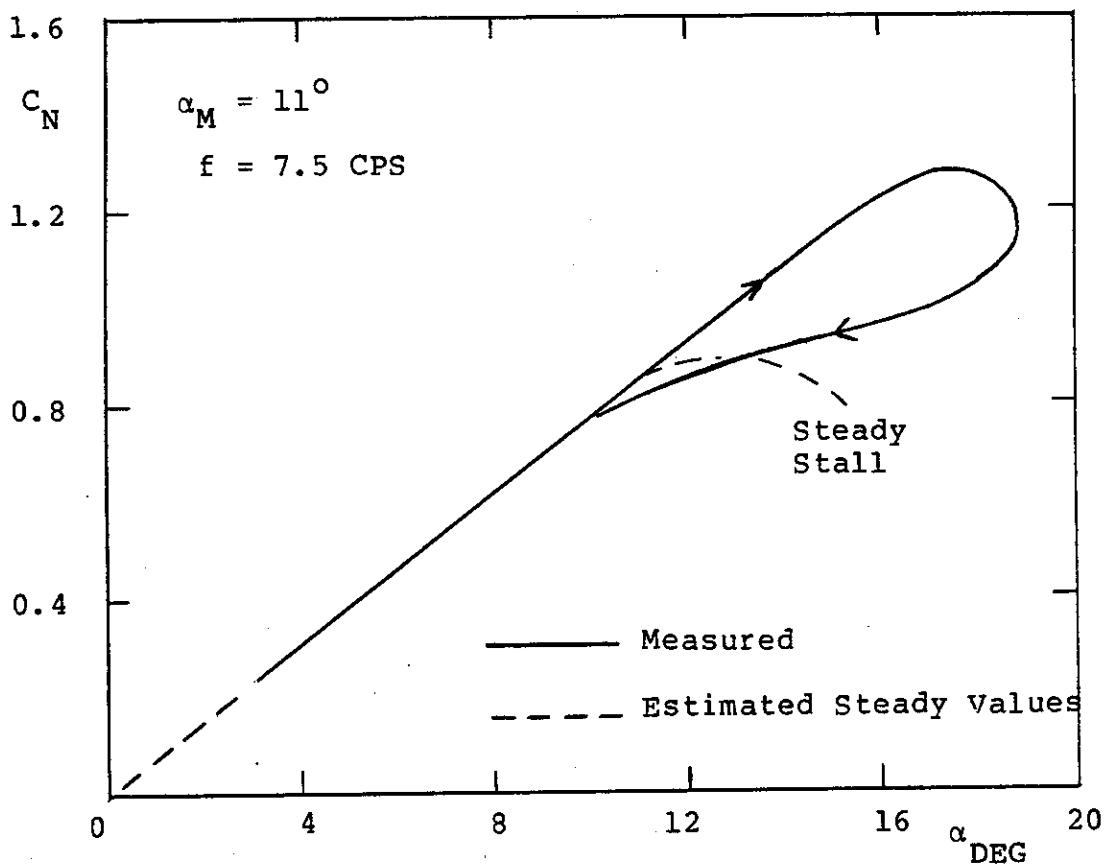


Figure 2. ILLUSTRATION OF DYNAMIC STALL FOR AN OSCILLATING AIRFOIL. MEASURED FORCE COEFFICIENT VS. ANGLE-OF-ATTACK FROM (6) AND ESTIMATED STEADY AIRFOIL DATA

in error. Third, the Wilson-Patton program is for steady states only and is therefore unable to include dynamic effects of yaw. These effects, which include gyroscopic loads, changing aerodynamic forces, and variable induced flow patterns are often significant in evaluation of rotor loads and performance. Finally, the algorithm fails if the induced flow factor exceeds one-half, because this implies that a blade element is operating in the vortex ring state (see Section 2.1.1) where momentum theory does not apply. However, since the induced velocities calculated in the algorithm are in error, (as described before), the vortex-ring-state boundaries based on local momentum theory are also in error.

1.3.2 Rotorcraft Experience

Since all rotorcraft (i.e., helicopters and autogyros) operate at advance ratios > 0 (i.e., yawed flow) when in forward flight, a significant amount of knowledge has been gained concerning the operation of rotors under these conditions. Although certain aspects of this knowledge can be applied directly to the operation of wind turbine rotors in yawed flow, as will be examined later, other aspects are not well suited for wind turbines. For example, although the MOSTAB (7) and MOSTAS (8) computer programs provide information on rotor performance in various operating conditions, they are difficult to adapt to specific wind turbine applications due to their complexity.

1.3.3 Test Results

Recent wind tunnel tests with wind turbines operating in yawed flow conditions (9) have provided some steady state performance data for small rotors. Studies of larger rotors in wind tunnels, (10) and (11), have provided data at high yaw angles. These data are useful and will be used later to aid in correlating both the theoretical and experimental data presented.

1.3.4 Analytical Results

Stoddard (12),(13) has developed numerous closed form analytical relationships, some of which can be easily programmed on small calculators, to predict wind turbine performance and blade loading in both axial and yawed flow conditions. Although the analytical formulations also take yaw rate into account, the effects of variable inflow are ignored as are the effects of transient yaw rate.

2. THEORETICAL DEVELOPMENTS

2.1 SIMPLIFIED YAWED FLOW PERFORMANCE THEORY

2.1.1 General Equations

A generalized theory for a rotor operating in yawed flow conditions is well developed by Gessow and Myers (14), and the theory lends itself well for adaptation here.

Three independent relationships are necessary to determine the steady state performance of the rotor for particular operating conditions. From axial momentum theory, and assuming uniform inflow across the rotor disk, one can write

$$C_T = 2v(\lambda^2 + \mu^2)^{\frac{1}{2}} \quad (1)$$

Using blade element theory and integrating over the blade radius and around the rotor disk, one can write:

$$C_T = \sigma a \left[\frac{1}{6} (1 + \frac{3}{2} \mu^2) \theta + \frac{1}{4} \lambda \right], \quad (2)$$

where one assumes: (a) constant rotor speed; (b) small flapping angles, β , so that $\cos \beta \cong 1$ and $\sin \beta \cong \beta$; (c) small inflow angles, ϕ , so that $\phi = U_P/U_T$ (see Figure 1); (d) constant lift curve slope, a ; (e) no effects of wake rotation and radial velocity components along the blade; and (f) untwisted and untapered blades.

From an energy balance at the rotor shaft one can write:

$$C_Q = \lambda C_T - \frac{\sigma}{8} C_{d0} \quad (3)$$

where C_{d0} is the drag of the airfoil at the mean blade angle of attack.

It is significant to note that equations (1) and (2) are based on axial momentum theory which breaks down in the vortex ring state, defined graphically in Figure 3 for axial flow, [see Reference (14)] while equation (3) is generally applicable.

By combining equations (1) and (2) one can write an expression for induced flow, v :

$$v = \frac{\frac{\sigma a}{12} (1 + (\frac{3}{2}\mu^2)) \theta + \frac{\sigma a}{8} \bar{\lambda}}{\frac{\sigma a}{8} + (\lambda^2 + \mu^2)^{\frac{1}{2}}} \quad (4)$$

2.1.2 Computer Algorithm

The computer algorithm starts with a given value of tip speed ratio, v , and yaw angle, χ , from which advance ratio, μ , and axial tip speed ratio $\bar{\lambda}$ can be calculated. Tip speed ratio, v , and yaw angle χ are varied as independent parameters. Solidity ratio, σ , profile drag, C_{d0} , lift curve slope, a , and blade pitch angle, θ , are held constant.

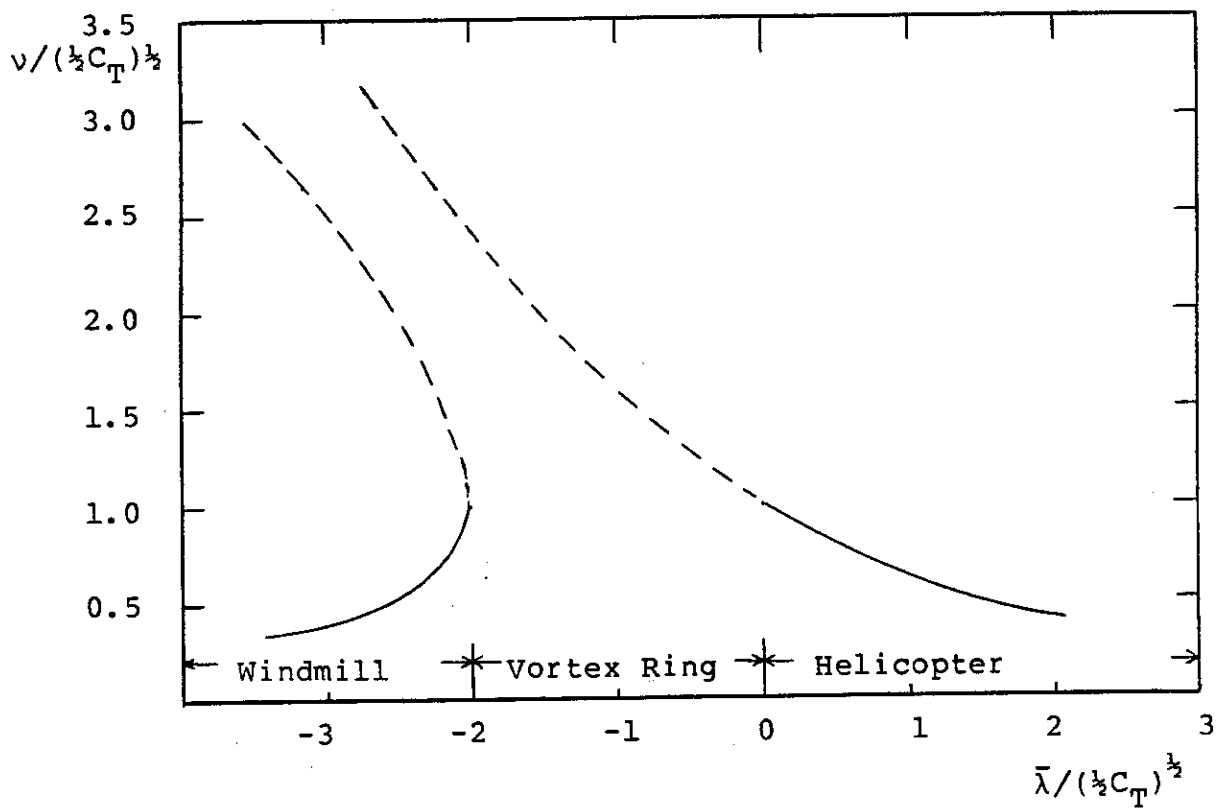


Figure 3. PLOT OF AXIAL TIP SPEED RATIO VS. INDUCED FLOW NORMALIZED ON $(\frac{1}{2}C_T)^{\frac{1}{2}}$ SHOWING THREE OPERATING STATES (14)

An initial value of induced flow ratio is chosen as

$$v \text{ initial} = \frac{1}{3} \bar{\lambda} \quad (5)$$

and iterations are performed using equation (4) until v converges within a specified error tolerance. The final calculated induced flow ratio is used in equations (1) and (3) to calculate C_T and C_Q .

The algorithm can be further refined if the drag coefficient, C_{do} , is allowed to vary as a function of average angle of attack over the rotor disk. Figure 4 illustrates a typical blade element operating at radial station r .

If one ignores both the periodic components of U_p and U_T that occur during yawed flow conditions and the flap rate component of U_p then

$$U_T = \Omega r \quad (6a)$$

and

$$U_p = \lambda \Omega R \quad (6b)$$

From the figure it is evident that

$$\alpha = \phi - \theta \quad (7)$$

and that for small θ , α varies from 90 degrees at the blade root ($r = 0$) to nearly λ at the tip. One can use the 70%

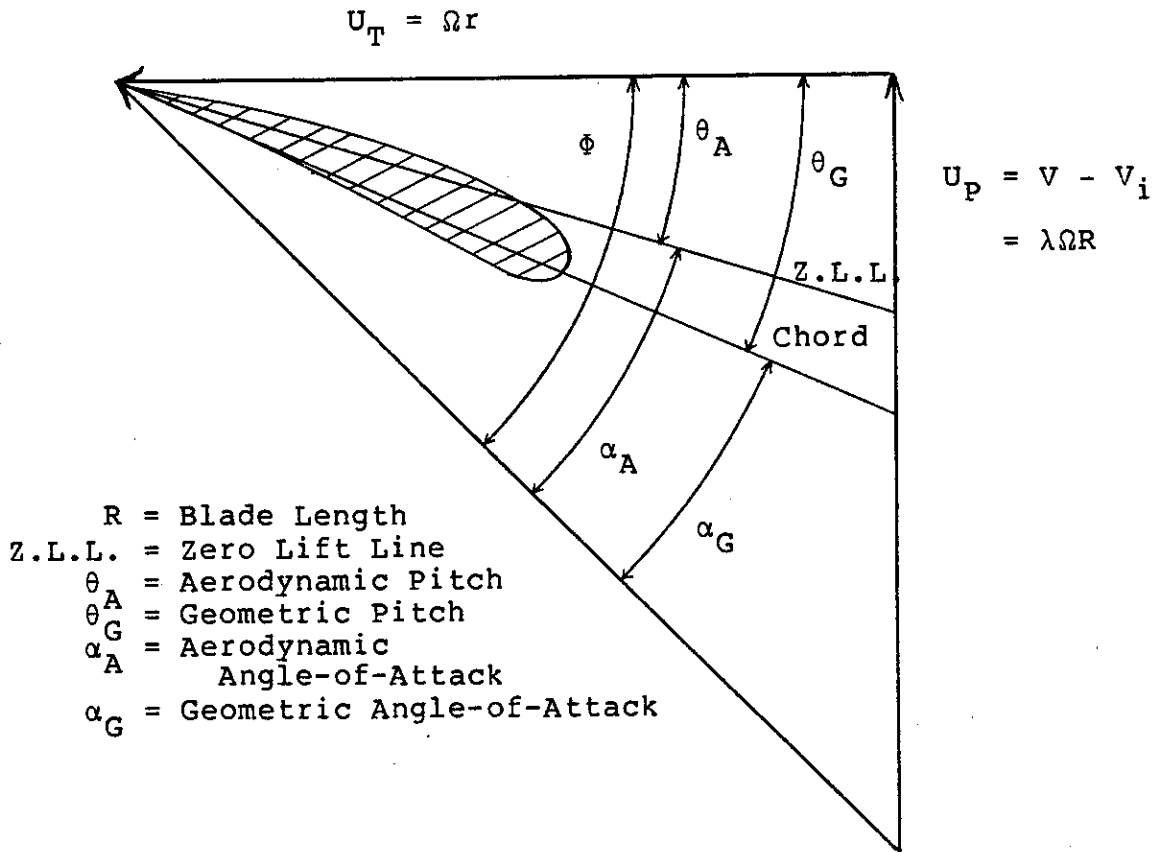


Figure 4. TYPICAL BLADE ELEMENT OPERATING AT RADIAL STATION, r

radius station to determine an average blade angle of attack. One can also approximate the value at that station, since ϕ is small,

$$\alpha = \frac{U_P}{U_T} - \theta \quad (8)$$

Substitution of (6) at the .70R station gives

$$\alpha_{\text{avg.}} = \frac{\lambda}{.7} - \theta \quad (9)$$

For most practical airfoils, not operating in stall, a parabolic function can be chosen that closely approximates the relationship between angle of attack and drag coefficient. A suitable choice for many airfoils is:

$$C_{d0} = .01 + .5 (\alpha_{\text{geometric}})^2 \quad (10)$$

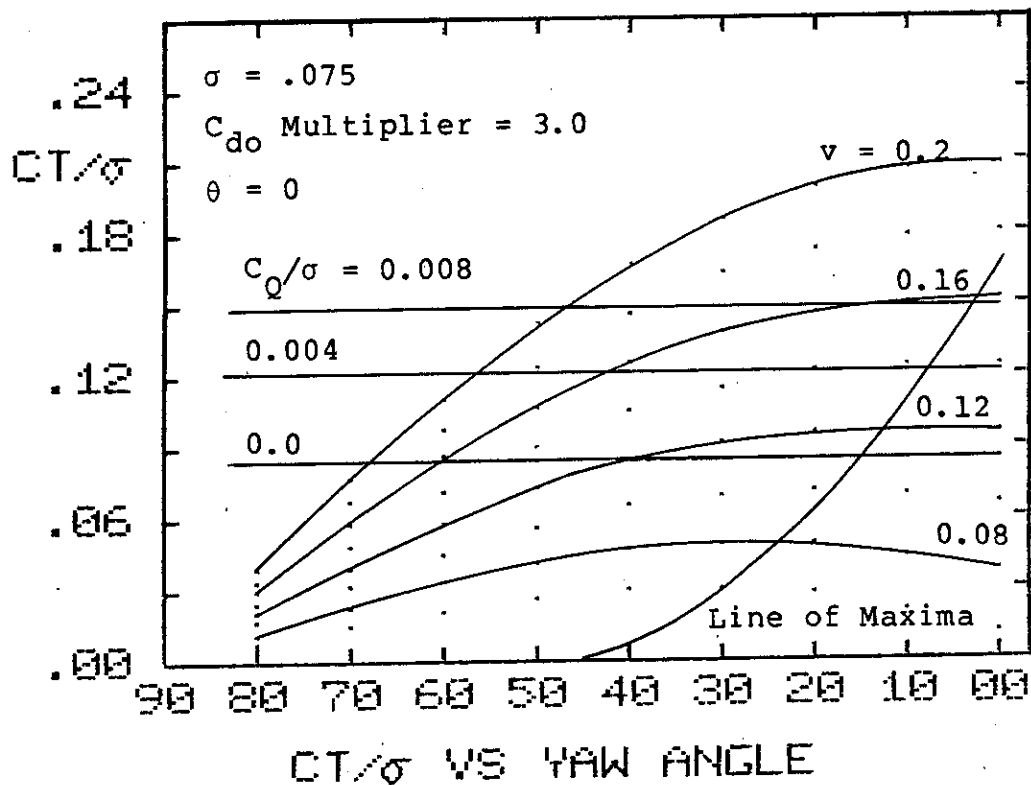
In the computer algorithm, v is calculated, λ is fixed and the average geometric angle of attack (as defined in Figure 4) is determined using equation (9). C_{d0} is then calculated using equation (10) and the geometric angle of attack. The resulting value is used in equation (3) to calculate C_Q .

2.1.3 Computer Algorithm, Results and Analysis

The algorithm presented in Section 2.1.2 is programmed in BASIC on an Apple II Plus microcomputer. The program listing is presented in Appendix 6.2.

The results of the computation are presented in three ways, each of which lends a particular insight into the operation of wind turbine rotors in yawed flow. In each case, however, conclusions drawn must be tempered with the restrictive assumptions used in the algorithm development. That is, the results are valid for the following operating conditions: (a) out of the region of stall, (b) where the assumption of uniform inflow may be valid, and (c) out of the vortex ring state where momentum theory does not apply.

One method of presenting the results of the algorithm is shown in Figure 5. Lines of constant C_Q/σ are generated from an interpolation routine that calculates C_T/σ for a given C_Q/σ . The Figure 5a shows that, for zero pitch angle, θ , lines of constant C_Q/σ are parallel, horizontal lines, and that the relationship between particular C_T/σ and C_Q/σ values is constant, regardless of yaw angle. For negative pitch angles, C_T/σ tends to decrease for a given C_Q/σ as yaw angle is increased. The change is proportional to pitch angle. For positive pitch angles C_T/σ increases for constant C_Q/σ as yaw angle is increased. The effect is shown in Figures 5b and c. The near constant relationship between C_T and C_Q with yaw angle suggests feasibility of a wind turbine system that limits power output to a constant value with a thrust limiting device that either yaws the rotor about a vertical axis or pitches the rotor about a horizontal axis, above rated thrust. A machine of this type



Note: Dots indicate intermediate tip speed ratio values.

Figure 5a. GRAPH OF C_T/σ VS. YAW ANGLE FOR $\sigma = 0.075$, A C_{d0} MULTIPLIER OF 3, AND $\theta = 0$ WITH v , C_Q/σ , AND THE MAXIMUM POWER POINTS PLOTTED AS PARAMETERS

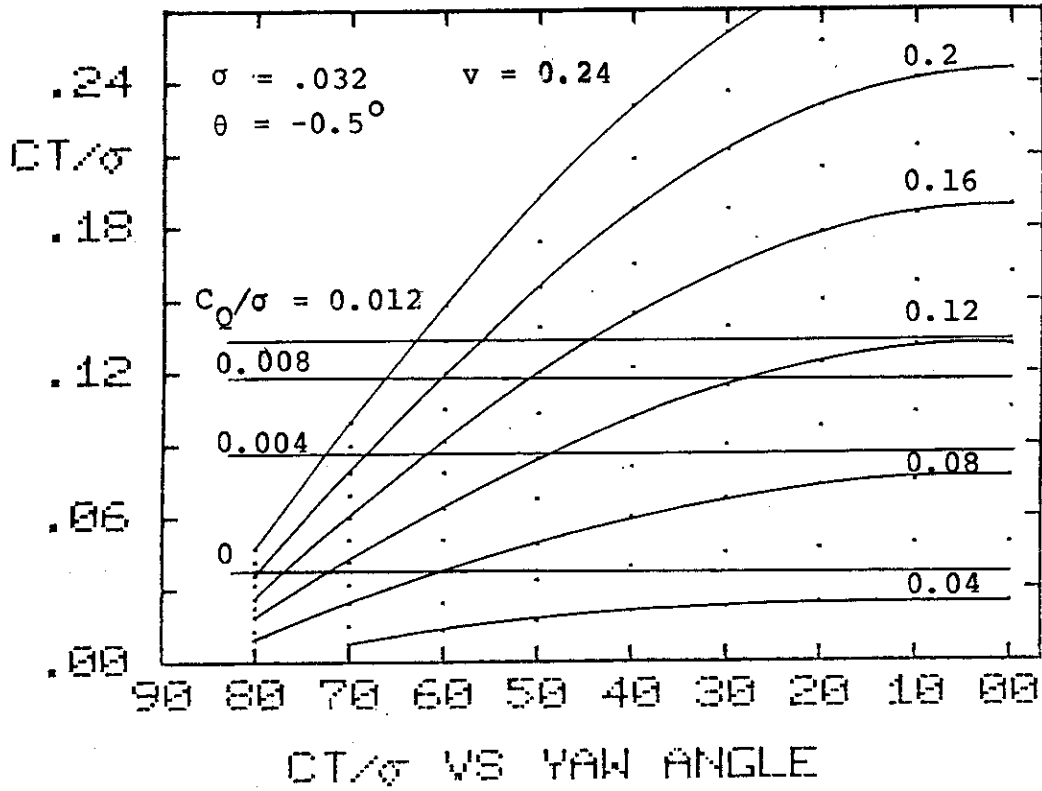


Figure 5b. GRAPH OF C_T/σ VS. YAW ANGLE FOR $\sigma = 0.032$ AND $\theta = -0.5^\circ$ WITH v AND C_Q/σ PLOTTED AS PARAMETERS

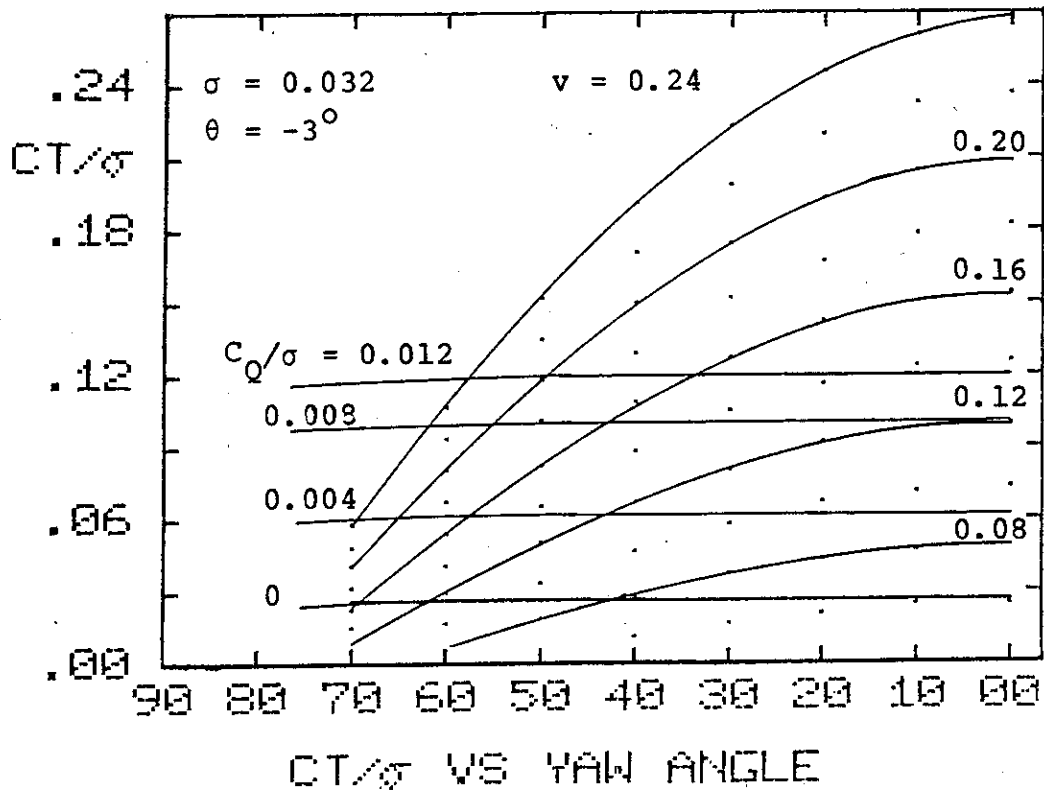


Figure 5c. GRAPH OF C_T/σ VS. YAW ANGLE FOR $\sigma = 0.032$ AND $\theta = -3^\circ$ WITH v AND C_Q/σ PLOTTED AS PARAMETERS

has been designed and constructed by North Wind Power Company (15). This machine consists of a rotor that is attached to the nacelle by means of a spring loaded horizontal hinge. For wind speeds above rated power, and therefore above rated thrust, the spring force is overcome by the thrust force and the rotor tilts up to the necessary pitch angle, thereby reducing rotor torque and thrust until equilibrium is established at rated power.

Another interesting result illustrated by Figure 5a is that the theory predicts that under certain conditions there may be more power available in yawed operation than in axial flow conditions. This may be seen from the line of constant tip speed ratio, $v = .12$. As yaw angle increases, the thrust coefficient and torque coefficient (i.e. power) first increase, reaching a maximum at 15° yaw angle, and then decrease at higher yaw angles. From the shape of the curves one can see that this effect increases for the $v = 0.8$ curve and is negligible for the $v = 0.2$ curve.

Although the phenomenon of increased power with yaw angle appears to be a moderate effect from the viewpoint of obtaining extra power from a given wind machine, and may not occur under certain operating conditions, the ability to predict and be aware of the effect is important in the consideration of yaw as a method of power control. First, it is advantageous to operate wind machines at yaw angles for maximum power extraction. Second, if the power output

of a constant rotor speed wind machine is to be controlled by a yaw actuated, feedback control system, the system would experience a control reversal in those regions where torque increased, rather than decreased, with yaw angle. Third, the increase in power with yaw angle provides a potential benefit in the prevention of overspeeding for yaw controlled wind turbines. In particular, if a machine operating at rated power and zero yaw angle were to lose its load due to mechanical or electrical failure, the tendency would be for the machine to overspeed. In yaw-controlled machines, this tendency must be countered by a rapid yawing of the rotor through nearly 90° . If, however, the machine could be operated at or near the yaw angle for maximum power (which is > 0) the rotor would be yawed through a considerably smaller angle. It follows that, in the latter case, the rotor RPM would have less time to increase before the furled position were obtained.

The calculation of the yaw angle for maximum power is outlined below. Using equations (1) and (2) and the definition of the λ , $\bar{\lambda}$, v and v , and neglecting μ^2 because it is small in equation (2) one can write: (See also Figure 6).

$$C_T = 2v(v \cos\chi - v)^2 + (v \sin\chi)^2)^{\frac{1}{2}} \quad (11)$$

$$C_T = \frac{\sigma a}{4} (v \cos\chi - v) - \frac{\sigma a}{6} \theta \quad (12)$$

we wish to find

$$\left. \frac{\partial C_T}{\partial X} \right|_{v = \text{constant}} = 0$$

in order to locate the maxima.

We therefore define:

$$C_T/2v^2 = G, \quad v/v = H, \quad \frac{\sigma a}{8v} = I \quad \text{and} \quad \frac{2\theta}{3v} = J$$

then

$$G = I(\cos X - H - J) \tag{13}$$

$$G = H(H^2 - 2H \cos X + 1)^{\frac{1}{2}} \tag{14}$$

Thus substituting

$$H = \cos X - G/I - J \tag{15}$$

one obtains

$$G^2 = (\cos X - G/I - J)^2 + (\cos X - G/I - J)^4 - 2(\cos X - G/I - J)^3 \cos X \tag{16}$$

Now taking the differential and setting all dX coefficients = 0 (since we wish $dG/dX = 0$) one obtains:

$$\begin{aligned} & -2 + 6(\cos X - G/I - J) \cos X \\ & - 2(\cos X - G/I - J)^2 = 0 \end{aligned} \tag{17}$$

Letting $A = G/I + J$ and solving the quadratic for $\cos\chi$;

$$\cos\chi = \frac{A + (9A^2 + 8)^{\frac{1}{2}}}{4}$$

Where

$$A = G/I + J = \frac{4C_T}{\sigma av} + \frac{2}{3} \frac{\theta}{v}$$

(18)

Plotting equation (18) on the graph of Figure 5a, one can see that the line connects the power maxima.

The physical reason for the phenomenon is illustrated as follows.

If one considers the mass flow through the rotor it can be expressed as a function of area and flow velocity as:

$$\dot{m} = \rho Av \quad (19)$$

When considering flow through a yawed rotor, one might expect the area, A , in equation (19) to be the projected area of the rotor disk normal to the direction of flow. However, the Prandtl-Glauert Hypothesis for flow over wings (16) indicates that the flow affected by the rotor is contained in a cylinder of radius R , independent of rotor disk orientation. Therefore, based on the Prandtl-Glauert Hypothesis, the area in equation (19) is constant with yaw angle and mass flow through the rotor is only a function of velocity. Figure 6 shows the non-dimensional velocity relationships with yaw angle. From the figure, the resultant

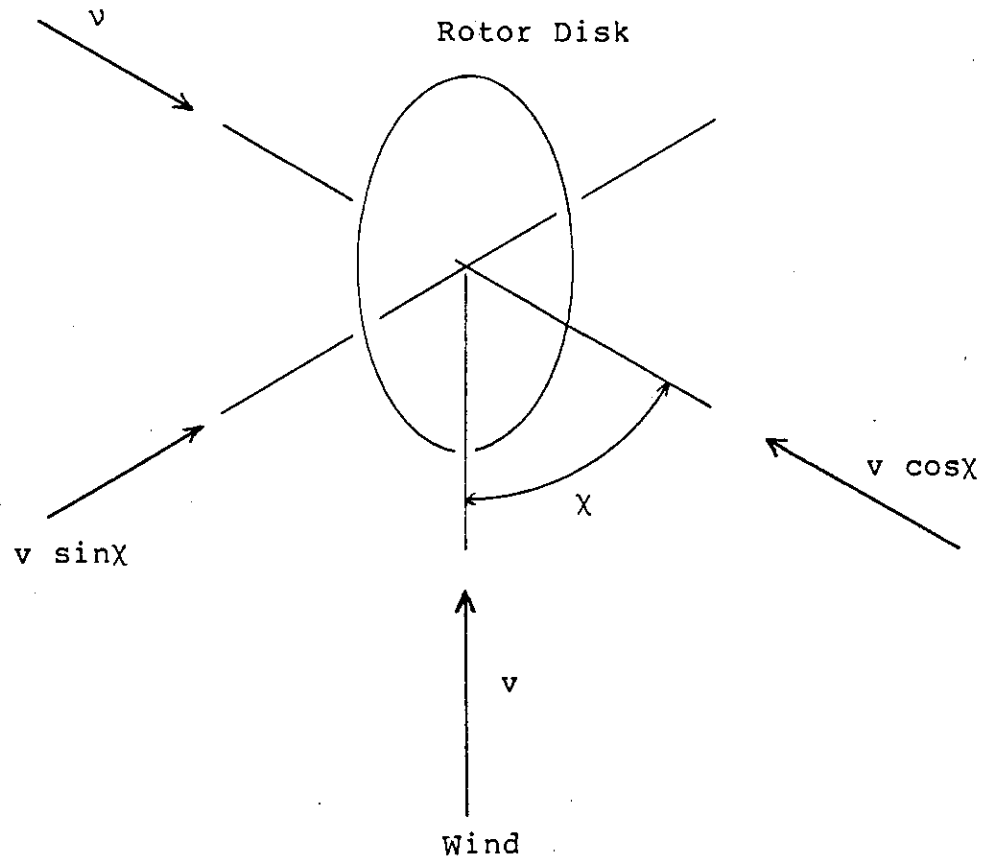


Figure 6. NONDIMENSIONAL VELOCITIES ACTING ON THE ROTOR DISK AT YAW ANGLE, χ

flow velocity at the disk is:

$$\text{net velocity} = \left[(v \cos X - v)^2 + (v \sin X)^2 \right]^{\frac{1}{2}} \quad (20)$$

or

$$\text{net velocity} = (v^2 + v^2 - 2v v \cos X)^{\frac{1}{2}} \quad (21)$$

If v and v are constant, a larger yaw angle results in a larger net velocity at the rotor, which, from equation (19) and the Prandtl-Glauert Hypothesis, indicates that mass flow will increase with yaw angle. From equation (11) it is evident that if the net velocity (and therefore mass flow) increases with constant v and v , then C_T (and C_Q) will increase with yaw angle.

However, the induced flow, v , is not constant with constant v and increasing yaw angle. In fact, the numerical results show that induced flow decreases with yaw angle. From equation (11) and (21) it is evident that decreasing induced flow, v , will result in decreasing C_T and C_Q values. Thus the existence of a power maximum at yaw angles other than zero depends on the competing effects of increased mass flow and decreased induced velocity with yaw angle.

Based on equation (18), one can show that for constant C_T/σ , a , and θ values, the occurrence of a maximum is strictly a function of tip speed ratio and one can calculate a critical tip speed ratio beyond which the maximum will not

occur at positive yaw angles, given the required constants. In addition, one can deduce that the smaller the value of A, the more pronounced will be the effect, and that there is a maximum value of A, ($A = 0.618$) above which the effect will not occur. Therefore, a decrease in C_T , C_Q , or θ , or an increase in σ or v will result in amplification of the effect of maximum performance at yaw angles other than zero. These effects are demonstrated in Figure 5.

Finally, a comparison of Figures 5b and c shows the large effect that small changes in collective pitch can have on turbine performance. A similar comparative approach can easily be extended to examine the effects on rotor performance of the parameters, σ , a , and C_{do} .

A second method of presenting the results of the computer algorithm is presented in Figure (7). Figure 7 is plotted for the same configuration as Figure 5b. C_P is calculated using particular C_Q and v values by the relation:

$$C_P = \frac{2C_Q}{v^3} \quad (22)$$

The computer program for the algorithm is listed in Appendix 6.2.

Several interesting results are easily obtained from Figure 7. However, one must interpret these results within the restrictive assumptions of the analysis stated previously. From the figure, one can determine wind turbine

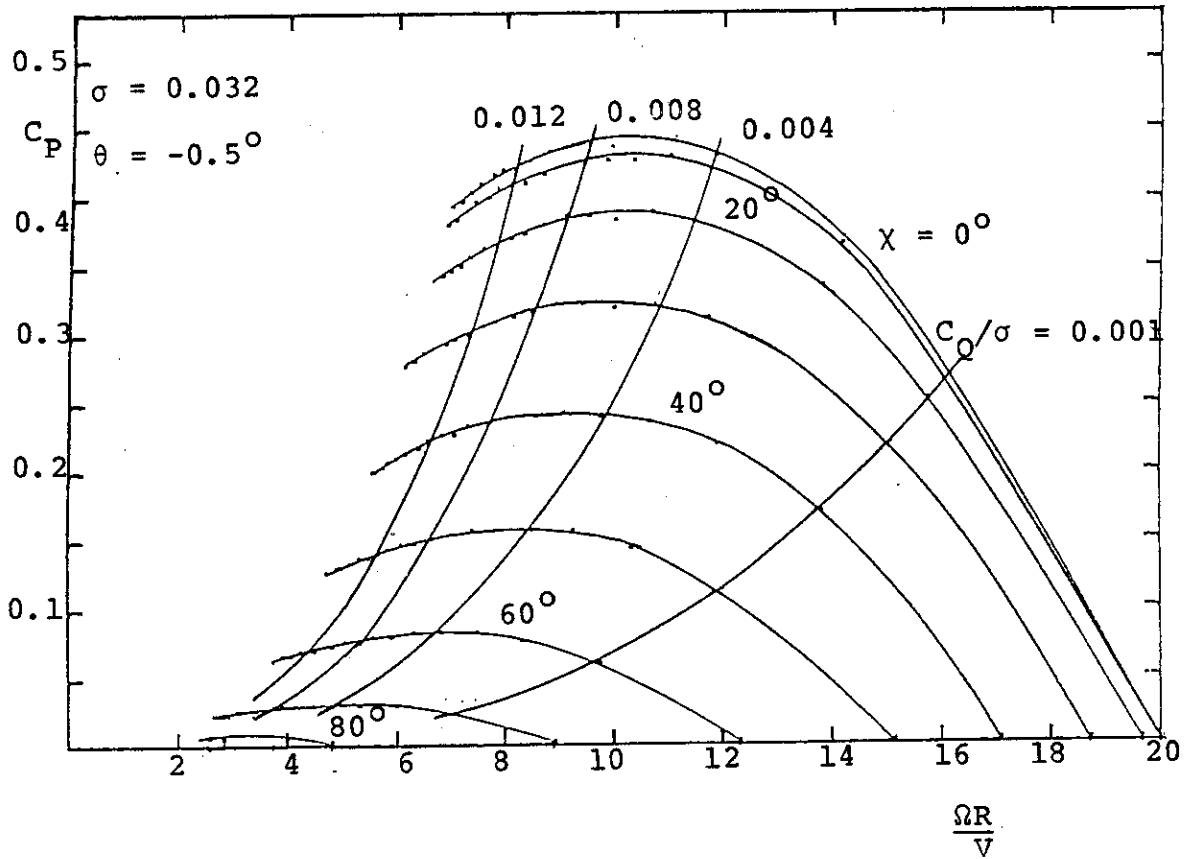


Figure 7. GRAPH OF C_p VS. SPEED RATIO $\Omega R/V$ FOR $\sigma = 0.032$ AND $\theta = -0.5^\circ$ WITH χ AND C_q/σ PLOTTED AS PARAMETERS. DATA IS THE SAME AS THAT PLOTTED IN FIGURE 5b

performance as a function of tip speed ratio and yaw angle. For example, in Figure 7, which is for parameters identical to Figure 5b, a yaw angle of 10° has a very small effect on performance. In addition, by considering lines of constant C_Q/σ and C_T/σ one can choose a rated power operating point that will result in optimum power coefficient and yet provide a stall margin, as necessary. (C_T/σ approaching .14 generally indicates an approach to stall conditions).

It is interesting that the theory predicts that there is a maximum performance coefficient, even without stall effects. A brief analysis will provide some insight into the phenomenon. By combining equations (2), (3) and (22) ignoring drag effects, and assuming zero pitch angle, one can write.

$$C_P = \left(\frac{\sigma a}{2}\right) \left(\frac{1}{v^3}\right) (v - v)^2 \quad (23)$$

Physically the $(1/v^3)$ term represents the power available in the wind while the $(v-v)^2$ term represents the power extracted, which conforms with the definition of the power coefficient, C_P . Rearrangement of equation (23) gives

$$C_P = \left(\frac{\sigma a}{2}\right) \left(\frac{1}{v}\right) \left(1 - \frac{v}{v}\right)^2 \quad (24)$$

one then takes

$$x = \frac{v}{v} \quad \text{with: } v = \text{constant} \quad (25)$$

(Letting $v = \text{constant}$ is a good assumption near maximum C_p values, as is shown by the numerical results). Setting the derivative $(\frac{dC_p}{dx})$ to zero, one can calculate two solutions,

$$x = \frac{v}{v} = 1, 1/3 \quad (26)$$

Since the solution $(v/v) = 1$ is in the vortex ring state it can be ignored. The other solution shows that the power coefficient will have a maximum, without stall effects, when the ratio of induced to free-stream flow is about one-third. The exact value will vary depending on variations in induced velocity, which were ignored. This result is related to the Betz coefficient, $C_p = 0.59$, the optimal value of C_p which occurs for $v/v = 1/3$. The optimal operating condition is shown in Figure 8, based on the Betz derivation and actuator-disk momentum theory.

A third presentation of the results of the algorithm for the simplified theory is shown in Figure 9. In this figure lines of constant, non-dimensional, induced flow velocity, v , have been added to the curves of Figure 5b. The graph allows one to evaluate quickly the induced flow for various operating conditions. For example, the ratio of induced flow to tip speed ratio at maximum power coefficient is easily seen, as is the fact that induced flow decreases with yaw angle for constant tip speed ratio, both discussed previously. Finally, the figure gives performance values

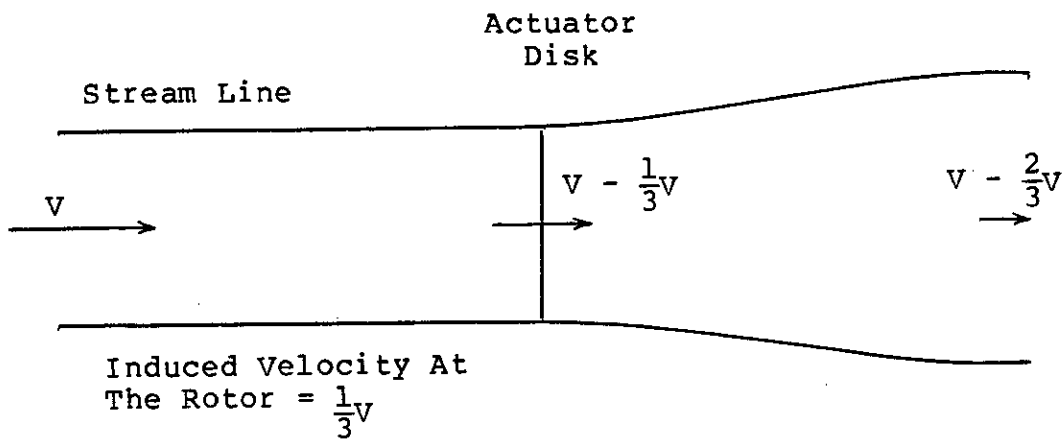


Figure 8. OPTIMUM OPERATING CONDITIONS FOR A WIND TURBINE ROTOR

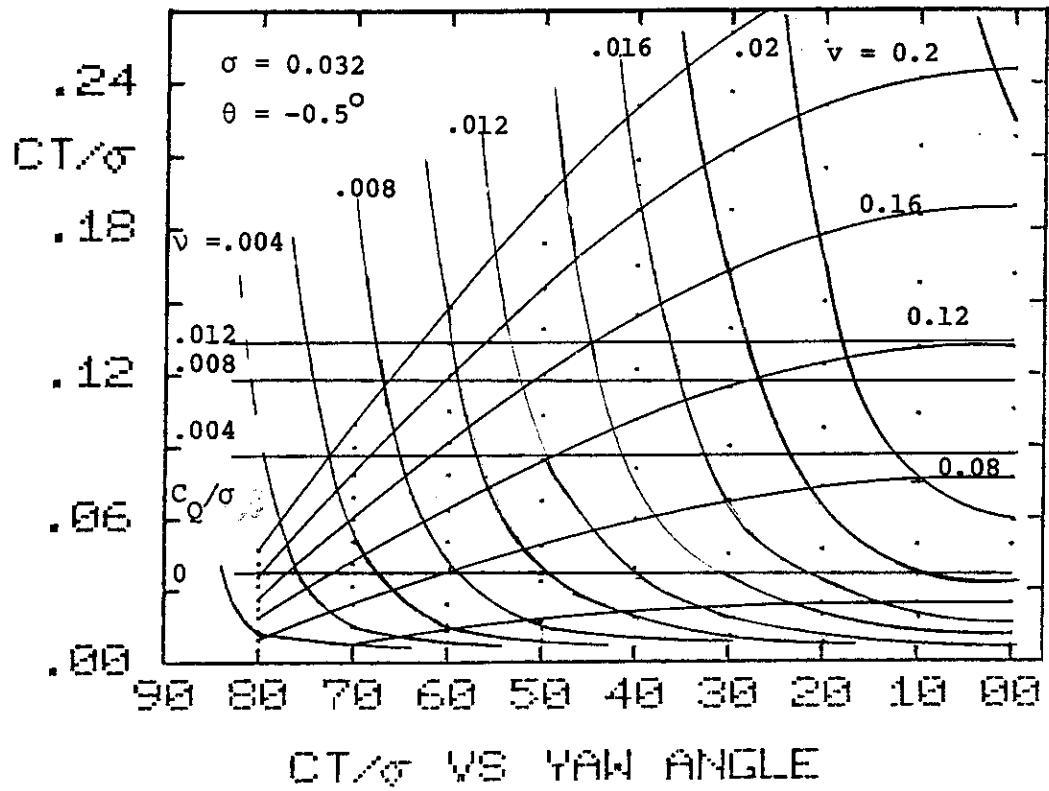


Figure 9. FIGURE 5b REPLOTED WITH LINES OF CONSTANT INDUCED VELOCITY ADDED

and induced flow velocities for various operating conditions which will be used to reduce computing time in the dynamic, yawed flow simulation developed next.

2.2 DYNAMIC YAWED FLOW ROTOR SIMULATION MODEL

2.2.1 Objectives

Although the previous simplified theoretical development provides a method to estimate yawed flow performance parameters, such as C_T , C_Q , v and v_i , it fails to provide a detailed analysis needed to examine other important factors such as unsteady blade loading, yaw rate, and local angle-of-attack. To provide a more detailed analysis in yawed flow conditions, a dynamic rotor simulation model was developed. The simulation was constructed with the following considerations:

- a.) Complexity: Complex computer simulations of rotors already exist that provide detailed analysis, e.g., MOSTAB (7). Therefore this analysis is designed to be simple enough that it can be easily applied and even programmed on a small, microcomputer system, and yet with sufficient complexity that the results are quantitatively useful.
- b.) Dynamic Effects: The simulation is constructed so that transient and dynamic effects can be analyzed. Since most analytical solutions provide only steady state or quasi-steady state solutions,

data generated from a dynamic simulation could yield new insights. Induced velocities, usually calculated using steady state momentum theory, are calculated using a dynamic inflow theory (17). The use of this theory in yawed flow or transient yaw conditions is expected to provide a more accurate induced velocity profile over the rotor disk than either the assumption of uniform inflow or of isolated induced velocities based on local momentum theory. Accurate induced velocity profiles are important in calculating local angle of attack and aerodynamic forces. The theory is discussed in more detail in Section 2.2.3.4.

- c.) Variable Wind Effects: The simulation is constructed so that variable wind speeds and yaw angles can be included to determine wind turbine response to gust conditions.
- d.) Stall Effects: Stall effects are ignored in the simulation. The justification for this is that in yawed flow rotors display the effects of dynamic stall (6). (Local blade elements experience an effective oscillatory angle of attack.) Since dynamic stall causes increased effective lift, local lift values are calculated based on a linear lift slope, a . As a result the model is not applicable for stalled operation, and may

overestimate lift coefficients as the angle of attack retreats from the maximum. See again Figure 2.

- e.) Drag Coefficients: Drag coefficients are calculated as a function of local geometric angle of attack using equation (10).
- f.) Passive Cyclic Pitch: Two-bladed rotors which operate in yawed flow at moderate to high advance ratios, or with high yaw rates, usually include a teetering hub, often with a positive pitch-flap coupling (i.e. $\delta_3 \gg 0$, passive cyclic pitch hub) in order to reduce steady blade and tower forces. Examples include the experimental rotor described in Section 3, the modified NASA MOD-0 and MOD-2 and several smaller wind machines. As a result, the simulation is developed to include hinged hub designs with variable pitch-flap coupling for a two-bladed rotor.
- g.) Elastic Flapping Effects: The simulation is developed to include elastic-blade flapping, in addition to the pitch-flap coupling effects just described. These effects are necessary for an adequate treatment of blade loads and may also be important for the calculation of performance for some rotors.

2.2.2 Simulation Model Algorithm Overview

The state variable approach, with a predictor-corrector integration routine, was selected to solve the system of first-order differential equations that describe the rotor behavior.

The coordinate system and directions are shown in Figure 10 for the rotor. The state variables for the system are: (a) angular rotation about the prelag axis and its angular velocity, τ and $\dot{\tau}$; (b) elastic flap angle and velocity, β_e and $\dot{\beta}_e$; (c) azimuth angle and velocity, Ψ and $\dot{\Psi}$, or Ω ; (d) yaw angle and velocity, χ and $\dot{\chi}$; and (e) induced flow velocity, v .

The state variables for the model are identified as:

$$\begin{aligned} Y1 &= \tau \\ Y2 &= \dot{\tau} \\ Y3 &= \beta_e \\ Y4 &= \dot{\beta}_e \\ Y5 &= v \\ Y6 &= \dot{\Psi} = \Omega \\ Y7 &= \chi \\ Y8 &= \dot{\chi} \end{aligned} \tag{27}$$

Note: Ψ is omitted in the system of equations since increments of Ψ will generate the time increment for the predictor-corrector algorithm.

and the state equations are:

$$\begin{aligned}\dot{Y}_1 &= Y_2 & (28) \\ \dot{Y}_2 &= f_1 \\ \dot{Y}_3 &= Y_4 \\ \dot{Y}_4 &= f_2 \\ \dot{Y}_5 &= f_3 \\ \dot{Y}_6 &= f_4 \\ \dot{Y}_7 &= Y_8 \\ \dot{Y}_8 &= f_5\end{aligned}$$

where the functions f_1 through f_5 are derived and explained in Section 2.2.3. In general, the functions f_1 through f_5 are functions of the state variables, Y_i and the aerodynamic forces on the rotor. Therefore, given the state variables and the aerodynamic forces on the rotor at time t , the new state variables are calculated at time $t + \Delta t$ using the state equations, the aerodynamic equations, and a predictor-corrector solution. Thus, a general algorithm for the model may be outlined in seven steps as follows:

1. Input initial conditions for Y_i , $i = 1$ to 8.
2. Determine azimuth step size and calculate time step, since $\Delta t = \Delta \Psi / \Omega$ (Note variable time step since Ω is variable).
3. Input wind speed as constant or function of time.
4. Calculate aerodynamic forces on each rotor blade at time, t and azimuth, Ψ .

5. Solve the state equations for time $t + \Delta t$ using a predictor-corrector algorithm such as described in (18) to specified error tolerance. This will require updating aerodynamic force calculations at time $t + \Delta t$ and again with each iteration of the state variables. Also, since Ω is changing, a corrected time step is calculated based on the average, corrected, Ω over the interval.
6. Store the values of the state variables at time $t + \Delta t$ and azimuth angle $\Psi + \Delta\Psi$.
7. Go to 3 and continue.

The algorithm described will result in a time based simulation model of the rotor from which instantaneous values of performance, aerodynamic forces and blade loadings can be determined and followed over time in response to steady or variable operating conditions.

2.2.3 Derivations

In order to apply the rotor model algorithm, the state equations f_1 through f_5 and the aerodynamic forcing equations must be developed. For each of the derivations the result must be in terms of the given state variables and the aerodynamic forces, for a solution to exist. Before deriving the individual state and aerodynamic equations, let us first derive the general equations of motion for a two-bladed rotor operating in yawed flow with variable yaw rate and pitch-flap coupling (i.e. δ_3). This result will be

necessary in deriving other equations. Figure 10 defines the coordinate directions. The general approach is to first write the kinetic energy of the rotor based on the velocities u_c , v_c , and w_c described in the rotating system. Next, one writes the Lagrangian and virtual work and forms the differential equations of motion in terms of τ and χ . The final equation takes the form:

$$2(M) \begin{Bmatrix} \dot{\tau} \\ \dot{\chi} \end{Bmatrix} + 2(G) \begin{Bmatrix} \dot{\tau} \\ \dot{\chi} \end{Bmatrix} + 2(K) \begin{Bmatrix} \tau \\ \chi \end{Bmatrix} = (F) \quad (29)$$

The matrices M, G, K and F are the equivalent mass or inertial matrix, the gyroscopic matrix (there is no explicit viscous damping), the stiffness matrix, and the aerodynamic forcing functions, respectively. The velocities in terms of u_c , v_c , and w_c are presented in Appendix 6.3 as are the details of the derivation and the resulting equations.

2.2.3.1 Aerodynamic Equations

In general terms, the aerodynamic forces are calculated from blade element theory and are integrated along each blade, at successive rotor azimuth angles, to obtain the aerodynamic forces. Figures 10 and 11 illustrate the quantities involved.

The aerodynamic forces to be calculated are the elemental thrust force, dT , and the elemental inplane force, dQ . From these, the aerodynamic thrust, thrust moment, inplane force and torque are calculated. For this

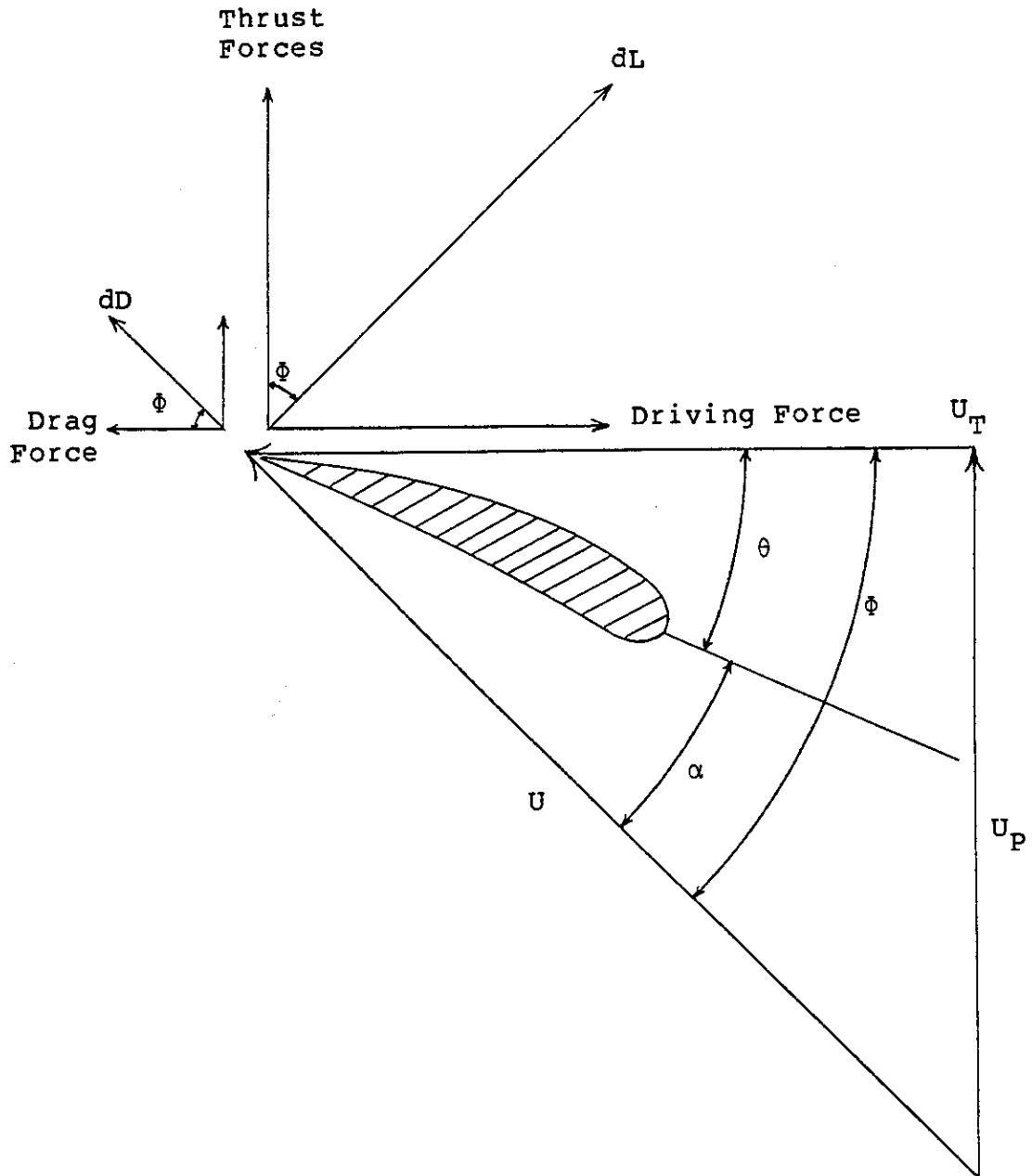


Figure 11. BLADE ELEMENT, dr , OPERATING AT RADIAL STATION r .

derivation, it is assumed that the lift is a linear function of angle of attack, (stall effects are ignored), and drag is a second order function of angle of attack. Based on the geometry of Figure 11 one can write:

$$dT = dL \cos\phi + dD \sin\phi \quad (30)$$

$$dQ = dL \sin\phi - dD \cos\phi \quad (31)$$

where

$$dL = q C_L \quad (32)$$

$$dD = q C_{D0} \quad (33)$$

and

$$q = \text{dynamic force} = \frac{1}{2} \rho dr c U^2 \quad (34)$$

$$C_{D0} = f(\alpha) \text{ See (10)}$$

since

$$\alpha = \phi - \theta \quad (35)$$

and θ is the known pitch angle based on blade geometry and the pitch-flap coupling for the rotor, the solution for dT and dQ is determined once the velocities U_P and U_T are established, since:

$$\phi = \tan^{-1} \frac{U_P}{U_T} \quad (36)$$

and

$$U^2 = U_P^2 + U_T^2 \quad (37)$$

Expressions for the velocities U_p and U_T are derived in detail in (14). For a rotor operating in yawed flow (i.e. advance ratio > 0), for small flapping angles (so that $\cos\beta \cong 1$ and $\sin\beta \cong \beta$), for constant yaw angle (no yaw rate and neglecting the effects of wake rotation, one can write:

$$U_T = \Omega r + V \sin\chi \sin\Psi \quad (38)$$

$$U_p = V \cos\chi - V_i - r\dot{\beta} - \beta V \sin\chi \cos\Psi \quad (39)$$

Since yaw rates are to be included in the rotor model, velocities due to yawing must be added to U_T and U_p .

From Figures 10 and 11, U_T and U_p are defined in the v_c and $-w_c$ directions. Equations (3.2) and (3.3) in Appendix 6.3 define the inertial velocities in these coordinate directions (i.e. no wind or induced velocities are present). If, for simplification, all terms of third order or higher are ignored, the equations become:

$$v_c = \Omega r - \dot{\chi} S \sin\Psi \quad (40)$$

$$w_c = \dot{\tau} r \cos\delta_3 + \dot{\chi} r \cos\Psi \quad (41)$$

The addition of these terms to the U_p and U_T velocities gives:

$$U_T = \Omega r + V \sin\lambda \sin\psi - \dot{\chi} S \sin\psi \quad (42)$$

$$U_P = V \cos\lambda - V_i - r\dot{\beta} - \beta V \sin\lambda \cos\psi - \dot{\chi} r \cos\psi \quad (43)$$

(Note that the Ωr term in the v_c equation is already included in the expression of U_T , and the $\dot{\chi} r \cos\psi$ term is included in the flap-rate term, $\dot{\beta}$, in the U_P equation. The latter point will be made evident in the derivation of the flapping equations).

Given the wind velocity and radial and azimuthal station (v , r and ψ), equations (42) and (43) express the tangential and normal velocities in terms of the known state variables. Thus the aerodynamic forces dT and dQ can be found.

Knowing the elemental aerodynamic forces one can now write the aerodynamic components of the forces and moments for the inplane and thrust directions as follows:

$$TB(j) = \sum_{n=1}^N dT = \text{Total thrust force per blade} \quad (44)$$

$$MB(j) = \sum_{n=1}^N dT \cdot r = \text{Total thrust moment per blade} \quad (45)$$

$$TQ(j) = \sum_{n=1}^N dQ = \text{Total inplane force per blade} \quad (46)$$

$$MQ(j) = \sum_{n=1}^N dQ \cdot r = \text{Total driving torque per blade} \quad (47)$$

where

N = number of blade elements

j = blade number (i.e. blade 1 or 2)

Note that all equations assume small flap angles, and no flap angle corrections are included.

Let us review the assumptions used in the derivation of the aerodynamic forces:

1. Blade geometry, wind speed, rotating velocity, Ωr , and induced velocity are constant over the blade element, dr . The more blade elements assumed, the less significant are the errors due to this assumption.
2. Flow along the blade is ignored. According to (14) radial flow may increase the profile drag slightly, but will have little effect on rotor thrust.
3. Wake rotation effects are ignored. These are usually small compared to Ωr .

4. Tip losses have been thus far ignored. These losses, however, can be easily included by the approximation of Prandtl and Betz as presented in (14).

$$B = 1 - \frac{(2C_T)^{\frac{1}{2}}}{b} \quad (48)$$

where B is the tip loss factor; blade elements out board of radius BR are assumed to have profile drag but no lift. C_T is the rotor thrust coefficient and b is the number of rotor blades.

5. The lift-curve slope and drag coefficient are assumed to be simple functions of angle of attack and constant over the blade elements, dr. Corrections in lift and drag coefficients due to variation in Reynolds Number, stall effects, surface roughness, etc. can be included if these effects are known quantitatively. These effects are not included in the present simulation model.
6. Flapping angles are assumed small so that the small angle assumptions hold, and total blade aerodynamic forces are not corrected for the cosine of the flapping angle.

7. Third order and higher inertial terms have been ignored in the calculation of U_T and U_P for simplicity. The error should be small for moderate yaw rates and τ angles.

2.2.3.2 State Variable Equations for Yaw Angle and Cyclic Pitch Deflection About the Pre-lag Axis

Derivation of the f1 function for state equation \dot{Y}_2 , (i.e. the equation of motion about the pre-lag axis) and the f5 function for state variable \dot{Y}_8 (i.e. the equation of motion about the yaw axis) are found at the beginning of this section and in Appendix 6.3.

The equations for $\dot{Y}_2 = \dot{\tau}$ and $\dot{Y}_8 = \dot{\chi}$ are obtained from premultiplication of equation (29) by $(M)^{-1}$. Thus

$$I \begin{Bmatrix} \ddot{\tau} \\ \ddot{\chi} \end{Bmatrix} = - (M)^{-1} (G) \begin{Bmatrix} \dot{\tau} \\ \dot{\chi} \end{Bmatrix} - (M)^{-1} (K) \begin{Bmatrix} \tau \\ \chi \end{Bmatrix} + (M)^{-1} \frac{1}{2} (F) \quad (49)$$

Since these matrix manipulations are best carried out in the computer program itself, explicit relationships for $\dot{\tau}$ and $\dot{\chi}$ are not presented here. The derived matrices and solutions are presented in Appendix 6.3. Examination of equations (3.17), (3.18) and (3.19) in the Appendix, shows that one can evaluate the state equations for $\dot{\tau}$ and $\dot{\chi}$ in terms of blade and nacelle moments of inertia, (I and I_N), blade mass, (M), delta three angle, (δ_3), the aerodynamic forces calculated in equations (44) to (47) and the state variables.

Let us review the assumptions used in the derivations.

1. Third order and higher terms are neglected in the expression for rotor kinetic energy.
2. All aerodynamic assumptions listed previously apply because these forces are included as the forcing function in the derivation.

2.2.3.3 State Variable Equations for Flapping Angle

Blade flapping angles, β , are actually determined from several components. The state variables $Y3 = \beta_e$ and $Y4 = \dot{\beta}_e$ represent the elastic flapping of the blades.

Figure 12 shows the components considered in the total flapping angle β . β_o is a constant precone flap angle; $\tau \cos \delta_3$ is a flapping angle due to rotation about the prelag axis; and β_e is the flap angle due to the elastic bending of a rigid blade about a simulated flap hinge with spring constant as shown in the figure. The equation of motion for one blade is:

$$I \ddot{\beta}_e + (\bar{I} \Omega^2 + K_s) \beta_e = \frac{MB(1) + MB(2)}{2} \quad (50)$$

where \bar{I} is the equivalent centrifugal inertia. Since the nonrotating frequency is given by

$$\omega_o^2 = \frac{K_s}{I} \quad (51)$$

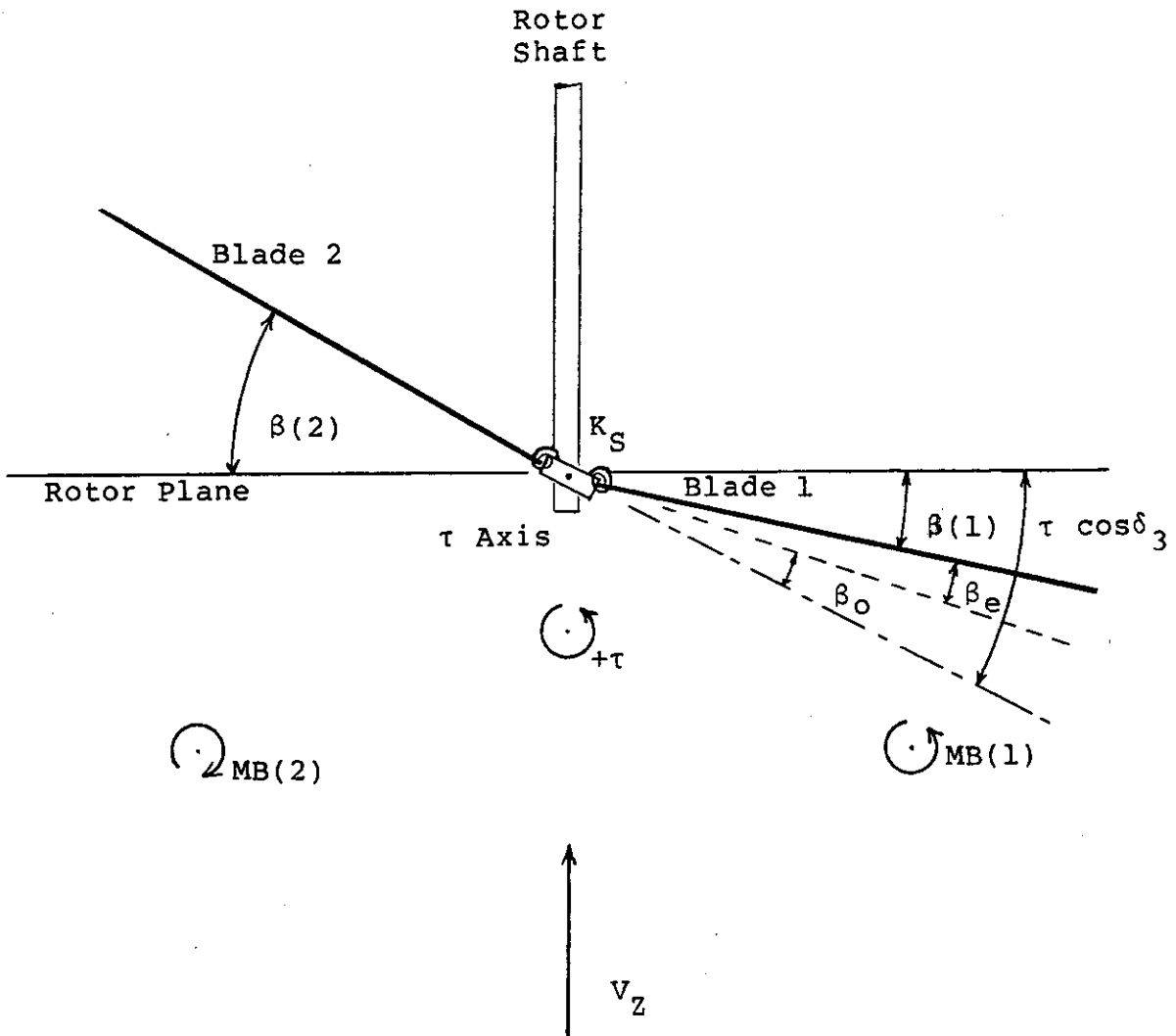


Figure 12. RIGID BLADE FLAPPING GEOMETRY AND DEFINITIONS

and since the elastic mode experiences rotational stiffening different from the centrally-hinged rigid blade ($\bar{I} \neq I$, $\bar{I}/I = \omega_1^2$), the rotational frequency is:

$$\omega_n^2 = \omega_o^2 + \Omega^2 \omega_1^2 \quad (52)$$

One can write, therefore,

$$\ddot{Y}_4 = f_2 = \ddot{\beta}_e = -(\omega_o^2 + \Omega^2 \omega_1^2) \beta_e + \frac{MB(1) + MB(2)}{2I} \quad (53)$$

Now one can write the total flap angle for blade 1 as

$$\beta(1) = \beta_o + \beta_e + \tau \cos \delta_3 \quad (54)$$

and for blade 2 as

$$\beta(2) = \beta_o + \beta_e - \tau \cos \delta_3 \quad (55)$$

The related derivatives are:

$$\dot{\beta}(1) = \dot{\beta}_e + \dot{\tau} \cos \delta_3 \quad (55)$$

$$\dot{\beta}(2) = \dot{\beta}_e - \dot{\tau} \cos \delta_3$$

Since:

$$Y1 = \tau; Y2 = \dot{\tau}; Y3 = \dot{\beta}_e \text{ and } Y4 = \dot{\beta}_e$$

these four equations are easily written in terms of the state variables and thus flapping angles and velocities for each blade are determined.

The assumptions for this derivation are:

1. The blade is modeled by a rigid blade with root hinge having an equivalent spring coefficient.
2. Small flap angles are assumed since thrust forces are not corrected for cosine of the flap angle.
3. Elastic damping is ignored.
4. Rotational stiffening is approximated by a second order function of natural flapping frequency.
5. The two blades are identical.

2.2.3.4 State Variable Equation for Dynamic Induced Flow

The application of a dynamic inflow theory in this simulation is one factor that sets this rotor model apart from other rotor simulations, e.g. (4). The relationships used have been recently developed by Pitt and Peters (17) in studies of dynamic inflow patterns for helicopter rotors in forward flight. The advantage gained in using dynamic inflow theory is that complex induced flow patterns that follow dynamic yawed flow conditions are easily expressed in concise analytical terms. Previous methods (4) use steady-state momentum theory to calculate isolated induced flow

velocities over the rotor disk. Such an approach ignores the dynamic response of the induced flow to unsteady variations in yaw angle. Previous methods also fail to account for the induced flow gradient under yawed conditions. Therefore, previous analyses often give poor estimates of induced velocities at moderate advance ratios.

There are two factors that affect induced velocity patterns over the rotor disk in unsteady yawed flow. First, in yawed flow (advance ratios > 0) there is a velocity component in the plane of the rotor disk as well as one normal to the disk. This fact causes the lift distribution that occurs at the leading edge of the disk to affect induced velocities over the whole disk. Therefore, the induced flow pattern over the disk can not be determined from local momentum theory, see Figure 13. Second, the induced flow patterns respond dynamically to changes in operating conditions, such as a yawing. The pattern responds in a fashion analogous to a mechanical spring and damper, in that there is a time lag between the application of lift and the development of induced flow.

Although Glauert (see Figure 13) proposed a profile shape for the induced flow pattern, the problem of analytically quantifying the pattern over the rotor disk has remained. One of the advantages of the method proposed by Pitt and Peters (17), and used in this simulation, is that not only is the average dynamic induced flow velocity

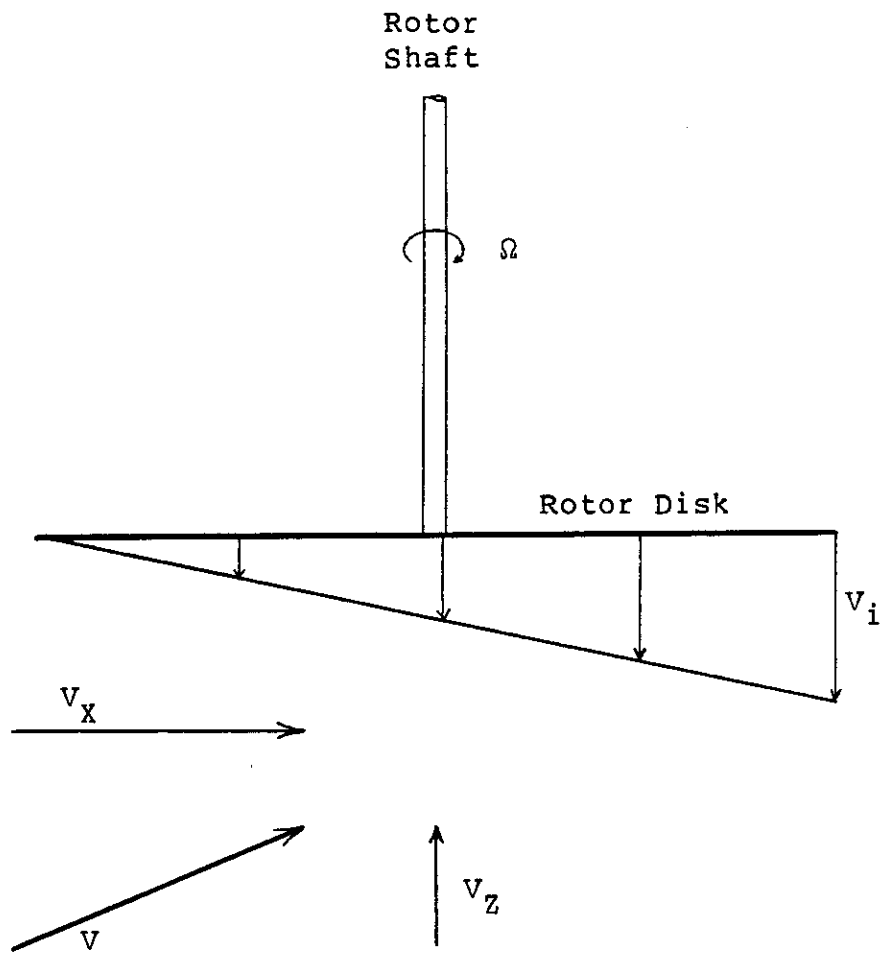


Figure 13. INDUCED FLOW PATTERN FOR YAWED FLOW PROPOSED BY GLAUERT (19)

calculated, based on dynamic rotor operating conditions, but the velocity gradient across the disk is also calculated as a function of yaw angle. The average induced velocity is calculated as a state variable, Y5, and correlates with steady state induced velocities calculated by momentum theory (see equation 14). The flow gradient (and therefore local induced velocities) is calculated based on this average induced velocity, on yaw angle, on blade radial position and on azimuth angle.

This explanation is a simplification of dynamic inflow and the interested reader is referred to (17).

From the analysis of Pitt and Peters (17) one can write the following equations applicable to wind turbine rotors operating in yawed flow.

$$\dot{Y}_5 = f_3 = \dot{v} = \frac{\Omega}{TT} \left[\frac{1}{2} \frac{C_T}{vv} - v \right] \quad (56)$$

$$TT = \left(\frac{1}{vv} \right) \left(\frac{64}{75\pi} \right)$$

$$vv = (\lambda^2 + \mu^2)^{\frac{1}{2}}$$

The local, dimensional induced velocity is then found from

$$V_i = v\Omega r \left[1.33 + \frac{15\pi}{64} \left(\frac{1-\cos\lambda}{1+\cos\lambda} \right)^{\frac{1}{2}} (\cos\Psi) \right] \quad (57)$$

The following notes and assumptions apply to these equations:

1. The effects of pitch moment and roll moment on induced flow are ignored, although these could be easily added from the results of (17) if desired.
2. Although, ideally, v should be calculated based on the average value of C_T over the rotor disk, instantaneous values of C_T are used in the present simulation for convenience. Numerical results thus far, however, show that instantaneous values of C_T do not vary appreciably around the rotor disk. Also, due to the lagging response of the dynamic induced flow equation, the effect of a twice per revolution variation in C_T is further diminished.

2.2.3.5 State Variable Equation for Rotor Speed

As mentioned above, rotor azimuth is not calculated as a state variable, instead incremental azimuth angles are set in the model and the resulting time step calculated based on average rotor speed, Ω , over the time interval. The equation of motion for the rotor is of the form

$$2I\dot{\Omega} - \text{net torque} = 0 \quad (58)$$

The net torque is the aerodynamic driving torque, $MQ(1) + MQ(2)$, minus the generator and gear box shaft torque which is, in general, a function of Ω , and $\dot{\Omega}$. This simulation

ignores the inertial terms for the generator. Thus, one can write for the rotor speed

$$\dot{\gamma}_6 = \dot{\Omega} = f_4 = \frac{1}{2I} \left[MQ(1)+MQ(2) - f_{\text{gen}}(\Omega) \right] \quad (59)$$

The assumptions applicable to equation (59) are:

1. All previous assumptions concerning the derivation of the aerodynamic forces apply, since MQ represents the aerodynamic driving torque.
2. Equal blade moments of inertia.
3. Inertial effects of the generator and gear box are ignored.
4. Gear box efficiencies must be included in the generator function, since shaft torque at the rotor is required.
5. Shaft torque must be expressible in terms of rotor speed, Ω .

2.2.4 Dynamic Yawed Flow Computer Simulation: Example Application

The computer algorithm developed in Section 2.2.3 is used to model a specific two-bladed, wind-turbine rotor with passive cyclic pitch. The actual rotor is used on an experimental wind turbine to investigate the feasibility of a two-bladed, yaw controlled wind energy conversion system. Physical details are presented later in Section 3. The present intent is to illustrate the application of the dynamic yawed flow simulation, previously described, to a

physical system and to compare some of the results with other theoretical results. Correlation with experimental results is reserved for Section 3.

2.2.4.1 Example Model Description

Details of the computer simulation are described here and are listed in full in Appendix 6.4. Equations and relationships are presented where they are necessary to describe the physical system or are required to amplify the equations presented in Section 2.2.3. The model is programmed in BASIC on an Apple II Plus microcomputer.

PROGRAM LOGIC

Dynamic Yawed Flow Model For Experimental, Two-Bladed Wind Turbine

1. Dimension arrays and variables.
2. Enter the following variable inputs.
 - o Date and notes.
 - o Autorotation/Power-on flag (removes generator torque in autorotation).
 - o Azimuth angle increment.
 - o Predictor-corrector error tolerance and maximum number of iterations allowed.
 - o Blade radial increment.
 - o Wind speed.
 - o Optional print-out routines desired.
 - o Initial values of 8 state variables.

3. Read or calculate the following constants.
 - o Solidity ratio.
 - o Aerodynamic pitch angle at .7R.
 - o Pitch correction for difference between aerodynamic and geometric pitch.
 - o Blade mass and moment of inertia.
 - o Nacelle moment of inertia without tail boom. (i.e. This is a fixed boom analysis).
 - o Distance from yaw axis to rotor.
 - o Blade precone angle.
 - o Delta three angle.
 - o Radius of rotor.
 - o Air density.
 - o Blade frequency coefficients.
 $(\omega_n = \omega_o^2 + \Omega^2 \omega_1^2)$
 - o Blade element span, dr.
4. Print-out input file if desired.
5. Initialize program counters.
6. Enter iterative azimuth loop.
7. Check counters for end of complete rotor revolution - update as necessary.
8. Go to aerodynamic forces subroutine and calculate aerodynamic forces on each blade.
9. Print out current dimensional rotor data and non-dimensional rotor data based on state variables, rotor position and aerodynamic forces, if desired.

10. If end of complete revolution, print out current state variables, selected averages and errors based on previous revolution. Change input variables, yaw rate, print out routines, or save data from previous revolution as desired. Finally, save current state variables for comparison with next revolution.
11. Go to the predictor-corrector subroutine and get state variables at new azimuth angle and time step.
12. Update counters.
13. Print out current value of state variables and some nondimensional data, as desired.
14. Update running averages.
15. Save current cyclic pitch position and induced flow, state variables 1 and 5 for optional print out to disk at end of the revolution, or save other variables, as desired.
16. Go to 7 and continue.

SUBROUTINES:

1. Aerodynamic force calculation.
 - 1.1 Reset total blade force and moment variables for each blade to zero (i.e. TB, MB, TQ, and MQ).
 - 1.2. For each blade calculate the following:

- 1.3 Total flap angle and velocity (see equations (54) and (55)).
- 1.4 Reset tip loss counter.
- 1.5 For each blade element calculate the following: (Refer to blade diagram in Figure 14).
- 1.6 Radial position of the center of the element, dr . The model assumes a center cut-out of 27%.
- 1.7 Blade element geometric pitch angle based on radial position, blade twist function, aerodynamic pitch angle set at the 70% station, and the current value of the cyclic pitch due to pitch flap coupling and deflection about the prelag axis. Thus:

$$\text{pitch}|_r = \text{twist}|_r + \text{pitch correction} \quad (60)$$

$$\pm \tau \sin \delta_3$$

((+) for Blade #1, (-) for Blade #2)

- 1.8 Chord width as a function of radial position.
- 1.9 U_T and U_P based on equations (42), (43), (56) and (57).
- 1.10 α , ϕ and U^2 from equations (35), (36) and (37).
- 1.11 Local Reynolds Number.
- 1.12 Save local value of α and V_i for Blade 1 (if not in a predictor-corrector iteration loop).

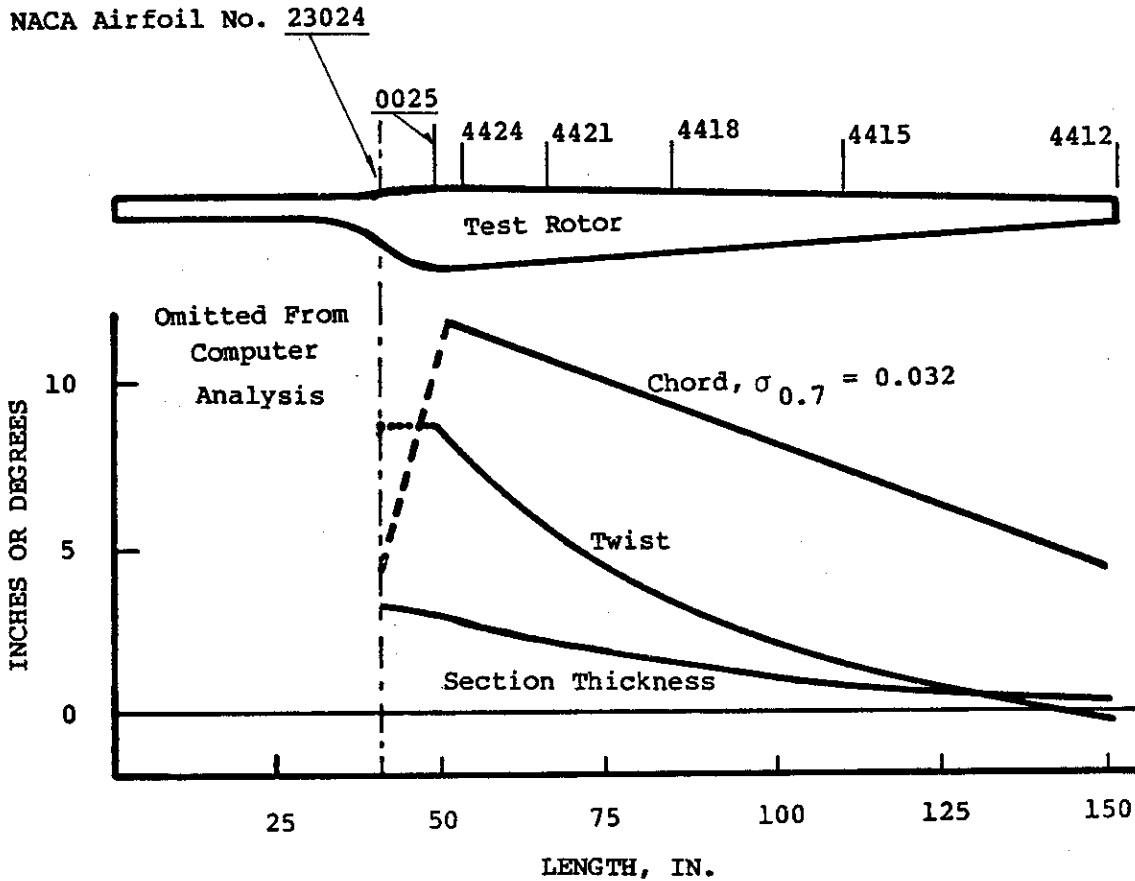


Figure 14. TEST ROTOR BLADE

- 1.13 Go to C_L and C_{d0} subroutine and obtain C_L and C_{d0} .
- 1.14 Make a tip loss correction if on the outboard element. The correction is based on equation (48). For power-on operation the steady state C_T/σ value for the rotor is approximately .1, while for power-off the value is approximately .03. For $\sigma = .032$ one can calculate from equation (48) that the tip loss factor will be

 .96:Power-on
 .98:Autorotation

Note that these are approximations since C_T/σ varies somewhat over the rotor disk in yawed flow and in transient conditions. Since accurate tip loss calculation based on local C_T would be an iterative process, the constant values calculated above are used in the model for the two operating modes to reduce computing time.
- 1.15 Local forces and moments are calculated and summed over the blade as shown in equations (44) to (47), and blade data is printed out if desired.
- 1.16 Go to step 1.5 or 1.2 until all elements and both blades are completed.
- 1.17 Return

2. Lift and Drag Coefficient Calculation.

2.1 Calculate C_L based on radial position and geometric angle of attack, α . From Figure 14 it is evident that the airfoil section is variable along the blade. The blade is divided into three sections outboard of the cut-out section and one lift curve slope and zero crossing is selected for each section. Airfoil data from reference (20) is used with standard roughness and a 3×10^6 Reynolds Number. This is an approximation since in normal operation the airfoils operate at a Reynolds Number of approximately 0.75×10^6 . However, the degrading effect of decreased Reynolds Number operation is offset by the assumption of standard roughness and it is assumed the effects approximately cancel for the real blade. Thus:

$$r < 0.407R; C_L = 0.075\alpha + .2 \quad (a = 4.3) \quad (61a)$$

$$0.407R \leq r < 0.656R; C_L = .0875\alpha + .3 \quad (a = 4.9) \quad (61b)$$

$$r \geq 0.656R; C_L = .1\alpha + .4 \quad (a = 5.7) \quad (61c)$$

(α is geometric angle of attack in degrees)

It is assumed that lift continues as α increases beyond the limits of steady stall in order to approximate dynamic stall conditions that occur in

yawed flow. (See again 2.2.1-d). Therefore, this simulation would not be applicable for a starting analysis, for an axial flow analysis beyond the static stall limits, for operation at reduced RPM with low Reynolds Numbers or near the stall limits, or for yawed flow operation resulting in extreme angles of attack.

The limiting case for the simulation is taken to be α (geometric) = 20° . These restrictions could be removed by including the effects of stall on the lift and drag coefficients. However, since a passive cyclic pitch rotor must be operated away from static stall limits due to inherent instabilities, and since dynamic stall conditions warrant a linear slope beyond static limits, calculation of lift coefficient is based on equations (61) only.

- 2.2 Check for angle of attack between zero and 90° for drag calculation.
- 2.3 Calculate drag coefficient. A single expression for drag coefficient was approximated from data for the respective airfoils at $3 \times 10^6 R_e$ and standard roughness from reference (20).

$$C_{d_o} = .01 + .5 (\alpha_{\text{radians}}^2) \quad (10)$$

(α is geometric)

As in the case of the lift coefficient, static stall effects are ignored.

2.4 Check for $\alpha \geq 20$ degrees. Print out warning if 20 degrees or above. Note this is the geometric angle of attack.

2.5 Return

3. Predictor-Corrector

3.1 Go to derivative subroutine and calculate all derivatives, \dot{Y}_i , at current time based on current state variables.

3.2 Store all current state variables and their derivatives at time, t .

3.3 Calculate Δt based on azimuth step size and Ω at time t .

$$\Delta t = \Delta \Psi / \Omega \quad (62)$$

3.4 Predict new state variable values at time $t + \Delta t$ by

$$Y_{i,t + \Delta t}^{(1)} = Y_{i,t} + \Delta t (\dot{Y}_{i,t}) \text{ (Euler Formula) } (63)$$

and save new $Y_{i,t + \Delta t}^{(1)}$ values.

3.5 Increment Azimuth values, as

$$\Psi = \Psi + \Delta \Psi \quad (64)$$

- 3.6 Set iteration counter to 1.
- 3.7 Go to aerodynamic forces subroutine and calculate new forces at new azimuth angle with new Y_i state variables.
- 3.8 Go to derivatives subroutine and calculate \dot{Y}_i at $t + \Delta t$ ⁽¹⁾ derivatives at new time.
- 3.9 Calculate new time step based on average between Ω at time t and new Ω at time $t + \Delta t$ (Ω is state variable Y_6) by:

$$\Delta t = \frac{2\Delta\psi}{\Omega_t + \Omega_{t+\Delta t}} \quad (1) \quad (65)$$

- 3.10 Correct Y_i at time $t + \Delta t$ by

$$Y_i(t + \Delta t)^{(2)} = Y_i(t) + \frac{\Delta t}{2} (\dot{Y}_i(t) + \dot{Y}_i(t + \Delta t)^{(1)}) \quad (66)$$

- 3.11 Calculate errors and print.

$$\% \text{ Error}_{t + \Delta t} = \frac{Y_i^{(2)} - Y_i^{(1)}}{Y_i^{(2)}} \quad (67)$$

- 3.12 Check for maximum number of iterations. If yes, then 3.15.
- 3.13 Check for errors within tolerance. If yes, then 3.15.

- 3.14 Rename $Y_{i_{t + \Delta t}}^{(2)}$ as $Y_{i_{t + \Delta t}}^{(1)}$. Increment iteration counter and go to 3.7 and repeat.
- 3.15 Exit predictor-corrector.
- 3.16 Calculate final Δt by equation (65), set iteration counter to zero.
- 3.17 Return

The predictor-corrector algorithm outlined above is explained fully in reference (18). Several points are worthy of note here. The error in the solution method is in the order of Δt^3 , an order of improvement over the Euler Method, the error of which is in the order of Δt^2 . (The Euler Method consists of using only the predictor part of the algorithm). Generally one or two applications of the corrector are sufficient and it is generally more efficient to reduce the step size (Δt , or in this case, $\Delta \Psi$) rather than apply more corrections to obtain desired accuracy. For this reason the maximum number of iterations suggested is 3 for the simulation. One final note; application of the corrector only once is also called a second order Runge-Kutta Algorithm, and is often used for the numerical solution of differential equations.

4. State Variable Derivatives

- 4.1 Calculate elements of the mass gyroscopic and stiffness matrices according to equation (3.17).

- 4.2 Calculate the first element of the forcing vector. F_1 in equation (3.17).
- 4.3 For constant yaw rate only, skip to step 4.6.
- 4.4 Calculate the second element of the forcing vector, F_2 in equation (3.17). Note that a yaw moment must be supplied here for variable yaw rate.
- 4.5 Calculate the inverse of the mass matrix. See Appendix 3.
- 4.6 Calculate the state variable derivatives.

$$\begin{aligned}\dot{Y}_1 &= Y_2 & (68) \\ \dot{Y}_2 &= f_1 \text{ (see equation (3.18))} \\ \dot{Y}_3 &= Y_4 \\ \dot{Y}_4 &= f_2 \text{ (see equation (53))} \\ \dot{Y}_5 &= f_3 \text{ (see equation (56))} \\ \dot{Y}_6 &= f_4 \text{ (see equation (59))} \\ \dot{Y}_7 &= Y_8 \\ \dot{Y}_8 &= f_5 \text{ (see equation (3.19))}\end{aligned}$$

For the simulation model under consideration, the generator torque function, $f_{gen}(\Omega)$, was determined by experiment to be $C_Q/\sigma = 0.008$ power-on and $C_Q/\sigma = 0.001$ in autorotation. By definition then

$$f_{gen}(\Omega) = \frac{C_Q}{\sigma} \sigma \rho \pi \Omega^2 R^5 \quad (69)$$

The autorotation flag determines whether the simulation is run power-on or in autorotation and substitutes the proper value of C_Q/σ .

4.7 Return

Although the equations for variable yaw rate are presented here and included in the computer model, simulations conducted to date were carried out only for the case of constant yaw rate. Therefore, the derivative equation

$$(\dot{Y}_8 = \ddot{\chi} = f_5)$$

was set equal to zero and the simplified equation (3.21), derived in Appendix 6.3, was used to calculate \dot{Y}_2 .

$$(\dot{Y}_2 = \ddot{\tau} = f_1)$$

The equations for variable yaw rate are included however, so that if the yaw forcing moment in equation (3.17) is known (for example in the use of an actuator driven yaw control system) a variable yaw rate can be simulated with this computer model.

2.2.4.2 Running the Simulation and Error Analysis

A sample input file is shown on the following page for a simulation to determine cyclic pitch response, discussed later in 2.2.4.3. The file is given to point out the constants used in this and other simulation runs and to

INITIALIZED DATA SET

1/30/81 EXAMINE CYCLIC PITCH FREQUENCY AND DAMPING AT RATED POWER

DELTA 3 (DEG)= 87
PRECONE ANGLE (DEG)= 0
BLADE I (KG M^2)= 40.7
BLADE NTL.FREQ (HZ)= 7.46
BLADE FREQ COEFF.(HZ)= .1765
RADIUS (M)= 3.81
AIR DENSITY (KG/M^3)= 1.23
AERO DYN. PITCH AT .7R (DEG)= -.5
DR (M)= .5588

OP. IN AUTOROT.? N

DELTA AZMTH.(DEG)= 15

BLADE ELEM. = 5

PRED.CORR. ERROR LMT= .05

PRED.CORR. ITER. LMT= 3

BLADE MASS (KG)= 15

NACELLE MOM.OF INERTIA (KG M^2)= 51.6 FOR ZERO YAW ANGLE ONLY

YAW MOM. ARM (M)= .61

SOLIDITY RATIO= .032

WIND SPEED (M/S)= 10

Y1 = .1745

Y2 = 0

Y3 = .01728

Y4 = 0

Y5 = .01803

Y6 = 24.207

Y7 = 0

Y8 = 0

SAMPLE INPUT FILE

discuss step size choice and resulting errors. Constants 1 through 8 and 15 through 18 are taken from data specific to the wind turbine to be simulated. See Table 5. The other items are variable. The blade element span, dr , depends on the number of blade elements selected. For all simulations presented, 5 elements were used; 3 elements having been tried and found to provide insufficient accuracy.

For simulations run to date an azimuth increment of 15 degrees and predictor-corrector iteration limit of 3 resulted in adequate accuracy. Errors in the rapidly changing variables, τ , $\dot{\tau}$, β_e , and $\dot{\beta}_e$, were generally less than 1 or 2 percent while errors in the slowly changing variables, v , Ω , and χ , were near zero. (Note that one method of increasing the program speed would be to provide variable iterations for either rapidly or slowly changing state variables). The error limit, set at 5%, was occasionally met before the 3 iteration limit, thus allowing for less iterations during that step. These constants and step size limitations are used for all simulation runs presented herein.

2.2.4.3 Comparison With Other Theoretical Results

Several operating conditions were simulated using the dynamic computer simulation model as described in 2.2.4.1 and results are compared in Table 1 with results obtained from the simplified theory for identical operating conditions.

TABLE 1

Comparison of Dynamic Simulation with Simplified Theory for Two-bladed Experimental Turbine Parameters.

Power Off (Autorotation)			
<u>Yaw Angle (degree)</u>	<u>Performance Variable</u>	<u>Simple Theory</u>	<u>Dynamic Simulation</u>
15	v	0.0639	0.0623
	v	0.01847	0.01743
	C_Q/σ	0.00106	0.00106
	C_T/σ	0.05345	0.04979
	C_P	0.26	0.2806
60	v	0.10204	0.1009
	v	0.00851	0.00781
	C_Q/σ	9.68×10^{-4}	9.68×10^{-4}
	C_T/σ	0.0522	0.04747
	C_P	0.0583	0.0603
80	v	0.26473	0.27126
	v	0.003143	0.00246
	C_Q/σ	9.723×10^{-4}	9.723×10^{-4}
	C_T/σ	0.0519	0.04166
	C_P	0.0034	0.0031
85	v	0.524	
	v	0.00156	
	C_Q/σ	0.001	--
	C_T/σ	0.051	
	C_P	0.0004	

Power-On

<u>Yaw Angle (degree)</u>	<u>Performance Variable</u>	<u>Simple Theory</u>	<u>Dynamic Simulation</u>
15	v	0.108305	0.1113
	v	0.020162	0.017128
	C_Q/σ	0.00798382	0.00798397
	C_T/σ	0.11213	0.10158
	C_P	0.4022	0.3706
<hr/>			
30	v	0.1176	0.1218
	v	0.01742	0.01479
	C_Q/σ	0.00797	0.00797
	C_T/σ	0.112	0.1009
	C_P	0.3136	0.2823
<hr/>			
60	v	0.1865	0.1996
	v	0.009734	0.00786
	C_Q/σ	0.00798	0.00798
	C_T/σ	0.1119	0.09615
	C_P	0.0787	0.0642

In determining the values for Table 1, one should note that, although average C_Q/σ for power-on and power-off operation is set to 0.008 and 0.001, respectively, for the calculation of torque, C_Q/σ varies, as do the other variables, around the rotor disk due to yawed flow conditions. The values in Table 1 for the dynamic simulation represent the average value around the disk, and thus due to rounding errors and finite step size the steady state averages do not exactly agree with the prescribed torque function. This average value of C_Q/σ is used to calculate the variables v , v and C_T/σ for the simple theory for comparison in the table. The data for the simple theory is represented graphically in Figure 9.

Examination of Table 1 shows the correlation between the simplified theory and the dynamic simulation operating in steady state yawed flow conditions to be quite good, with the following exceptions:

- (a) Reliable data from the dynamic simulation at 85° yaw angle is not possible due to stall conditions on the retreating blade.
- (b) In autorotation the simple theory predicts a slightly higher C_T/σ and slightly lower C_p than the dynamic simulation. With power-on, the simple theory again predicts higher C_T/σ values, than does the dynamic simulation; and it also over predicts C_p . This is probably due to the effects

of tip losses which are included in the dynamic theory and more pronounced at higher C_Q/σ .

- (c) The simple theory predicts higher induced flow values in all cases.

The good correlation between the two theoretical approaches is rather surprising, especially when one considers the diversity of the two methods. Due to the compatibility of results from the two methods, the simplified theory can provide a short-cut approach to obtaining average conditions for dynamic operation. Thus, these averages are valuable as starting conditions for the dynamic simulation, which decreases the computer time required to reach steady state values for a desired simulation. The use of a chart such as Figure 9 can be used to obtain these starting conditions. One could alternatively devise a combined program in which steady-state values are first calculated using the simplified theory and these values are used as initial values for the dynamic simulation model.

A second theoretical correlation with the dynamic simulation model can be obtained from the transient cyclic pitch response. There are approximate formulas for the frequency and damping for the cyclic pitch and these can be compared with results of the dynamic simulation model.

Using a basic rotor equation of motion, it can be shown, (21), that the frequency and damping ratio of the cyclic pitch angle, τ , can be approximated by the formula:

$$\omega_n^2 = 1 + \frac{\gamma}{8} \tan \delta_3 \quad (70a)$$

and

$$\zeta = \frac{\gamma}{16} \quad (70b)$$

Thus:

$$\omega_d = \left(1 + \frac{\gamma}{8} \tan \delta_3 - \left(\frac{\gamma}{16}\right)^2\right)^{\frac{1}{2}} \quad (71)$$

The frequencies are measured in cycles per revolution. Since the lift curve slope for the blades varies with radial position (see again equation (61)), an average lift curve slope for use in γ can be calculated by:

$$a_{avg} = \frac{\sum r_i^3 a_i}{\sum r_i^3} \quad (72)$$

Where r_i is the radial station and a_i the corresponding lift slope. For the dynamic simulation, the blade Lock number can then be calculated as:

$$\gamma_{avg} = 5.7$$

with

$$a = 5.5, B = 0.96, \text{ and } c_{.7} = 0.1915 \text{ m}$$

Substituting into equations (70) and (71) gives:

$$\omega_n = 1.64$$

$$\zeta = .218$$

$$\omega_d = \omega_n (1 - \zeta^2)^{\frac{1}{2}} = 1.6$$

(cyc. per rev.)

The dynamic simulation was initialized from equilibrium conditions at rated power and zero yaw angle ($v = 0.108$), but with the cyclic pitch, τ , deflected to $+ 10^\circ$. (Equilibrium value is 0° since there is no yawed flow). The initial conditions and response are shown in Figure 15. Response frequency is easily determined directly from the figure, while the damping ratio is calculated using the log decrement method. The results are:

$$\omega_d = 1.532 \text{ cycles per rev.}$$

and

$$\zeta = 0.1882$$

Thus, the simulation predicts a cyclic pitch response close to that obtained from simple, uncoupled rotor equation of motion (70). Some of the neglected coupling effects in equation (70) are dynamic inflow, elastic coning and periodic coefficients, which are included in the dynamic simulation, and which may account for the difference in the results.

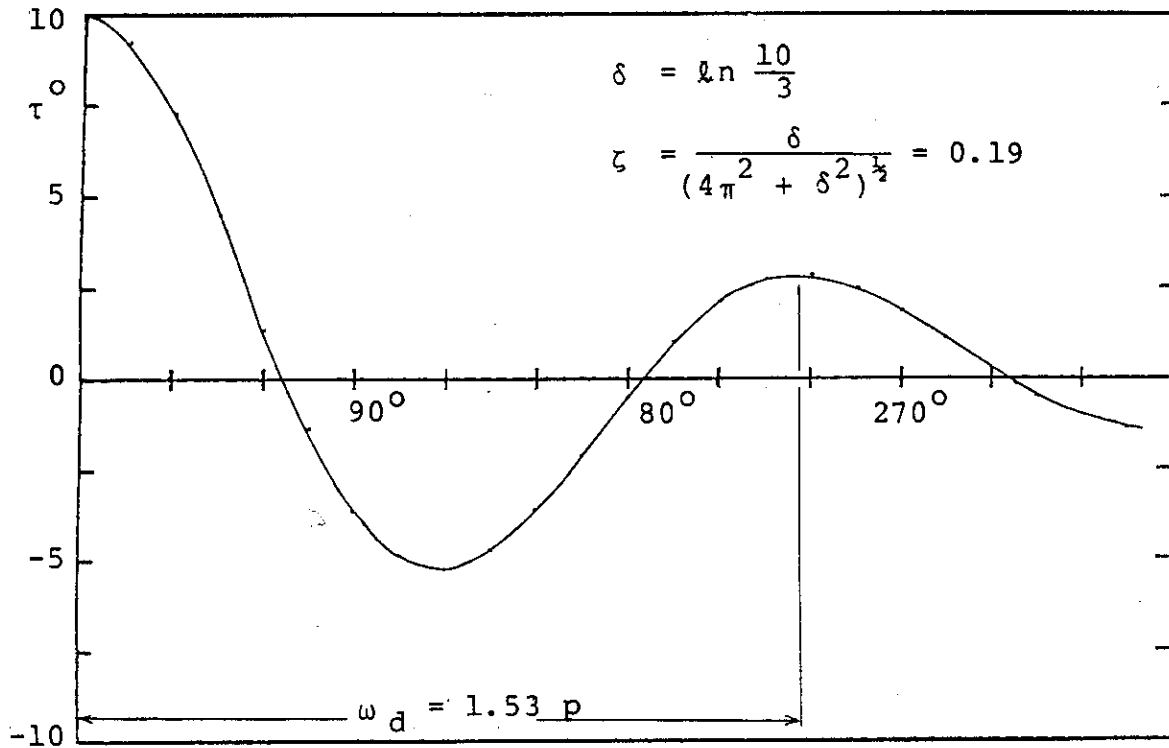


Figure 15. τ RESPONSE TO $+10^\circ$ DEFLECTION

A third theoretical correlation for the dynamic simulation model is obtained by comparisons with results from the Wilson-Lissman program for axial flow (3). The Wilson-Lissaman program was run on the DEC-20 computer system at the Washington University Center for Computational Mechanics in order to analyze the experimental test rotor with blade element sections. Lift and drag coefficients were calculated using a table look-up with stall effects included (22). Resultant performance coefficient (for -0.5 degree blade pitch angle, and a tip speed ratio, $\Omega R/v$, of 9.6) is 0.37 which compares well with the dynamic simulation, which gives $C_p = 0.40$ at a tip speed ratio of 9.22 for identical operating conditions. One would expect the simulation to predict a slightly higher performance value since drag effects are underestimated at the inboard sections for which the airfoils are thicker and have higher drag coefficients. The Wilson-Lissaman program included these effects. Also, neither program includes hub and shank losses, and therefore both probably over-predict actual C_p values.

3. EXPERIMENTAL TESTING

In order to further examine the effects of yawed flow on wind turbine rotors, two sets of experimental data are presented from recent tests at Washington University. The first set consists of results from a small model rotor operated in the Washington University wind tunnel. The second set consists of results from a 7.6 meter (25 foot) diameter, two-bladed experimental wind turbine with passive cyclic pitch operated at the Washington University Tyson Research Center. Both the model and full scale wind turbine were designed and constructed under contract to the Solar Energy Research Institute by Washington University Technology Associates, under the direction of Dr. K. Hohenemser, in order to examine the feasibility of yaw controlled wind turbines with passive cyclic pitch. (2) The author has acted as Research Assistant on both projects. Much of the test equipment descriptions and test data presented herein are summarized from project reports and publications. The interested reader is referred to (22), (23) and (24) for further details.

3.1 Wind Tunnel Testing

3.1.1 Wind Tunnel Model Description

The model rotor and blade design are shown in Figures 16 and 17 with appropriate dimensions. The hub design consists of a cyclic pitch hinge with large delta δ angle that provides a flat tracking rotor in yawed flow operation.

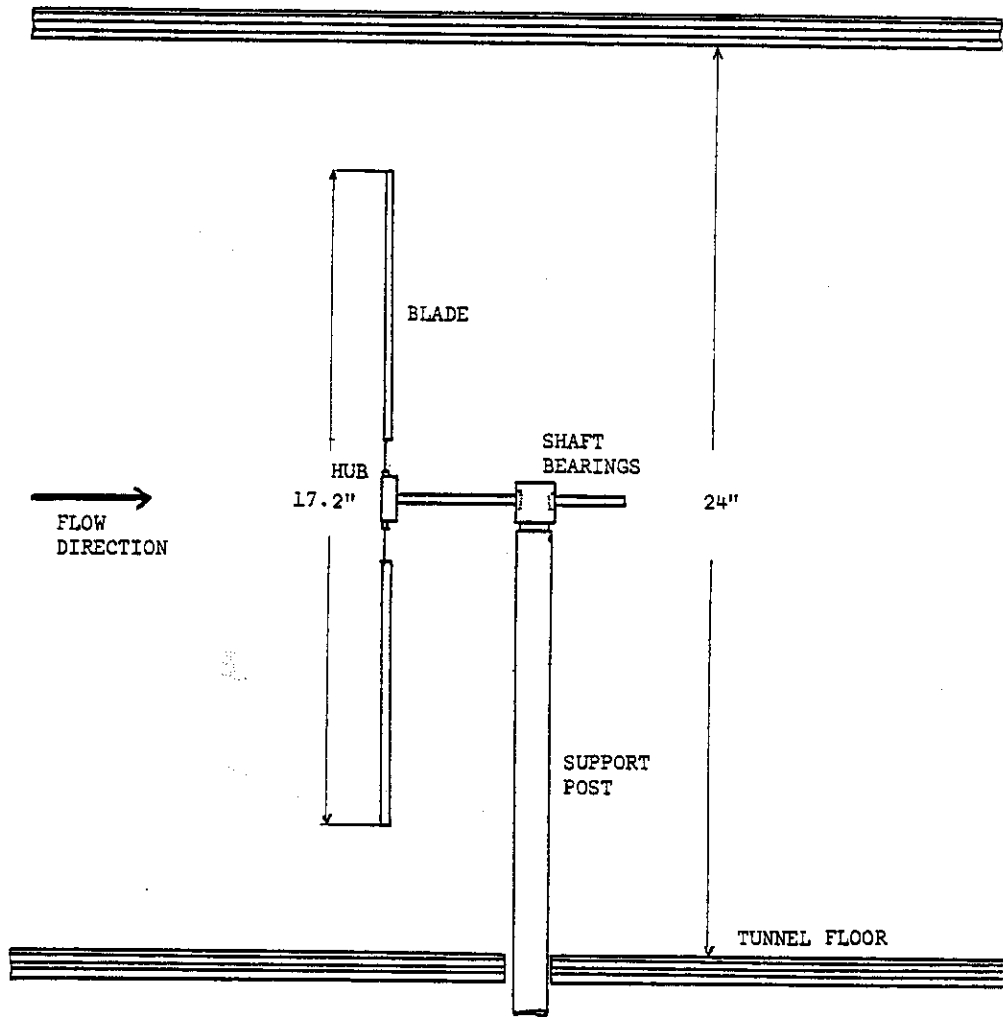


Figure 16. MODEL ROTOR IN WIND TUNNEL

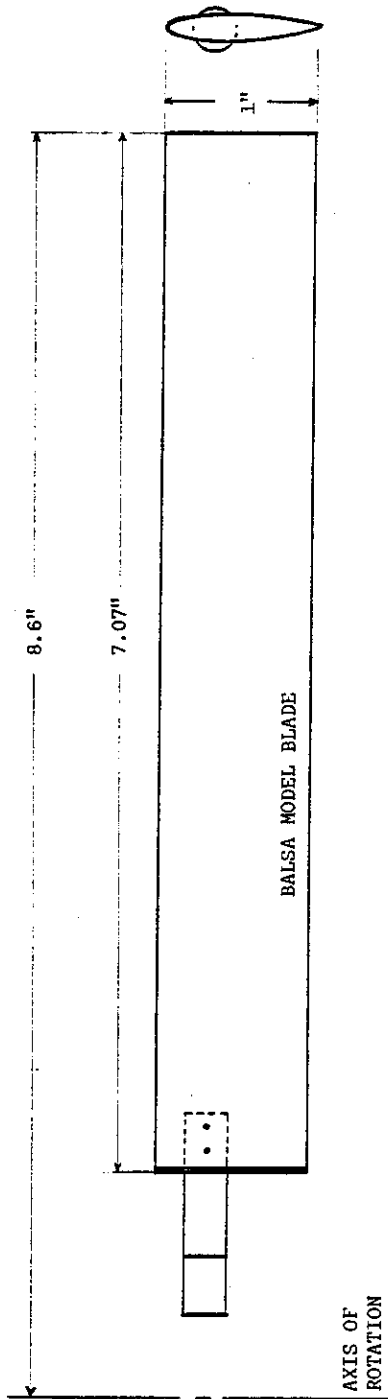


Figure 17. MODEL ROTOR BLADE

The hub design shown in Figure 18. The model is designed to operate in two modes: (i) a freely yawing, vane-stabilized mode, (see Figure 19a and b), and (ii) a fixed yaw mode, Figure 19c. The latter mode was included so the yaw angle could be varied and controlled during tunnel operation. Figures 20 and 21 show photographs of the model in each operating mode. Rotor solidity is 0.075 and blade Lock number is 6.4.

3.1.2 Test Procedures and Results

The model rotor was operated in both modes, but for autorotation only. The operation was in a wind tunnel test section of 0.61 X 0.61 meters (24 X 24 inches) at wind speeds from zero to 9.91 m/s (22 MPH). Yaw angles were measured with a yaw angle gauge mounted on the tunnel floor, and rotor RPM was measured with a strobe light. Autorotational tip speed ratios were calculated for each mode as functions of yaw angle. The data are presented in Tables 2, 3 and 4. Table 2 contains the data from fixed yaw tests with tunnel speeds near 8 m/s (27 ft/s, 18 mph), while Table 3 contains data from free yaw tests with a tunnel speed of 5.7 m/s (19 ft/s, 12.86 mph). Table 4 contains data from a fixed yaw test at 1800 RPM. All data are for zero degrees blade pitch angle.

From the tables, it is evident that the tip speed ratio for a given yaw angle varies widely with rotor speed. It is presumed that this is caused by a substantial effect of

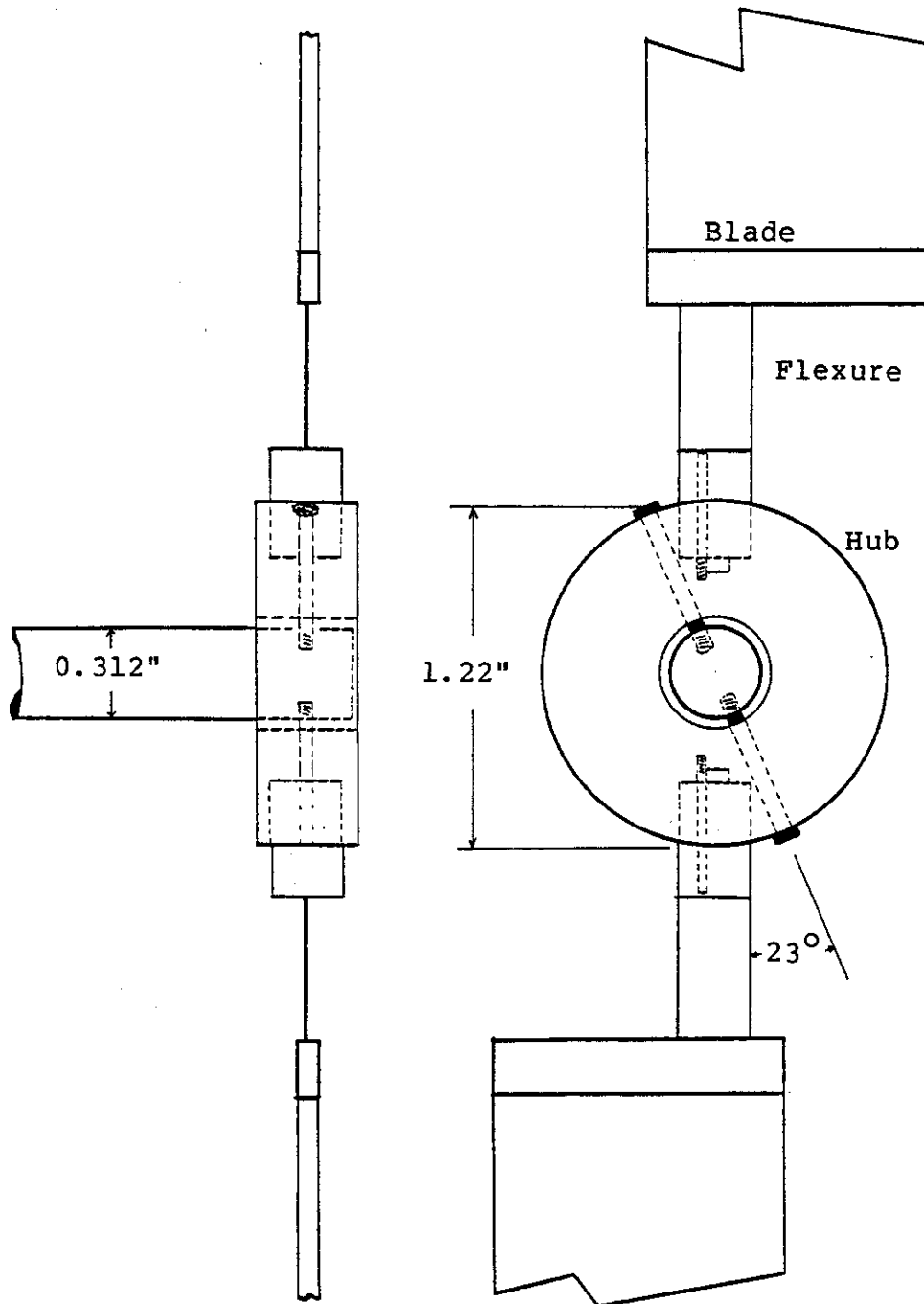


Figure 18. HUB AND CYCLIC PITCH HINGE FOR WIND TUNNEL MODEL ROTOR

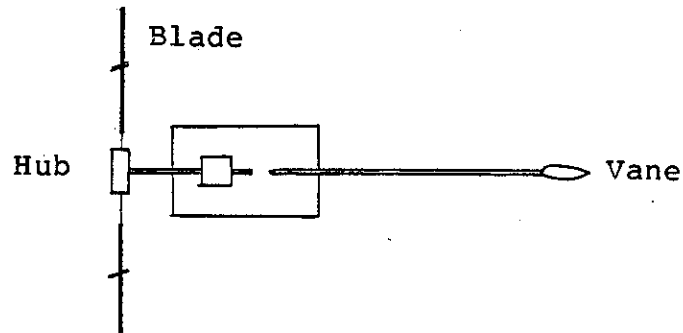


Figure 19a. FREE YAW MODE, TOP VIEW

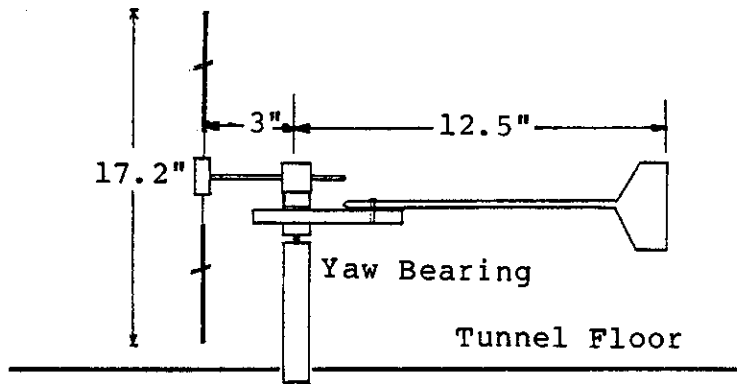


Figure 19b. FREE YAW MODE, SIDE VIEW

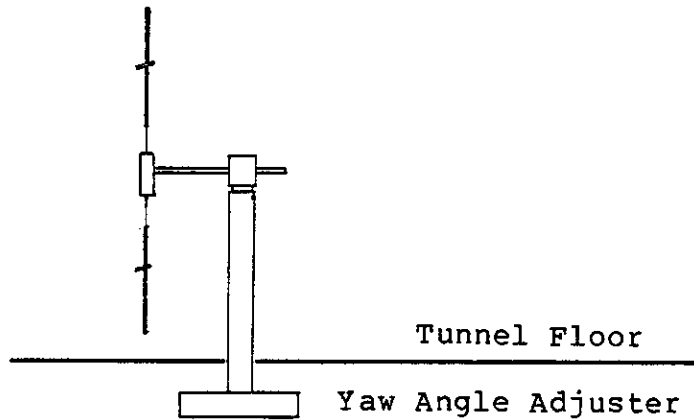


Figure 19c. FIXED YAW MODE, SIDE VIEW

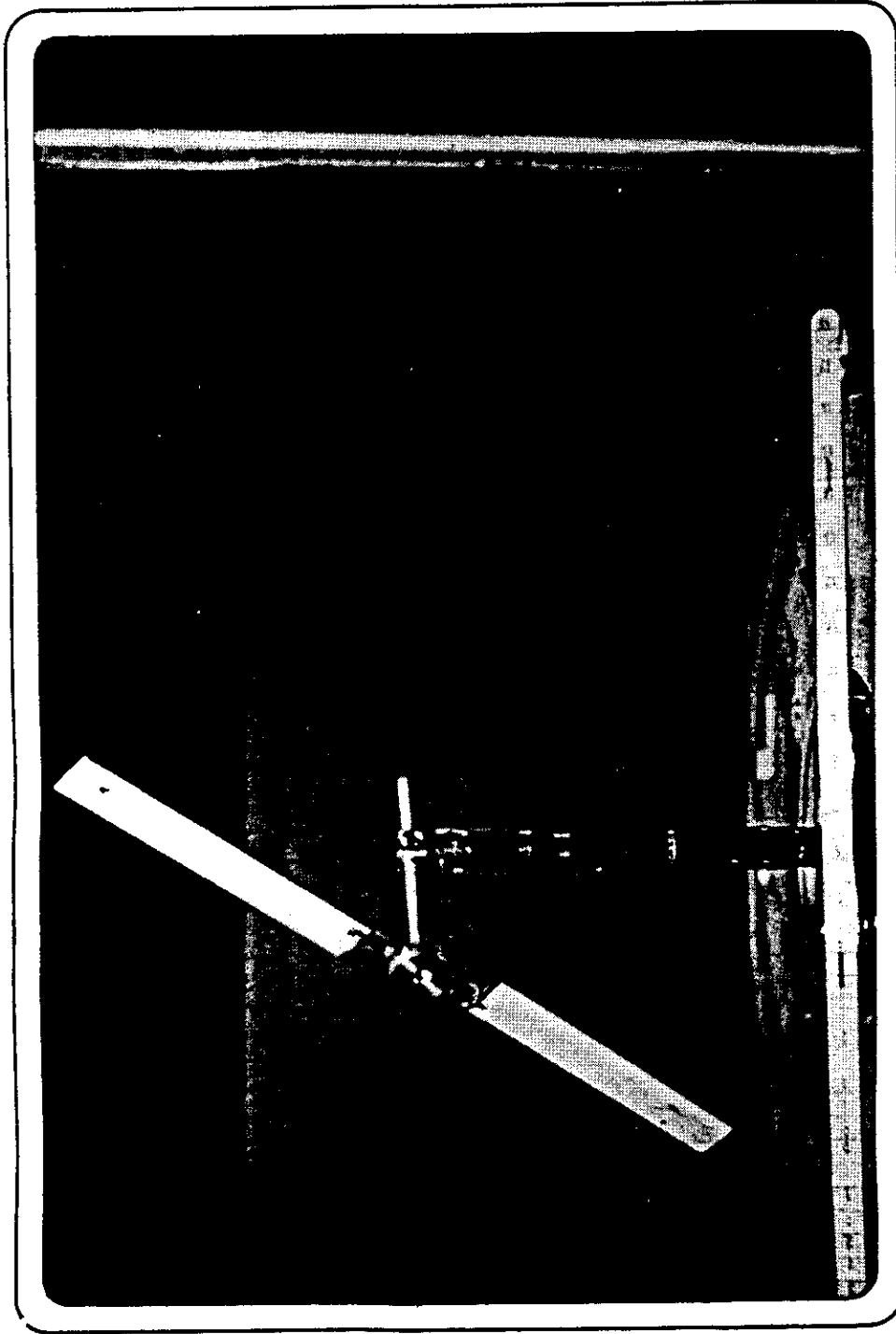


Figure 20. PHOTOGRAPH OF WIND TUNNEL MODEL, FIXED YAW MODE

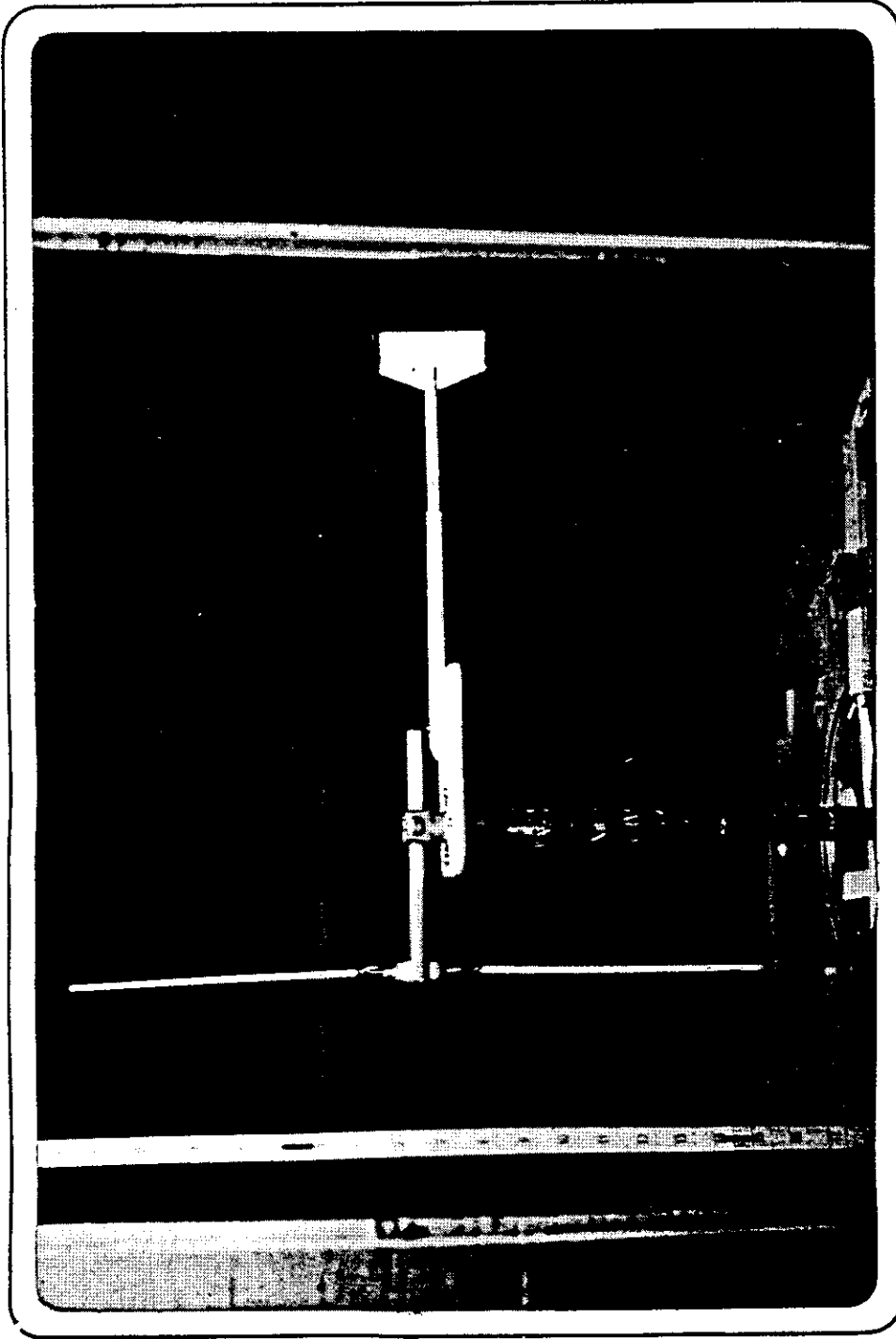


Figure 21. PHOTOGRAPH OF WIND TUNNEL MODEL, FREE YAW MODE

TABLE 2

Wind Tunnel Data

Fixed Yaw Angle

0 Degrees Blade Pitch

R = .216 m (8.6 inches)

<u>Yaw Angle</u> <u>Degrees</u>	<u>Tunnel Speed</u> <u>m/s</u>	<u>Speed</u> <u>(ft/s)</u>	<u>Rotational Speed</u> <u>RPM</u>	<u>Speed</u> <u>(rad/s)</u>	<u>V</u> <u>ΩR</u>	<u>ΩR</u> <u>V</u>
0	7.75	(25.4)	1525	(159.7)	0.225	4.44
0	8.00	(26.25)	1600	(167.6)	0.221	4.52
0	8.59	(28.17)	1770	(185.4)	0.214	4.67
0	9.40	(30.83)	2400	(251.3)	0.173	5.78
15	7.87	(25.83)	1510	(158.1)	0.231	4.33
30	8.13	(26.67)	1340	(140.3)	0.268	3.73
40	9.91	(32.50)	1770	(185.4)	0.247	4.05
45	8.33	(27.33)	1100	(115.2)	0.335	2.99
60	8.51	(27.92)	535	(56.0)	0.704	1.42
70	8.64	(28.33)	350	(36.7)	1.09	0.92

TABLE 3

Wind Tunnel Data

Free Yawing Configuration

0 Degrees Blade Pitch

R = .216 m (8.6 inches)

<u>Yaw Angle</u> <u>Degrees</u>	<u>Tunnel Speed</u>		<u>Rotational Speed</u>		<u>$\frac{V}{\Omega R}$</u>	<u>$\frac{\Omega R}{V}$</u>
	<u>m/s</u>	<u>(ft/s)</u>	<u>RPM</u>	<u>(rad/s)</u>		
0	5.72	(18.75)	920	(96.3)	(0.275)	3.64
5	5.72	(18.75)	940	(98.4)	(0.269)	3.72
10	5.72	(18.75)	950	(99.5)	(0.266)	3.76
15	5.72	(18.75)	880	(92.2)	(0.287)	3.48
30	5.72	(18.75)	760	(79.6)	(0.332)	3.01

TABLE 4

Wind Tunnel Data

Constant RPM Test - 1800 RPM

0 Degrees Blade Pitch

R = .216 m (8.6 inches)

<u>Yaw Angle</u> <u>Degrees</u>	<u>Tunnel Speed</u>		<u>Rotational Speed</u>		<u>$\frac{V}{\Omega R}$</u>	<u>$\frac{\Omega R}{V}$</u>
	<u>m/s</u>	<u>(ft/s)</u>	<u>RPM</u>	<u>(rad/s)</u>		
0	8.53	(28.00)	1800	(189.0)	0.210	4.76
10	8.46	(27.75)	1800	(189.0)	0.208	4.81
20	8.79	(28.83)	1800	(189.0)	0.216	4.63
30	8.89	(29.17)	1800	(189.0)	0.218	4.59
40	9.75	(32.00)	1800	(189.0)	0.240	4.17
50	10.97	(36.00)	1800	(189.0)	0.270	3.7

Reynolds number on the airfoil drag (25). Figure 22 illustrates the effect of Reynolds number on airfoil performance for an airfoil similar to that used on the model. At lower Reynolds number, appreciably higher wind speed is required to autorotate the rotor at a given RPM. Figure 23 shows, for zero yaw angle, the measured dependence of tip speed ratio, v , on rotor speed. The Reynolds number, taken with the rotational speed at the 70 percent radius station is also shown. Re is 50,000 at 1800 RPM for the model rotor. This curve was used in order to correct v for RPM values other than 1800 to that expected at 1800 RPM (or 50,000 Reynolds number) in order to obtain consistent results of the tests. With this correction, all test results can be approximated by a single curve of tip speed ratio vs. yaw angle. The results are indicated by the solid line in Figure 24. Note that the tip speed ratio actually decreases through the first 15 degrees of yaw below the zero yaw value, which indicates a slight increase in the power available for the model between 0 and 15 degrees yaw angle. This experimental result confirms the existence of operating conditions at which the maximum power occurs at yaw angles greater than zero, as predicted by the simplified theory. Also plotted in Figure 24 are the results of the simplified theory from Figure 5a for autorotation, $\sigma = 0.075$ and $\theta = 0$. A drag multiplier of 3 is assumed in order to account for poor airfoil quality and for the low Reynolds number effect

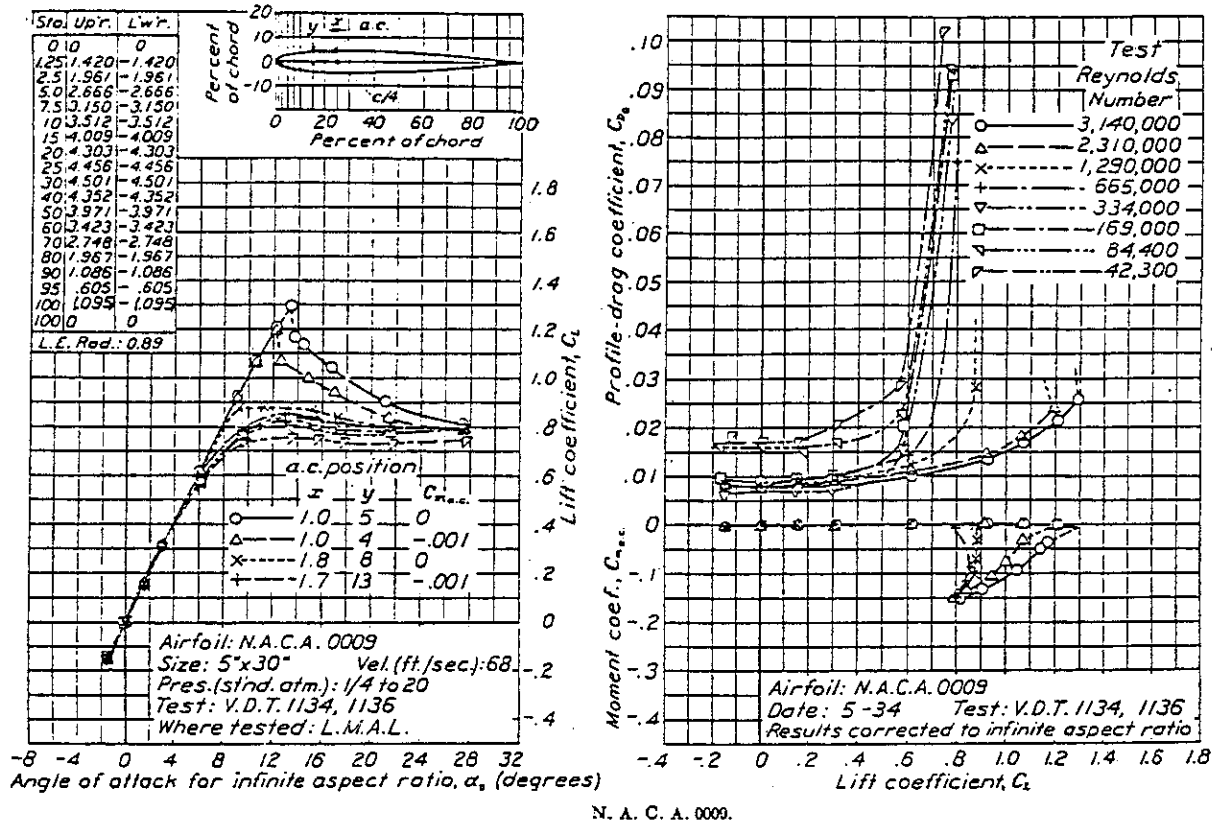


Figure 22. EFFECT OF REYNOLDS NUMBER ON AIRFOIL PERFORMANCE (25)

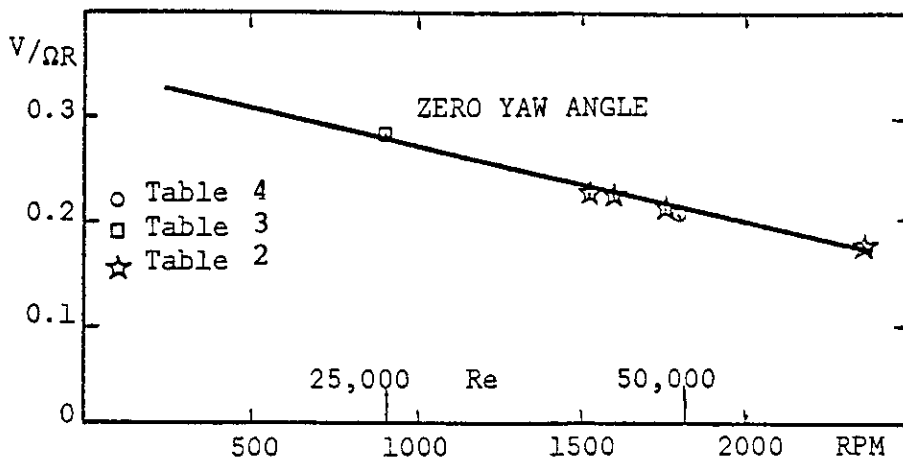


Figure 23. EFFECT OF ROTOR SPEED OR REYNOLDS NUMBER ON TIP SPEED RATIO

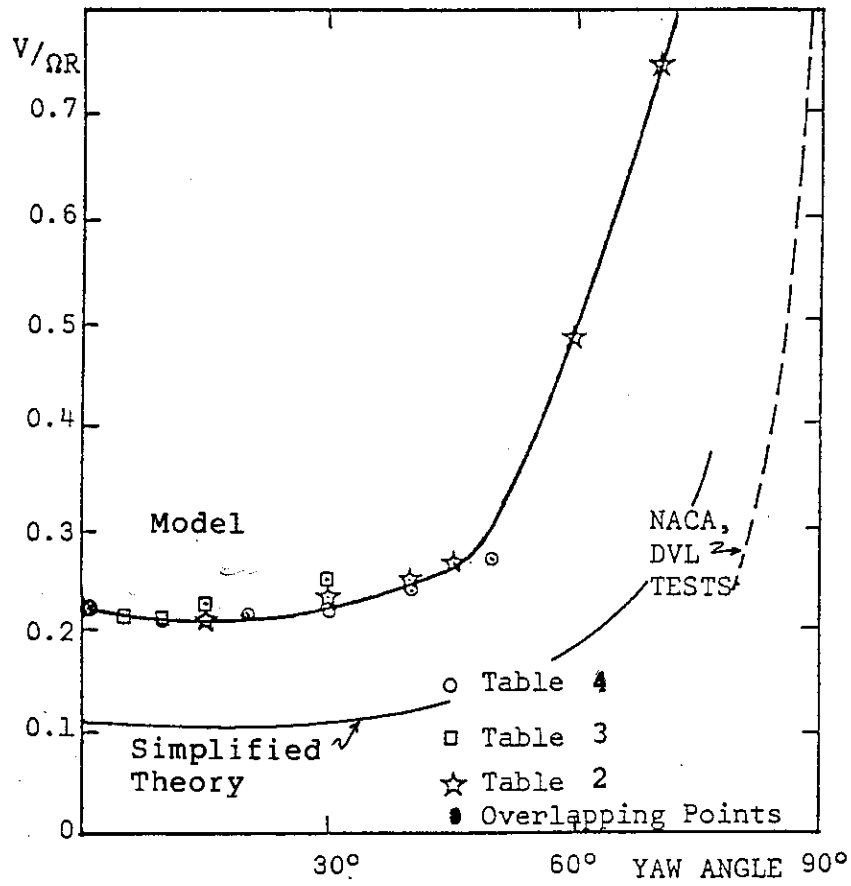


Figure 24. SPEED RATIO $V/\Omega R$ VS. YAW ANGLE FOR VARIOUS WIND TUNNEL TESTS (10), (11) AND FOR SIMPLIFIED THEORY

as shown in the drag curve of Figure 22. From the figure it is evident that although the quantitative correlation is quite poor, the shape of the curves and the prediction of a power maximum near 15° yaw angle correlates well. One should not expect a numerical correlation here, due to the nature of the wind tunnel model and wind tunnel effects. For example, the model airfoil data is unknown, blade pitch angles were set by eye, wind tunnel wall effects were present, and the model was operated at low Reynolds numbers. These factors all affect the quantitative results. Therefore, the fact that the theory predicts the qualitative trends of the model operation is considered a positive result.

3.1.3 Qualitative Comparison With Other Wind Tunnel Test Results

In order to better substantiate the performance trends predicted by the simplified theory, theoretical results are compared with other wind tunnel test data. The first was a 1935 NACA test (10) of a 3.05 meter (10 ft.) diameter rotor which had 4 individually hinged blades with a total solidity ratio of 0.133. The pitch angle varied within wide limits. The dashed curve in Figure 24 refers to a -3° pitch setting. (Negative angles indicate away from feather.) The blades are untwisted with a 4418 airfoil. The RPM was constant at 550, representing (at the 70 percent station) a Reynolds number of 620,000. One will note from the dashed curve,

that the Washington University model autorotated at a higher value of v for a given yaw angle, than does the NACA model. Again, this must be explained by the low Reynolds number effect and is consistent with the trend seen in Figure 23. One will also note that the simplified theory predicts a similar trend at high yaw angles, although the solidity ratio and drag coefficients differ.

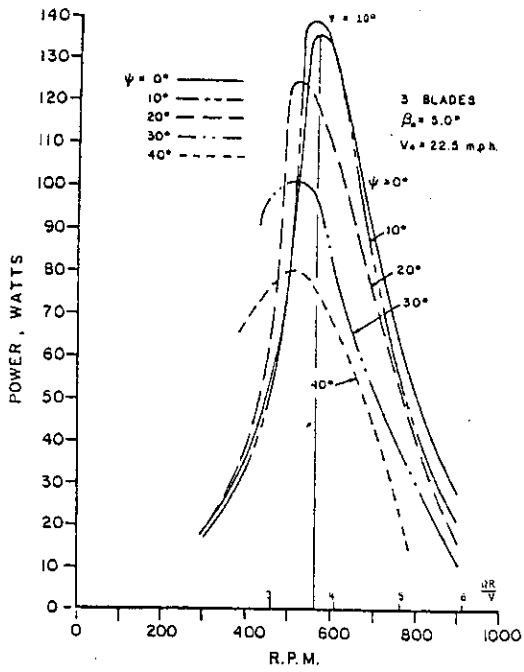
The second data source for comparison is a German DVL test of 1939 (11). These tests were conducted with a 4 bladed, individually hinged, synchropter model of 0.06 total solidity ratio, also with a wide variation of pitch settings. The RPM was constant at 430, which represents a Reynolds number of 260,000 at the 70 percent station. A -3° pitch setting (3° away from feather) was selected for the chart. Despite the difference in solidity and Reynolds number, the dashed curve of Figure 24 represents these data as well as the NACA data. The DVL tests were performed not only for autorotation (as were the NACA tests), but also for driving and driven conditions (i.e. helicopter and windmill). Therefore, based on these two tests it appears the the simplified theory correctly predicts that operating tip speed ratios, v , are extremely sensitive to variations in yaw angle when operating at higher yaw angles.

The third test results used for comparison are recent wind tunnel tests conducted at the University of Massachusetts, Amherst, in June 1978 (9). The rotor from a 200

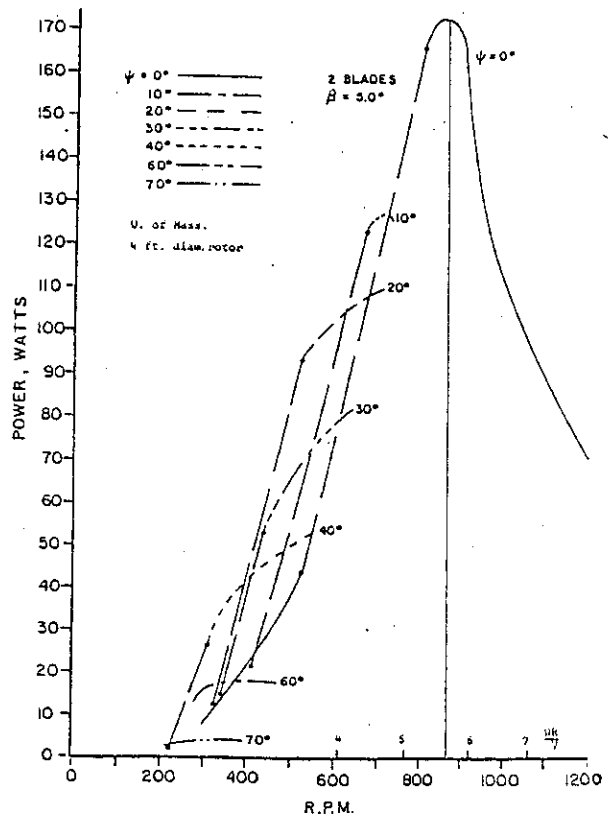
watt, Windcharger wind turbine was modified to accept either two or three blades, and was tested at a variety of yaw angles and blade pitch angles. Rotor solidities were $\sigma = 0.115$ and $\sigma = 0.174$ for the two- and three-bladed rotors, respectively. The speed of the open-jet tunnel was 10 m/s (22.5 MPH). Figures 25a and b show the test results for the three and two bladed rotors at a pitch angle of 5 degrees. (As before pitch angles are measured positive toward feather.) Operating inverse tip speed ratios, $1/v$, have been added to the bottom of the figures. Reynolds numbers, calculated at the 70 percent radius station, were near 230,000 in the maximum power range. The point of maximum power extraction occurs at a yaw angle of 10 degrees for the 3-bladed rotor operating at a $1/v$ ratio of 3.7 and at zero degrees yaw angle for the two-bladed rotor. According to the derivation presented in Section 2.1.2 based on the simplified theory, the existence of a power maximum at yaw angles greater than zero depends on the variable A. (See equation (18)). From equation (18), one would expect the effect to be evident for large values of solidity ratio, σ , and small tip speed ratios, $1/v$, as is indeed the case in Figure 25.

In summary, although the quantitative comparison between wind tunnel test results and the results of the simplified theory does not correlate well (for reasons

POWER vs. R.P.M. FOR VARIOUS YAW ANGLES, ψ



(A)



(B)

Figure 25. WIND TUNNEL TESTS FOR WINDCHARGER 200 (9)

previously discussed), the trend identification and qualitative correlation between the theoretical results and wind tunnel test data is quite good. The theory correctly predicts the existence of a power maximum occurring at yaw angles other than zero, it identifies the significant rotor parameters necessary in determining the yaw angle for maximum power extraction, and it illustrates the sensitivity of rotor performance to rotor angle of attack at high yaw angles.

3.2 Full Scale, Atmospheric Testing

3.2.1 Experimental Wind Turbine Description

The atmospheric test equipment consists of a modified Astral Wilcon 10B wind turbine mounted on a tiltable, 18.3 meter (60 ft.) Unarco-Rohn steel tower. The Astral Wilcon 10B wind turbine is a tail vane stabilized, upwind turbine with a self-excited alternator. The original 7.6 meter (25 ft.) diameter, three-bladed rotor is replaced with a two-bladed rotor with passive cyclic pitch using two of the original Astral Wilcon fiberglass blades. A new hub and blade retention structure has been constructed which incorporates a cyclic pitch hinge mounted at a delta 3 angle of 67 degrees, with a ± 13 degree limit to limit deflection allowable. Data for the turbine are presented in tabular form in Table 5 and further details are available in (22), (23) and (24). Photographs of the machine are presented in Figure 26.

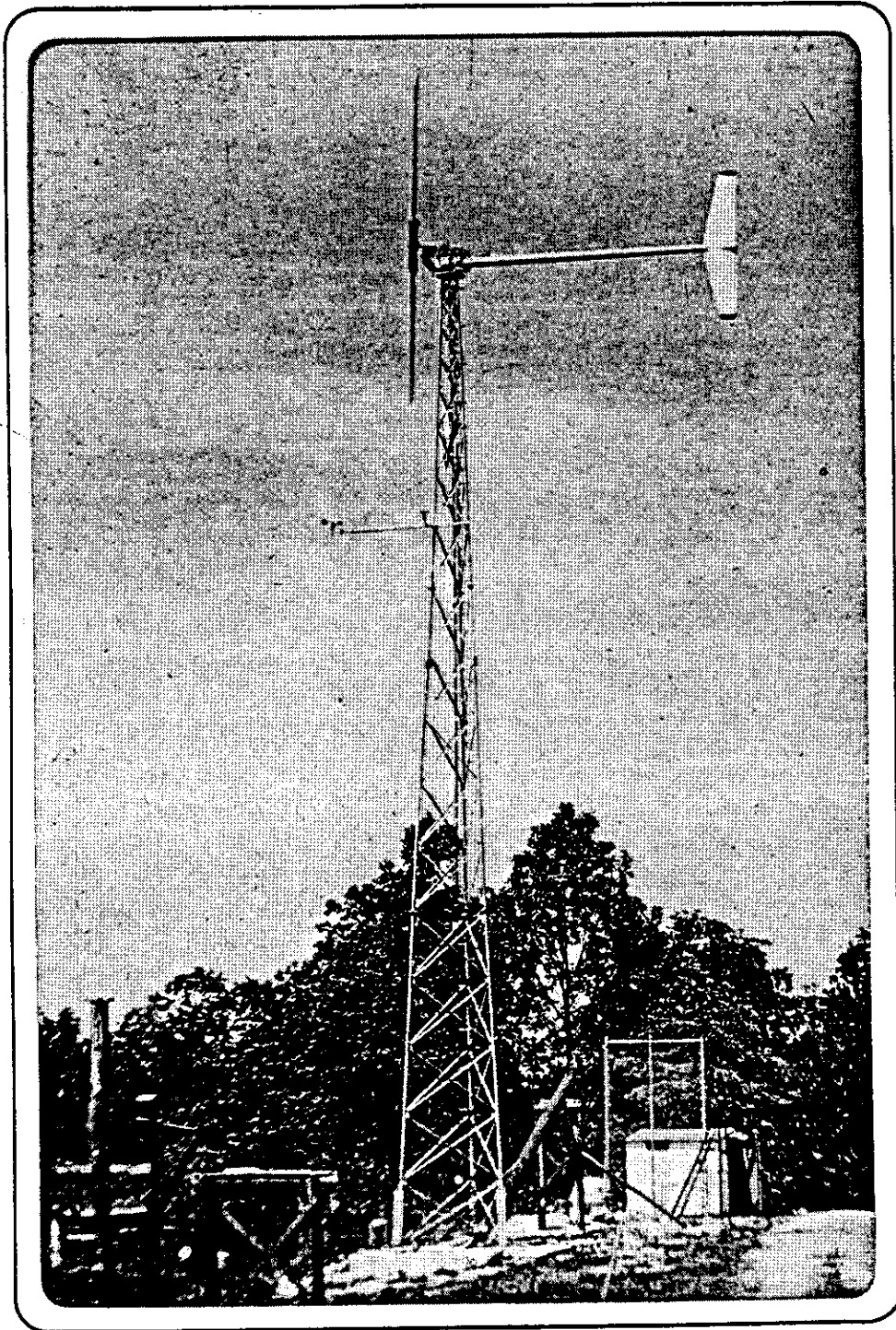


Figure 26a. PHOTOGRAPH OF EXPERIMENTAL WIND TURBINE AT TEST SITE SHOWING TOWER AND INSTRUMENT SHED

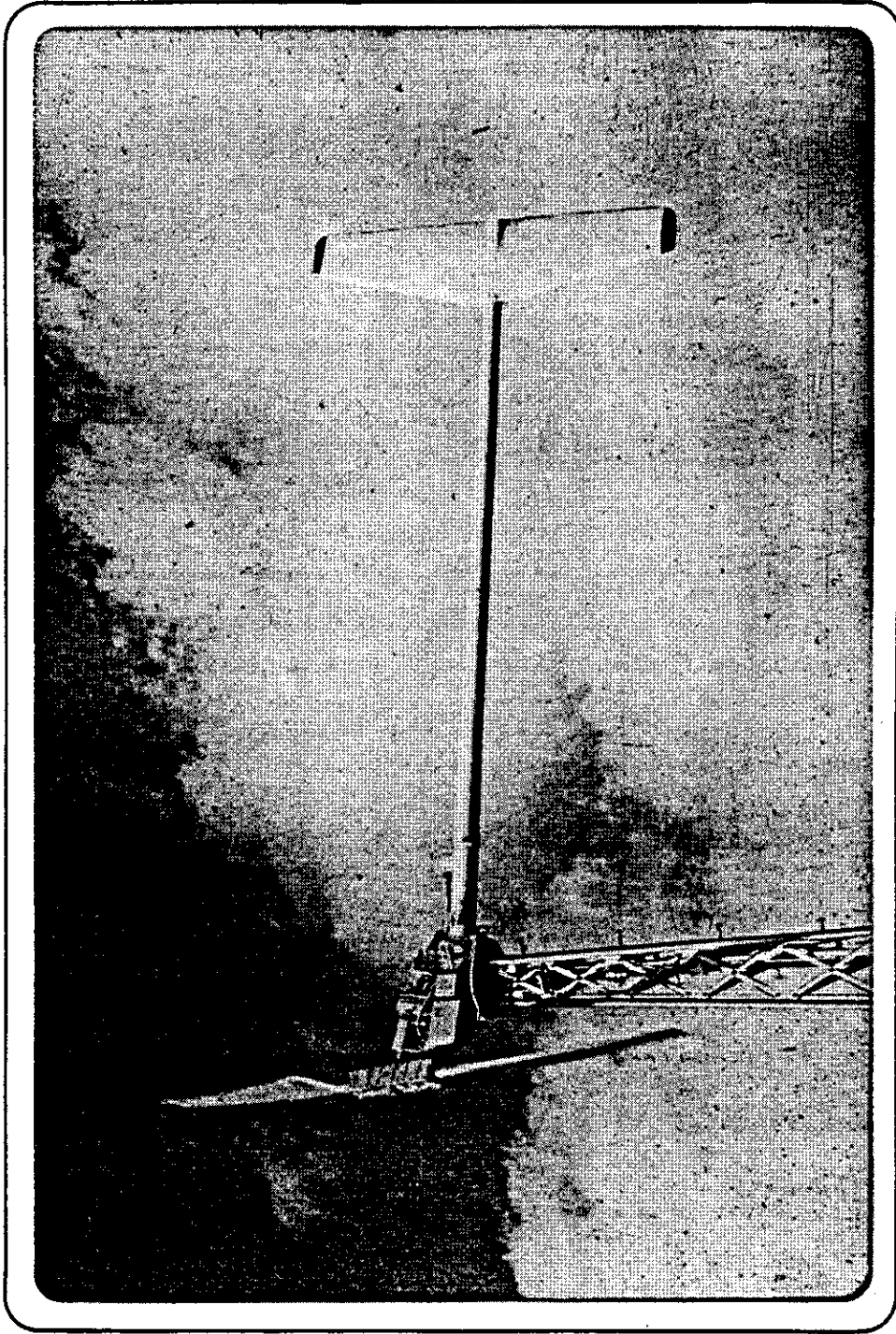


Figure 26b. PHOTOGRAPH OF WIND TURBINE, SIDE VIEW

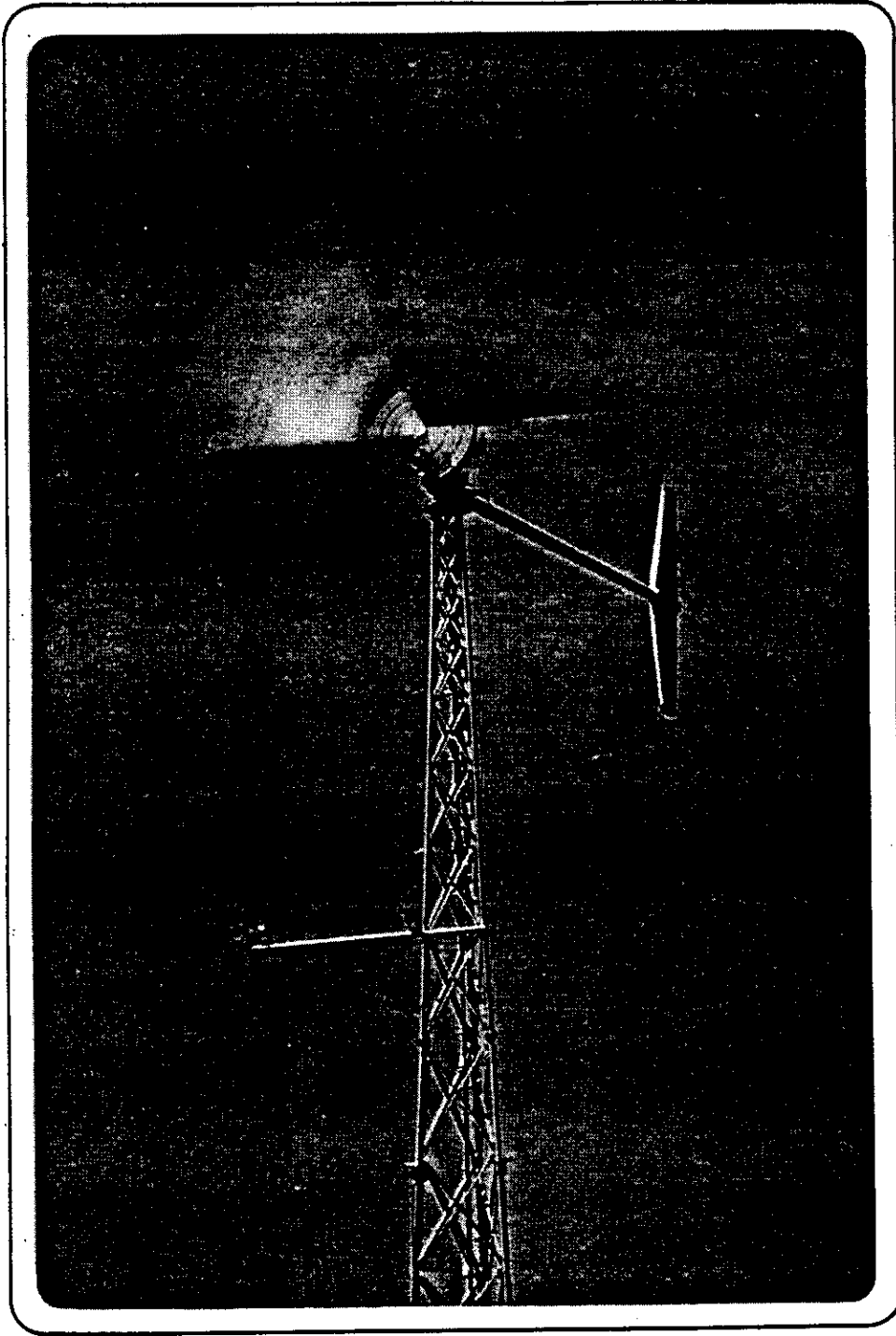


Figure 26c. PHOTOGRAPH OF WIND TURBINE, FRONT VIEW

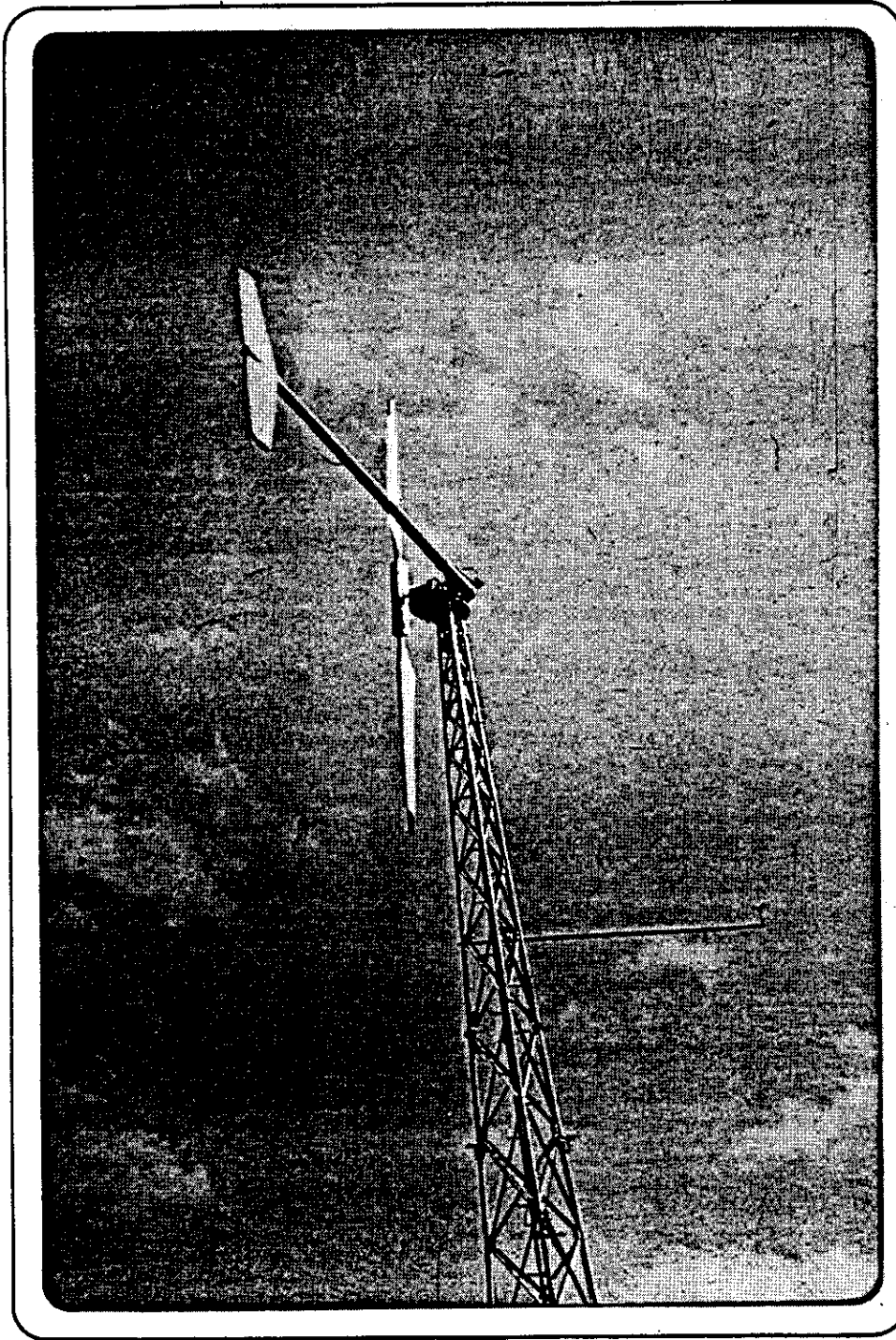


Figure 26d. PHOTOGRAPH OF WIND TURBINE, FURLED

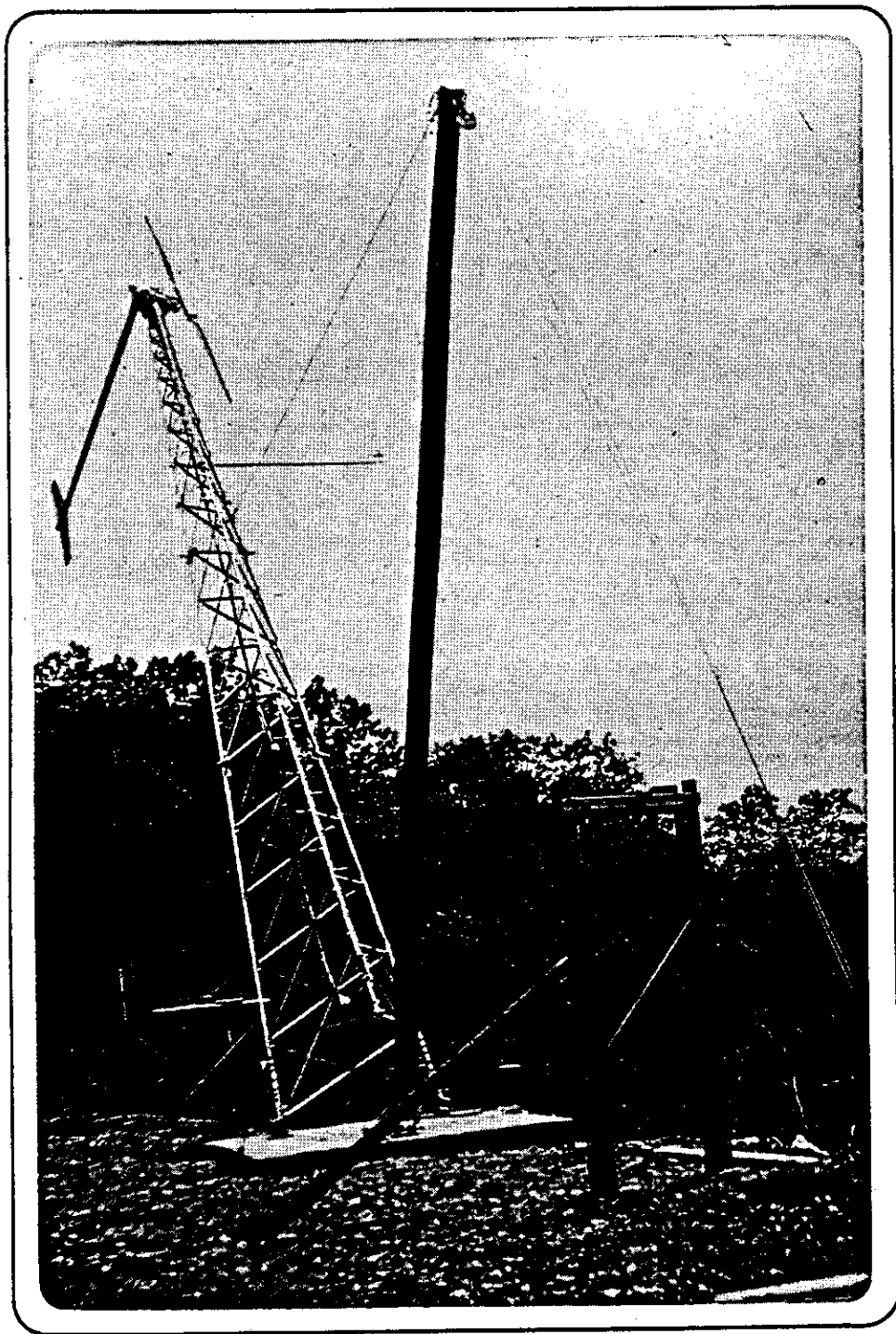


Figure 26e. PHOTOGRAPH OF TOWER OPERATION

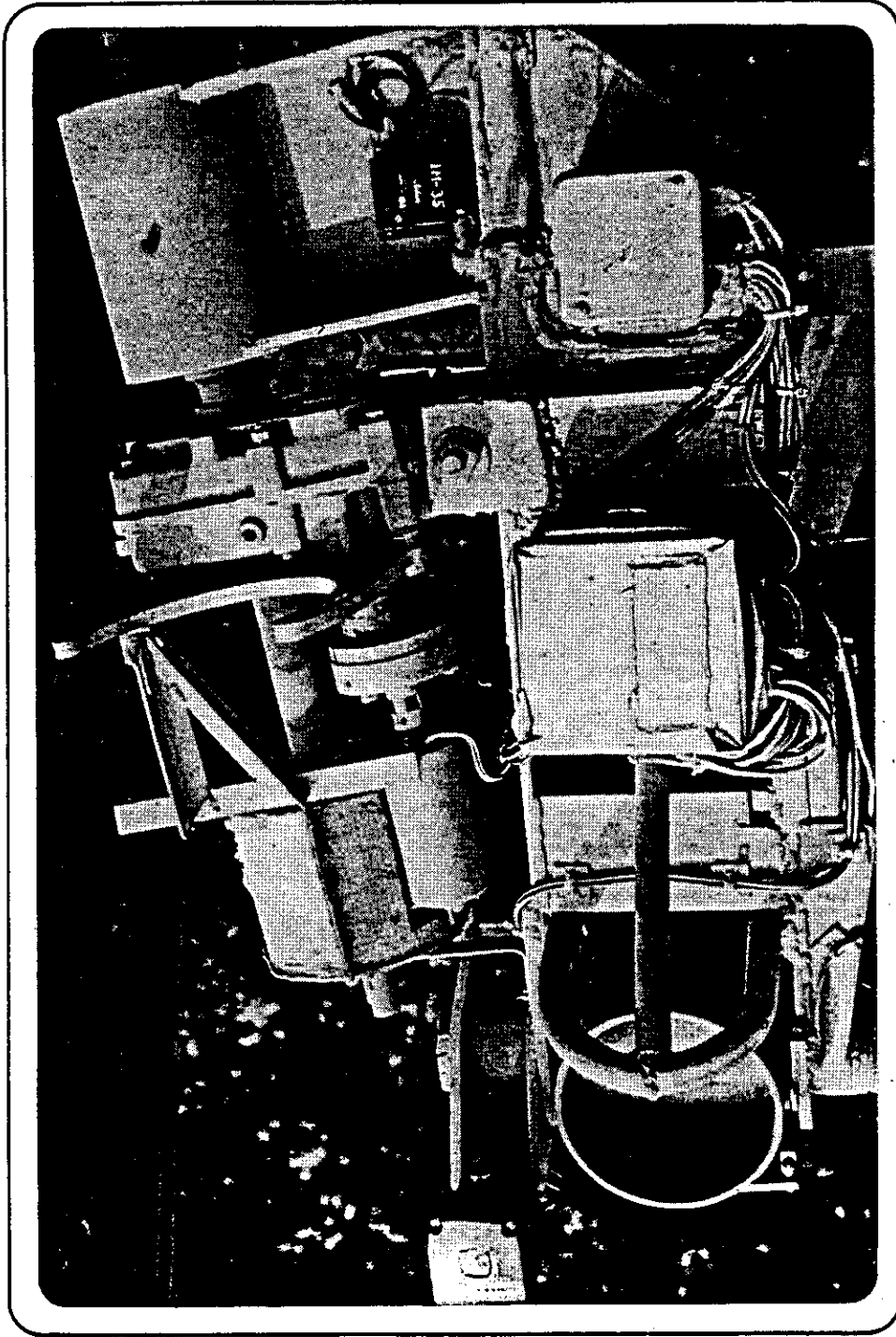


Figure 26f. PHOTOGRAPH OF EXPERIMENTAL WIND TURBINE NACELLE DETAIL SHOWING SLIP RINGS, GEAR BOX, MAIN BEARINGS, FURL ACTUATOR AND INSTRUMENTATION BOXES

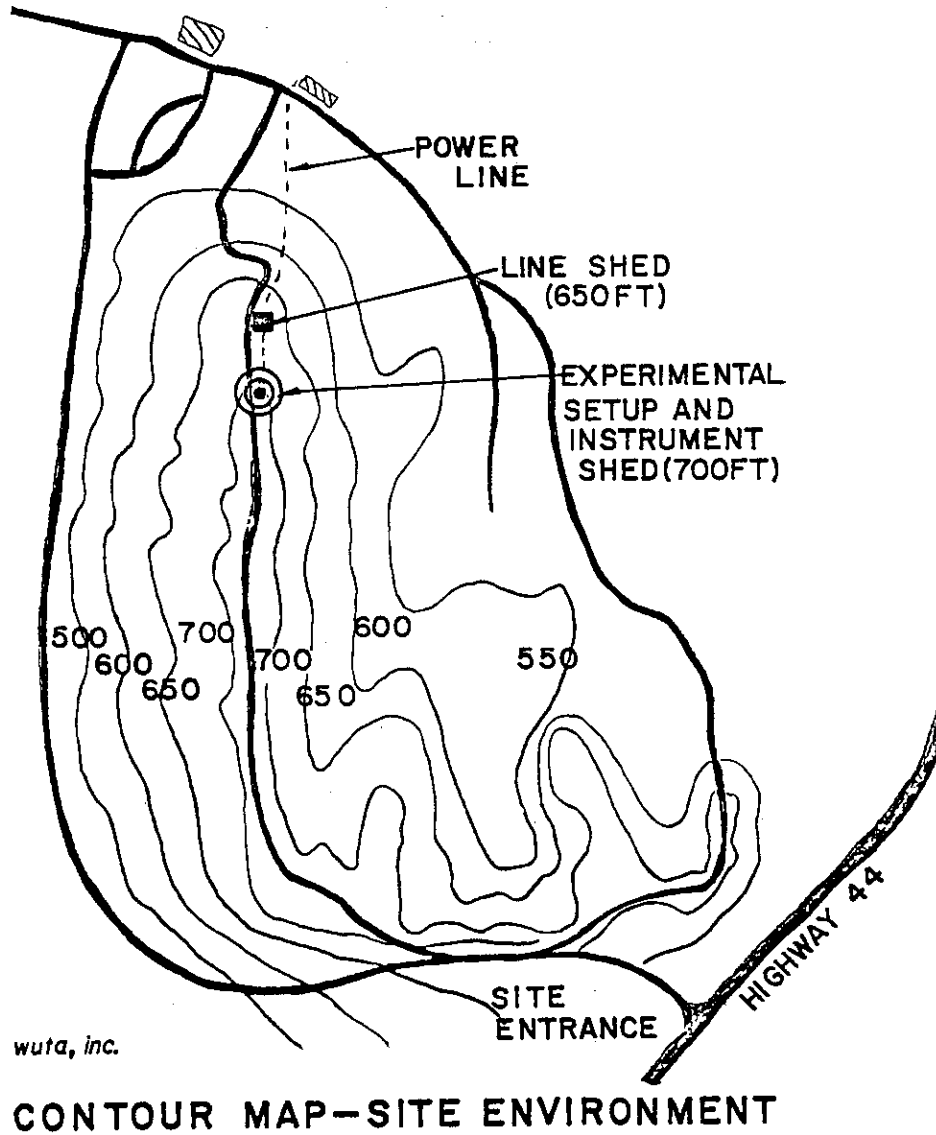


Figure 27. SITE CONTOUR MAP

The atmospheric tests were conducted atop a 214 meter (700 ft.) north-south ridge at the Washington University Tyson Research Center during the summer and fall of 1980. The center is located about 32 km (20 miles) west of the university campus on Interstate Highway 44. (See Figure 27).

TABLE 5

Full Scale Machine Data

Rotor Diameter 7.6 m (25 ft.)

Blade Material Reinforced Fiberglass

Blade twist, chord, and airfoil section, See Figure 14

Blade mass 15 kg (33 lbm)

Blade solidity ratio 0.032 at .7R

Blade moment of inertia 40.7 kgm² (30 slug ft²)

Blade Lock number 7.0 at .7R

Prelag angle 23°

δ_3 angle 67°

Cyclic pitch stops +13°

Reference rotor RPM 225

Reynolds number 640,000 at .7 R

Tail vane 1.16 m² (12.5 ft²) - Fiberglass - 12.7 kg (28 lbm)

Vane arm 5.2 m (17 ft) - aluminum - 42 kg (92 lbm)

Blade retention and hub - aluminum - 36 kg (80 lbs) -

clamped at fixed pitch setting

Gear box: Morse type, shaft mounted 15:1 speed increaser

Alternator: Maremont E-95 rewound brushless alternator designed for truck use. Output is rectified and delivers 220 VDC, 40 amps at 5500 RPM. The alternator is driven by a pulley from the gear box with a total speed increase of 25:1. The alternator weighs 16 kg (35 lbm)

Carrier beam: I-type steel with Roulon bearings for tail boom

Yaw post: 0.076 m (3 inch) steel tube attached by flange to the carrier beam and freely rotating in an upper self-aligning bearing and lower Roulon bearing.

Furl control actuator: 12 VDC - Saginaw steering actuator with 0.305 m (12 inch) stroke and 3338 N (750 lb) operating load and 13,350 N (3000 lb) static load.

Furl rate due to actuator: approximately 15 deg/sec. (depends on wind condition and furl or unfurl direction)

Distance from yaw axis to rotor 0.6 m (2 ft)

Starter motor/tachometer generator: 12 VDC permanent magnet motor or mounted on output shaft of the gear box.

3.2.2 Instrumentation

A list of monitored variables and the instrumentation used for data collection is presented in this section. A detailed description is provided since the resulting data will be used to compare theoretical and experimental results. Three types of instruments are used for recording the test quantities:

- o A multi-channel "Consolidated" oscillograph recorder.
- o A microprocessor data acquisition system including analog to digital converter, an internal clock and a 12 inch screen monitor and printer-plotter.
- o Display instruments for both monitoring and manual recording.

Auxiliary recording equipment includes a twenty channel "Vishay" model 2100 strain gauge conditioner and amplifier system, a twelve ring slipring unit to transmit signals from the rotating system, and various signal conditioning filters and output buffers. The recording instrumentation was either destroyed or severely damaged during lightning strikes on June 28, 1980. The repaired recording instrumentation has been in use since September 1980.

The measured quantities are divided into slowly varying quantities (for which a sampling rate of one per second is adequate), and rapidly varying quantities (which are either sampled at a rate of 128 samples per second or continuously recorded on the oscillograph). The slowly varying measured quantities are: wind speed, rotor speed, furl position, yaw post position, load voltage, alternator temperature, and ambient temperature. There are display instruments for each of these quantities. The first five quantities can also be recorded with the oscillograph and with the microprocessor.

The signals are conditioned to vary between 0 and 5 volt DC, which is the range that the microprocessor accepts. This 5 volt range is divided into 255 intervals. The analog-to-digital converter assigns each measured voltage point to one of these intervals. The largest conversion error is ± 0.01 volt or $\pm 0.2\%$ of the total range of the measured quantity.

The oscillograph channels use a damping resistance of 470 ohms and have a sensitivity of 4 volts/inch. Thus the 5 volt range of the measured quantities corresponds to a 1.25 inch range on the oscillograph record. The light sensitive paper moves with a speed of either 0.25 or 1.00 inch/second. In the range of operating speeds (between 100 and 225 RPM) the time for one rotor revolution corresponds to 0.15 - 0.066 inches at 0.25 inch/ second or 0.6 to 0.267 inches at 1 inch/second on the oscillograph record. The recording rolls are seven inches wide, so that five quantities, in addition to the rotor speed signal, can be recorded simultaneously without overlap. The rotor speed signal consists of 0.1-inch event marks in response to a magnetic pickup. The RPM signal is taken for all oscillograph records.

The rapidly varying measured quantities for the rotor are: blade flap-bending, blade in-plane bending, shaft torque, and blade cyclic pitch. The signal wires from the strain gauge bridges pass through the hollow rotor shaft to the silver slipring assembly at the rear end of the shaft, down the tower, and on to the instrument shed located 24 m

(70 ft.) from the tower base. The rapidly varying measured quantities for the non-rotating structure are: vertical and sidewise tail boom bending, fore-to-aft and lateral yaw post bending, and fore-to-aft and lateral linear accelerations of the rotor bearing block. The lightning strike on June 28, 1980 destroyed one of the linear accelerometers. Since it had been found that the lateral accelerations are always substantially smaller than the fore-to-aft accelerations, the destroyed accelerometer was not replaced. After resumption of the atmospheric tests in September, 1980, only fore-to-aft accelerations were recorded. Here are some more detailed comments on each measured quantity.

3.2.2.1 Wind Speed

Until June 28, 1980 a A7-104-4 anemometer sold by Natural Power, Inc. was used. The signal frequency was proportional to wind speed (1.7 mph/Hz, or 0.76 m/s/Hz). A frequency to DC converter was adjusted during the wind tunnel calibration such that the display voltmeter and the microprocessor received 0.18 volt/m/s. A "bin" of 1/2 m/s corresponded to 0.090 volt. The 5 volt range of the signal corresponded to a wind speed range of 0 to 27.8 m/s (62 mph). The anemometer was first installed on a horizontal boom attached to the tower at about 13.4 (44 ft.) height. The anemometer boom had a natural frequency of 3 Hz (180 CPM) and was strongly excited by the rotor. To avoid reading errors and damage to the anemometer, it was

relocated on a fixed mast of 12 m (40 ft.) height installed 15 m (50 ft.) to the north of the tower. On June 28, 1980 the replacement anemometer was struck by lightning and destroyed, together with all of the recording equipment in the adjacent instrument shed. It was then recognized that a separate pole for the anemometer increases the danger of a lightning strike and that relocation on the tower attached boom is desirable. Since the A7-104-4 anemometer had been found to be sensitive to vibrations of its support boom it was decided to acquire, instead, a TV 102 Texas Electronics anemometer which produces a DC signal proportional to wind speed and has the required range of 0-5 volt. A frequency to DC converter is not needed. When checking out this instrument it was found that it produced a ± 1 volt oscillation with the frequency of its rotation. It was returned to the manufacturer and was repaired under the warranty without charge. The oscillation, though reduced to ± 0.1 volt, still persisted. A wind speed signal conditioning circuit with active filter and three buffers was developed, shown in Figure 28. The circuit completely removes the signal oscillations. It also provides three outputs. One to the microcomputer, one to the oscillograph and one to the display DC meter for monitoring. These three outputs do not interfere with each other due to a buffer in each of them. (Previously the signal to one of the recording instruments had some effect on the signals to the others.) The TV 102

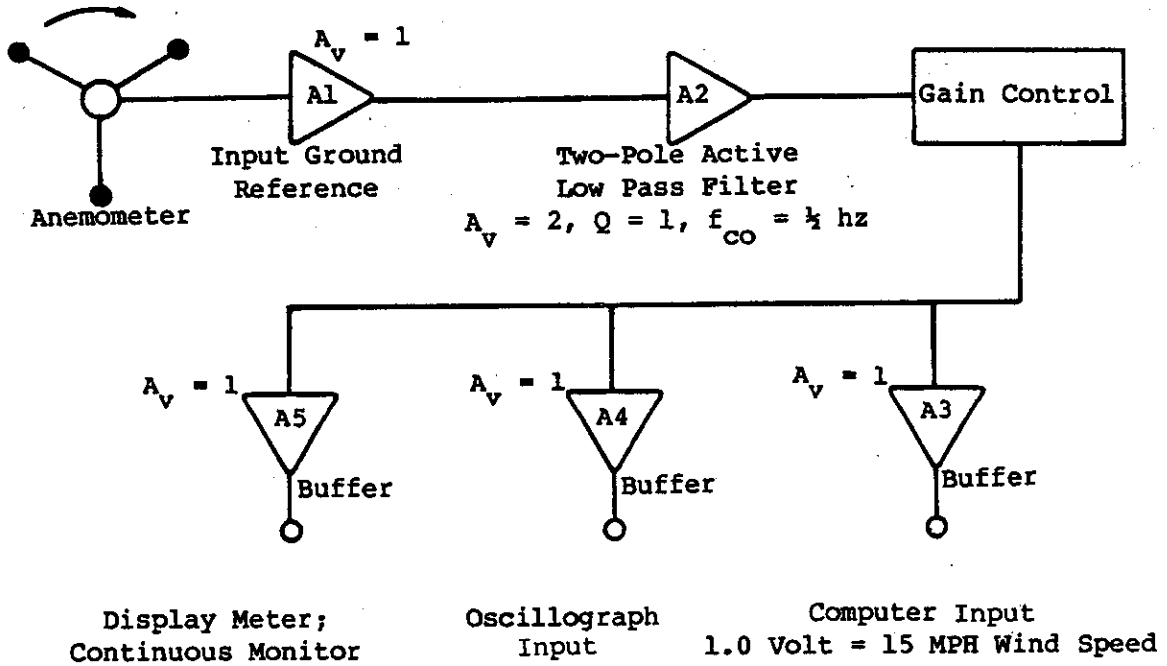


Figure 28. WIND SPEED SIGNAL CONDITIONING CIRCUIT

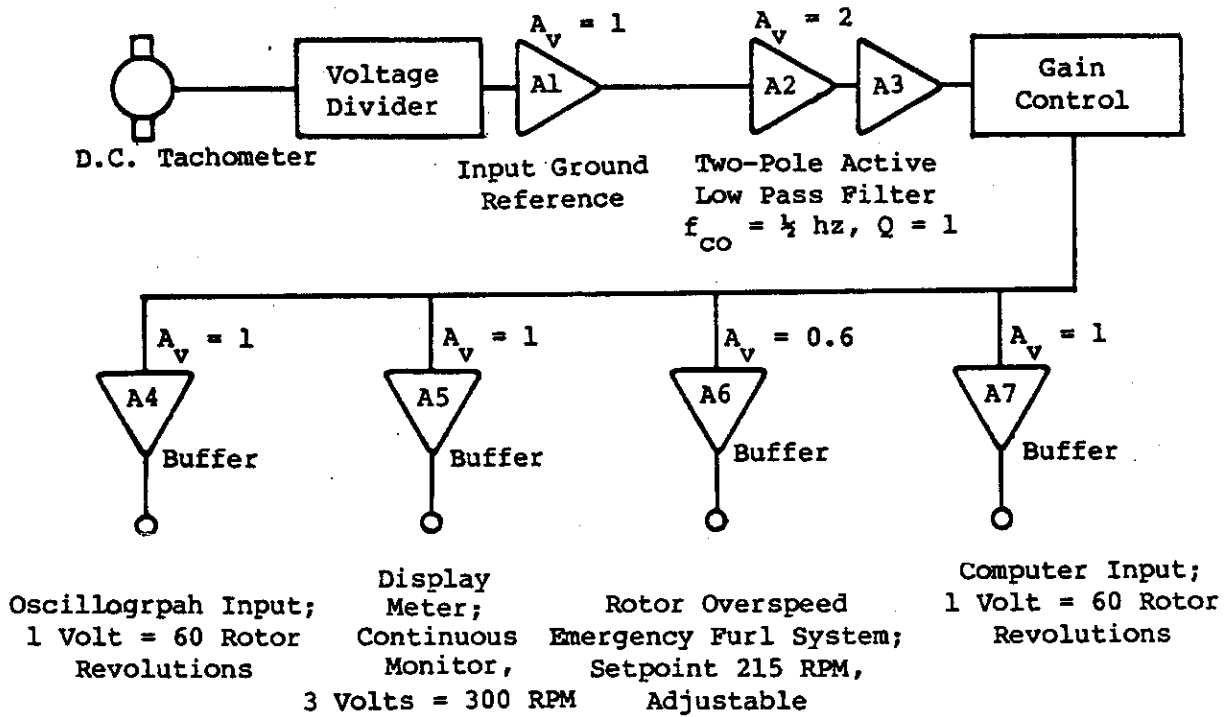


Figure 29. ROTOR SPEED SIGNAL CONDITIONING CIRCUIT

anemometer has a calibration constant of 6.705 m/s (15 mph)/volt and a range of 0 to 33.5 m/s (75 mph). On the oscillograph the calibration constant is 26.82 m/s (60 mph)/inch.

The anemometer boom extends to the west of the tower and is not in the wake of obstacles for the prevailing wind direction. However, easterly winds will produce a wake from the tower structure. It is located 5.5 m (18 ft.) below the rotor center. Due to the updraft from the ridge on which the wind turbine is located, the wind speed can be higher at the anemometer than at the rotor center. This appears to be true for westerly winds. For northerly or southerly winds the speed at the anemometer location can be expected to be lower than at the rotor center. Because of the uncertainty about the average wind speed over the rotor disk, the performance coefficient C_p based on the anemometer readings is not a reliable efficiency measure.

3.2.2.2 Rotor Speed

There are two rotor speed signals available. One signal originates in a magnetic pickup that gives one impulse per rotor revolution. It is recorded by the oscillograph and allows an accurate determination of the rotor speed by measuring the distance between impulses. It also indicates phase angle. The other signal originates in the tach generator which produces up to 17 volts, contaminated by brush noise. During the initial statistical data

sampling the signal was merely reduced in strength by a voltage divider, so that the standard deviation for the rotor speed included the brush noise. Later, a rotor speed conditioning circuit was developed, shown in Figure 29. The circuit has a low pass filter and has three buffer amplifiers for the three outputs. One to the microcomputer, one to the DC meter and one to the oscillograph. This arrangement prevents interference errors from the coupling of these three outputs, as was originally experienced. The calibration constants are 1 volt/60 RPM for the microcomputer which thus accepts up to 300 RPM, 1 volt/100 RPM for the DC meter, and .0254 m (1 inch)/240 RPM for the oscillograph record.

3.2.2.3 Furl and Yaw Post Position

The electronic configurations for the Boom Position Detector (furl angle) and the Yaw Post Angular Position Detector are essentially identical. Each consists of a high quality, rotating, wire-wound potentiometer as the movable or sensing element. Each is excited from an adjustable voltage regulator having load regulation of $\pm 0.2\%$ with noise and voltage ripple less than 2 mV maximum over the adjustable excitation range. Each position detector is excited at a DC voltage level in the range from five to eight volts, dependent upon the calibration constant of the given circuit. The input voltage to the Vishay Series 2100 Signal Conditioner is essentially potentiometric in nature. The

configuration of the selected input circuit allows high-level voltage signals rather than millivolt level signals to be transmitted from the position detector to the signal conditioner. Since the transmission distance is approximately 45.72 m (150 ft.), high level signals are desirable. Maximum current flow in the signal input circuit never exceeds 40 microamperes, thereby assuring minimal line loss. Further, the ratio of detector resistance to transmission line resistance is greater than 100,000/1. Measurement error resulting from line resistance is therefore not significant. The amplifier input, after scaling, varies from five through 20 millivolts. Scaling is accomplished directly at the input to the amplifier by 0.1% MIL-R-55182J divider networks. Amplifier input stability is $\pm 2\mu\text{V RTI}/^{\circ}\text{C}$ (maximum) with noise and drift of less than 10 $\mu\text{V RTI}/\text{day}$. The amplifier input is common mode connected and has input impedance approaching 26 M ohms. Amplifier Gain (A_v) is set in the range from 100/1 to 300/1 depending upon maximum output voltage level required. Amplifier linearity is $\pm 0.05\%$ at DC. Circuit calibration and amplifier operational tests can be performed at the control panel of the Vishay Signal Conditioner. Additionally, the circuit is configured to allow the "balance potentiometer" (normally used for strain gauge circuit balance) to function as a voltage level offset control.

The Boom Position Detector is a 270 degree, rotary, linear, wire-wound potentiometer, mounted on the underside of the tail boom pivot pin. The potentiometer slider (wiper) is driven by a linear mechanical linkage connected to the tail boom. Overall position sensitivity is 0.3 volts per 10° of furl angle. Zero output voltage corresponds to the fully unfurled position.

The Yaw Post Angular Position Detector is a 360° , linear, wire-wound potentiometer mounted on a tower brace and the lower yaw post support plate. It is driven by a timing belt connected to the yaw post. Overall position sensitivity is 1.00 volt per 100 degrees of yaw post rotation. Zero output corresponds to a North position. The furl and yaw post position signal conditioning circuit is shown in Figure 30.

3.2.2.4 Load Voltage

The alternator load voltage is measured across the resistive load bank consisting of seven resistors with a nominal resistance of 40 ohm each. The load resistors are located just outside the instrument shed. Since the voltage is used to compute the power output of the alternator (power output equals the squared voltage divided by the resistance), it is important to estimate the possible error from a change in resistance with temperature. One of the resistors was connected to a 250 volt source and the resistance measured as it heated up to about 70°C .

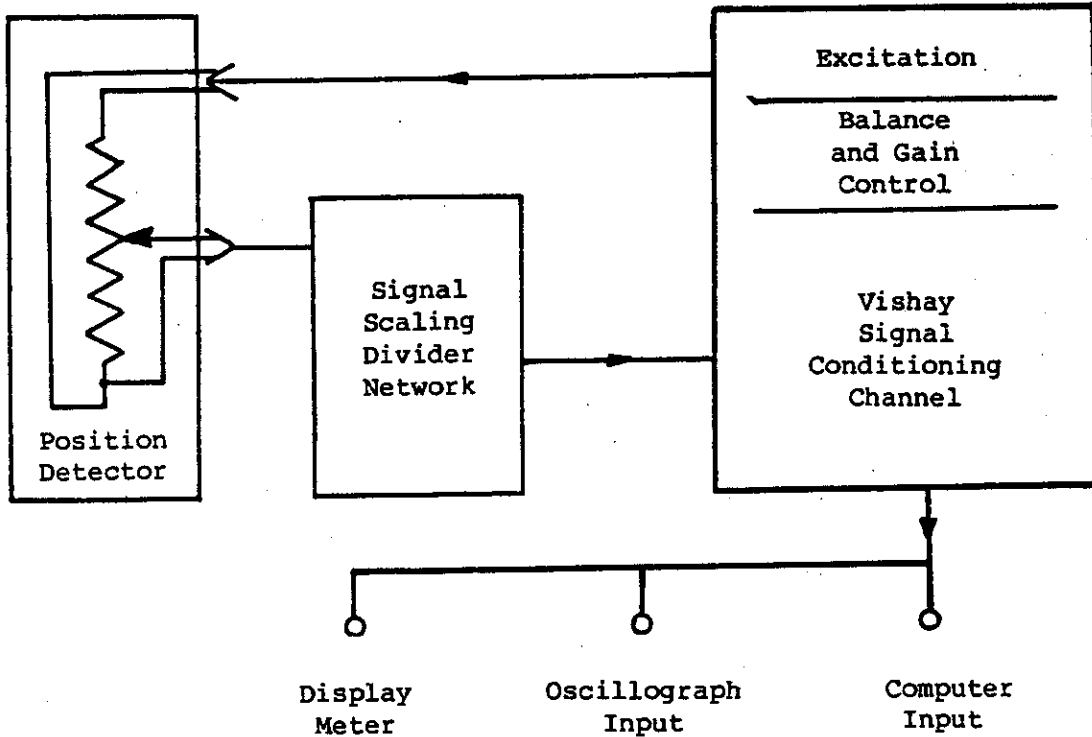
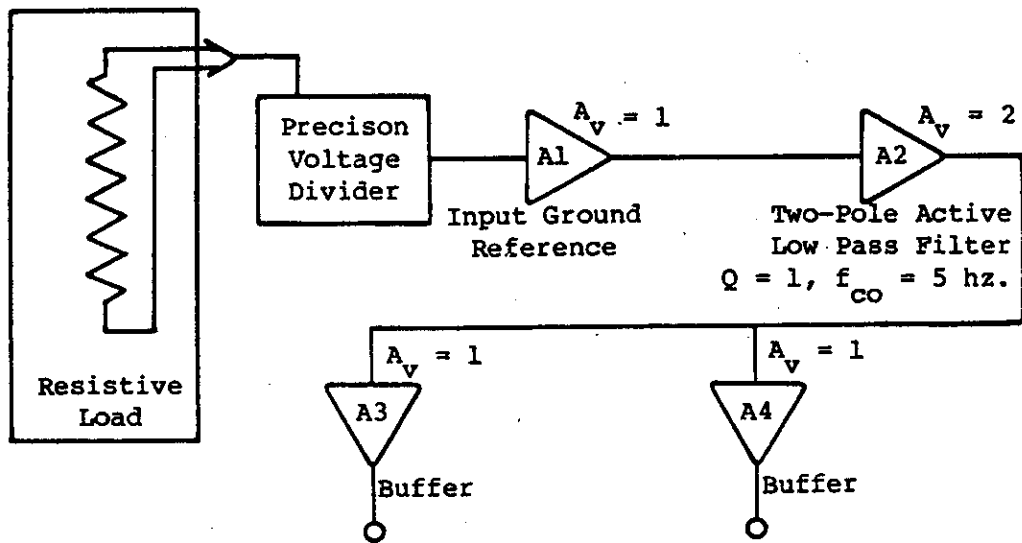


Figure 30. FURL AND YAW POST POSITION SIGNAL CONDITIONING CIRCUIT



Auxilliary Input; Computer Input;
1 Volt = 100 Load Volts 1 Volt = 100 Load Volts

Figure 31. LOAD VOLTAGE SIGNAL CONDITIONING CIRCUIT

Equilibrium temperature was reached in 10 minutes. The increase in resistance was from 40.84 to 41.46 ohm, or a 1.5% increase. Since the alternator voltage is limited to 225 volt and is mostly below this value, it was considered unnecessary to correct for the effect of temperature on the load resistance. The total load bank resistance is 5.8 ohm. The total resistance (including that of DC cable to the shed), is 6.0 ohm when measured at the machine. A correction of $6/5.8 = 1.03$ is made to the voltage measured across the load resistors in order to obtain the voltage at the alternator location. The alternator power output is thus determined as $(1.03 \text{ volt})^2 / 6.00 \text{ watts}$.

During initial tests, the three phase current from the alternator was conducted down the tower and to the shed, where the rectifier and tuning capacitors were located. The alternating current in the cables adjacent to the signal caused a severe noise in all signals. Rectifier and tuning capacitors were then moved to the tower top so that only the DC cables reached the shed. The signal noise was greatly reduced but still unacceptable. It was apparently caused by the AC ripples in the DC current. The DC cables were then inserted into a grounded metal conduit that extended from the tower top to the instrument shed. The noise in all signals is now completely eliminated except that the DC load voltage still contains a small AC ripple. A voltage signal conditioning circuit, shown in Figure 31, was added which

has a low pass filter and buffer amplifiers for the microcomputer input and for the oscillograph input. The average calibration constant is 1 volt/100 load volts. The DC meter receives the load voltage directly. The voltage signal conditioning unit produces some errors in the generator output measurements because the signal-voltage relationship is somewhat nonlinear at low power outputs, and because the gain is temperature dependent. The meter readings are believed to be more accurate and have been used when possible.

3.2.2.5 Strain Gauge Circuits

Micro Measurement 350 ohm strain gauges type CEA-06-250UW-350 are used on all locations. Each bridge is made up of four gauges, two in tension, two in compression. The gauge factor for each gauge is 2.1 volt/unit strain. For most bridges the gain in the Vishay 2100 is set at 10:10 corresponding to 2020 amplification factor. The excitation level is 10 volts. For a complete four gauge bridge the strain is then given by

$$\epsilon = \text{Volt}/(10 \times 2020 \times 2.1)$$

The stress is $\sigma = \epsilon E$, where E is the modulus of elasticity. For the aluminum blade retention and for the tail boom $E = 10.4 \times 10^6$ psi. For the steel yaw post and cyclic pitch flexure, $E = 30 \times 10^6$ psi. The moment calibrations are made in

terms of nominal bending moments at the rotor center, at the tail boom hinge and at the upper yaw post bearing. The cyclic pitch flexure, driven by an eccentric, is calibrated in terms of degrees cyclic pitch deflection. The following table gives the Vishay 2100 gain, the volt/unit, the psi/unit, and the oscillograph inch/unit for the strain gage bridges. For the sake of completeness, the gains and calibration constants for the linear accelerometer, for the furl and yaw post potentiometers and for the load voltage are added.

A yaw post position signal of 0.0 or 3.6 volt indicates that the rotor axis points North. Zero volt for the furl position signal indicates zero furl angle (90° rotor angle-of-attack). The magnetic pick-up signal for rotor speed is always at the bottom of the oscillograph record. Time moves from left to right. Positive voltage (there is no negative voltage) is from top to bottom of the oscillograph record. The yaw post bending gain has been reduced to one quarter beginning in October, 1980, in order to limit the output to the 5 volt level compatible with the microcomputer analog-to-digital input board.

3.2.2.6 Microcomputer System

The microcomputer system for statistical data processing consists of:

- o A 48K, 6502 microprocessor based, "Apple II Plus" Central Processing Unit;

TABLE 6
Instrument Gains

Vishay Channel	Signal	Gain Setting	Volt/Unit	Psi/Unit	Oscillograph Inch/Unit
1	Cyclic Pitch	2:6	2v/10 ⁰	10.100/10 ⁰	.5"/10 ⁰
2	Blade In-plane Bending	10:1	4.6v/10 ⁴ #	1.120/10 ⁴ #	1.15"/10 ⁴ #
3	Blade Flap Bending	10:1	3.2v/10 ⁴ #	770/10 ⁴ #	.80"/10 ⁴ #
4	Rotor Torque	10:1	1.2v/10 ³ #	840/10 ³ #	.30"/10 ³ #
5	Accelerometer	7:8	5v/g		1.25"/g
6	Tail Boom Bending	10:1	3.9v/10 ⁴ #	950/10 ⁴ #	.97"/10 ⁴ #
7	Yaw Post Position	2:5	1v/100 ⁰		.25"/100 ⁰
8	Yaw Post Bending	10:1	5.8v/10 ⁴ #	4100/10 ⁴ #	1.45"/10 ⁴ #
9	Since Oct. '80 Furl Position	2:52 0:5	1.45v/10 ⁴ # 0.3v/10 ⁰	4100/10 ⁴ #	.36"/10 ⁴ # .75"/10 ⁰
10	Load Voltage		1v/100 ⁰		.25"/100 ⁰

*Gain = Setting X 2--

SI Units: Nm in. lb X 0.113
kPa = psi X 6.9

- o An AI02, 16 channel analog-to-digital (A/D) conversion module compatible with the Apple II Plus C.P.U.;
- o Plug-in, Mountain Hardware real time clock;
- o An "Apple" mini-disk drive unit;
- o A "Trend Com 200" Thermal Printer; and,
- o A black and white video monitor.

Some of the special features available with this system include floating point BASIC capability incorporated in the read only memory; built in, high resolution graphics capability; and print-out capability of the graphics display in both standard and expanded scales. Further details concerning the hardware are available in the Apple II Plus Hardware Manual and other product literature.

In order to integrate the computer system into the project instrumentation system, several peripheral devices were added. Between the computer power supply and the available grid power, three protective devices were added. First a 120 volt, constant voltage, "Sola" transformer was installed to protect against voltage transients. Second, a filter and surge protection circuit were installed to protect against lightning and high voltage power surges. And third, a standby power source, purchased from the Apple Company, was added to provide reserve power in order to protect data and programs currently stored in the computer memory in the event of a line power failure.

It is significant to note that although the constant voltage transformer and reserve power supply were installed as buffers to the line power at the time of the lightning strike, on June 28, 1980, the computer was still severely damaged, indicating the sensitive nature of these devices to electrical transients.

In addition to the power supply protection devices, a special interface box was constructed for the 16 channel, 0 to 5 V DC A/D board. It consists of self-grounding audio jack inputs (i.e. the input connections are automatically grounded when the patch plugs are removed to guard against static electric discharges across the input ports), and 10 volt Zener diodes placed across each input to protect against reverse and over voltages. The use of 5.6 volt Zener diodes was attempted, but the input signals became non-linear at voltages in excess of 3 to 4 volts.

Accuracy of the A/D interface board was determined using a "Fluke" digital voltmeter and reference voltage source. It was determined that the board, which converts 0 to 5 V DC to a digital scale of 0 to 255 (0 to FF hexadecimal), reads approximately 6% higher over its entire range. This error was compensated during data processing by use of 54 digital units per volt rather than 51, as indicated by the A/D board scaling factor. Although this limited the upper scale reading to approximately 4.6 volts, it had little effect on data accuracy since most data were

collected at values well below the 4.6 volt DC limit.

Program and data storage was, in general, accomplished using the mini-disk system with one disk acting as an "operating disk" containing the sampling programs, a second disk containing the graphical plotting routines, while the bin data was stored on separate "data" disks.

Copies of all data and programs were made on separate disks to protect against disk failure or operator errors, both of which occurred several times during the course of data sampling and analysis.

3.2.2.7 Lightning Protection

The test site selected for the wind turbine generator is at an elevation of approximately 213.4 m (700 ft.). It is in an isolated wooded area and is without question the tallest conductive structure in the area. The test site is located 22 miles southwest of St. Louis, Missouri in an area prone to strong atmospheric disturbance. The test site is likely to be affected by three main disturbances; direct lightning strikes, main power surges and induced transients. Direct lightning strikes are the most severe source of atmospheric disturbance. The significant factors of concern for direct lightning strikes are the pulse rise time, current amplitude and current duration. The 50 percentile probabilistic stroke peak current is about 18,000 amperes, with about one in one hundred strikes exceeding 120,000 peak amperes. The stroke duration can persist up to 100

milliseconds and the rise time of the pulse can approach a few nanoseconds. Most lightning strikes reach 90 percent of their peak current in less than one microsecond. These data were obtained from Lightning Elimination Associates.

A severe thunderstorm occurred in the area of the test site on June 28, 1980. The concentration of high frequency energy resulted in significant damage to the wind turbine instrumentation. The test site was so severely struck that the test equipment was subjected to direct strikes, power main surges and electromagnetic pulses from nearby lightning. The electrical storm lasted several hours and resulted in nearly 7000 dollars damage to instrumentation. Signal transducers including strain gauge bridges, accelerometers, position sensing potentiometers and the site anemometer were destroyed by direct strikes. Computer circuits and the integrated circuits for the signal conditioning instrumentation were destroyed by line transients and electromagnetic pulses. Fortunately, the turbine hardware and generator sustained no damage, although the fuse protecting the field winding of the generator was blown. The following discussion describes the steps taken to insure safety to equipment from subsequent electrical storms.

The turbine generator is mounted on top of a tiltable steel tower and each leg of the tower is connected by a large copper cable to individual grounding rods driven 3 m (10 ft.) into the earth at the base of the tower. The tower is

grounded to the wind turbine generator by three large carbon brushes which bear against the yaw post. The machine frame is grounded to the main shaft. The main shaft extends through the gear box to the rotor and passive cyclic pitch mechanism and is grounded by two large carbon brushes. The blade retention mechanism is grounded to the main shaft using woven copper straps. The cyclic pitch mechanism effectively isolates the blade retention box beam from the main shaft because Rulon bearings are used in the mechanism. The woven copper straps provide a flexible ground path around the Rulon bearings.

The grounding arrangement described above provides shunt paths around all mechanical components likely to sustain damage from a direct lightning strike. The key components to be protected are the cyclic pitch mechanism bearings, the gear box bearings and the yaw post bearings. The tail boom is effectively grounded to the machine frame through the shunt path of the furl actuator mechanism.

Site protection was further improved by installation of a lightning rod mounted to the top of the wooden tower tilt boom (gin pole). The boom is in the full upright position when the tower is lowered and resting in its cradle. The lightning rod is connected to two grounding rods at the base of the boom. The lightning rod is the preferred strike point for any lightning strikes in the vicinity of the test site and helps insure protection of the

tower (lowered) and instrument shed during periods when testing is not in progress.

Metal Oxide Varistors (MOVS) are passive low cost devices used extensively on all tower instrument and power wiring. All MOVS are connected to grounding rods. They serve a dual function. During operational tests, they function as low energy, high amplitude noise clamps, protecting signal conditioners and A/D computer input boards from excessive input voltage. They are very effective when used to bypass furl - unfurl actuator switching noise and commutator noise from the tach generator.

The MOVS provide a second protective function when the tower is in the lowered position and unattended. All signal inputs are disconnected from the signal conditioning equipment and the computer during unattended periods. The MOVS effectively tie the transducer signal wires to the ground. In the event of a lightning strike or other atmospheric disturbance, the MOVS break down and drain the voltage to ground. Breakdown occurs in nanoseconds and all conductors form shunt drain paths to ground, helping to insure the survival of the transducers and the integrity of the wiring insulation.

During normal operation and data acquisition, the instrumentation power inputs are protected by a "Sola" transformer and surge isolators. The surge isolators protect the instrumentation from power line surges caused by

lightning strikes, earth currents, magnetic induction, switch arcing and inductive switching transients.

The main power is disconnected from the instrument shed by a large knife action switch when unattended. The power line ground connector is not disconnected by this switch. The power line ground connector is connected to an earth grounding rod at the instrument shed to insure power line ground conductor integrity.

3.2.3 Data Acquisition and Processing Methods

Two types of data acquisition methods have been used: analog data acquisition with an oscillograph, and digital data acquisition with a microcomputer. Approximations to steady state data have been obtained both from oscillograph records and from meter readings. Data on transients have been extracted from oscillograph records. Digital data acquisition and processing by the microcomputer have been used to obtain statistics on performance parameters and on loads.

3.2.3.1 Analog Data

Steady state data are difficult to obtain during atmospheric testing since wind speed and rotor speed are continuously changing. All oscillograph records contain the traces of wind speed and rotor speed so that it is possible to judge when a more or less steady state occurs over several seconds.

Sometimes it is not possible to find a steady state record. For example, conditions with high wind speeds are only obtained during gusts. In order to include the gust conditions in the steady state rotor power evaluation, the angular rotor acceleration was determined from the oscillograph record, and the inertia torque was added to the measured rotor shaft torque. The sum of rotor inertia torque and rotor shaft torque is equal to the aerodynamic torque. It was found that the inertia corrected rotor torque agrees with the steady state torque values and can be considered a quasi steady aerodynamic torque. It is multiplied by the angular rotor speed to obtain rotor power.

The steady values of the measured quantities show little scatter when plotted vs. rotor speed. The larger scatter when plotted vs. wind speed is caused by the difference between the wind speed reading from the anemometer located 5.5 m (18 ft.) below the rotor center and the average wind speed seen by the rotor. Scatter is also caused by the fact that the rotor speed, due to rotor inertia, follows wind speed changes only after a certain delay.

In addition to steady state evaluations vs. rotor speed and vs. wind speed, some time histories have been extracted from the oscillograph records. They show starting and furling processes and responses to gusts.

3.2.3.2 Statistical Data Processing

Five computer programs have been developed for statistical data sampling using the method of bins as described previously. The five programs sample data as follows:

- P1. Two performance variables vs. wind speed using only BASIC.
- P2. One dynamic variable, usually cyclic pitch amplitudes, vs. yaw rate.
- P3 & P4. Two or six performance variables vs. wind speed using a high speed sampling machine language routine.
- P5. Six dynamic load variables vs. rotor speed.

The first program collects, for each wind speed bin, the mean value, standard deviation, the global maximum and the global minimum for rotor speed and cyclic pitch amplitude. The second program collects, for each yaw rate bin, the mean and standard deviation of the cyclic pitch amplitude. From the oscillograph records a clear dependence of cyclic pitch amplitude on yaw rate was observed. It was decided to collect statistical data on this dependence. The third and fourth programs collect statistical data required for performance vs. wind speed. The fifth program collects dynamic loads statistical data in rotor speed bins.

In addition to the five sampling programs, two analysis programs were developed. The first converts the digital voltage data stored in each bin array into a graphical plot.

The second completes a statistical data evaluation of the rotor power vs. wind speed data and calculates and plots the power coefficient both as a function of average wind speed and also for each wind speed bin.

A more detailed description of these programs follows. The documentation of the programs is presented in Appendix 6.5.

Pl. Power-off Data vs. Wind Speed

The "Wind-2" program was developed to sample cyclic pitch amplitude and rotor RPM as functions of wind speed using only BASIC programming commands. This was the first sampling program developed and was used to collect data in autorotation before a faster and more sophisticated machine language sampling program was developed. See Appendix 5 for details.

The program samples the wind-speed port and rotor-RPM port twice using BASIC commands available in the Apple command structure. It then takes the average of each and stores the value. The program then samples the cyclic pitch position for approximately 1 second (47 times), stores the values, and, after sampling, determines the maximum and minimum values sampled. Next, the cyclic pitch amplitude is determined by calculating one-half of the difference of the maximum and minimum value. A 56 unit wind-speed bin array is used based on a 0.5 m/s bin width. Values of the maximum, minimum, mean, standard deviation and number of samples are

updated for both RPM and cyclic pitch amplitude for the current wind speed bin number.

The program also has several control and monitoring features. The furl angle is tested to insure it is set properly and no automatic furling has occurred. Since the rotor is tilted 8 degrees, actual furl angles are a geometric combination of rotor tilt and furl set angles. The program calculates the required furl set angle for a chosen furl angle and insures the angle is within limits for data sampling. RPM is tested to insure the wind turbine is not in a starting mode which may bias the higher wind speed bins if gusts occur during starting. Wind speed is tested to insure the winds are not zero. If any of these tests fail, a message is printed to the user and the bin arrays are not updated.

In addition, cyclic pitch amplitude is tested. If it is approaching the stop limits, the speaker is toggled for an audible warning and a visual warning appears on the screen. This alerts the operator to possible stop pounding during operation.

Finally, machine performance is monitored by a screen display of current values of wind speed, RPM, cyclic pitch amplitude and tip speed ratio.

At the conclusion of data sampling, as determined by the operator, the bin array data are output to a data disk and a "hard-copy" is produced on the thermal printer.

A plotting routine that uses the Apple high resolution graphics capability then presents the bin data for analysis. Elapsed time of the test and approximate rotor revolutions occurring during the test are also printed. The program is capable of sampling at a rate of about one sample for each variable every 3.5 seconds.

P2. Cyclic Pitch Amplitude vs. Yaw Rate

The "Yawrate" Program was developed to relate a dynamic variable, usually cyclic pitch amplitude, to yaw rate by the method of bins based on yaw rate. The program samples both yaw position and the real time clock, (which reads time in milliseconds) and stores these values. Next, cyclic pitch position is sampled for approximately one-half second (24 times) and these values are also stored. Yaw position is then sampled again, followed by the clock and the elapsed time is calculated. The elapsed time and the recorded yaw position, before and after the cyclic pitch sampling, are used to calculate an approximate yaw rate in degrees per second. The yaw rate is an approximation since it assumes constant, linear yaw rate over the 0.5 second interval. There are 35 yaw-rate bins, each 1 degree per second in width, for both positive (unfurl direction) and negative (furl direction) yaw rates. After determining that the calculated yaw rate is within limits (i.e. between 0 and 36 degrees per second) the cyclic pitch amplitude is calculated and the yaw rate bin arrays are updated as in the "Wind-2" program.

At the conclusion of testing, as determined by the operator, both the positive and negative yaw rate bin arrays are output to data disk and then to the printer. The data is then plotted using a graphical plotting routine for analysis.

The program monitors rotor RPM and only allows data within specified RPM limits since cyclic pitch amplitudes are a function of RPM as well as yaw rate. Furl angle is set at the beginning of the test and held constant during the sampling. Sampling is monitored during operation by a display on the video monitor of current yaw rate and cyclic pitch amplitude.

P3. Power-on Data vs. Wind Speed

The "Wind-6" program was developed subsequent to the development of a machine language, high-speed sampling program through consultation with "Micro Systems Development" of St. Louis. The high speed sampling program uses assembly language mnemonics for the Apple, 6502 based microprocessor chip. Briefly, the program, used as a subroutine of the "Wind-6" program, samples five input channels 128 times in one second in a multiplexing fashion and then samples eight more input channels once each at the end of the five channel, high-speed sampling routine. These data are stored in the computer with 32 previous data sets (i.e. 32 previous seconds worth of data). Next, for each "high speed" channel the amplitude and the mean value are

calculated and then stored. In addition, the global maximums and minimums for all channels are stored as a function of bin number.

By calling this subroutine, up to five rapidly varying high speed dynamic channels and eight slowly varying dynamic channels can be sampled in approximately one second. Next, using BASIC to address the locations in which the mean values and amplitudes of the current sample set are stored, one can obtain these values to update the bin arrays, as was done in the previous two programs, with data from each of the variables being sampled.

The "Wind-6" program was developed to provide a wind speed-bin analysis on six variables using the high speed sampling routine. The variables chosen are RPM, cyclic pitch amplitude, rotor power output, generator power output, rotor to generator efficiency, and thrust loading. In order to determine instantaneous values of these variables the following signals are sampled using the high speed subroutine. RPM is sampled directly as a slowly changing variable, (i.e. once per second). Cyclic pitch is sampled as a rapidly changing variable (i.e. 128 times per second) and the amplitude read at the stored address. Rotor power is determined by treatment of rotor torque as a rapidly changing variable with mean rotor torque read at the stored address. This value, multiplied by present RPM, provides rotor power. Generator power is determined by treatment of

generator voltage as a slowly changing variable. (i.e. sampled once per second), (voltage squared divided by resistive load equals generator power.) Efficiency is determined from the ratio of generator power to rotor power, and thrust is determined from the mean fore-to-aft yaw post strain-gauge value divided by the moment arm to the rotor shaft.

The "Wind-6" program incorporates all the testing procedures and performance monitoring features of the "Wind-2" program. In addition, atmospheric parameters for the test are input to the program and recorded so that the performance results can be corrected to standard air density conditions for the calculation of nondimensional coefficients.

P4. RPM and Rotor Torque vs. Wind Speed (Fast Sampling Rate)

The "Wind-2 Fast" program was developed to enhance rapid data collection of two significant variables as rapidly changing variables. Although the machine language sampling subroutine, (described above for the "Wind-6" program) was quite fast, the time to sort the data in six bin arrays, to perform the operational testing procedures, and to output performance parameters required overall collection times of approximately 3.5 seconds per sample set. This resulted in rather lengthy tests to accumulate the data necessary to determine meaningful bin values, especially with rapidly changing wind conditions. Thus, the "Wind-2

"Fast" program was developed as an abbreviated version of the "Wind-6" program with all extraneous features deleted. The program is used both to sample mean RPM and rotor power as fast variables (i.e. 128 times per second) and to store these variables in bin arrays. All testing for furl angle, RPM, etc. was removed from the sampling iteration, and video output was reduced to only the two parameters being sampled. This resulted in a 1.4 second iteration time per sample set compared with the 3.5 seconds mentioned previously. Otherwise, this program operates the same as the "Wind-6" program.

P5. Load Amplitudes

The "RPM-6" program, based on the high speed, machine-language sampling subroutine, was developed to determine structural and cyclic pitch response to varying RPM. The program operates in a manner directly analogous to the "Wind-6" program with wind speed bins replaced by RPM bins and performance replaced by structural loads. The RPM bins are 8.8 RPM in width. The variables sampled and stored in the bin arrays are cyclic pitch amplitude; vertical boom bending amplitude; either in-plane bending amplitude or torque amplitude; mean flap bending; flap bending amplitude; and either yaw post bending amplitude or front accelerometer amplitude. Each of these variables are sorted and stored in bin arrays as described above and then the data plotted in graphical form. The only data output during the test is RPM

bin number and warnings if furl angle, RPM or cyclic pitch exceed preset limits. These tests and warnings are the same as described in the "Wind-6" program.

P6. Plotting Routines

Bin array data is stored on the data disks as digital voltage values determined directly from the A/D board output. These values are then converted into appropriate units and plotted on axes stored in binary form on the bin plot disk. In addition, a sample distribution plot is completed showing the log of the number of samples vs. wind speed. The program uses the high resolution graphics feature of the Apple computer system to print the graph in either a standard or expanded scale.

P7. Coefficient of Performance Analysis

The " C_p " program was developed to calculate rotor performance and mean wind speeds based on a given performance test. Bin array data for the desired rotor power test are read into the program along with a standard atmospheric correction factor that is based on ambient pressure and temperature recorded during the data collection.

First, the mean wind speed that occurred during the test is calculated using the number of samples present in each bin. Next, mean wind power during the test is calculated using a corrected air density, based on the atmospheric correction factor for the test period and on the rotor disk area using the equation

$$P = \frac{1}{2} \rho_{\text{corr.}} A_{\text{rotor}} V_{\text{wind}}^3 \quad (74)$$

Then, the wind speed at mean power is calculated. Next mean rotor power over all bins is calculated and an average coefficient of performance for the rotor during the test period is printed. Finally, for each bin, mean rotor power is compared with power available at that wind speed and a plot of performance coefficient vs. wind speed bin is printed.

3.2.4 Full Scale Test Results

The full scale experimental wind turbine was operated for a total of 96 hours between May and October, 1980. A summary of the results that are relevant to the effects of yawed flow on rotor loads and performance follows. The reader is referred to (22), (23) and (24) for more details.

3.2.4.1 Power-Off Analog Data

Figure 32 shows the speed ratio $V/\Omega R$ vs. yaw angle (yaw angle is assumed to be equal to the furl angle.) NACA test results from Figure 23 are superimposed. The full-scale rotor autorotates at lower $V/\Omega R$ than does the model. This is caused by the lower solidity and by the higher Reynolds Number of the full-scale machine. The discontinuity of the model curve at 50° yaw angle, (see Figure 23) interpreted as a stall effect, is not seen for the full-scale rotor. The measured $V/\Omega R$ curve blends into the NACA curve, which is probably representative of 6.26 to 12.1 m/s (14 to 27 MPH)

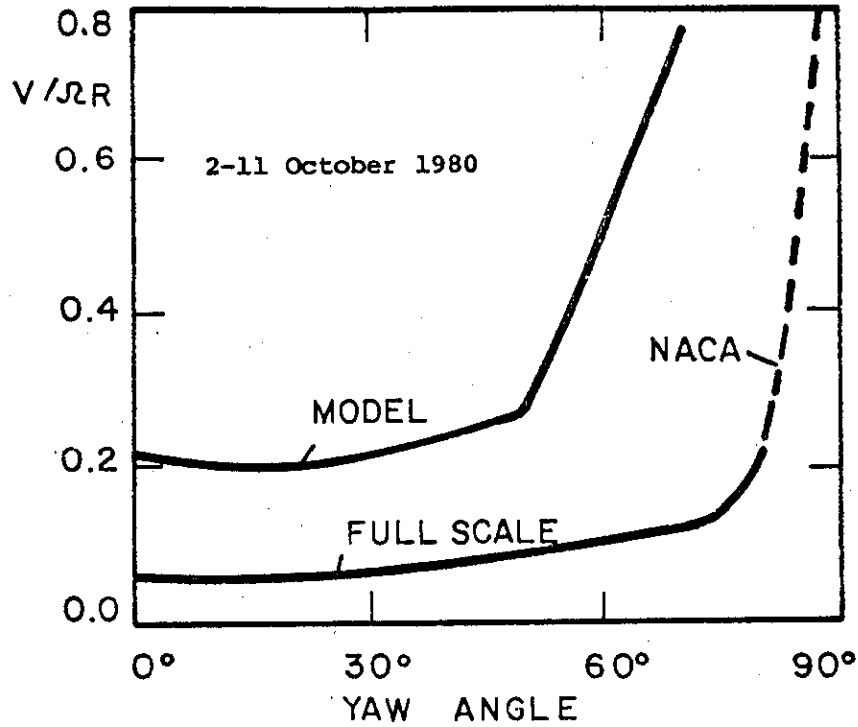


Figure 32. STEADY STATE AUTOROTATION TEST RESULTS FOR MODEL AND FULL SCALE MACHINE

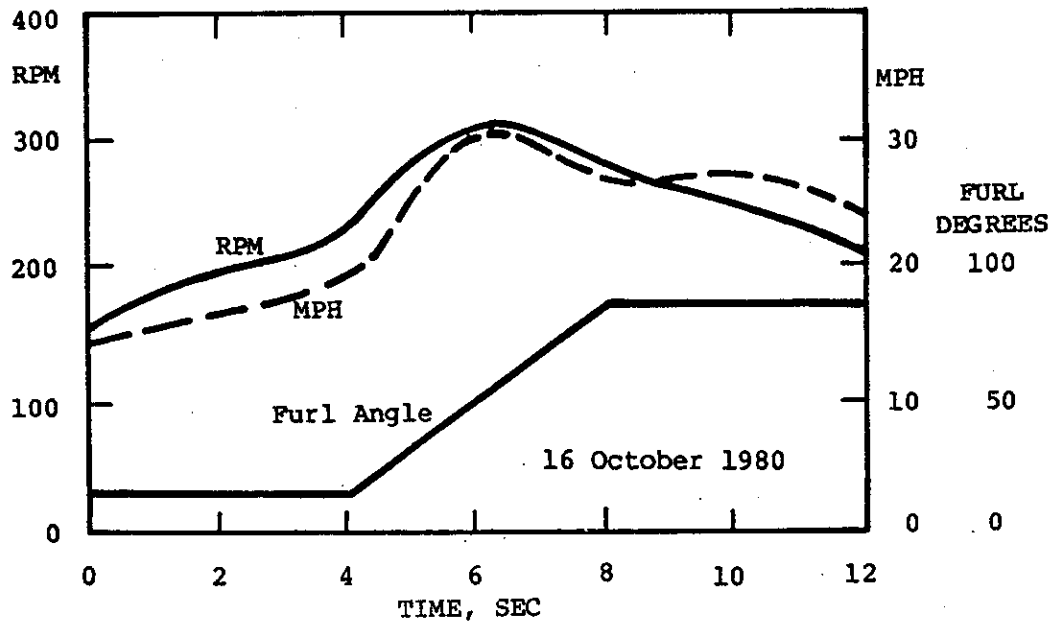


Figure 33. POWER-OFF AUTOMATIC FURLING RESPONSE TO STRONG WIND GUSTS; ROTOR SPEED, WIND SPEED AND FURL ANGLE VS. TIME

and between 160 to 250 RPM.

Figure 32 illustrates the difficulty of a power-off rotor speed control at small yaw angles. For example, a gust at zero yaw angle that doubled the wind velocity would require a change in yaw angle (equal to furl angle) of 70° . The first 30° of yaw angle change would not change $V/\Omega R$ and would be ineffective for the purpose of rotor speed control. In normal operation there is no need for a power-off rotor speed control at low yaw angle. For power-off operation at high yaw angle, envisioned for storm survival, rotor speed control requires only small changes in yaw angle. For example, Figure 32 shows that a doubling of the wind velocity at 60° yaw angle and zero power operation would require a change in yaw angle of only 20° and would be immediately effective. As will be shown, the automatic furl control is not capable of preventing sizeable overspeed from a gust when the unfurled rotor is operated power-off in autorotation. This characteristic is evident from Figure 32. Unfurled power-off operation can and should be avoided except in the case of power failure.

The flap bending amplitude increases along the power-off operational line in Figure 32 from ± 170 Nm (± 1500 in-lb) at 15° yaw angle to ± 350 Nm (± 3100 in-lb) at 80° yaw angle. The in-plane amplitude remains nearly constant at ± 204 Nm (± 1800 in-lb). The stresses in the blade retention are quite low, up to ± 1655 kPa (± 240 psi) for flap bending.

and ± 1310 kPa (± 190 psi) for in-plane bending. The cyclic pitch amplitude is $\pm 2^\circ$ to $\pm 4^\circ$ and is affected by changes in wind direction.

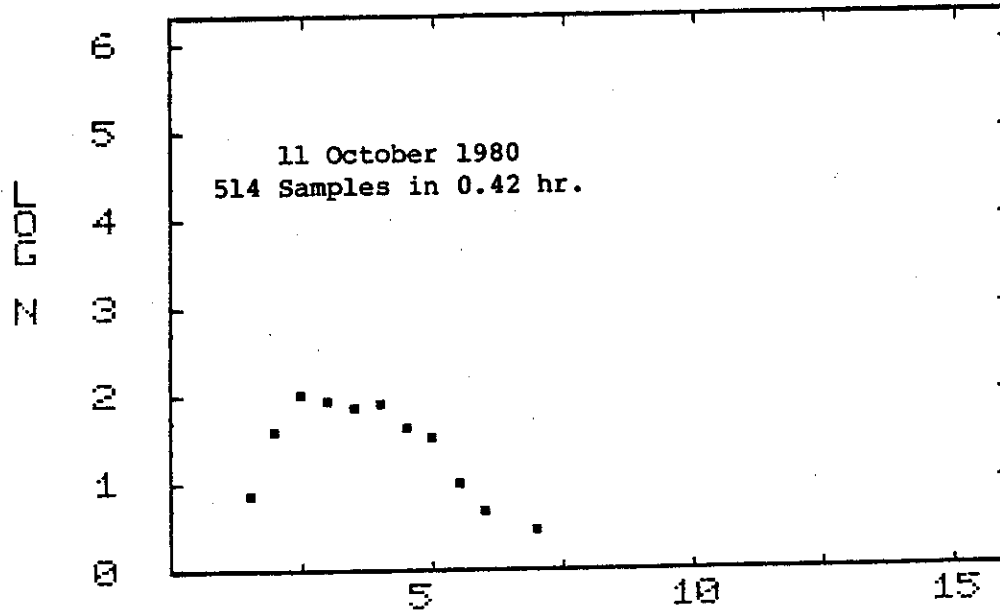
To establish the autorotational characteristics as shown in Figure 32 , some low furl angle tests had to be conducted power-off. The automatic furl control was set to be tripped at 228 RPM. Figure 33 shows an automatic furling process initiated by strong gusts that increased the wind speed at the anemometer location from 6.26 to 14.1 m/s (14 to 30 MPH) in 6 seconds. Automatic furling began when 228 RPM was reached and stopped 4 seconds later, at 85° furl angle. The maximum rotor speed was 310 RPM at 45° furl angle. Without furling, the equilibrium rotor speed for 14.1 m/s (30 MPH) wind velocity is 540 RPM when a tip speed ratio of $\Omega R/V = 16$ is assumed. The maximum flap bending amplitude occurred directly after the start of furling and displays a 2P oscillation of ± 1130 Nm ($\pm 10,000$ in-lb). The maximum rotor torque amplitude which occurred at the same time as the maximum bending was a 4P oscillation with ± 188 Nm (± 1660 in-lb) corresponding to ± 9653 kPa (± 1400 psi) shear stress in the rotor shaft. The maximum rotor thrust, as estimated from a static flap bending moment of 1809 Nm (16,000 in-lb), was about 1424 Nm (320 lb). Such an overspeed condition can occur in power-on operation if the power suddenly fails. The test results prove that the overspeed condition is benign. No damage was

caused to any component, and the dynamic loads and stresses remained well within allowable limits. To cover the emergency case of sudden power loss, the wind turbine must be capable of withstanding, without damage, a 35% overspeed.

3.2.4.2 Power-Off Digital Data

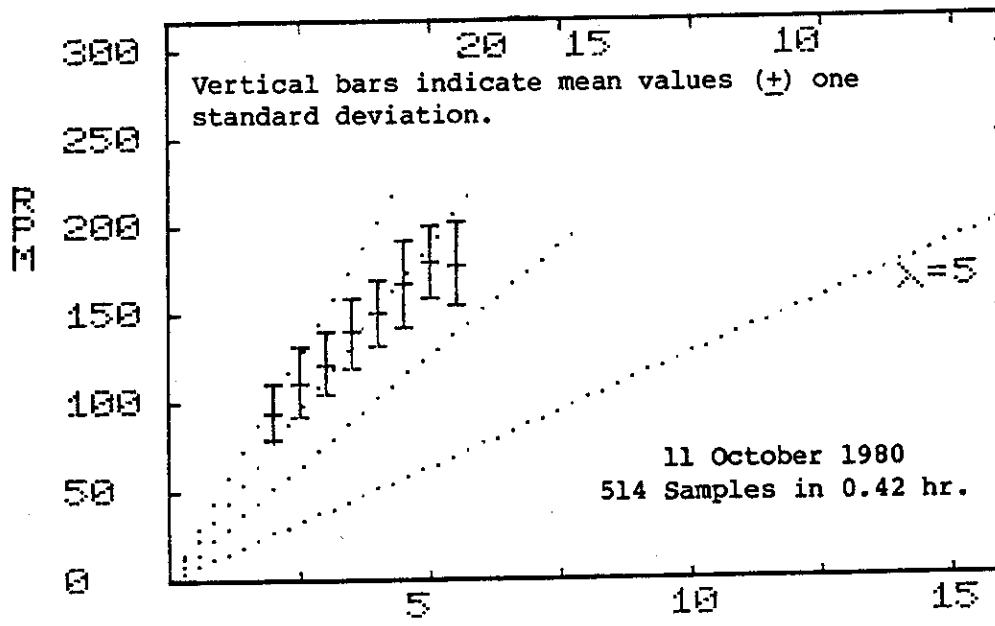
Digital data have been processed to obtain the statistics of aerodynamic and loads parameters during extended runs of one hour or more. Figure 34 shows some results of digital data acquisition for power-off conditions. Figure 34a is for 15° furl angle, and Figure 34b is for 45° furl angle. The first graph in each figure gives log N vs. wind speed bin, where N is the number of samples in the bin. The wind speed bin mid-points correspond to wind speeds of 0.5, 1.0, 1.5, 2.0, etc. meter per second. One or two points farthest to the right have been neglected because they represent very few samples so that the statistics are not meaningful for these bins.

The second graph of each figure gives the mean and standard deviation of the rotor speed for each wind speed bin. The dotted lines represent constant tip speed ratios $\Omega R/V = 5, 10, 15, 20$. It is seen that for Figure 34a, the mean values of the RPM represent tip speed ratios larger than 15 at the low end, and tip speed ratios smaller than 15 at the high end of wind speed and RPM. For a steady wind, the tip speed ratio is constant and, according to Figure 32, it has the value of $\Omega R/V = 16$ for 15° furl angle. For



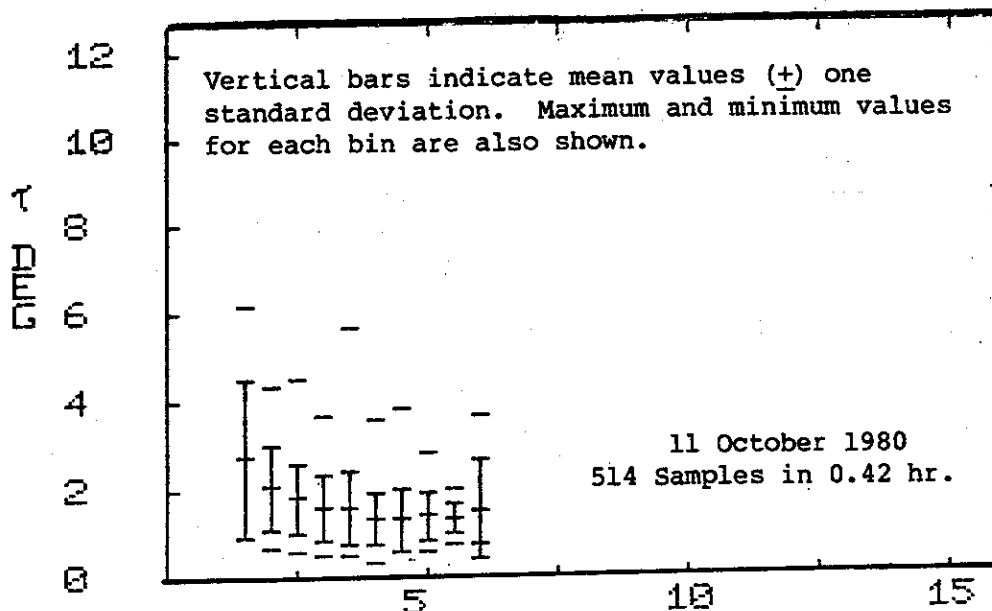
LOG SAMPLES (N) VS WIND SPEED (M/S)

Figure 34a-1. POWER-OFF RUN, SAMPLE DISTRIBUTION, LOG (N) SAMPLES VS. WIND SPEED FOR 15 DEGREE FURL ANGLE



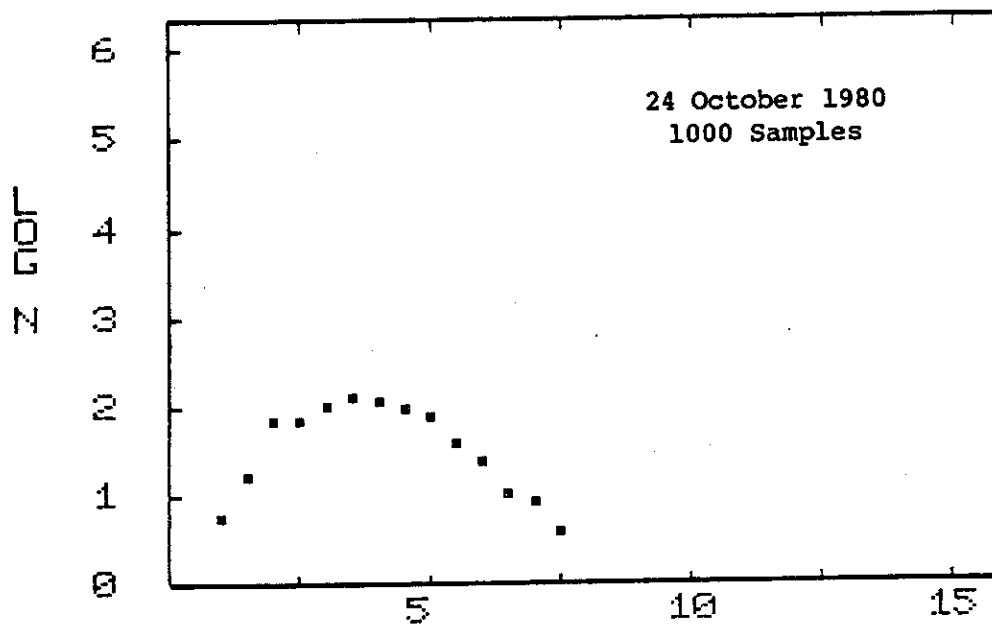
RPM VS WIND SPEED (M/S)

Figure 34a-2. POWER-OFF RUN, RPM VS. WIND SPEED FOR 15 DEGREE FURL ANGLE



CYCLIC PITCH VS WIND SPEED (M/S)

Figure 34a-3. POWER-OFF RUN, CYCLIC PITCH AMPLITUDE VS. WIND SPEED FOR 15 DEGREE FURL ANGLE



LOG SAMPLES (N) VS WIND SPEED (M/S)

Figure 34b-1. POWER-OFF RUN, SAMPLE DISTRIBUTION, LOG (N) SAMPLES VS. WIND SPEED FOR 45 DEGREE FURL ANGLE

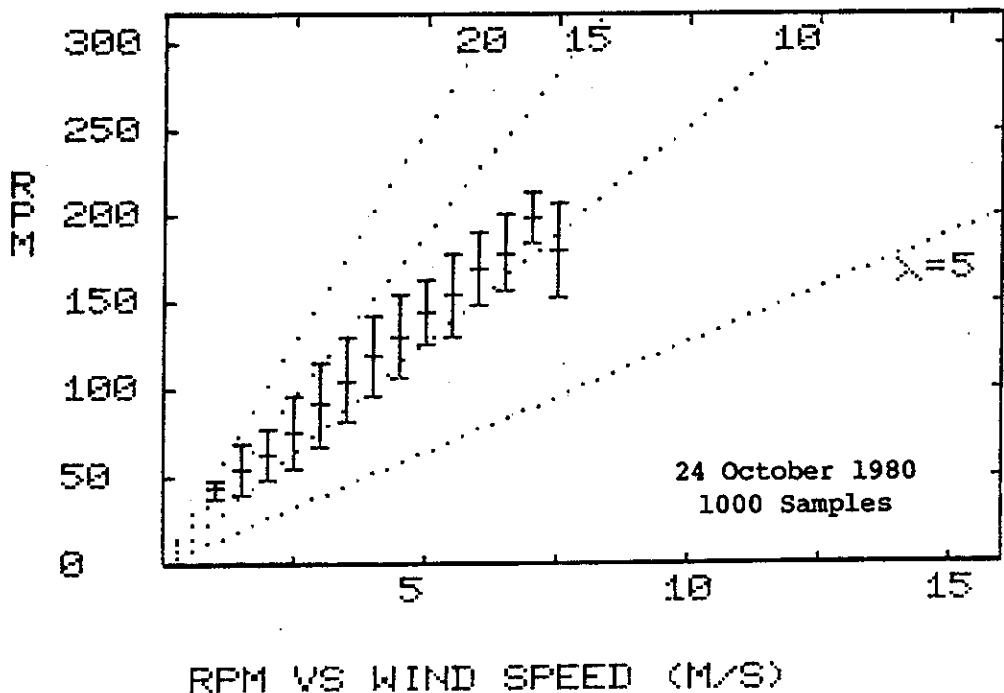


Figure 34b-2. POWER-OFF RUN, RPM VS. WIND SPEED FOR 45 DEGREE FURL ANGLE

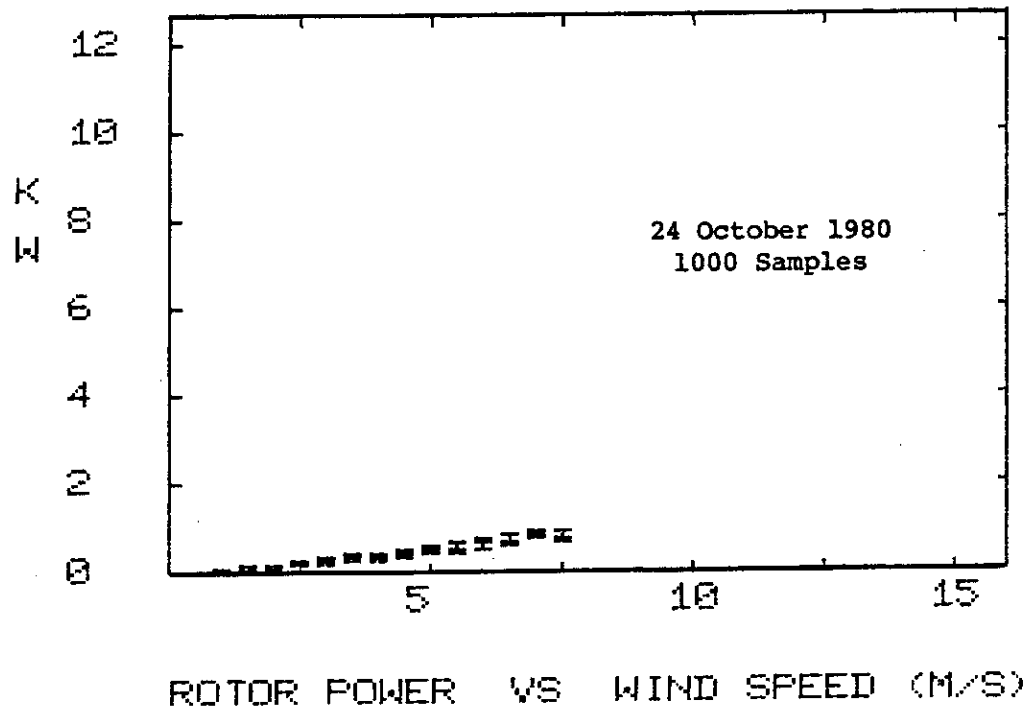


Figure 34b-3. POWER-OFF RUN, ROTOR POWER VS. WIND SPEED FOR 45 DEGREE FURL ANGLE

fluctuating wind speed, the tip speed ratio varies because the inertia of the rotor keeps the RPM lower than equilibrium for gust peaks and higher than equilibrium for gust valleys. If one computes the root-mean-cubed wind speed, which represents the mean power in the wind, one obtains:

$$V_{MP} = \sum (V^3_N) / N^{1/3} \quad (75)$$

Thus, one can obtain, for the corresponding bin, a tip speed ratio close to that found in a steady wind. For example, V_{MP} for the sample distribution of Figure 34a has the value 3.6 m/s (8.1 MPH). It is seen that for this velocity the tip speed ratio is in fact close to 16, while at the low end it is 18 and at the high end it is 13.

The third graph of Figure 34a shows the cyclic pitch amplitude vs. wind speed. The mean, standard deviation and global maximum and minimum for each wind-speed bin are plotted. For low wind speed the mean values are about $\pm 3^\circ$; and for high wind speeds, they are about one-half this value.

Figure 34b, shows a lower tip speed ratio of about 12 for a furl angle of 45° . For steady conditions, the tip speed ratio should be 12.5, according to Figure 32, so that the digital data agree with the analog data. The trend toward higher tip speed ratios at lower wind speed is also

recognizable in Figure 34b, though it is not as pronounced as in Figure 34a. This could be due to the higher number of samples taken, or possibly due to the relative absence of rapid gusts. The third graph of Figure 34b shows the rotor power vs. wind speed. The appreciable rotor power produced at high wind speed and high rotor speed with the generator switched off is either caused by air pumping losses of the generator (windage loss) or by the tightening of the belt from centrifugal forces. Without the belt the rotor power is quite small.

Loads are not presented for power-off conditions, although they have been measured. The power-on dynamic loads at a given furl angle and RPM were found to be either the same or somewhat higher than for power-off and are presented later.

3.2.4.3 Power-On Analog Data

Analog data taken with the oscillograph provide both an estimate of steady state characteristics as well as the time histories of special events.

Figure 35 shows rotor power vs. rotor speed for the unfurled position (actually 15° furl angle) and for 40° furl angle. The data are taken from oscillograph records over periods of several seconds during which the rotor speed was approximately constant. The solid line corresponds to a torque coefficient of $C_Q/\sigma = 0.008$. With two exceptions, the measured rotor power points are reasonably well

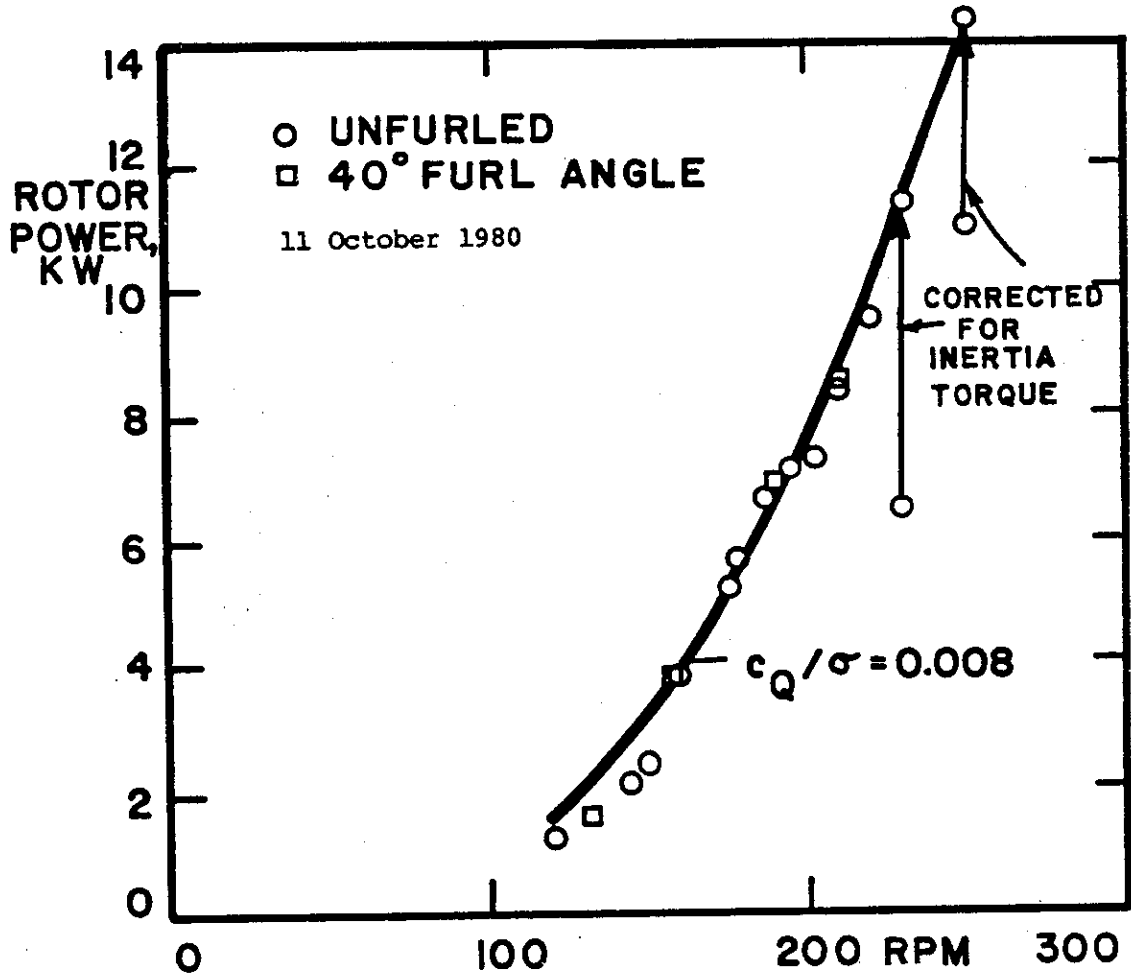


Figure 35. ROTOR POWER VS. ROTOR SPEED; 25/1 GEAR RATIO

represented by the constant torque coefficient, which implies that the rotor power varies with the cube of the rotor speed. The two highest rotor power points are taken during a period of rotor acceleration. If one corrects the measured shaft torque by the inertia torque from the angular rotor acceleration, the corrected rotor power values agree with the cubic power curve. For example, at 250 RPM the acceleration was 15 RPM/sec. or 1.57 rad/sec^2 . The torque correction is, 136 Nm (1200 in-lb), where a rotor moment of inertia of 88 kgm^2 (65 slug ft.^2) is used. The shaft torque is $414 + 136 = 550 \text{ Nm}$ (4880 in-lb). The rotor power computed with this torque is 14.6 kW at 250 RPM rather than 11 kW as found without the inertia torque correction. In the same manner the second point is corrected, which shifts the rotor power from 6.6 to 11.4 kW at 230 RPM.

Figure 36 shows one of many recorded time histories of power-on automatic furling. The furling relay was set at 228 RPM, and a gust of 13.4 m/s (30 MPH) tripped the relay. The rotor speed reached a maximum of 250 RPM, and the furl actuator stopped at 70° furl angle as the rotor speed dropped below 228 RPM.

Figure 37 shows the time history of a power-on gust peaking at 16.1 m/s (36 MPH). The automatic furling device had been switched off, so that the machine was in a manual furling mode. The operator, not expecting the strong gust (which doubled the wind speed at the anemometer site from 8

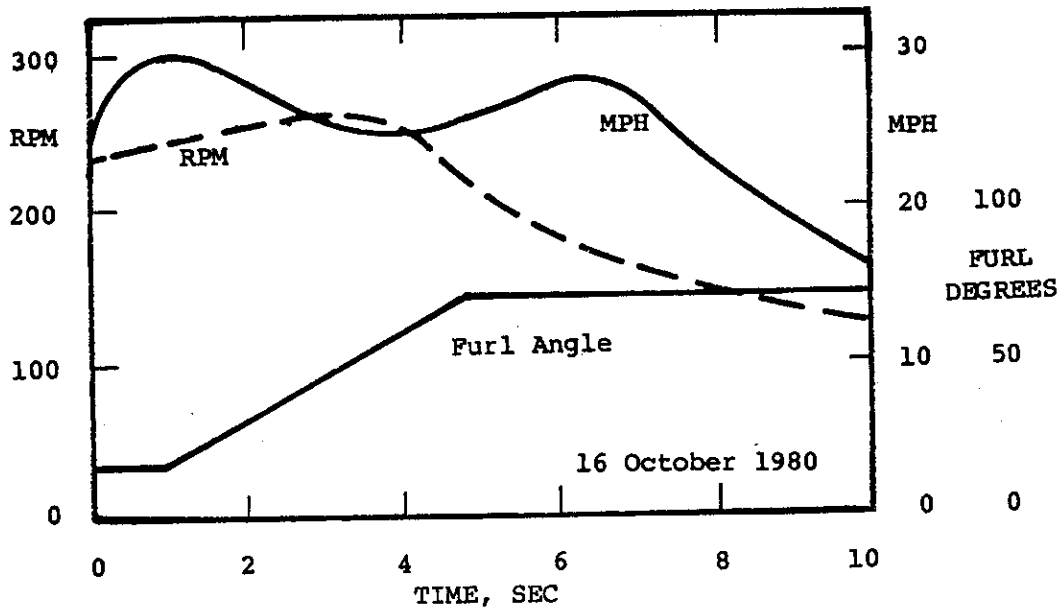


Figure 36. POWER-ON AUTOMATIC FURLING RESPONSE TO WIND GUSTS; ROTOR SPEED, WIND SPEED AND FURL ANGLE VS. TIME

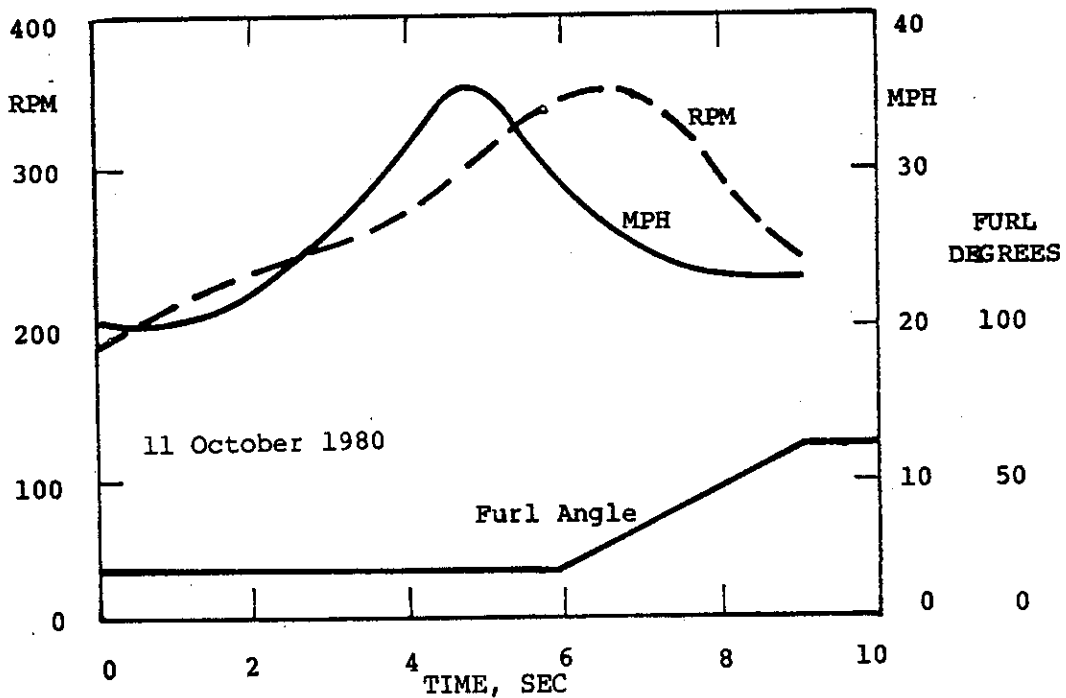
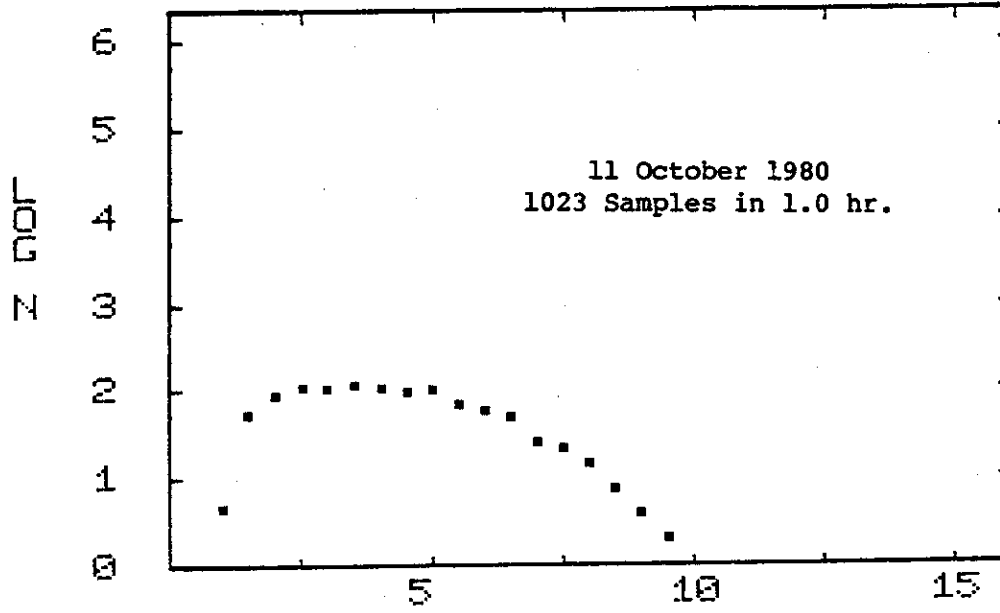


Figure 37. POWER-ON ROTOR RPM RESPONSE TO WIND GUST AND DELAYED FURLING; ROTOR SPEED, WIND SPEED AND FURL ANGLE VS. TIME

to 16.1 m/s (18 to 36 MPH) within 4 seconds), delayed manual furling by about 4 seconds. Furling was too late to prevent a rotor overspeed of 360 RPM which occurred 2 seconds after the peaking of the gust. This is the highest wind velocity and the highest overspeed encountered so far. A careful check after the event revealed no damage. The alternator experienced an overspeed to 9000 RPM. According to the manufacturer it is designed for 10,000 RPM. The tach generator experienced 5400 RPM. It is designed for 4000 RPM. The aerodynamic rotor power, including rotor inertial torque, reached nearly 30 kW. The alternator power output at 9000 RPM was only 5.5 kW which explains the rapid increase in rotor speed. The alternator power probably peaks at about 7000 RPM and then rapidly declines with increasing RPM. During the delayed furling the cyclic pitch amplitude went from 3° to 11° ; the shaft torque 4P amplitude went from 75 to 373 Nm (660 to 330 in-lb) \pm 19,306 kPa (\pm 2800 psi).

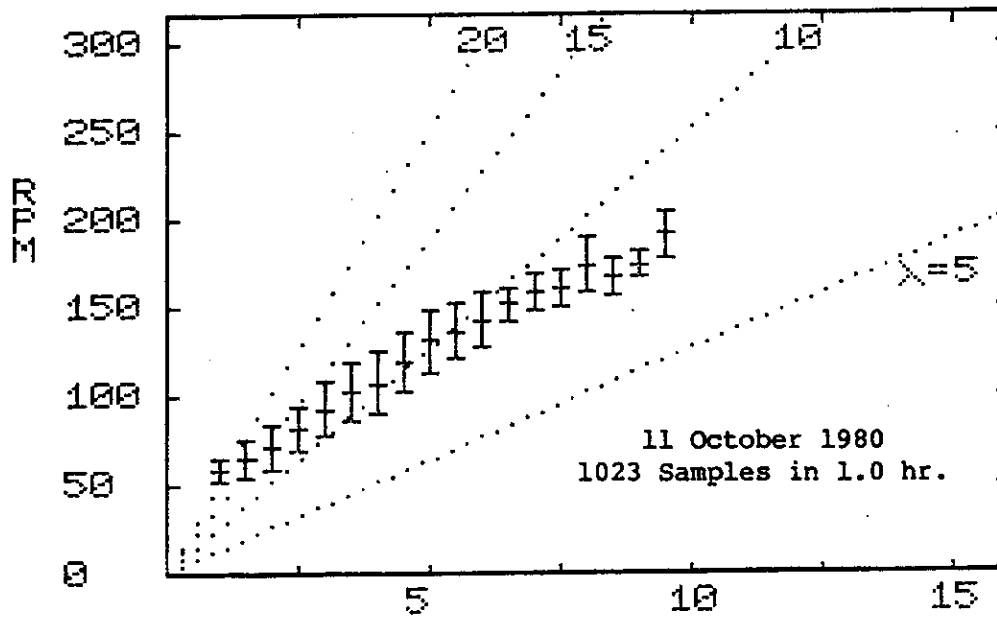
3.2.4.4 Power-On Digital Data

Digital data are used to obtain the "bin" characteristics over extended time periods, as with the power-off data. Figures 38 and 39 show the performance sampling results of power-on runs both in the unfurled position (15° furl angle) and in the 45° furl position, respectively. Winds are from the northwest and west. It was found that the data for the upper end of the wind speed scale were biased if



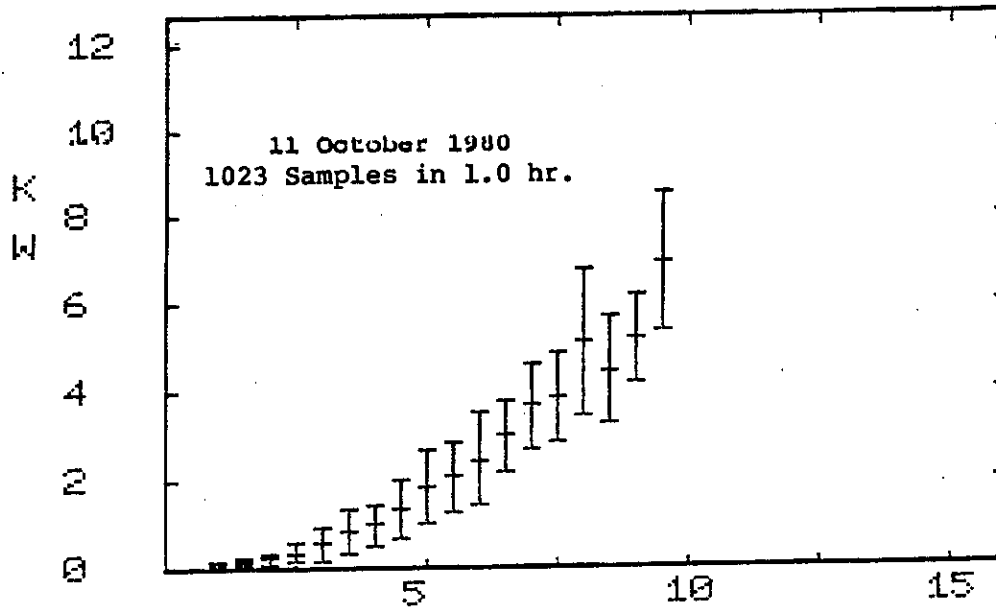
LOG SAMPLES (N) VS WIND SPEED (M/S)

Figure 38a. POWER-ON RUN, SAMPLE DISTRIBUTION, LOG (N) SAMPLES VS. WIND SPEED FOR 15 DEGREE FURL ANGLE



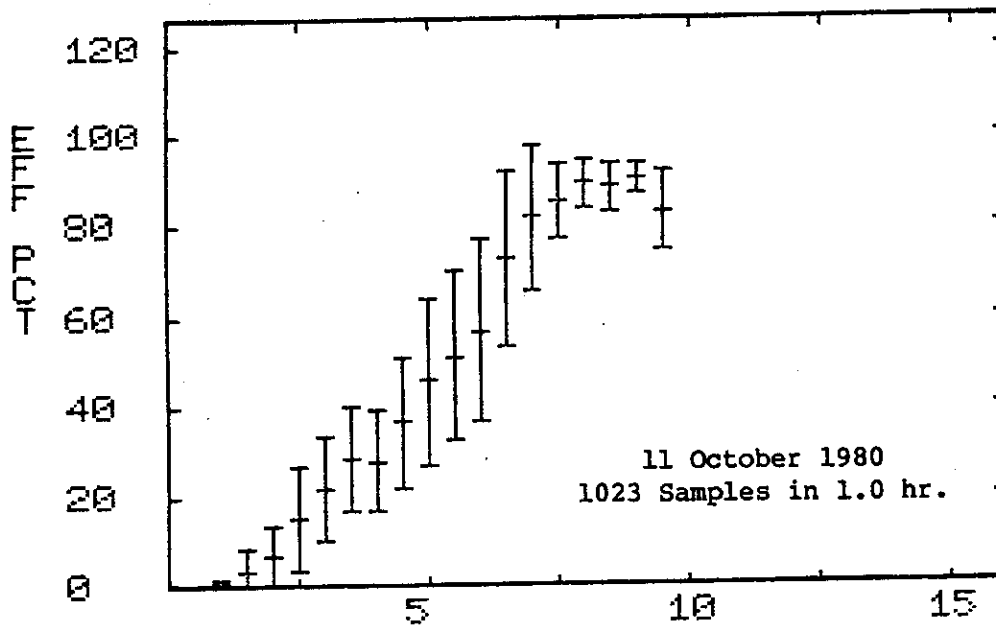
RPM VS WIND SPEED (M/S)

Figure 38b. POWER-ON RUN, RPM VS. WIND SPEED FOR 15 DEGREE FURL ANGLE



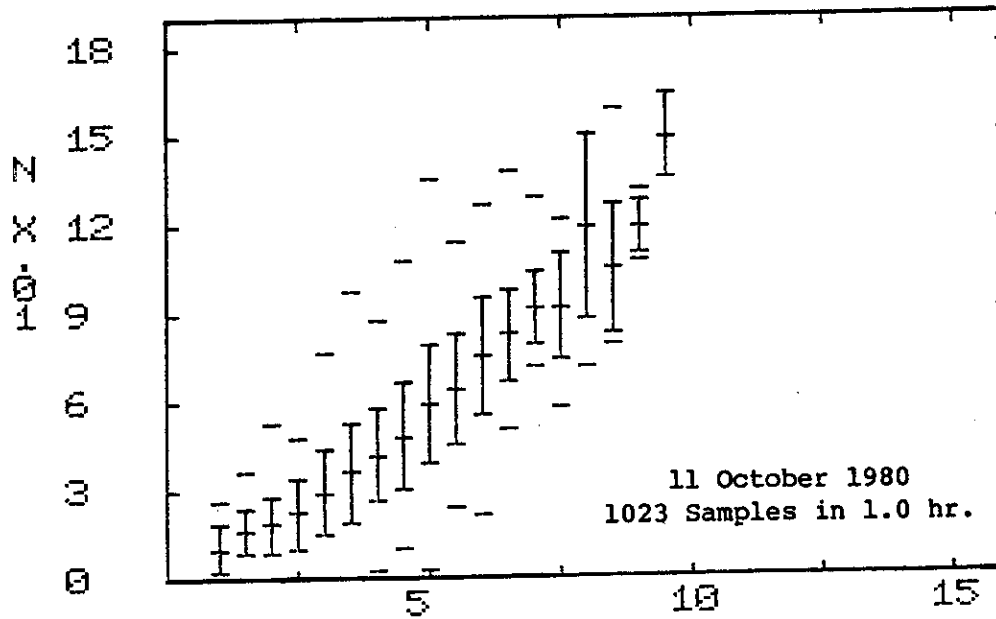
ROTOR POWER VS WIND SPEED (M/S)

Figure 38c. POWER-ON RUN, ROTOR POWER VS. WIND SPEED FOR 15 DEGREE FURL ANGLE



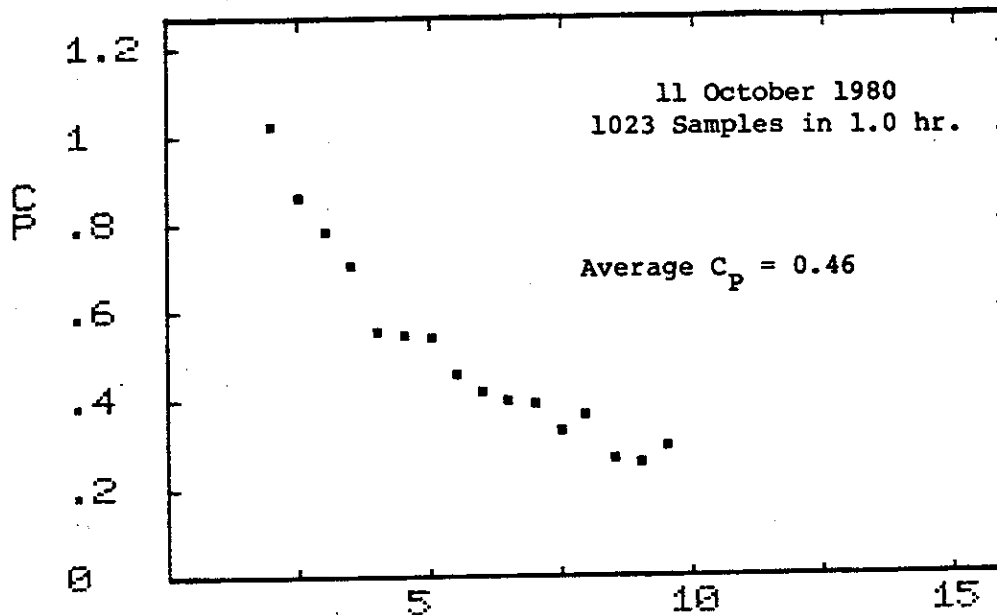
GEN. TO ROTOR EFF. VS WIND SPEED (M/S)

Figure 38d. POWER-ON RUN, GENERATOR TO ROTOR EFFICIENCY VS. WIND SPEED FOR 15 DEGREE FURL ANGLE



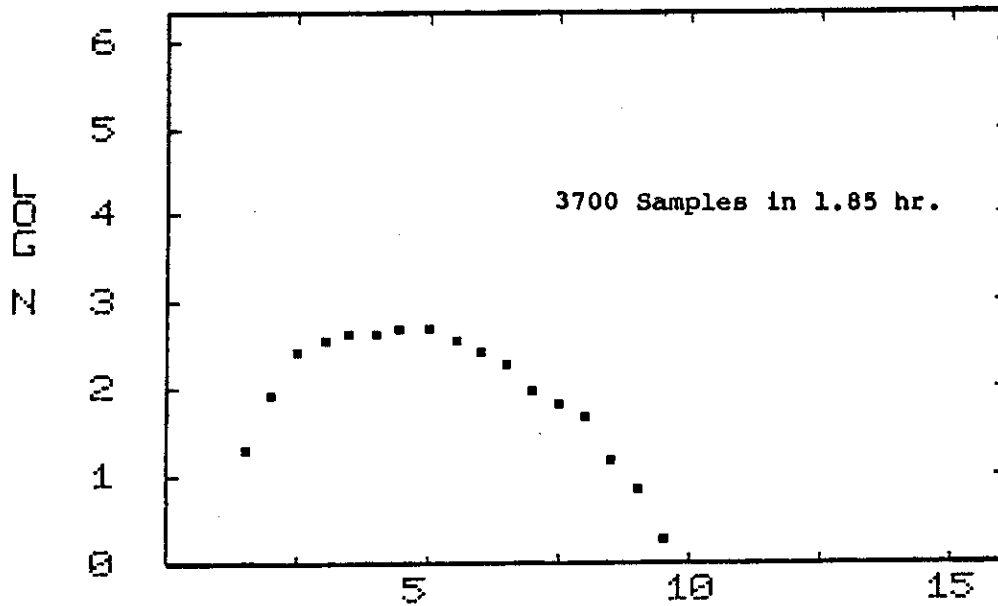
THRUST (N X 0.01) VS WIND SPEED (M/S)

Figure 38e. POWER-ON RUN, THRUST VS. WIND SPEED FOR 15 DEGREE FURL ANGLE



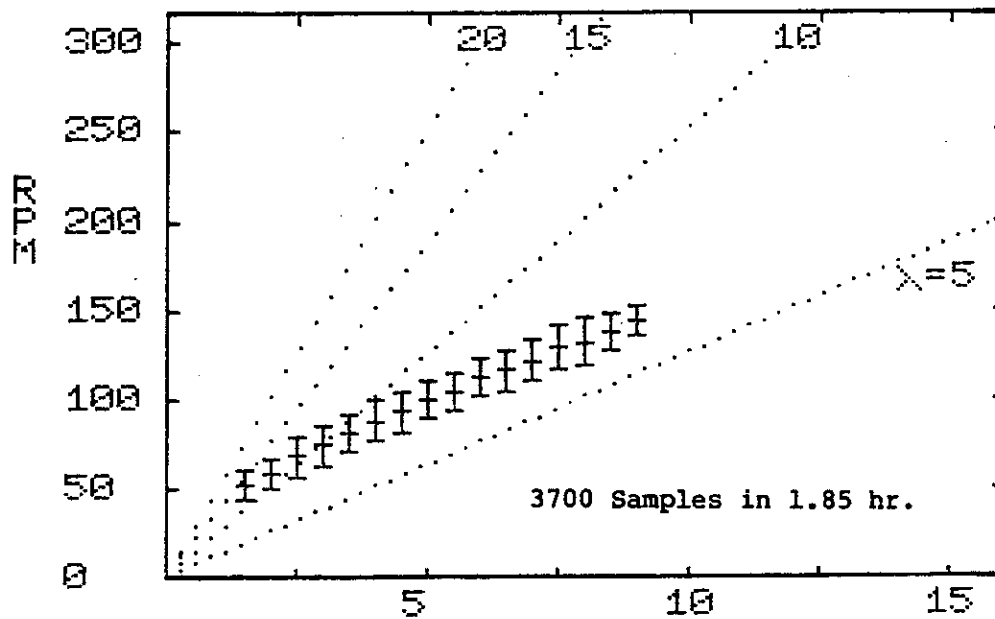
CP VS WIND SPEED (M/S)

Figure 38f. POWER-ON RUN, POWER COEFFICIENT VS. WIND SPEED FOR 15 DEGREE FURL ANGLE



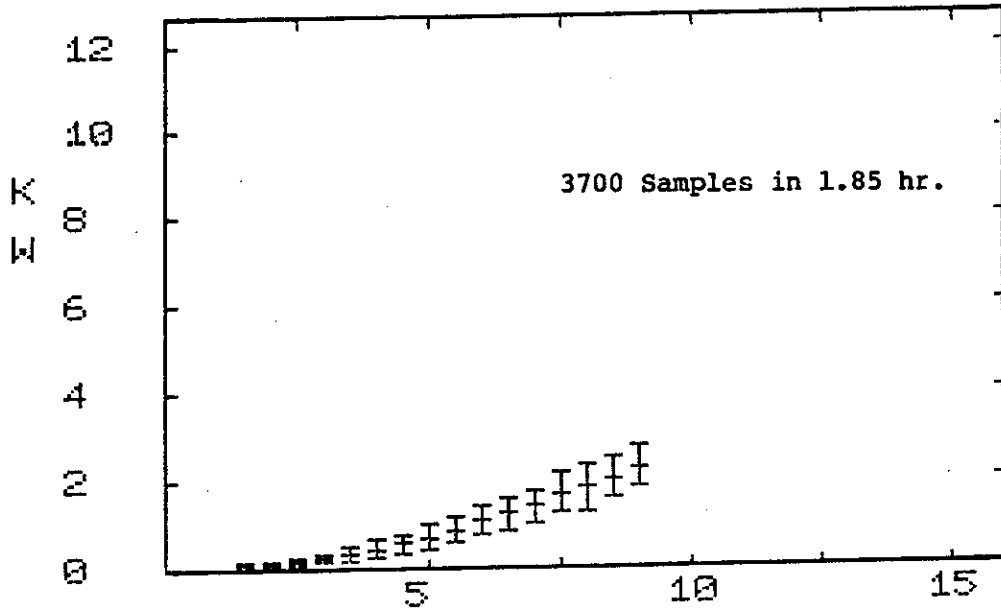
LOG SAMPLES (N) VS WIND SPEED (M/S)

Figure 39a. POWER-ON RUN, SAMPLE DISTRIBUTION, LOG (N) SAMPLES VS. WIND SPEED FOR 45 DEGREE FURL ANGLE



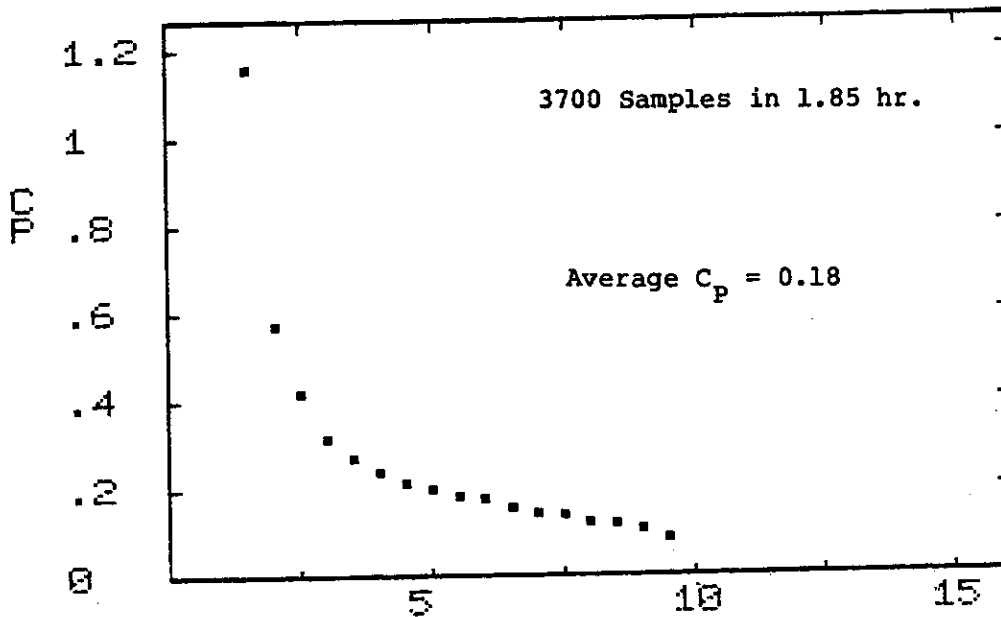
RPM VS WIND SPEED (M/S)

Figure 39b. POWER-ON RUN, RPM VS. WIND SPEED FOR 45 DEGREE FURL ANGLE



ROTOR POWER VS WIND SPEED (M/S)

Figure 39c. POWER-ON RUN, ROTOR POWER VS. WIND SPEED FOR 45 DEGREE FURL ANGLE



CP VS WIND SPEED (M/S)

Figure 39d. POWER-ON RUN, POWER COEFFICIENT VS. WIND SPEED FOR 45 DEGREE FURL ANGLE

frequent automatic furlings occurred during the test run, although sampling was interrupted during furling and unfurling. The two runs presented in Figures 38 and 39 were performed in wind conditions where no automatic furling occurred. Figures 38a and 39a show the sampling distributions which are smooth for both runs. In contrast, sampling distributions taken in south wind were ragged with substantial differences in the number of samples for adjacent wind speed bins. The other measured variables also showed much more scatter and average C_p was substantially lower with southerly winds. Winds coming from the south pass over woods that extend close to the site. The wind from the south is apparently quite turbulent which degrades the rotor performance. All performance data presented are for tests in which the winds were from the open west or northwest. Load data, however, includes tests in which winds were from the south. The point to the farthest right in Figure 38a and 39a has been neglected because it represents too few samples.

Figures 38b and 39b show a similar pattern of RPM vs. wind speed as previously discussed for the power-off test (Figure 34). Toward the high end of the wind-speed scale, the tip speed ratio is lower; and toward the low end of the scale, the tip speed ratio is higher. The rotor power shown in Figure 38c and 39c has a substantial standard deviation in each wind speed bin caused both by the variation of RPM

and by the sensitivity of rotor power to RPM, as indicated by Figure 35. The generator-to-rotor efficiency of Figure 38d shows efficiencies over 0.80 for the higher wind speeds, but very low efficiencies for lower wind speeds. Much of the wind turbine operation will be at wind speeds of 5 to 6 meter per second (11 to 13 MPH) where the efficiency is only 40%. Though the distribution between mechanical and electrical losses is not known, it is likely that most of the loss is electrical and caused by the tuning capacitors needed to increase the peak power output from 5 kW to 8 kW. Obviously a prototype should not use the alternator in its present configuration. Subsequently we will ignore the alternator performance and only present the rotor performance.

Figure 38c shows the rotor thrust in newtons. The rotor thrust is obtained by dividing the yaw-post bending moment by the distance between the upper yaw bearing and the rotor axis, 0.521 m (205 inches). From Figure 38e, the rotor thrust at 9 m/s (20 MPH) is 1200 newtons (270 lbs).

Figures 38f and 39d show the mean aerodynamic rotor efficiency, C_p , for each wind speed bin. At low wind speed, C_p is large; at high wind speed, C_p is small. There are two reasons for this. First, the rotor RPM and rotor power during gusts is lower than for steady state operation, since the rotor speed cannot follow the gust. Second, the rotor RPM and rotor power are higher in lulls than for steady state

operation. The mean aerodynamic efficiency, C_p , has been computed by relating the mean rotor energy during the entire run to the total mean energy in the wind.

$$C_p = \frac{\sum N \bar{P}_R}{\sum N A \rho \bar{V}^3 / 2} \quad (76)$$

where \bar{P}_R is the mean rotor power in each bin, and where \bar{V} is the mean wind speed in each bin.

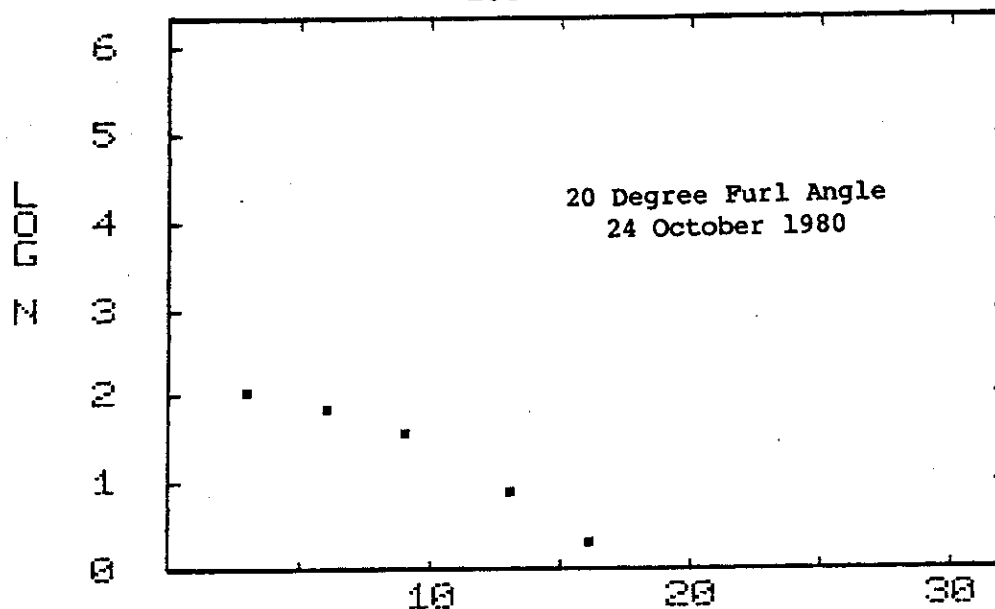
Since the samples are taken at constant time intervals, the above expression is the ratio of the time averaged rotor power over the time averaged wind power. For the test run represented by Figure 38, $C_p = 0.46$; for that represented by Figure 39 $C_p = 0.18$. ρ is the calculated air density for the test run and is obtained by correcting standard sea level air density to a value at the test site based on measured temperature and pressure readings. This correction factor was 0.98 for the run of Figure 38 and 0.959 for the run of Figure 39.

The true relation between the wind speed as measured at the anemometer site and the wind speed at the rotor center is not known and could reduce the cited C_p . If one uses the wind profiles measured at the University of Massachusetts 25 kW wind turbine site (26), one would conclude that the rotor center sees a 5% higher wind speed than the anemometer. The cited C_p values would then be reduced by 15%. In any case,

it appears that the storage of wind energy in the rotor during gusts and its release during lulls is quite efficient. A certain amount of loss as compared to steady state operation is unavoidable since the rotor operates both above and below the tip speed ratio for maximum C_p . This is similar to a constant speed wind rotor, only with less variation in the tip speed ratio.

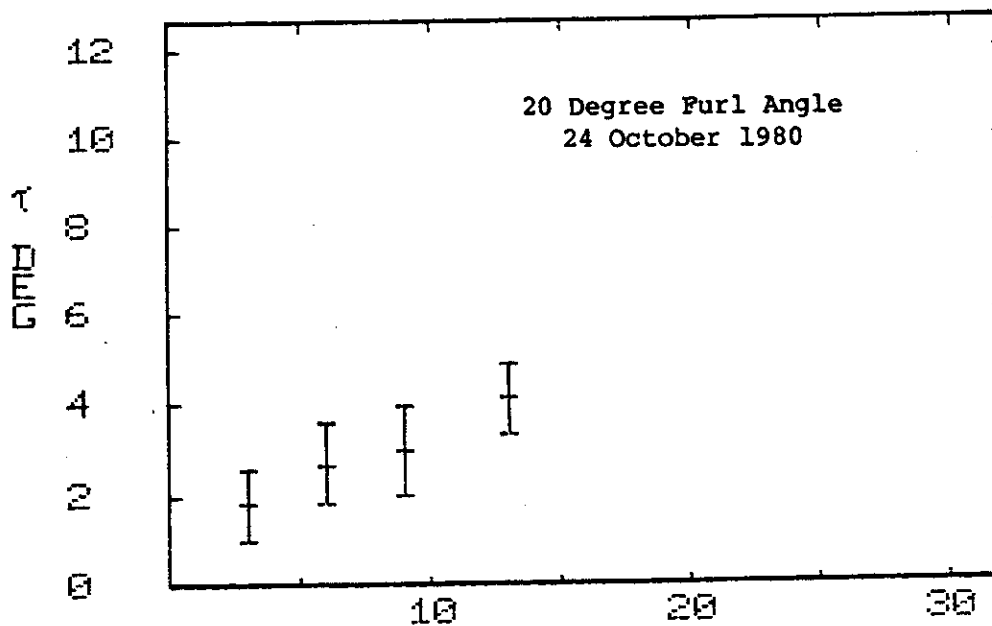
In summary, the measurements have shown that the two-bladed yaw controlled, wind rotor with passive cyclic pitch variation does not degrade turbine performance and may actually enhance it due to the rapid adaptation of the machine to changes in wind direction.

Figure 40 shows, for the 20° furlled position, the digital data correlation between cyclic pitch amplitude and yaw rate. It had been observed that yaw rates in the furl direction (counter clockwise seen from above) cause higher cyclic pitch amplitudes than the opposite yaw rates. The reason for this is that even for zero yaw rate, there is a nominal cyclic pitch amplitude due to velocity gradients over the disk. This nominal value has the same phasing as that caused by a yaw rate in furl direction, so that these two effects superimpose. In the unfurl direction, yaw rate phasing is reversed and dynamic cyclic pitch deflection due to unfurl yaw rate is reduced by the nominal cyclic pitch deflection. This will be discussed further in Section 3.2.5. The digital program differentiates between the two



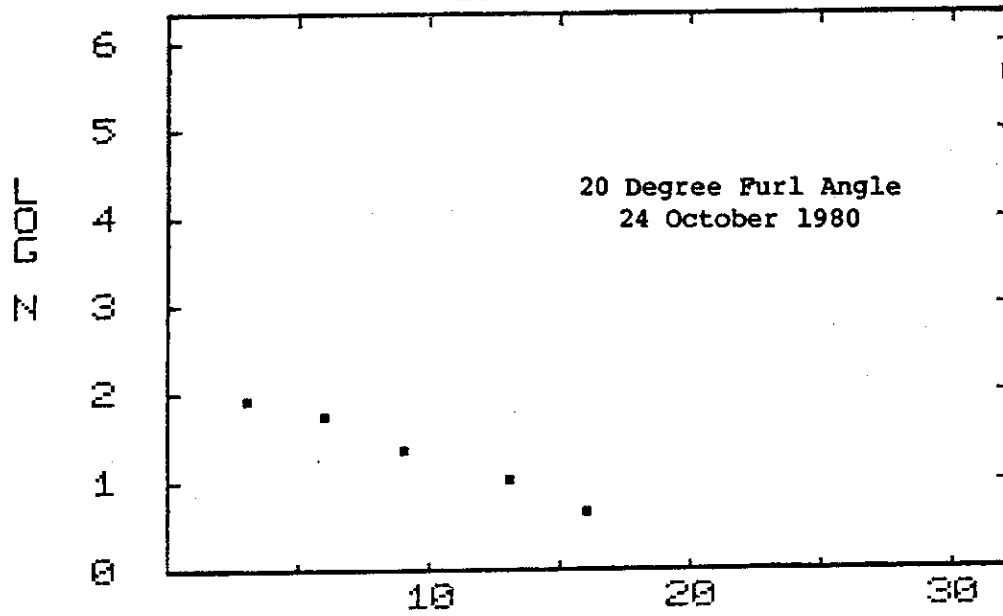
LOG SAMPLES (N) VS YAWRATE (DEG/SEC)

Figure 40a-1. SAMPLE DISTRIBUTION, LOG (N) SAMPLES VS. YAW RATE; MOTION IN FURL DIRECTION



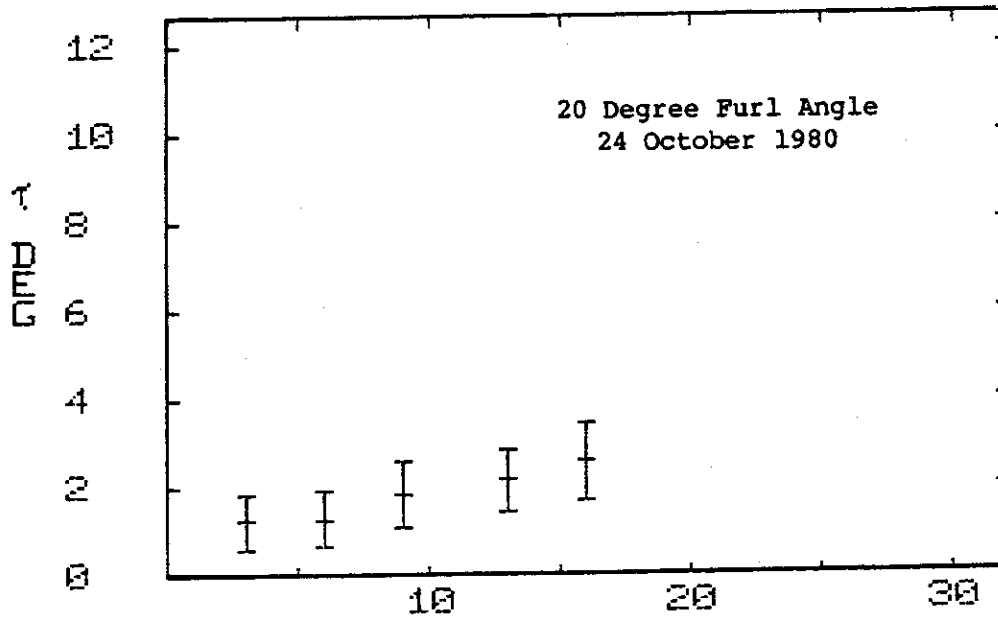
CYCLIC PITCH VS YAWRATE (DEG/SEC)

Figure 40a-2. CYCLIC PITCH AMPLITUDE VS. YAW RATE; MOTION IN FURL DIRECTION



LOG SAMPLES (N) VS YAWRATE (DEG/SEC)

Figure 40b-1. SAMPLE DISTRIBUTION, LOG (N) SAMPLES VS. YAW RATE; MOTION IN UNFURL DIRECTION



CYCLIC PITCH VS YAWRATE (DEG/SEC)

Figure 40b-2. CYCLIC PITCH AMPLITUDE VS. YAW RATE; MOTION IN UNFURL DIRECTION

yaw rate directions. Figure 40a refer to yaw rates in the furl direction. Figure 40b refer to yaw rates in the opposite direction. It is clearly seen that the increase of cyclic pitch with yaw rate is larger for the furl direction than for the unfurl direction.

Figure 41 shows the results of the loads digital program for 30° furl angle. The results for 15° furl angle are nearly identical and are not presented. The fore-to-aft accelerometer data have been omitted since the acceleration amplitude did not exceed ± 0.1 g. The graphs represent volt vs. rotor RPM. The relation between the volt scale and the physical units is noted at the top of each graph. Figure 41a shows the sample distribution which is a smooth curve with two humps. The point to the farthest right represents only three samples and has been neglected. Figure 41b shows the mean flap bending moment. The highest mean value is $4.1 \times 355 = 1455$ Nm (12,873 in-lb). Assuming the aerodynamic center to be at $2/3$ of the radius (at 2.5 meter), the calculated rotor thrust is $2 \times 1455/2.5 = 1164$ N (260 lb) which is close to the rotor thrust of 1200 N (270 lb) obtained from yaw-post bending (Figure 38e) at 9 m/sec (20.1 MPH) wind velocity. Figure 41c gives the flap bending amplitude with a maximum mean value of 276 Nm (2440 in-lb). Figure 41d gives the in-plane bending amplitude with a maximum mean value of 204 Nm (1745 in-lb). Figure 41e shows the bending amplitude for the vertical boom which is equal

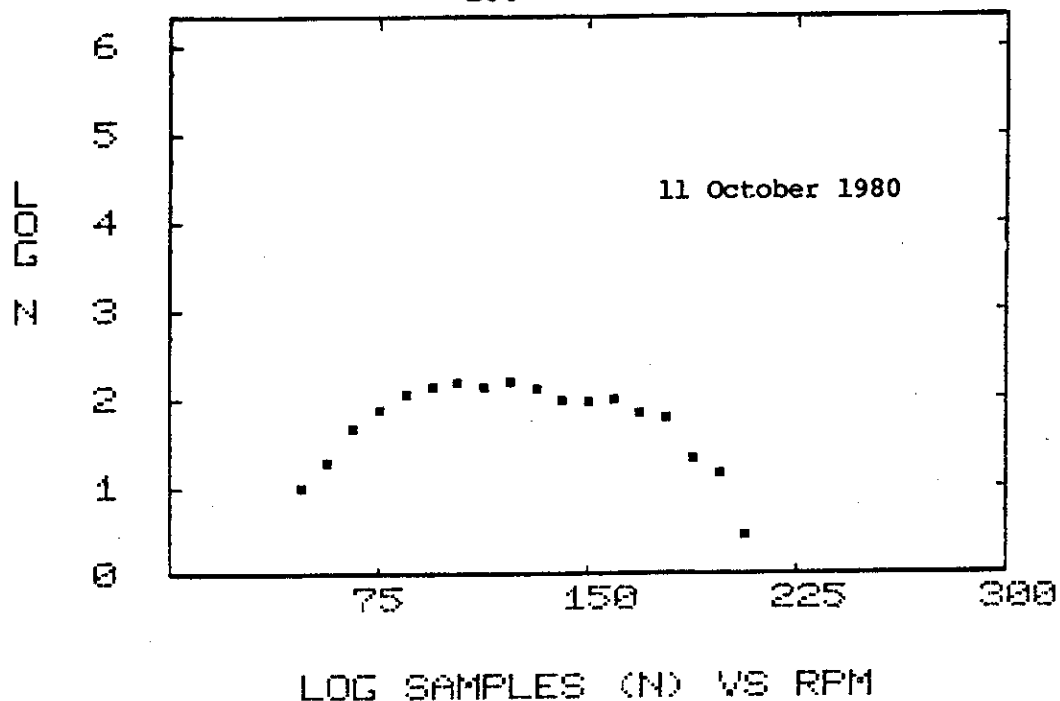


Figure 41a. SAMPLE DISTRIBUTION, LOG (N) SAMPLES VS. RPM FOR 30 DEGREE FURL ANGLE

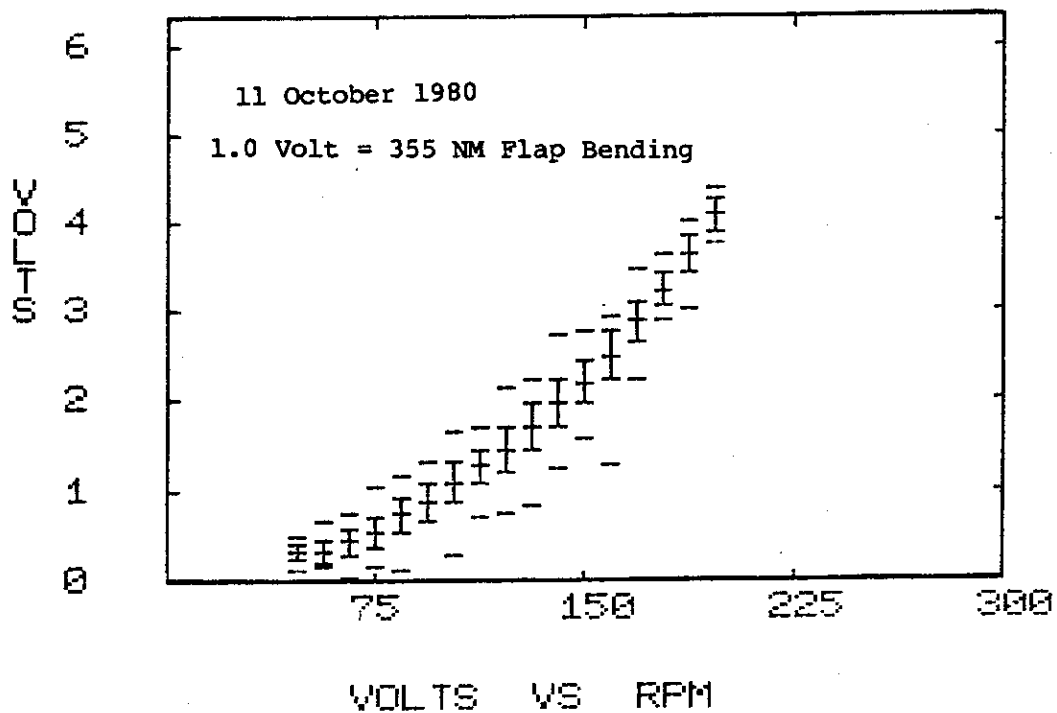


Figure 41b. MEAN FLAP BENDING VS. RPM FOR 30 DEGREE FURL ANGLE

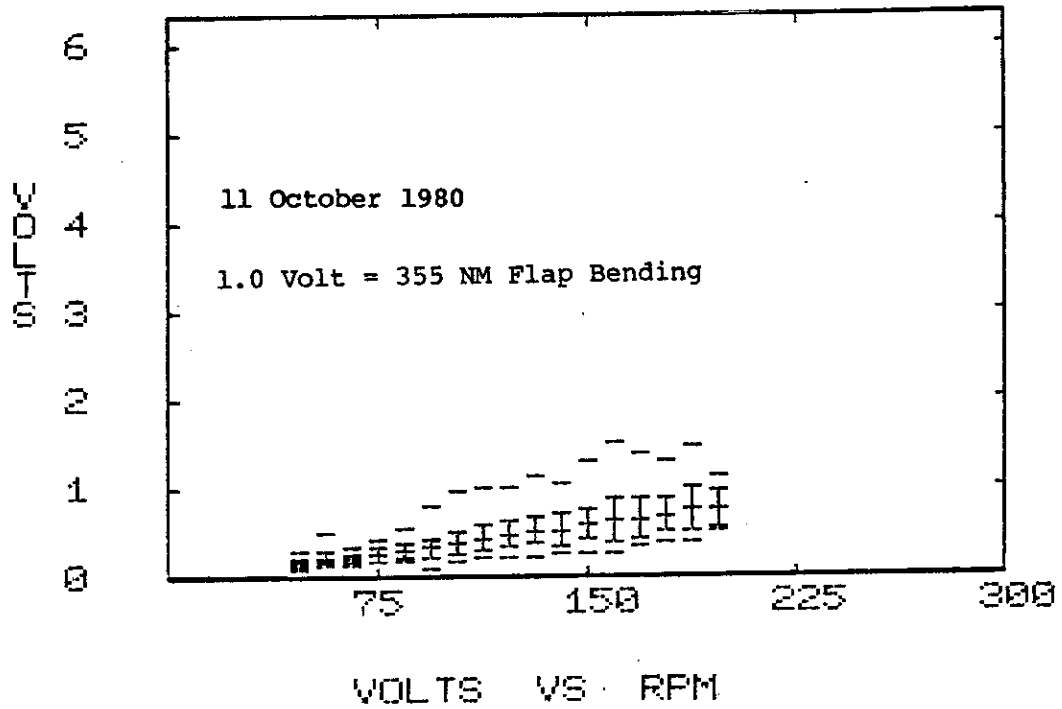


Figure 4lc. FLAP BENDING AMPLITUDE VS. RPM FOR 30 DEGREE FURL ANGLE

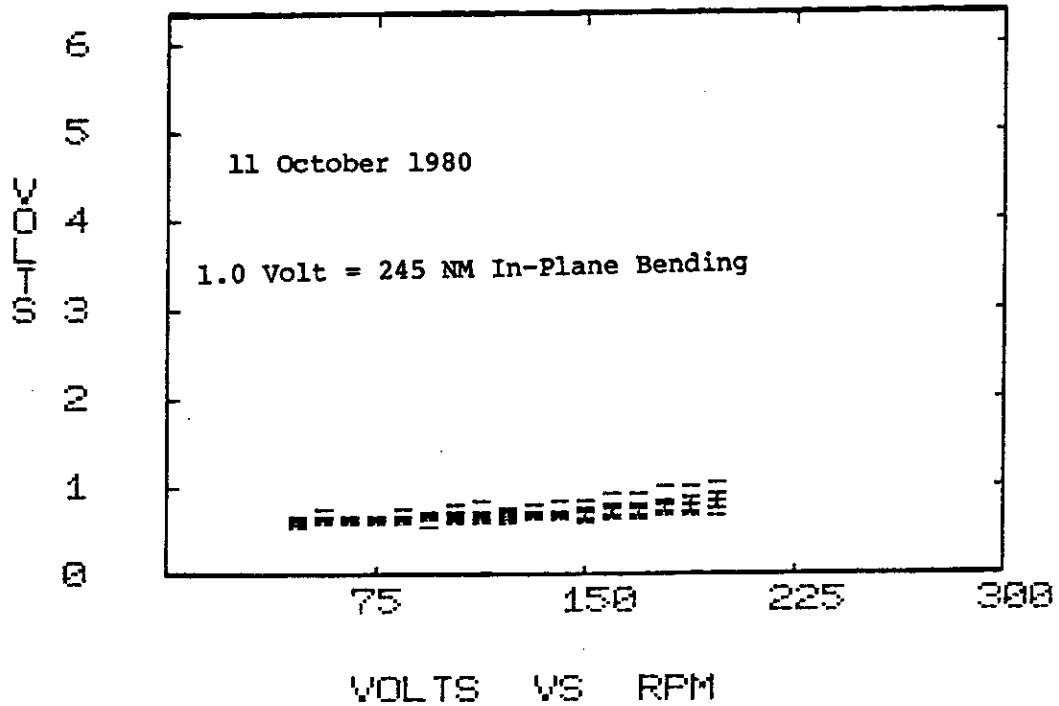


Figure 4ld. IN-PLANE BENDING AMPLITUDE VS. RPM FOR 30 DEGREE FURL ANGLE

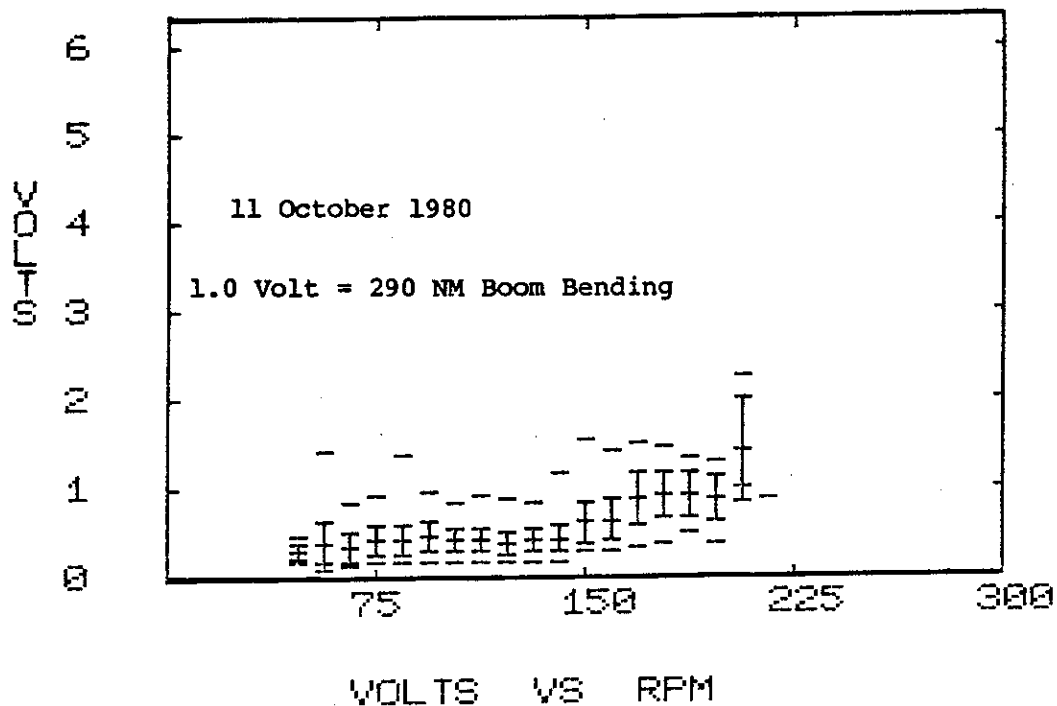


Figure 41e. VERTICAL BOOM BENDING AMPLITUDE VS. RPM FOR 30 DEGREE FURL ANGLE

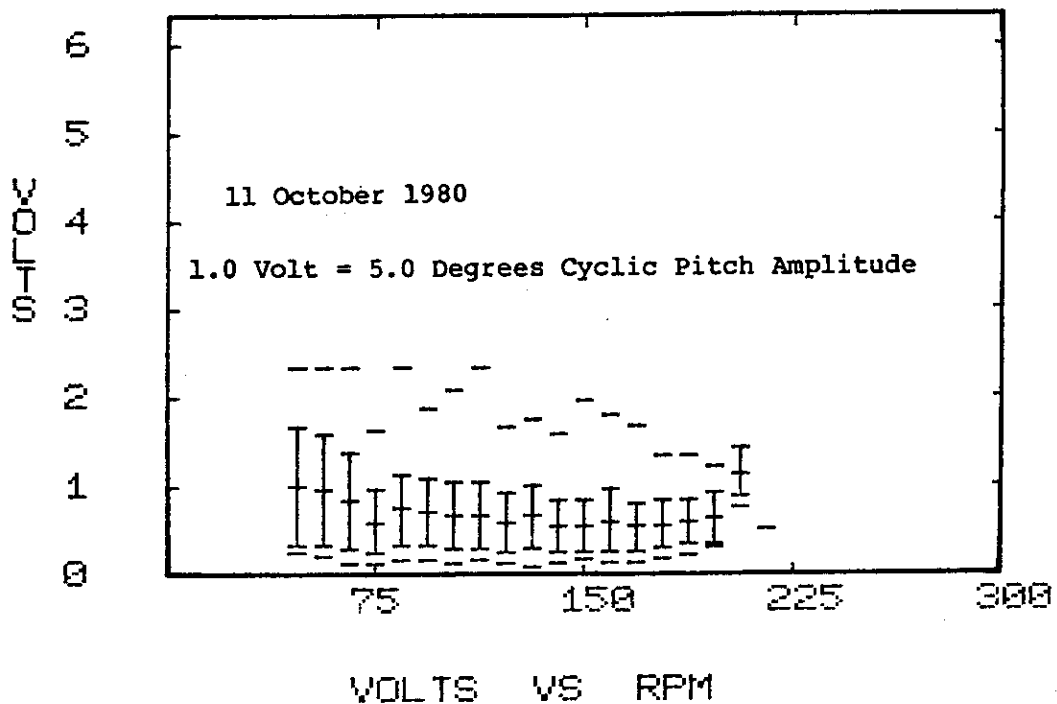


Figure 41f. CYCLIC PITCH AMPLITUDE VS. RPM FOR 30 DEGREE FURL ANGLE

to the bending amplitude of the yaw post at the upper yaw bearing. The maximum for the boom occurs at the vertical 1P resonance, (about 160 RPM) and is 290 Nm (2566 in-lb). These dynamic loads agree reasonably well with the values obtained from oscillograph records. They represent very low alternating stresses, see Table 6. Finally, Figure 41f shows the cyclic pitch amplitude. Its mean is $\pm 5^\circ$ at 50 RPM and decreases to $\pm 3^\circ$ at 200 RPM.

3.2.4.5 Steady-State Loads Survey

More or less steady-state conditions have been identified from the oscillograph records. For such conditions RPM and wind speed change only slightly over an interval of several seconds. From the records taken on September 9, 1980, four such points have been selected at 125, 150, 162 and 171 RPM. The rotor was unfurled (15°). The generator-to-rotor gear ratio was 25:1. The second replacement generator was installed which has a different power-RPM relation than the first replacement generator used for most tests (22). The dynamic loads are not much affected by this difference.

Figure 42 shows the moment amplitudes vs. RPM. The bending moment of the vertical boom is not plotted because it is almost equal to the bending moment of the yaw post. The in-plane blade bending moment is not plotted because it is almost independent of RPM. It is about ± 204 Nm (± 1800 in-lb). (See Figure 41d.) It originates almost exclusively

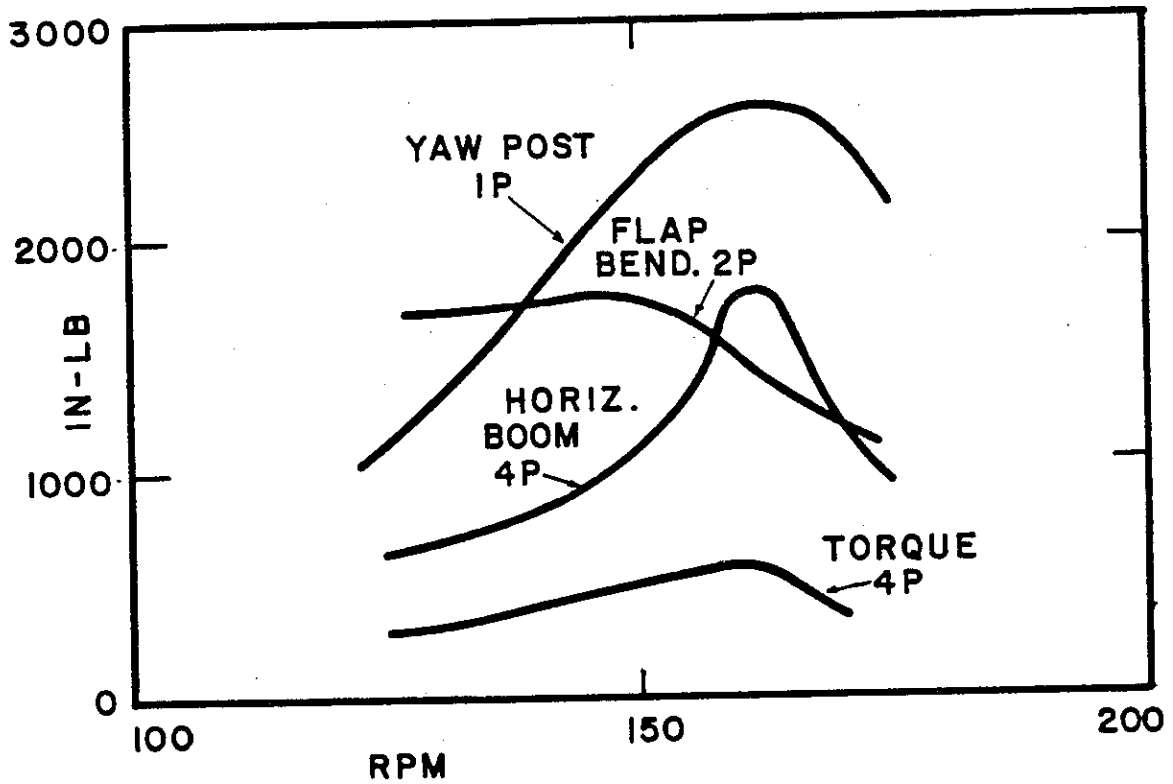


Figure 42. DYNAMIC LOADS VS. ROTOR RPM FOR 15 DEGREE FURL ANGLE

in the 1P gravitational blade moment. As mentioned before, the bending moments are given at the natural reference locations, and not at the location of the strain gauges. The bending moment for the yaw post is taken at the upper yaw bearing, the bending moment for the tail boom is taken at its hinge, and the bending moment for the blades is taken at the rotor center. Figure 42 indicates that all moments peak at about 160 RPM which is the resonance RPM for vertical boom bending. The yaw post and vertical boom oscillate with 1P, as does the in-plane blade moment, not plotted in the figure. The flap bending moment oscillates with 2P, and both the horizontal boom bending moment and the shaft torque oscillate with 4P. This may indicate a coupled mode. The stresses at the strain gauge locations are quite small. Using the values of Table 6 one obtains the maximum alternating stresses for steady conditions shown in Table 7. The maximum steady moments and stresses shown in Table 7 are also based on the following assumptions. The maximum steady yaw post and boom moment originates in the gravity moment of the tail boom of 1696 Nm (15,000 in-lb). The maximum blade flap bending moment originates in the thrust. This can be estimated to be 890 N (200 lbs) thrust per blade acting at 2.54 m (100 inch). This does not include centrifugal relief. The maximum steady in-plane moment originates in the torque per blade of 226 Nm (2000 inlb) and the maximum steady rotor shaft torque is 452 N (4000 in-lb). The steady

TABLE 7
 Maximum Loads for Steady States Unfurled (15°)

SI Units: Nm = in-lb. X 0.113

kPa = psi X 6.9

Component	Maximum Alternating Moment		Maximum Steady Moment		Yield psi
	in-lb.	psi	in-lb.	psi	
Yaw post	2,700	1,100	15,000	6,150	20,000
Tail Boom	2,700	260	15,000	1,420	20,000
Blade Flap Bending	1,900	150	20,000	1,540	20,000
Blade In-plane Bending	1,800	200	2,000	220	20,000
Rotor Shaft Torque	600	500	4,000	3,360	100,000

TABLE 8
Effect of Furl Angle on Loads
SI Units: Nm = in-lb. x 0.113

Furl Angle	RPM	MPH	Yaw Post + in-lb.	Flap Bending + in-lb.	Torque + in-lb.	Power
15°	160	10	3500	1900	600	off
15°	160	21	2800	1900	670	on
15°	200	27	4100	2500	1170	on
30°	160	24	3500	2800	670	on
30°	200	24	3500	3100	1160	on
45°	144	22	3700	4400	670	on
80°	160	27	2800	3100		off

moments are merely rough estimates in order to see the alternating moments and stresses in perspective. For the determination of fatigue margins, both steady and alternating stresses must be considered. The yield limits in the last column are also approximate values. The rotor shaft is mainly stressed from the torque arm of the shaft mounted gear box. As mentioned before, the alternating stress from this source is about $\pm 71,708$ kPa ($\pm 10,400$ psi) in addition to the steady 23,167 (3350 psi) from the torque. In view of the high strength of the rotor shaft, the safety margin is quite high. Both the steady and alternating stress of the yaw post are, in relation to its yield limit, much higher than for the other components. The yaw post gravity moment is really not a steady load since it varies with furl angle so that it will occur with a certain number of load cycles. The yaw post is by far the weakest structural element and will need special attention in a prototype design.

3.2.4.6 Transients Loads Survey

Rather than selecting steady state conditions, the maximum loads encountered for a given RPM are now presented. The effect of furl angle on the loads could not be determined at rated RPM but only at lower RPM values since the high wind speeds required for sustaining the rated RPM at the larger furl angles have not been available. 30° furl angle was tested up to 200 RPM, and 45° furl angle up to 144

RPM. Table 8 gives a comparison of the maximum loads for four furl angles.

The in-plane bending moment remained at about ± 204 Nm (± 1800 in-lb) independent of furl angle or RPM. The vertical boom bending moment is always nearly equal to the yaw post bending moment, while the horizontal boom bending moment is lower. The stresses for the maximum loads are shown in Table 9. Though the stresses are in part substantially higher than for the steady states shown in Table 7, they should be well below the infinite life fatigue allowables, except possibly for the yaw post.

3.2.4.7 Overspeed Conditions Loads Survey

Several overspeed conditions were encountered due to testing outside the normal operation envelope. Figure 33 shows one such overspeed case for which the power-off operation in unfurled condition, led to a 310 RPM overspeed in a strong gust. Only blade flap bending and rotor torque were measured. They reached a maximum ± 1130 Nm ($\pm 10,000$ in-lb) (2P) and ± 188 Nm (± 1660 in-lb), respectively.

Another overspeed case, which reached 360 RPM, is shown in Figure 37. This was caused by delayed furling in power-on operation. The only load measured during this overspeed was the rotor torque amplitude which reached 373 Nm (330 in-lb) at 4P during furling near 360 RPM. The torque amplitude in the unfurled position was only 75 Nm (660 in-lb) despite the high RPM. Table 10 compares the overspeed loads, as far

TABLE 9

Maximum Stresses

SI Units: kPa = psi x 6.9

Component	Stress, <u>±</u> psi
Yaw post	1680
Tail Boom	390
Blade Flap Bending	340
Blade In-plane Bending	200
Rotor Shaft Torque	980

TABLE 10

Overspeed Loads

SI Units: Nm = in.lbf. x 0.113

kPa = psi x 6.9

RPM	MPH	Flap Bending		Torque		Power
		<u>±</u> in-lb.	<u>±</u> psi	<u>±</u> in-lb.	<u>±</u> psi	
200	27	2,500(2P)	190	1,170(4P)	980	on
310	30	10,000(2P)	770	1,660(4P)	1400	off
360	36			3,300(4P)	2770	on

as they are known, with the loads at 200 RPM.

The high 2P flap bending load is probably caused by the coning mode which has a 2P resonance at 280 RPM (22). The high 4P torque may be caused by the symmetrical in-plane mode which, theoretically has a 4P resonance at 220 RPM. However, the resonance is probably modified by coupling with a boom mode (22). Furling at any rotor speed produces rather high 4P torque amplitudes. In the laboratory, it was observed that furling without the rotor produced large 12 Hz oscillations in the boom and in the actuator motor current. These furling actuator oscillations may couple with the symmetrical in-plane mode (torque mode) via the speed reducer torque arm. These oscillations occur only during actuator motion and almost disappear when the actuator motion stops. Even the highest overspeed stress, a torque amplitude of $\pm 19,099$ kPa (± 2770 psi), is small compared to the rotor shaft bending stress of $\pm 71,708$ kPa ($\pm 10,400$ psi), which is caused by the torque arm of the shaft-mounted speed reducer. One-half of the 373 Nm (3300 in-lb) torque is in the blade root, causing a stress of only 1241 kPa (180 psi). Although the overspeed stresses, particularly during furling, are several times higher than the stresses at 200 RPM, they do not represent any structural risk.

3.2.5 Correlation of Theoretical Results With Full Scale Experimental Results

In an attempt to verify the theoretical developments presented in Section 2, it is desirable to correlate the

experimental results of the previous section with the results obtained using both the simplified yawed-flow theory and the dynamic simulation model. These correlations, however, are hindered by numerous factors, so that numerical correlations within a specified error tolerance are difficult, if not impossible. For example, although wind speeds are measured at the tower, actual wind velocities across the rotor disk are unknown, due to vertical gradients in wind velocity and due to turbulence. Since both theoretical models assume a uniform wind velocity over the disk, this is a probable source of large errors. Furthermore, due to the continual variability of wind velocity, steady state conditions are rarely obtained and can only be approximated by review of oscillograph data which makes correlations with theoretical, steady-state data difficult. Finally, when one reviews the assumptions used in the development of both the simple and dynamic simulation model theory, one can at best expect only an approximate agreement between the theoretical and experimental results. In spite of these difficulties, correlation of certain experimental and theoretical results are useful in gaining confidence in the theoretical models developed and in illustrating these limitations.

3.2.5.1 Correlation of Autorotational Data

Figure 43 repeats autorotational tip speed data for the full scale wind turbine as was shown in Figure 32. Also

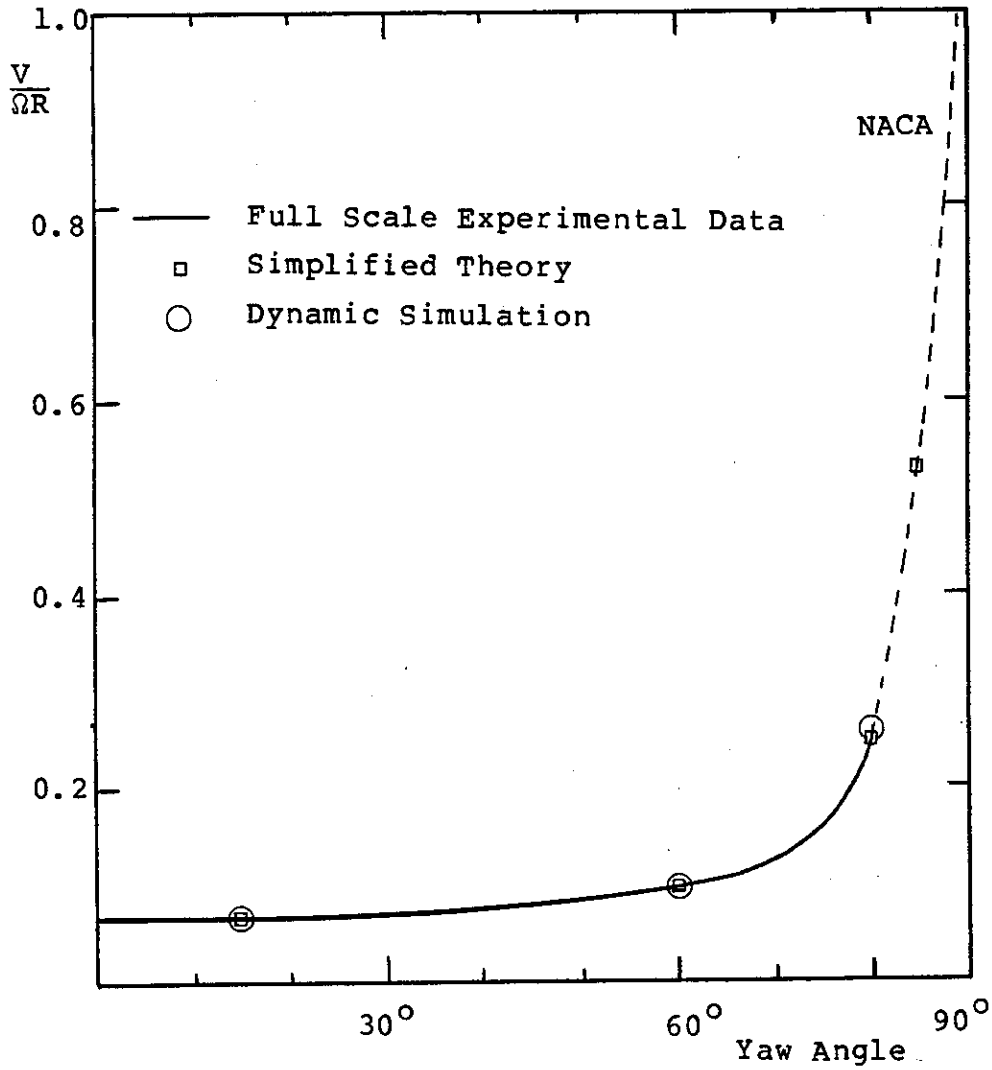


Figure 43. AUTOROTATION DATA CORRELATION FOR THE FULL SCALE EXPERIMENTAL WIND TURBINE

shown are data points from both the simplified and dynamic simulation models for the full scale rotor. The power loss due to friction shown in Figure 34b can be used to calculate that the wind turbine autorotates at a C_Q/σ of approximately 0.001. This value was used for both the simplified and dynamic theories to calculate autorotational states.

The figure shows excellent agreement between the experimental and theoretical data. Full-scale autorotational tests were only conducted up to 80 degree yaw angle due to low wind conditions; therefore, the NACA test results (10) are included for higher yaw angles. Note that the dynamic simulation model is discontinued at 80 degree yaw angle. This is because at 80 degrees the retreating blade experiences angles of attack exceeding 20° on the inboard section which is the assumed stall limit for the simulation model.

3.2.5.2 Correlation of Power-on Data

Figure 44 shows power-on data vs. wind speed for the full scale turbine at 15 and 40 degree yaw angle taken from Figure 35. It is evident that at small yaw angles both the simple theory and dynamic theory correlate well, while at 40 degree yaw angle, either theoretical result overestimates the power produced. The simple theory is worse than the dynamic theory. (Recall that the simple theory has no tip loss correction, which is more significant when the rotor is producing power than in autorotation). The dynamic theory,

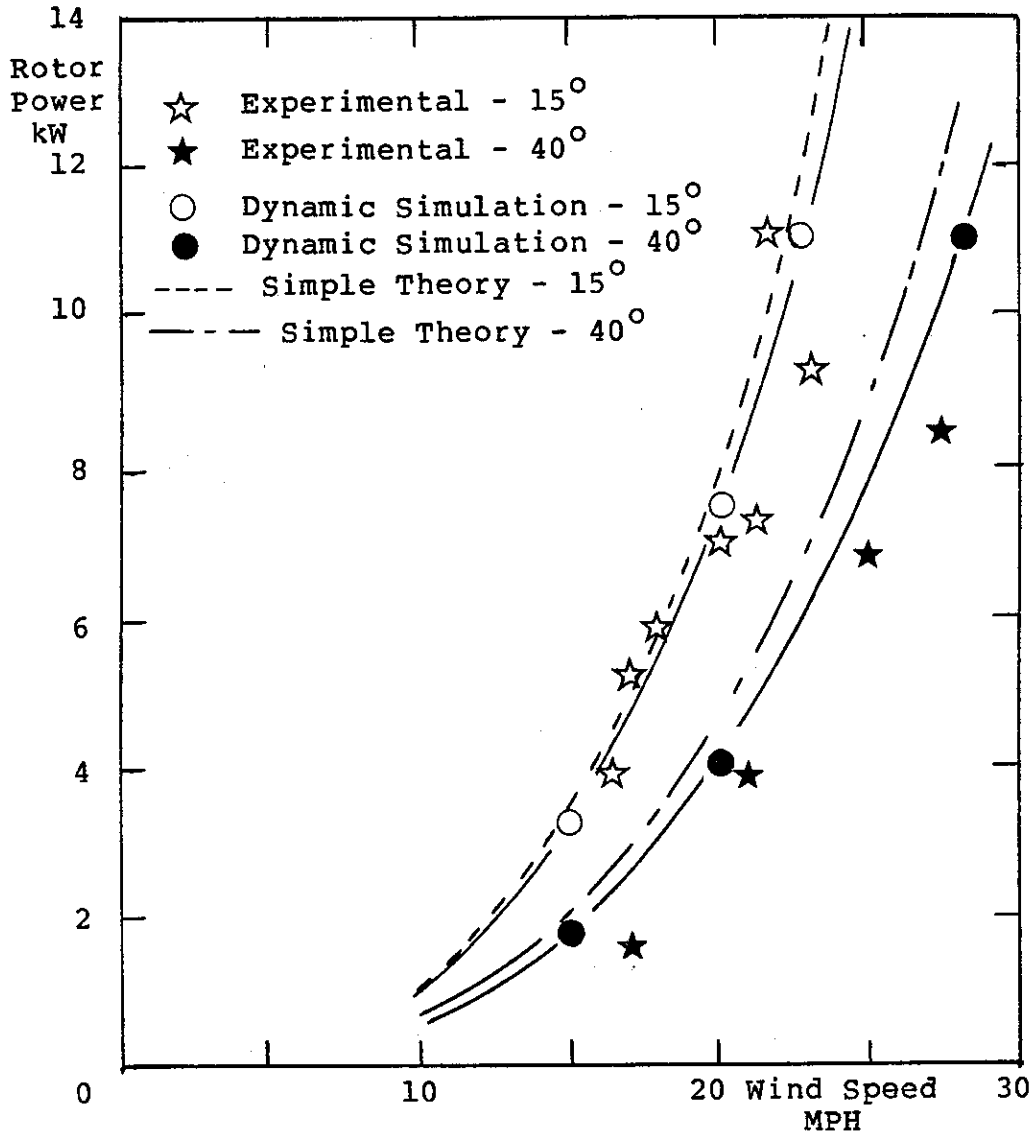


Figure 44. POWER-ON DATA CORRELATION FOR THE FULL SCALE EXPERIMENTAL WIND TURBINE

on the other hand, has a tip loss correction, but does not include hub and shank losses which probably become more significant at higher yaw angles.

3.2.5.3 Correlations of Cyclic Pitch Deflections

One advantage of the dynamic simulation model is that it can calculate cyclic pitch deflections in various operating conditions, which the simplified theory cannot do.

In Section 3.2.4 it was noted that cyclic pitch deflections were affected by yawing direction (furl or unfurl), yaw rate, and RPM. Figures 40a and 40b illustrate the effects of yaw direction and yaw rate while Figure 41f illustrates the effect of RPM.

The dynamic simulation model was run for 20° yaw angle at 146 RPM (minimum RPM for Figure 40 was 120 RPM) with yaw rates of 3 and 9 degrees per second in both directions. Table 11 shows the results of the simulations compared with the average experimental values obtained from Figure 40.

TABLE 11

Effect of Yaw Rate and Direction on τ

Condition	τ Experimental	τ Dynamic Model
Furl Direction, $3^\circ/\text{S}$	$\pm 1.9^\circ$	$\pm 1.1^\circ$
Unfurl Direction, $3^\circ/\text{S}$	$\pm 1.2^\circ$	$\pm 0.2^\circ$
Furl Direction, $9^\circ/\text{S}$	$\pm 3.1^\circ$	$\pm 2.5^\circ$
Unfurl Direction, $9^\circ/\text{S}$	$\pm 1.9^\circ$	$\pm 1.6^\circ$

By extrapolating the experimental data one finds that for zero yaw rate there exists a cyclic pitch deflection larger than one would expect from steady operation at 20° yaw angle. This fact is confirmed by oscillograph records, for which a nominal background cyclic pitch deflection of approximately 2 degrees appears consistently. As a result, one would expect τ values predicted by the dynamic simulation to be less than experimental values by 1 or 2 degrees, as in the case in Table 11.

To further correlate the effects of yaw direction and yaw rate on τ , two simulations were run and correlated to oscillographic records for similar operating conditions. The results are shown in Figure 45. The phase of the cyclic pitch response is determined by using the magnetic pickup on the main rotor shaft, while the cyclic pitch amplitude is determined by the cam follower on the cyclic pitch hinge. The figures illustrate the effects of yaw direction on τ . The phase of the background cyclic pitch deflection is shown by the steady state simulation curves. The amplitude of the steady state value is greater in the full scale turbine, probably due to turbulence and wind sheer effects, but it has the same phase relationship as in the simulation model. From Figure 45a it is evident that the τ response to a yaw rate in the furl direction has approximately the same phase, thereby amplifying the response. Yaw rates in the unfurl direction cause a phase reversal in the τ response and the

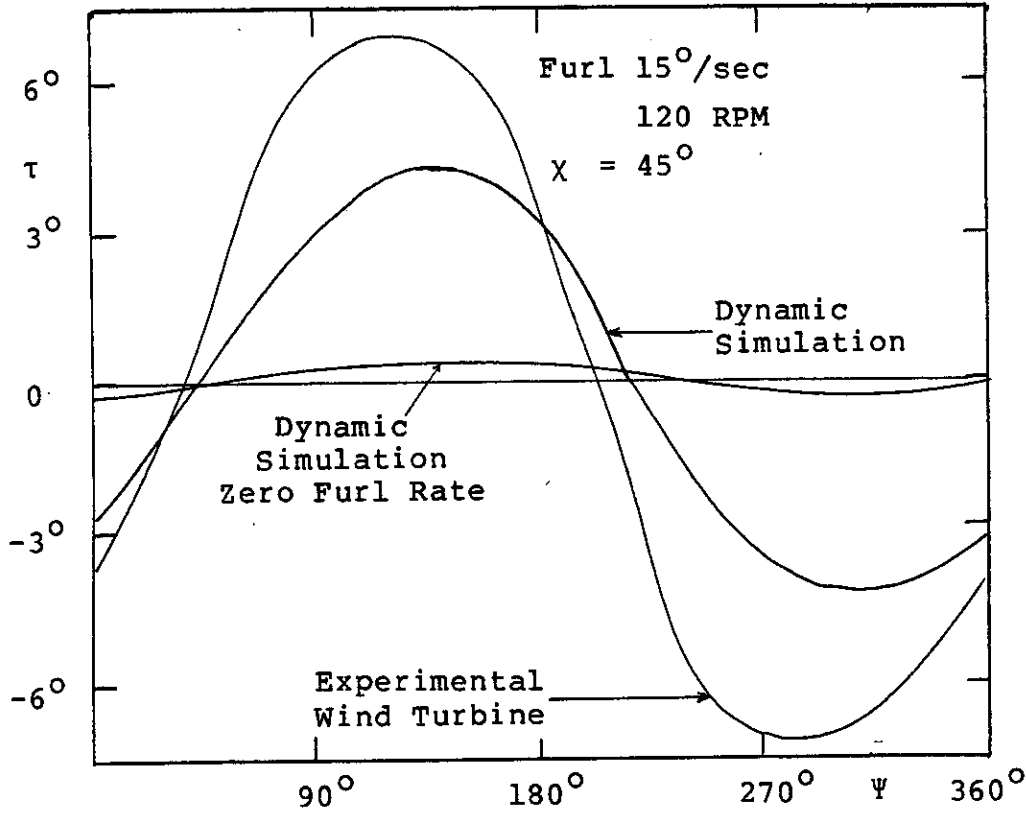


Figure 45a. CORRELATION OF CYCLIC PITCH DEFLECTION, FURL DIRECTION

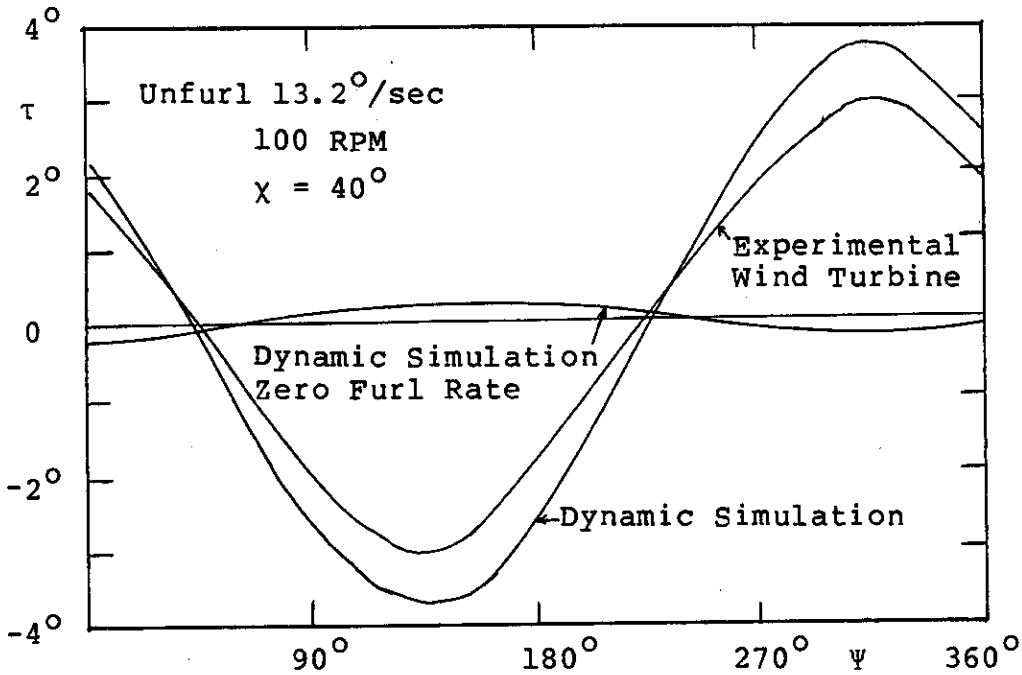


Figure 45b. CORRELATION OF CYCLIC PITCH DEFLECTION, UNFURL DIRECTION

net effect is a reduced τ . Note that these effects are not simply additive. Comparing only the simulation data, the steady τ response is $\pm 0.34^\circ$. If the responses were additive, there would be a difference of 0.68° in peak amplitudes between the furl and unfurl directions. The actual difference is 1.5° , about twice that value. This explains why the simulation for the unfurl direction more closely approximates the experimental data, while the simulation for the furl direction is underpredicted by more than the 1 or 2 degrees background deflection. In general, one may conclude that the dynamic simulation correctly predicts phase relationships and cyclic pitch response to yawed flow conditions and yaw rates, provided that corrections are applied to account for the background cyclic pitch due to factors not considered in the simulation model, such as wind shear or turbulence.

As mentioned above, cyclic pitch deflections are also affected by rotor RPM, as shown in Figure 41f. The dynamic simulation was run at 40° yaw angle at rated power, (230 RPM) and at 118 RPM, power-on, and in steady-state conditions. A yaw rate of 25° per second in the furl direction was applied, and the τ response recorded. The results are shown in Table 12.

TABLE 12

Effect of RPM on τ
 Simulation Yaw Angle = 40° ; 25°
 Per Second Furl Yaw Rate Applied
 After One Revolution

	RPM = 230	RPM = 118
+ τ	3.9°	6.6°
- τ	-4.8°	-8.3°

Note: If furl rate were expressed nondimensionally based on tip speed there would be no change in τ .

There is approximately a 70% increase in τ at the lower RPM, which confirms the trend shown in Figure 41f. (One would expect only a trend correlation in this comparison due to the numerous variables averaged into the RPM bin data.)

3.2.5.4 Correlations of The Effects of Yaw Angle On C_T/σ and C_Q/σ

Both the simple theory and dynamic simulation predict that C_T/σ is approximately constant with yaw angle, for constant C_Q/σ , up to yaw angles of at least 60 degrees for the experimental wind turbine (see Table 1). Since the wind turbine operates power-on at a constant C_Q/σ of 0.008, it is of interest to compare the data of Table 1 with experimental power-on data. Figure 41b shows flap bending deflection at a furl angle of 30 degrees. The maximum thrust was calculated previously to be 1164 N (260 lb) at 197 RPM. The C_T/σ value for this case, using corrected air density, is 0.107. The same methodology is used to calculate C_T/σ at other rotor speeds. These are recorded in Table 13.

TABLE 13

C_T/σ Comparisons for $C_Q/\sigma = 0.008$

Yaw Angle Degrees	RPM	Experimental Wind Turbine	Simple Theory	Dynamic Theory
15	75	0.106		
15	150	0.108		
15	159	0.112		
15	178	0.110		
15	Avg.	0.109	0.112	0.102
30	75	0.097		
30	150	0.099		
30	178	0.104		
30	197	0.107		
30	Avg.	0.106	0.112	0.101

Note 1. Higher yaw angle tests not available.

Note 2. Results for the dynamic theory showed C_T/σ to be independent of RPM. The experimental variation of C_T/σ with RPM is most probably due to unsteady effects and too few samples.

Figure 46 shows a similar plot for a furl angle of 15 degrees. C_T/σ is again calculated and recorded in Table 13. Finally, C_T/σ from Table 1 is recorded for 15 and 30 degree yaw angles for power-on conditions. (Note that, although not strictly identical, furl angle and yaw angle can be assumed equal with little error due to the large lifting area of the tail vane.)

The table shows that for the two angles tested, C_T/σ is independent of yaw angle and falls between values predicted by the simplified theory and the dynamic simulation. The simplified theory tends to slightly overpredict the calculated values from the flap bending data. One should temper these numerical correlations with the restrictions and the assumptions used in calculating thrust forces based on flap bending data.

3.2.6 Applications of the Theoretical Models

As discussed previously, the simplified theory can be effectively utilized to find approximate steady-state performance points which can be used as inputs to the dynamic simulation in order to save computer time. In addition, the simplified theory can be used to estimate performance, to identify trends and to determine the effects of pitch angle, solidity ratio, drag coefficients, lift curve slope and operating tip speed ratio on performance as a function of yaw angle. The previous sections have shown

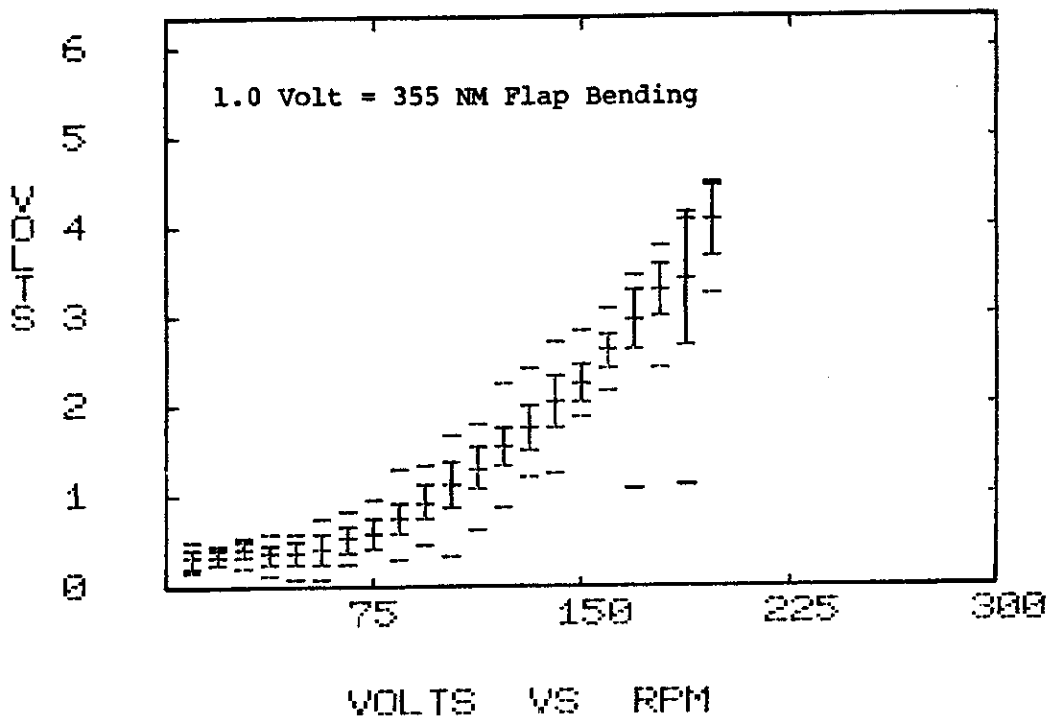


Figure 46. MEAN FLAP BENDING VS. RPM FOR 15 DEGREE FURL ANGLE

the theory to be remarkably accurate in spite of its simplicity.

For all its advantages, the simplified theory predicts neither aerodynamic blade forces and moments, local induced flow or local angle of attack, cyclic pitch response, nor transient yaw effects. One must use the dynamic simulation model to estimate these parameters. In order to illustrate some possible applications of the simulation, several operating conditions of interest were simulated and the results are presented in this section.

3.2.6.1 Prediction of Stall Limits

Since the two-bladed rotor with passive cyclic pitch should be operated out of stall conditions, estimates of operating conditions which might encounter blade stall are valuable so that these conditions might be avoided. An angle-of-attack of 20 degrees is assumed to be the limiting value for approaching stall conditions. (This value is large to account for dynamic stall.) It should be noted that this is only an assumption and that actual stall depends, not only on angle-of-attack, but also on dynamic effects and the percentage of the blade actually stalled. Figure 47 shows polar angle-of-attack plots for a yaw angle of 60 degrees, power-on, and a yaw angle of 80 degrees power-off. Since 20 degrees angle-of-attack limit is reached on the inboard section in these two cases, they are

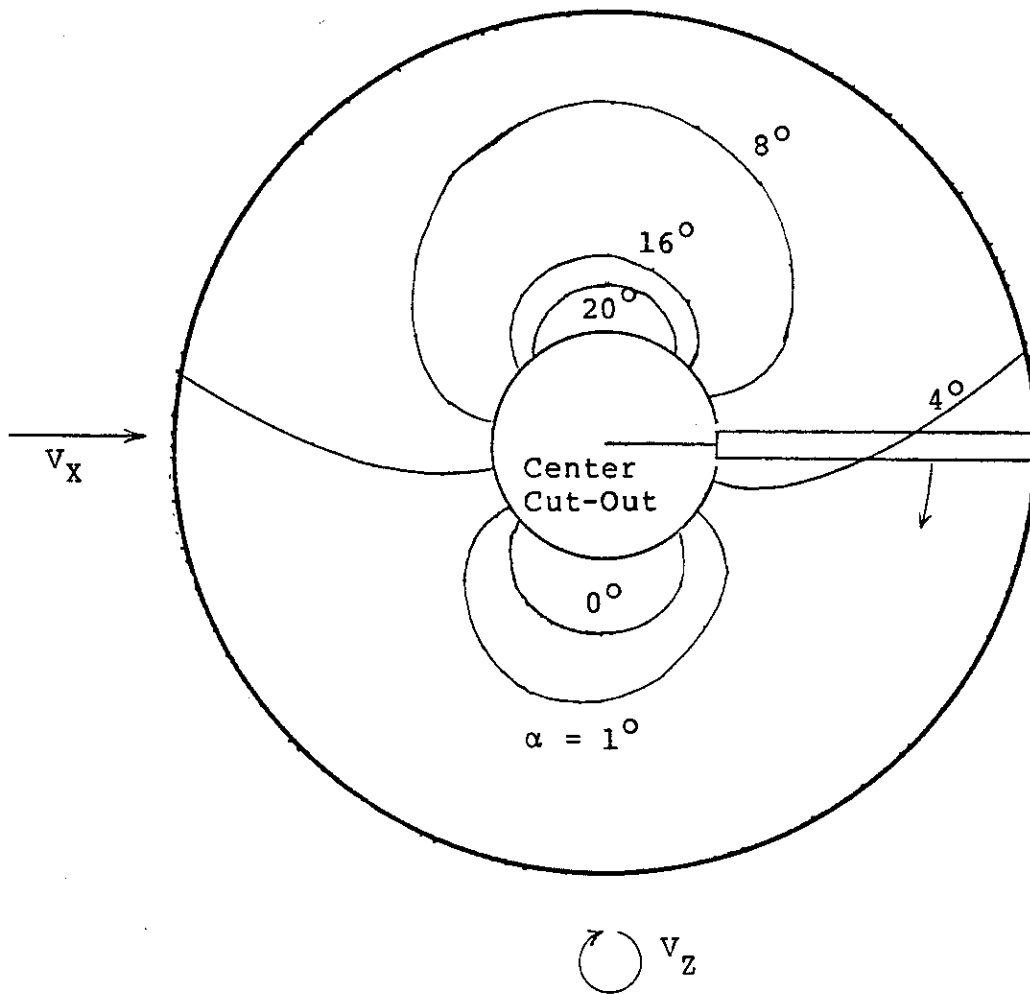


Figure 47a. ANGLE-OF-ATTACK PROFILE, YAW = 60° , RATED POWER, WIND SPEED = 18.4 m/s

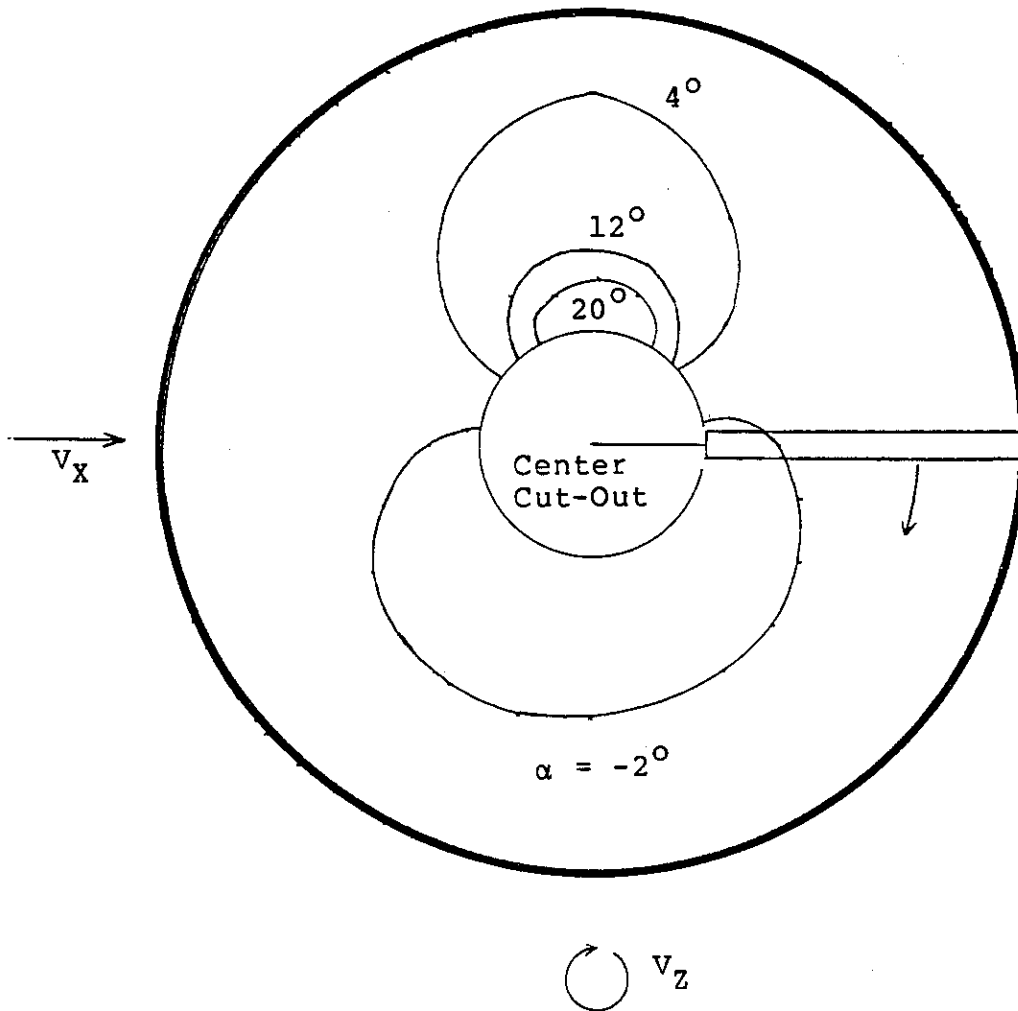


Figure 47b. ANGLE-OF-ATTACK PROFILE, YAW = 80° , AUTO-ROTATION, 230 RPM, WIND SPEED = 25 m/s

conservatively assumed to be limiting cases for the dynamic simulation model.

Relating these polar plots to actual operating conditions, one can conclude that the wind turbine generator power should be cut out at a yaw angle of 60 degrees at a corresponding wind speed of 18.4 m/s (41 MPH) to avoid possible blade stall. Although an autorotational limit of 80 degrees is shown for the model, actual rotors are capable of operating above this value without stall (10) and (11). It has been theorized that, since the retreating blade can enter regions of reverse flow at high advance ratios, the airfoil may produce lift again and thus avoid stall. Therefore, although operation power-on may not be possible above 60 degree yaw angles, operation at high advance ratios in autorotation at yaw angles greater than 80 degrees is possible, even though high angles of attack and reverse flow are encountered.

3.2.6.2 Loss of Load, Overspeed Simulation

If, during operation at rated power and rated wind speed with yaw angle equal to zero, there occurs a loss of load due to power transmission or electrical failure, the wind turbine rotor will tend to overspeed, even if equipped with an automatic furling device or speed governor. This operating condition was simulated during the full scale tests in autorotational conditions and resulted in a 35% speed increase. (See again Figure 33).

The dynamic simulation model was used to simulate such an occurrence and the results are shown in Figure 48. The model predicts a 41% overspeed, with constant wind conditions. No stall is encountered and the cyclic pitch remains within allowable limits.

3.2.6.3 Gust Response

Gusty wind conditions can cause unexpected operating conditions at the rotor and can lead either to stall conditions or excessive cyclic pitch response that may result in stop pounding of the cyclic pitch mechanism. Since gusts can include a change in wind direction as well as in wind speed, and since these gusts may cause furling operations, three gust response cases were simulated. The first consists of simply a 50% increase in wind speed at a constant yaw angle. The second combines a 50% increase in wind speed with a 20 degree per second yaw rate in the furl direction. The third consists of a 20 degree per second yaw rate in the unfurl direction. The simulated gust has a two second period and is shown in Figure 49. One will note that although shorter in period than most gusts, this gust profile compares well with the actual gust encountered during testing shown in Figure 33. All simulations started at 40 degree yaw angle, steady-state conditions. The results are shown in Table 14. The table shows that furl direction yaw rates or furling conditions during a gust tend to aggravate both cyclic pitch response and the approach to

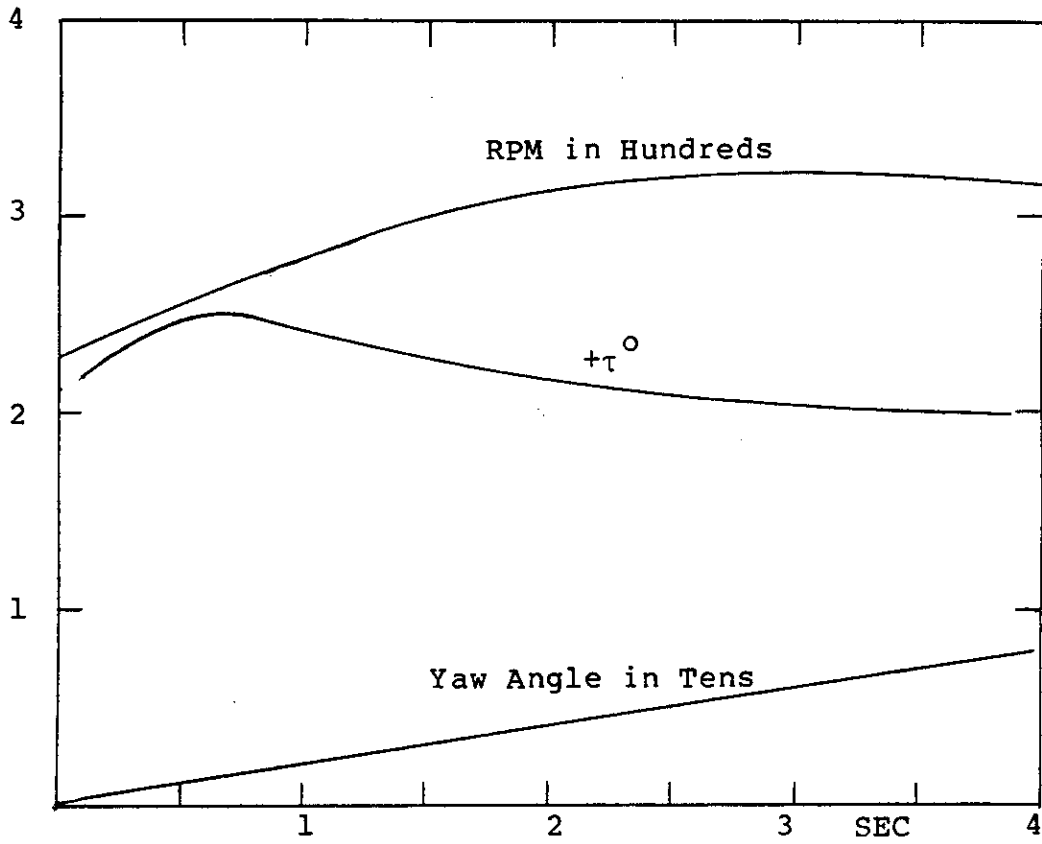


Figure 48. SIMULATED OVERSPEED WITH POWER LOSS

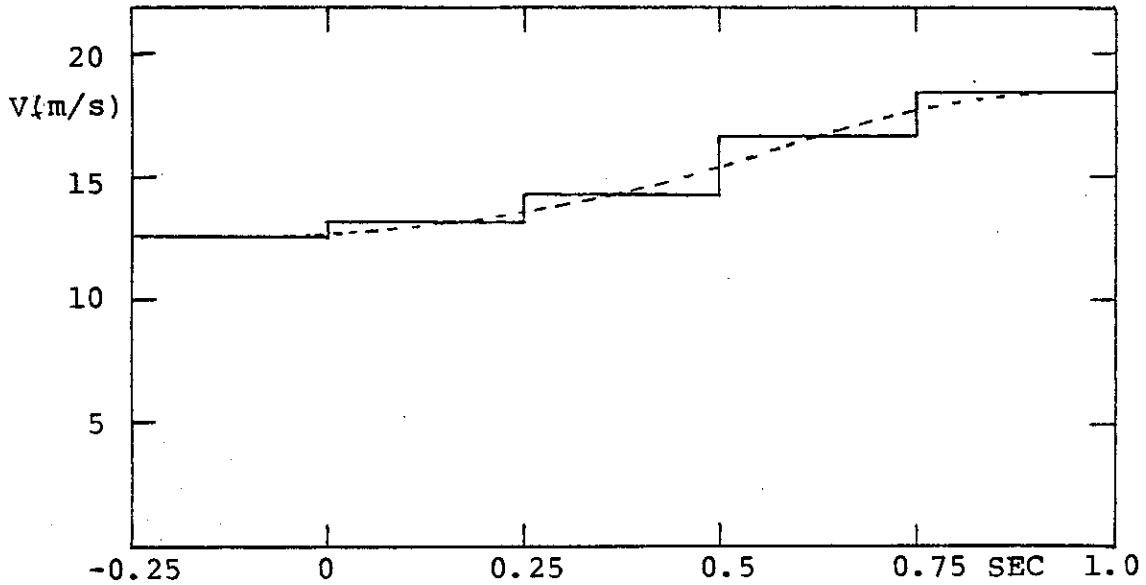


Figure 49. SIMULATED WIND SPEED GUST

TABLE 14

Gust Response

(dr-1 is the Inboard Element of 5 Blade Elements)

<u>Time, s</u>	α° <u>Blade 1</u>	ψ°	<u>dr</u>	$+\tau$ <u>Degrees</u>	$-\tau$	<u>RPM</u>
<u>I. YAW = 40° NO YAWRATE</u>						
0	< 20					230
0.25	< 20			1	1.1	232
0.50	< 20			1.2	1.3	237
0.75	20	270	1	1.6	1.6	248
1.0	21	255	1			
	22	270	1			
	21	285	1	1.7	1.7	263
<u>II. YAW = 40° to 60° 20°/s FURL DIRECTION</u>						
0	< 20					230
0.25	< 20			3.4	4.1	231
0.50	< 20			4.0	3.9	231
0.75	21	255	1			
	22	270	1			
1.0	21	285	1	4.3	4.3	234
	21	240	1			
	24	255	1			
	25	270	1			
	23	285	1			
	20	300	1	4.5	4.5	235
<u>III. YAW = 40° to 20° 20°/s UNFURL DIRECTION</u>						
0	< 20					230
0.25	< 20			2	1.5	233
0.50	< 20			1.5	1.6	242
0.75	< 20			1.2	1.3	260
1.00	< 20			1.2	1.2	285

blade stall. Unfurling, on the other hand, decreases these factors. A gust with no associated yaw rate will have an increasing effect on cyclic pitch and will aggravate the approach of blade stall.

It is of interest to examine and compare angle-of-attack and induced flow patterns during gust and yaw rate conditions, as they are calculated by the dynamic simulation model. Figures 50a and b show angle-of-attack patterns and induced flow patterns for a yaw angle of 60 degrees, at rated power, with no yaw rate, and no transients included. Figures 50c and d show the same charts at rated power during a 20 degree per second furl from 55 to 60 degree yaw angle (one rotor revolution) at the same rotor speed and wind speed. The transient effects are quite evident in the figures.

3.2.6.4 The Effects of Passive Cyclic Pitch on Aerodynamic Blade Forces in Yawed Flow Conditions

One reason for the use of a passive cyclic pitch hinge in the rotor system is the relief of unsteady aerodynamic thrust forces and moments that occur in yawed flow operation. The reduction in these forces and moments are easily examined using the dynamic simulation model.

The simulations were run at a 60 degree yaw angle in steady conditions at rated power. In one simulation the cyclic pitch response was included, as usual, while in the second simulation the τ response was forced to zero to

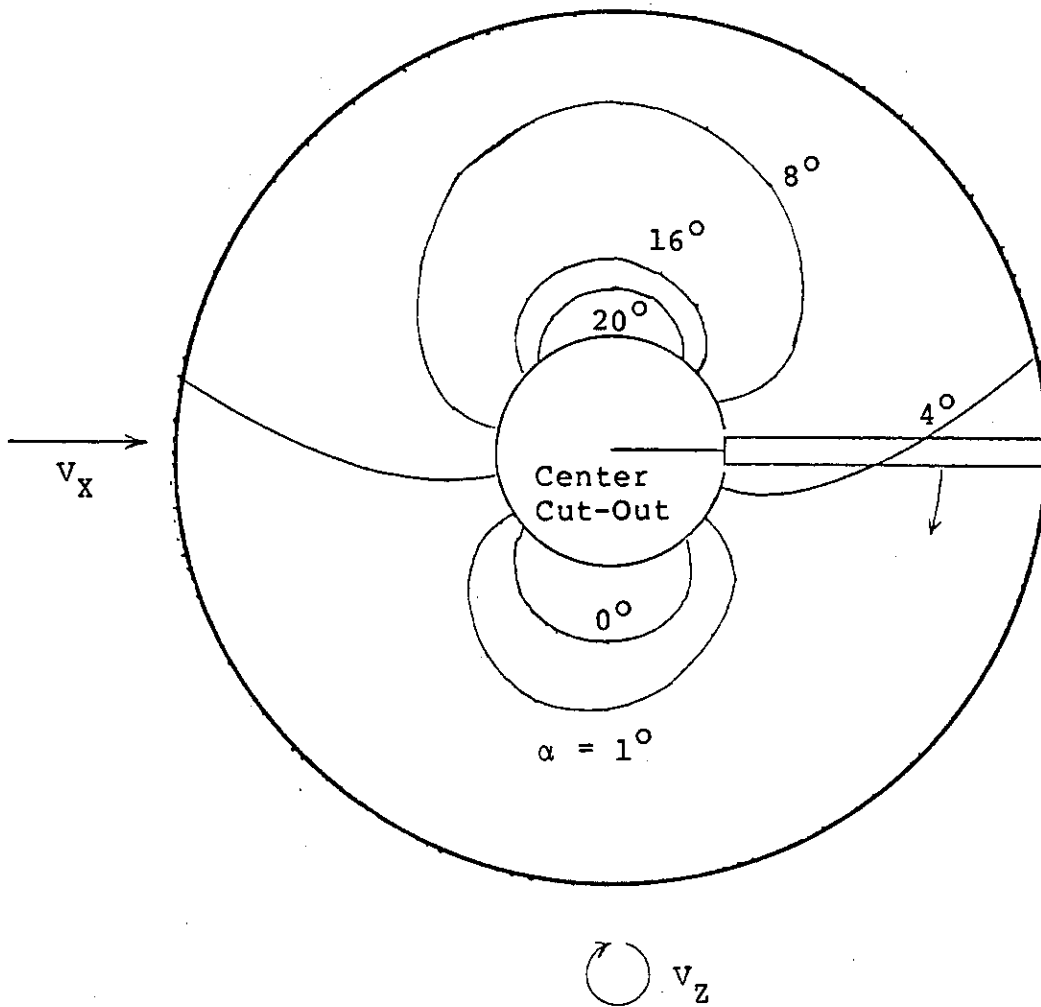


Figure 50a. ANGLE-OF-ATTACK PROFILE YAW = 60°, RATED POWER, STEADY STATE

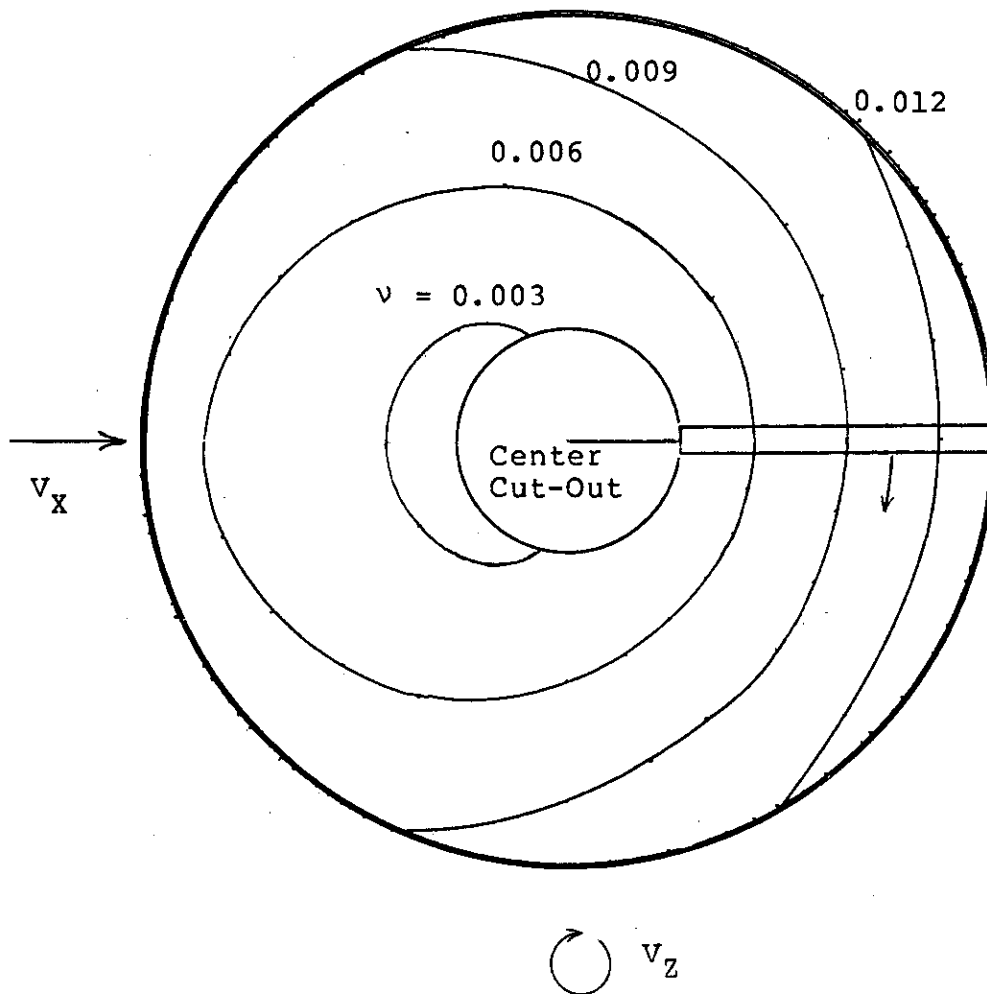


Figure 5b. INDUCED VELOCITY PROFILE, YAW = 60° , RATED POWER, STEADY STATE

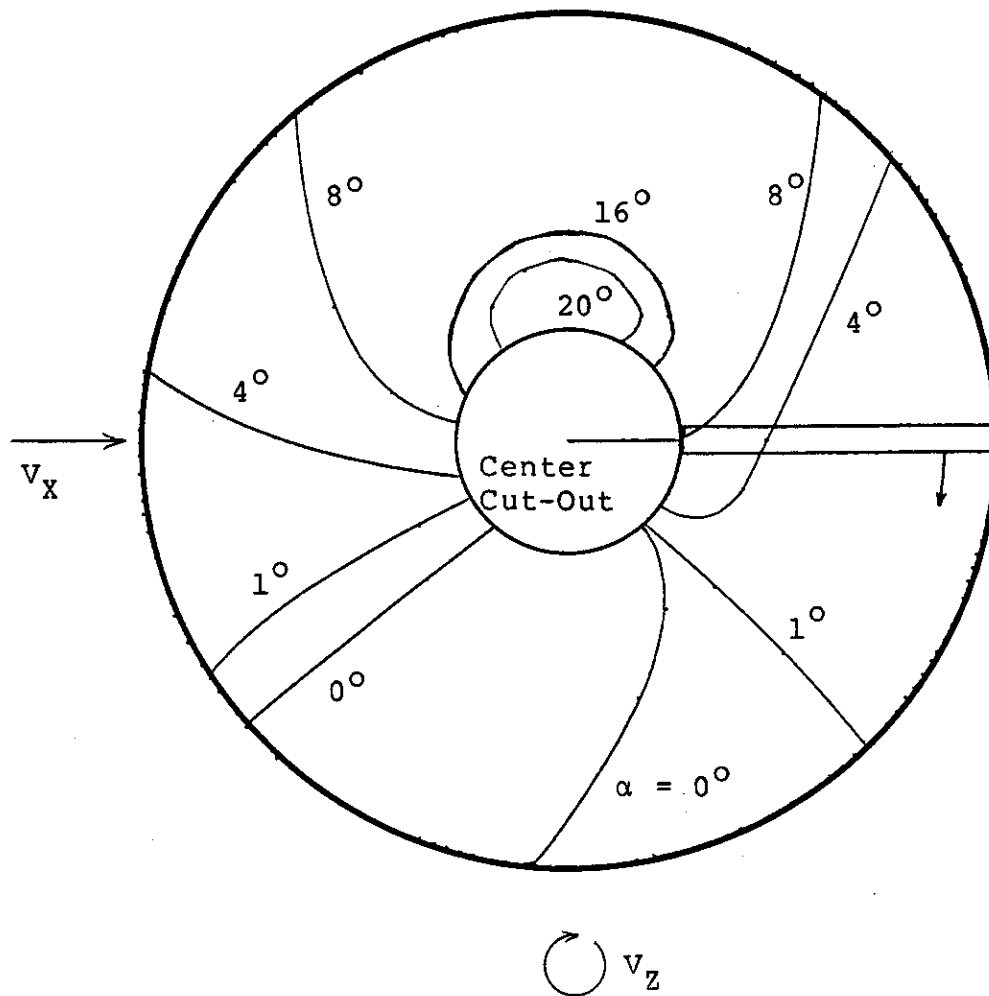


Figure 50c. ANGLE-OF-ATTACK PROFILE, YAW = 55° TO 60°,
RATED POWER, YAW TRANSIENT, 20° PER SECOND

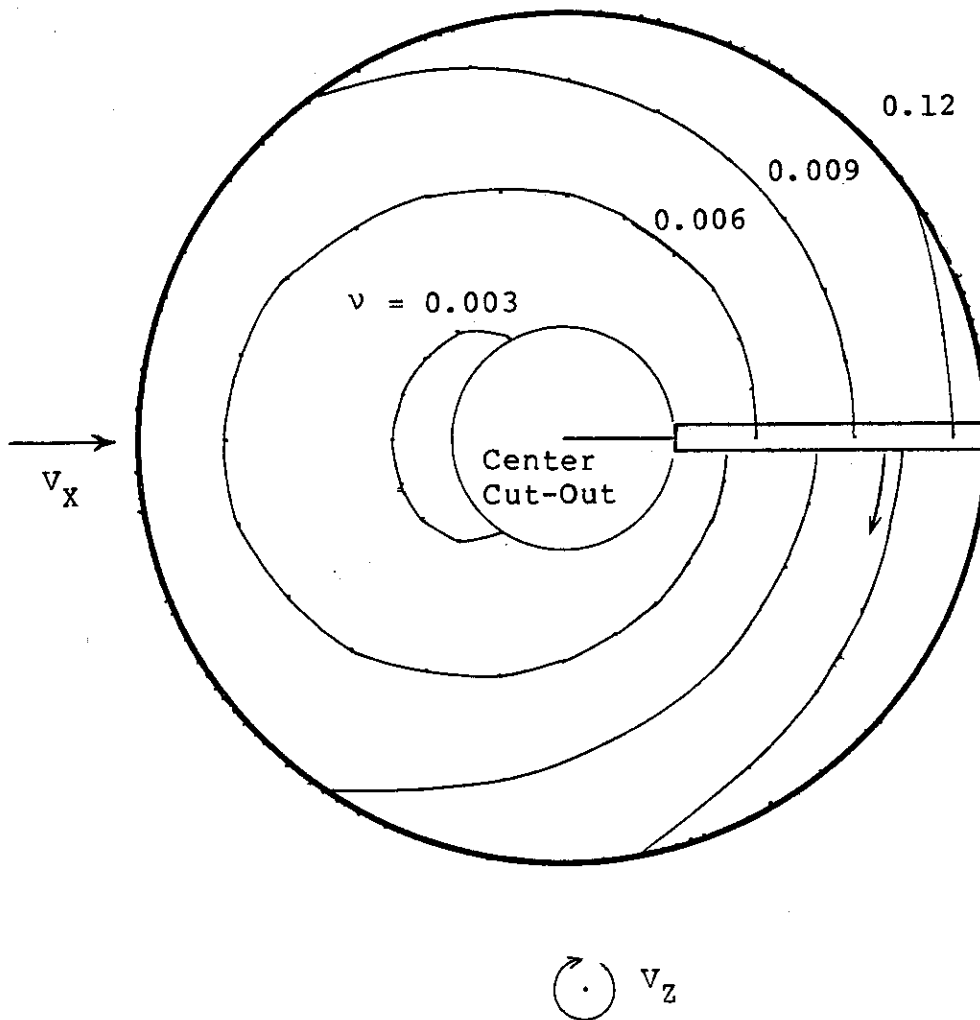


Figure 50d. INDUCED VELOCITY PROFILE, YAW = 55° TO 60° ,
RATED POWER, YAW TRANSIENT, 20° PER SECOND

simulate a rigid rotor. The resulting aerodynamic forces and moments in the thrust direction are shown in Table 15.

TABLE 15

1P Aerodynamic Forces and Moments
Per Blade For Rigid Blade Rotor and
Passive Cyclic Pitch Rotor

Yaw = 60° Rated Power
Wind Speed = 18.4 m/s (41 MPH)
RPM = 230 Steady State

<u>τ (degree)</u>	<u>Thrust (N)</u>	<u>Thrust Moment (Nm)</u>
+ 1.9	734 ± 4%	1966 ± 3%
0	768 ± 24%	2049 ± 25%

It is evident from the table that although the average forces and moments are nearly equal, the excursions about the average are markedly decreased when a passive cyclic pitch hinge is included. This should lead to decreased blade flapping fatigue loads.

3.2.6.5 Dynamic Loads

Although the dynamic simulation model is well suited to calculate blade aerodynamic forces and moments, in its present form, the accurate calculation of the dynamic loads due to these forces and moments is more difficult. In spite of this, a few observations are possible from simulation results.

Since the model includes elastic blade flap-wise deflections as a state variable (β_e), flap-wise blade loads

can be calculated using the simulation model. However, due to the assumption of a rigid blade with equivalent root spring (Figure 12), blade loads calculated in the simulation are probably not completely accurate. However, the calculation of resonant rotor frequencies that affect blade loading can be calculated using the present simulation model because aerodynamic damping terms are included in the simulation.

For example, since the rotor has a damping ratio of about 0.2, see equation (70b), one would expect a relatively flat resonance peak. Based on the frequency and damping of simple blade flapping see equation (53) one would expect a mild flap-wise resonance at 265 RPM with half-power points at 193 and 366 RPM. Simulations run at 230, 250, and 270 RPM indicate a relatively constant resonant amplification factor of 6 for flap-wise bending at all three speeds.

In order to adapt the simulation model to calculate dynamic blade loads as well as resonant frequencies, one could include an actual blade mode shape rather than use the assumption of a rigid blade with hinge spring.

4.0 CONCLUDING REMARKS

This section presents a summary of the dissertation, conclusions that can be drawn from work presented, and possible directions for further work in this area.

The simplified theory, which is developed from three basic, rotor performance equations, predicts average rotor performance in yawed flow with surprising accuracy, despite numerous simplifying assumptions. The theory, which is developed in the form of a computer algorithm, illustrates several valuable points. First, it shows for blades with zero pitch, C_T and C_Q are linearly related by a constant which is independent of yaw angle. This suggests that rotor control could be maintained from a feedback of rotor thrust rather than from the more conventional feedback of rotor power. Second, the simple theory shows that maximum rotor power may be obtained at yaw angles other than zero, and illustrates that the rotor parameters C_T , σ , v and θ can be used to determine the yaw angle for best performance. Third, the simplified theory provides a quick method by which one can determine steady-state rotor parameters that can be used as initial conditions in the dynamic simulation. This results in considerable savings in computing time in the dynamic simulation.

The dynamic simulation in yawed flow, although rather complex and computationally slow in comparison with the

simplified rotor theory, is used to provide detailed rotor operational characteristics that cannot be determined using the simplified theory. These include local angle-of-attack teeter or cyclic pitch response, and variable aerodynamic blade forces.

The dynamic simulation differs from some other simulation models in that it does not consider steady blade stall effects but does include a dynamic inflow theory to calculate induced flow velocities over the rotor disk. Since many horizontal axis wind turbines include a teetering or passive cyclic pitch hinge (in order to reduce blade loading in yawed flow or during yaw transients), this simulation is developed specifically to model these types of rotors.

Since the operation of teetering or passive cyclic pitch rotors in stall can produce a stop pounding instability, as, for example, the stop pounding instability that occurred in the modified MOD-0 teetering rotor during gust conditions (27), they must be operated out of stalled conditions. Therefore, it is unnecessary to calculate performance in stalled conditions for a teetering rotor. The simulation incorporates a constant lift curve slope for all blade angles of attack that occur during yawed flow operation. Although stall is not included, an important application of the dynamic simulation model is to identify operational limits that may lead to blade stall so that

these conditions can be avoided. Actual stall prediction is quite difficult due to the uncertainties that exist in the prediction of dynamic stall (28). For example, (28) shows that dynamic stall with unsteady free-stream (as occurs in rotors) exhibits entirely different characteristics than does a similar oscillating airfoil in steady airflow conditions, such as in Figure 2. Thus dynamic rotor stall is not well understood. One can, however, make a conservative assumption for limits on the local angle of attack for stall and thereby determine operating limits. This method is used in Section 3.2.6 with an angle-of-attack limit of 20° and from it one may conclude for the turbine modelled herein, that: (a) it should not be operated power-on at yaw angles in excess of 60 degrees, (b) that an increase in wind speed of more than 50% in less than 1 second may lead to stall conditions, and (c) that a gust coupled with a simultaneous 20 degree per second yaw rate in the furl direction will aggravate the stall while the same yaw rate in the unfurl direction will relieve the stall conditions. This type of analysis should be of significant value in the operational development of teetering and passive cyclic pitch wind turbine rotors.

In addition to the above considerations, the simulation model is also of value in predicting teeter or cyclic pitch response to various operating conditions so that stop limits can be determined and stop pounding avoided. For example,

the simulation demonstrated that a 50% wind gust causes a 70% increase in cyclic pitch response for the experimental wind turbine.

The simulation model can also be utilized to calculate instantaneous aerodynamic forces on the blades. It showed a 22% decrease in aerodynamic, oscillatory thrust moment due to the passive cyclic pitch, at a 60 degree yaw angle as compared to a rigid rotor. In its present form, blade flapwise resonant frequencies can be calculated from the simulation model, although blade loads are not well predicted due to the rigid-blade assumption. Further work on the simulation could include the actual blade mode shape to more accurately calculate blade loads and resonant frequencies.

The dynamic simulation is compared in this work to both the simplified theory and experimental results from full scale wind turbine tests at Washington University. Both correlations are quite good, providing confidence in the simulation.

Although the dynamic simulation is capable of modelling transient yaw rate conditions, simulations conducted to date and presented herein have been limited to constant yaw rate. Further development of the simulation could incorporate any governing device that might be used to control rotor speed or rotor torque. Such a simulation could use the equations as developed, except that a yaw-rate equation would be

added. One could also simulate a passive, thrust controlled wind turbine by including the yaw equilibrium equation developed in Appendix 3 and simulating thrust limited power control.

It is quite evident that the dynamic, yawed flow simulation which has been developed has not been exercised to its full potential. Much work could be done in this area.

The result of the wind tunnel model tests presented here illustrate both the usefulness and limitations of small-scale rotor experiments. The experiments were valuable in obtaining general characteristics and trends associated with a passive cyclic pitch rotor and yawed flow operation. They showed that the passive cyclic pitch rotor operated well as long as stall was avoided, that a power maximum can occur at yaw angles different from zero, and that rotor speed control with yaw angle was possible. However, due to low Reynolds Number effects, tunnel wall effects, and model construction limitations, numerical correlations between the wind tunnel results and either the full scale experimental results or theoretical results was impossible.

The full scale experimental studies provided both operational experience and data that is useful in examining the effects of yawed flow on wind turbine performance and loads, and on the operation of a yaw controlled wind turbine with passive cyclic pitch. Difficulties were encountered in

obtaining estimates of average operating conditions (due to variable flow over the rotor disk, wind turbulence, and continual variability of wind speed and direction). Nevertheless, oscillographic records and digital data-collection techniques using the method of bins provided data that correlated within reasonable limits with the theoretical performance results. The data was also useful in assessing the effects of yawed flow operation on a rotor with passive cyclic pitch. It was found that:

- (a) The passive cyclic pitch rotor operates with about the same efficiency as other horizontal axis wind rotors in steady, axial flow and may extract more power than a rigid rotor during wind direction changes because it more closely follows the wind.
- (b) The machine autorotates at yaw angles up to 80 degrees with the measured tip speed ratios agreeing with theoretical values and with those of large wind tunnel studies. Also, yaw angle variations while operating at yaw angles above 70 degrees cause large changes in rotor performance.
- (c) One should expect rotor overspeed of at least 35% with a yaw controlled wind turbine operating in autorotation during gusts or loss of load. This is due to the relatively flat performance curve (tip speed ratio vs. yaw angle) that exists up to yaw angles of 60 degrees.

- (d) The variable speed rotor efficiently stores energy at higher wind speeds (during gust peaks) and releases that energy during wind speed "lulls".
- (e) Cyclic pitch response is a function of RPM, yaw angle, yaw rate, and yaw rate direction.
- (f) Self-excited alternator efficiencies, like induction generator efficiencies, decrease rapidly below rated power, and may be only one-half their rated value during much of the wind turbine operating time.
- (g) Dynamic loads remained within allowable limits at various yaw angles and during yaw transients. The most highly stressed component is the yaw post. The dynamic loads exhibit a peak at the rotational frequency corresponding to the tail boom resonance.

In summary, it was found that the full scale yaw controlled wind turbine with passive cyclic pitch operated well and provided valuable data concerning the effects of yawed flow on wind rotors and passive cyclic pitch operation. The next phase of experimental testing will include the addition of a hydraulically controlled speed governor to control yaw angle with variable wind speed and a thrust controlled governing mode.

It is significant to note the important role that the microcomputer system played in this work. The significance

lies partly in the fact that the computer was able to provide on-site data collection, programmable data filtering, operational testing monitor and control, statistical data processing, on-site graphical results at the conclusion of each test, data storage both on disk and hard copy, and both simple and complex simulation rotor models. Although these capabilities have existed for some years now in larger, dedicated computers, the Apple microcomputer system used for this project was very compact, portable, and quite inexpensive (\$3500) making the above capabilities available to most experimenters, researchers and analysts. It is for this reason that the dynamic simulation program, developed here, in addition to the other programs developed and included in the Appendicies, were all written in BASIC programming language. This affords most potential users of these programs the opportunity to apply them without the necessity of access to a large computer system.

5. ACKNOWLEDGEMENTS

This dissertation is dedicated to my father, Andrew H. P. Swift, M.D. (1915-1981) who encouraged me to begin and complete my doctoral program.

Very few, if any, research studies of this magnitude are the effort of a single individual, and this work is no exception. I would first like to thank my advisors, Dr. D. Peters and Dr. K. Hohenemser for their assistance and patience in instructing me in rotary wing theory and practice. Next, I would like to thank Mr. Pat Rice and the other Washington University Technology Associate employees who assisted in the design, construction and report preparation for the experimental wind turbine. Also, my thanks to Bryan Hayden of the Mechanical Engineering Department for his technical and photographic assistance and to Kathy Windish of WUTA for the many hours spent typing and proof-reading the manuscript. In addition, thanks to Dr. R. Coles and the Tyson Research Center staff, especially Ross Vollmar and Bob Lewis for their assistance in the experimental work conducted at Tyson.

I would also like to extend my appreciation to my wife Linda and my daughter Carolyn for their patience and encouragement during the past two years of work on this project.

Funding for the experimental work was provided through Solar Energy Research Institute, Subcontract Number XH-9-8085-3.

6.0 APPENDICES

APPENDIX 6.1

Nomenclature

A	$\frac{4 C_T}{\sigma a v} + \frac{2\theta}{3v}$	Used For Determining λ for Maximum Power.
a		Lift Curve Slope (1/rad.).
\bar{a}		Axial Induced Flow Factor.
\bar{a}'		Flow Rotation Factor.
B		Tip Loss Factor.
BR		Effective Blade Radius for Lift Calculation.
b		Number of Rotor Blades.
C_{d0}		Drag Coefficient.
C_L		Lift Coefficient.
C_N		Normal Force Coefficient.
C_P		Rotor Coefficient of Performance =
	$\frac{P}{\frac{1}{2} \rho \pi R^2 v^3}$	
C_Q		Rotor Torque Coefficient = $\frac{Q}{\rho \pi \Omega^2 R^5}$
C_T		Rotor Thrust Coefficient = $\frac{T}{\rho \pi \Omega^2 R^4}$
c		Chord Width.
dD		Elemental Drag.
dL		Elemental Lift.
dQ		Elemental Torque.
dr		Elemental Span.
dT		Elemental Thrust.
f		Frequency

f1-f5	State Variable Functions.
I	Blade Moment of Inertia.
I_N	Nacelle Moment of Inertia.
\bar{I}	Equivalent Centrifugal Inertia.
i	Dummy Index.
j	Dummy Index.
K_S	Flap Hinge Spring Force Coefficient.
M	Blade Mass.
MB(i)	Thrust Moment Per Blade.
MQ(i)	Driving Torque Per Blade.
m	Elemental Blade Mass.
N	Number of Samples.
n	Dummy Index.
P	Rotor Power
p	Per Revolution Frequency.
\bar{P}_R	Mean Rotor Power Per Bin
Q	Torque
R	Blade Radius.
r	Local Blade Radius Station.
T	Thrust Force.
TB(i)	Total Thrust Force Per Blade.
TQ(i)	Total In-plane Force Per Blade.
t	Time
U	Resultant Blade Element Velocity.
U_P	Normal Blade Element Velocity.
U_T	Tangential Blade Element Velocity.

V	Wind Speed
v	Tip Speed Ratio = $V/\Omega R$
V_i	Induced Flow Velocity.
V_x	In-plane Wind Speed Component = $V_x = V \sin\chi$.
V_z	Axial Wind Speed Component, $V_z = V \cos\chi$.
v_x	In-plane Tip Speed Ratio, $v_x = v \sin\chi$.
v_z	Axial Tip Speed Ratio, $v_z = v \cos\chi$.
\bar{V}	Average Wind Speed Per Bin.
x	v/v Definition.
Y_i	State Variables: $Y1 = \tau$ $Y2 = \dot{\tau}$ $Y3 = \beta_e$ $Y4 = \dot{\beta}_e$ $Y5 = v$ $Y6 = \Omega$ $Y7 = \chi$ $Y8 = \dot{\chi}$
α	Blade Angle-of-attack.
α_M	Mean Rotor Angle-of-attack.
β	Blade Flap Angle.
β_e	Blade Elastic Flap Angle.
β_o	Blade Precone Angle.
γ	Blade Lock Number.
Δ	Increment

δ_3	Delta Three Angle. An angle measured from an axis normal to the blade pair of a two-bladed rotor, in the plane of the rotor, to the axis of rotation about the prelag hinge.
ζ	Damping Ratio.
θ	Blade Pitch Angle.
λ	Inflow Ratio = $\frac{V_z - V_i}{\Omega R}$
λ	Tip Speed Ratio = $\Omega R / V$
$\bar{\lambda}$	Axial Tip Speed Ratio = $v_z = \frac{V_z}{\Omega R}$
μ	Advance Ratio = $v_x = \frac{V_x}{\Omega R}$
ν	Induced Flow Ratio = $\frac{V_i}{\Omega R}$
ρ	Air Density (Standard = 1.23 kg/m ³).
σ	Solidity Ratio = $\frac{bc}{\pi R}$
τ	Cyclic Pitch Deflection. Actually this represents deflection about the prelag axis. For rotors with $\delta_3 = 0$, movement about this axis represents only blade flapping motion. In rotors, such as those considered herein, with large δ_3 values, movement about the prelag axis is almost all a blade pitch change, since $\text{Flap} = \tau \cos \delta_3$ $\text{Pitch} = \tau \sin \delta_3$ <p>Thus the definition of cyclic pitch for τ is slightly in error. When τ reaches its physical limit of travel it is called stop pounding.</p>
ϕ	Inflow Angle.
χ	Yaw Angle.
ψ	Blade Azimuth Position.

Ω	Rotor Speed
ω_n	Natural Frequency.
ω_o	Nonrotating Frequency.
ω_1	Rotating Frequency Component.

APPENDIX 6.2

Documentation for

The "Yawflow" and "Yawplot" Programs

A	Lift Curve Slope
AA	Angle-of-attack Selected for Plotting
AD	Angle-of-attack Array (degrees).
AE	Iteration Error Variable.
ALPHA	Calculated Angle-of-attack (radians).
CD	Drag Coefficient.
CHI	Yaw Angle (radians).
CP	Performance Coefficient = $2 CQ/v^3$.
CQ	Torque Coefficient _ Nondimensionalized on Sigma if Desired).
CT	Thrust Coefficient Nondimensionalized on Sigma if Desired).
FLAG	Iteration Counter.
GTHETA	Geometric Pitch Angle.
INFLOW	Inflow Ratio.
J	Yaw Angle Counter.
JJ	Yaw Angle Limit.
K	Tip Speed Ratio, $v/\Omega R$, Counter
KK	Tip Speed Ratio Limit.
LAMBAR	Axial Flow Ratio.
MCD	Drag Multiplier
MU	Advance Ratio

NU	Induced Flow Ratio.
N1U, N2U	Induced Flow Iterative Variables.
PI	π
THETA	Aerodynamic Pitch Angle.
U \$	Title String Variable.
V	Tip Speed Ratio, $V/\Omega R$.
XSIG	Solidity Ratio.
XQ	Selected Torque Coefficient for Plotting.
YAW	Yaw Angle (degrees).
YAW.AA	File Name for Angle-of-attack Plotting.
YAW.DAT	File Name for CT vs. Yaw Angle Plotting.
YAW.CQ	File Name for Torque Coefficient Plotting.

JPR#0

JLIST

```
1 REM YAWFLOW PROGRAM CALCULATED STEADY STATE PERFORMANCE IN YAWED FLOW
2 REM REVISION 2/2/81
3 REM ALPHA AND DRAG ARE CALCULATED BASED ON GEOMETRIC ANGLES WHILE EQUATIONS
USE AERODYNAMIC PITCH ANGLES
5 D$ = CHR$(4)
7 HOME : UTAB 5
10 DIM ADX(10,20),YAWK(10,20),UK(10,20),CQK(10,20),CT(10,20)
12 DIM XQ(5),AA(5)
14 INPUT "ENTER DATE AND NOTES > ";US$
15 INPUT "INPUT DRAG MULTIPLIER ? ";MCD
20 INPUT "INPUT SIGMA? ";XSIG
30 INPUT "ENTER AERODYN. PITCH IN DEG. > ";THETA
31 INPUT "ENTER GEOMETRIC PITCH IN DEG. > ";GTHETA
35 INPUT "DO YOU WANT OUTPUT NON-DIMENSIONALIZED ON SIGMA ? (Y/N) ";Z$
38 INPUT "INPUT ITERATIONS ON J(YAW) ? ";JJ
39 INPUT "INPUT ITERATIONS ON K(U) > 2 ? ";KK
40 A = 5.7:PI = 3.14159
45 THETA = THETA * PI / 180
46 GTHETA = GTHETA * PI / 180
50 FOR J = 0 TO JJ
60 FOR K = 2 TO KK
70 YAWK(J,K) = J * 10
80 CHI = YAWK(J,K) * PI / 180
90 UK(J,K) = .02 * K
100 LAMBAR = UK(J,K) * COS(CHI)
110 MU = UK(J,K) * SIN(CHI)
130 REM ITERATE FOR NU
140 N1U = LAMBAR / 3
150 FLAG = 1
160 XX = (XSIG * A / 12) * (1 + (1.5 * MU ^ 2)) * THETA + XSIG * A * LAMBAR / 8
170 YY = (XSIG * A / 8) + SQR((LAMBAR - N1U) ^ 2 + MU ^ 2)
180 N2U = XX / YY
190 AE = ABS(N2U - N1U)
200 IF AE < .0001 THEN 220
210 IF FLAG > 10 THEN 220
212 FLAG = FLAG + 1
214 N1U = N2U
216 GOTO 170
220 REM
230 NU = N2U
235 INFLOW = LAMBAR - NU
240 IF NU < 0 OR NU > LAMBAR THEN 260
250 GOTO 270
260 PRINT " NU NOT BETWEEN 0 AND LAMBAR"
270 REM
300 REM ALPHA AND DRAG CALCULATION BASED ON GEOMETRIC ANGLES
310 ALPHA = (1.43) * INFLOW - GTHETA
320 ADX(J,K) = ALPHA * 180 / PI
330 CD = .01 + .5 * ALPHA ^ 2
401 CD = CD * MCD
402 CT(J,K) = 2 * NU * SQR((LAMBAR - NU) ^ 2 + MU ^ 2)
410 CX = (LAMBAR - NU) * CT(J,K)
420 CY = 1 - (XSIG / 8) * (CD / CX)
430 CQK(J,K) = CX * CY
440 IF Z$ = "N" THEN 500
450 CT(J,K) = CT(J,K) / XSIG
460 CQK(J,K) = CQK(J,K) / XSIG
500 NEXT K: NEXT J
```

```
550 REM INSERT TEST STOP HERE
600 REM PLOT U PARAM.**STORE AS YAH.DAT
601 PRINT D$;"MON C,I,0"
602 PRINT D$;"OPEN YAH.DAT"
604 PRINT D$;"DELETE YAH.DAT"
606 PRINT D$;"OPEN YAH.DAT"
608 PRINT D$;"WRITE YAH.DAT"
610 FOR J = 0 TO JJ: FOR K = 3 TO KK
620 X = 42 + (90 - YAH(J,K)) * 21 / 10
625 X = INT (X + .5)
630 Y = ( - 128 / .24) * CT(J,K) + 148
635 Y = INT (Y + .5)
645 PRINT X
646 PRINT Y
650 NEXT K: NEXT J
655 PRINT "99999"
660 PRINT D$;"CLOSE YAH.DAT"
700 REM PLOT CQ= PARAM**STORE AS YAH.CQ
702 INPUT "HOW MANY CQ'S WILL YOU PLOT ? (<S) ? ";RR
703 FOR R = 1 TO RR: PRINT "CQ# ";R: INPUT " INPUT CQ/SIGMA ? ";XQ(R)
704 NEXT R
705 PRINT D$;"OPEN YAH.CQ"
706 PRINT D$;"DELETE YAH.CQ"
707 PRINT D$;"OPEN YAH.CQ"
708 PRINT D$;"WRITE YAH.CQ"
710 FOR R = 1 TO RR
720 FOR J = 0 TO JJ
730 K = 3
740 BB = CQ(J,K) - XQ(R)
750 IF BB >= 0 THEN 785
760 K = K + 1
770 IF K > KK THEN 900
780 GOTO 740
785 IF K = 3 THEN 900
800 RT = BB / (CQ(J,K) - CQ(J,K - 1))
810 XT = CT(J,K) - RT * (CT(J,K) - CT(J,K - 1))
820 X = 42 + (90 - YAH(J,K)) * 21 / 10
825 X = INT (X + .5)
830 Y = ( - 128 / .24) * XT + 148
835 Y = INT (Y + .5)
840 PRINT X
850 PRINT Y
900 NEXT J
902 NEXT R
905 PRINT "99999"
910 PRINT D$;"CLOSE YAH.CQ"
1000 REM PLOT ANGLE OF ATTACK FOR STALL
1010 REM STORE AS YAH.AA
1012 INPUT "HOW MANY AA'S WILL YOU PLOT? (<S) ";RR
1014 FOR R = 1 TO RR
1016 PRINT "ANGLE OF ATTACK # ";R
1018 INPUT "INPUT AA ? ";AA(R)
1019 NEXT R
1020 PRINT D$;"OPEN YAH.AA"
1030 PRINT D$;"DELETE YAH.AA"
1040 PRINT D$;"OPEN YAH.AA"
1050 PRINT D$;"WRITE YAH.AA"
1060 FOR R = 1 TO RR
1070 FOR J = 0 TO JJ
1080 K = 3
1090 BB = AA(J,K) - AA(R)
```

```
1091 IF BB > = 0 THEN 1099
1092 K = K + 1
1093 IF K > KK THEN 1180
1094 GOTO 1090
1099 IF K = 3 THEN 1180
1100 RT = BB / (ADK(J,K) - ADK(J,K - 1))
1110 XT = CT(J,K) - RT * (CT(J,K) - CT(J,K - 1))
1120 X = 42 + (90 - YAK(J,K)) * 21 / 10
1130 X = INT (X + .5)
1140 Y = (- 128 / .24) * XT + 148
1150 Y = INT (Y + .5)
1160 PRINT X
1170 PRINT Y
1180 NEXT J
1185 NEXT R
1190 PRINT "99999"
1200 PRINT D$;"CLOSE YAW.AA"
1210 PRINT D$;"PR#1"
1220 PRINT : PRINT
1230 PRINT " DATE: ";U$: PRINT
1240 PRINT " SIGMA= ";XSIG
1250 PRINT " THETA= ";THETA * 180 / PI;" DEG"
1260 PRINT " DRAG MULTIPLIER= ";MCD
1270 PRINT " ANGLE OF ATTACK #1= ";AAK1;" DEG"
1280 PRINT " CO/SIGMA #1= ";XOK1)
1290 PRINT : PRINT : PRINT
1295 PRINT D$;"PR#0"
1298 END
```

JPR#0

JLIST

```
5  REM  YAWPLOT PROGRAM
10  D$ = CHR$(4)
20  HGR
25  HCOLOR= 3
30  REM  PLOT AXIS
31  FOR Y = 4 TO 144 STEP 140: FOR X = 63 TO 231 STEP 21
32  HPLOT X,Y + 1 TO X,Y + 3
33  NEXT X: NEXT Y
35  HPLOT 42,4 TO 238,4 TO 238,148 TO 42,148 TO 42,4
36  FOR X = 42 TO 234 STEP 192: FOR Y = 20 TO 132 STEP 16
37  HPLOT X + 1,Y TO X + 3,Y
38  NEXT Y: NEXT X
39  PRINT D$;"BLOAD AXIS-YAWPLOT"
40  PRINT D$;"OPEN YAW.DAT"
50  PRINT D$;"READ YAW.DAT"
60  INPUT X: IF X = 99999 THEN 80
61  INPUT Y
65  IF Y < 5 OR Y > 147 THEN 75
70  HPLOT X,Y
75  GOTO 60
80  PRINT D$;"CLOSE YAW.DAT"
90  PRINT " U DOTS PLOTTED"
100 REM  PLOT CQ
110 PRINT D$;"OPEN YAW.CQ"
120 PRINT D$;"READ YAW.CQ"
130 INPUT X1
140 INPUT Y1
150 INPUT X2
160 IF X2 = 99999 THEN 210
170 INPUT Y2
180 HPLOT X1,Y1 TO X2,Y2
190 X1 = X2:Y1 = Y2
200 GOTO 150
210 PRINT D$;"CLOSE YAW.CQ"
230 PRINT " CQ LINES PLOTTED"
300 REM  PLOT ANGLE OF ATTACK LINES
310 PRINT D$;"OPEN YAW.AA"
320 PRINT D$;"READ YAW.AA"
330 INPUT X1
340 INPUT Y1
350 INPUT X2
360 IF X2 = 99999 THEN 500
370 INPUT Y2
375 IF Y1 > 147 OR Y1 < 5 THEN 390
376 IF Y2 > 147 OR Y2 < 5 THEN 390
380 HPLOT X1,Y1 TO X2,Y2
390 X1 = X2:Y1 = Y2
400 GOTO 350
500 PRINT D$;"CLOSE YAW.AA"
600 END
```

IPR#0

JLIST

```
1 REM YAWFLOW PROGRAM FOR PLOTTING STEADY STATE PERFORMANCE IN YAWED FLOW AS A
  FUNCTION OF CP
2 REM REVISION 2/2/81
3 REM ALPHA AND DRAG ARE CALCULATED BASED ON GEOMETRIC ANGLES. EQUATIONS USE A
  AERODYNAMIC ANGLES.
4 REM PLOTS CP VS TIP SPEED RATIO
5 D$ = CHR$(4)
8 HOME : UTAB 5
10 DIM CQ(9,20),CT(9,20)
14 INPUT "INPUT DATE FOLLOWED BY NOTES FOR THE RUN > ";U$
15 INPUT "INPUT DRAG MULTIPLIER ? ";MCD
20 INPUT "INPUT SIGMA? ";XSIG
30 INPUT "ENTER AERODYNAMIC PITCH ANGLE, DEG. > ";THETA
31 INPUT "ENTER GEOMETRIC PITCH ANGLE, IN DEG. > ";GTHETA
35 INPUT "DO YOU WANT OUTPUT NON-DIMENTIONALIZED ON SIGMA ? (Y/N) ";Z$
38 INPUT "INPUT ITERATIONS ON J(YAW) ? ";JJ
39 INPUT "INPUT ITERATIONS ON K(U)>1 ? ";KK
40 A = 5.7*PI = 3.14159
45 THETA = THETA * PI / 180
46 GTHETA = GTHETA * PI / 180
50 FOR J = 0 TO JJ
60 FOR K = 1 TO KK
80 CHI = J * 10 * PI / 180
90 U = .02 * K
100 LAMBAR = U * COS(CHI)
110 MU = U * SIN(CHI)
130 REM ITERATE FOR NU
140 N1U = LAMBAR / 3
150 FLAG = 1
160 XX = (XSIG * A / 12) * (1 + (1.5 * MU ^ 2)) * THETA + XSIG * A * LAMBAR / 8
170 YY = (XSIG * A / 8) + SQRT((LAMBAR - N1U) ^ 2 + MU ^ 2)
180 N2U = XX / YY
190 AE = ABS(N2U - N1U)
200 IF AE < .0001 THEN 220
210 IF FLAG > 10 THEN 220
212 FLAG = FLAG + 1
214 N1U = N2U
216 GOTO 170
220 REM
230 NU = N2U
235 INFLOW = LAMBAR - NU
240 IF NU < 0 OR NU > LAMBAR THEN 260
250 GOTO 270
260 PRINT "NU NOT BETWEEN 0 AND LAMBAR"
270 REM
300 REM ALPHA AND CD BASED ON GEOMETRIC ANGLES
310 ALPHA = (1.43) * INFLOW - GTHETA
320 Q = ALPHA * 180 / PI
340 IF Q > - 8 AND Q < 20 THEN CD = .01 + .5 * ((Q * PI / 180) ^ 2)
380 IF Q > 20 OR Q < - 8 THEN PRINT "AA OUT OF RANGE **"
401 CD = CD * MCD
402 CT(J,K) = 2 * NU * SQRT((LAMBAR - NU) ^ 2 + MU ^ 2)
410 CX = (LAMBAR - NU) * CT(J,K)
420 CY = 1 - (XSIG / 8) * (CD / CX)
430 CQ(J,K) = CX * CY
440 IF Z$ = "N" THEN 500
450 CT(J,K) = CT(J,K) / XSIG
460 CQ(J,K) = CQ(J,K) / XSIG
470 PRINT J,K
```

```
490 NEXT K: NEXT J
491 GOTO 600
495 REM PRINTOUT ROUTINE
500 PRINT D$;"PR#1"
510 PRINT "DATE: ";U$
520 PRINT : PRINT "SOLIDITY RATIO= ";XSIG
530 PRINT "AERODYN PITCH ANGLE= ";THETA * 180 / PI;" DEG"
535 PRINT "DRAG MULTIPLIER= ";MCD
537 PRINT : PRINT "VERT AXIS IS CP. ONE UNIT=.05"
538 PRINT "HOR AXIS IS TSR. ONE UNIT=2"
539 PRINT "CQ/S RANGES FROM 0 TO .018 STEP .001"
545 PRINT : PRINT : PRINT D$;"PR#0"
546 CALL - 16046
547 END
600 GOSUB 1500: REM PLOT AXIS
601 REM GET CP-TSR VALUES
605 INPUT "ENTER YAW ANGLE (99=EXIT)> ";J
606 IF J = 99 THEN 1230
607 J = .1 * J
610 FOR C = 0 TO 18
620 CQS = .001 * C
630 REM GET CT VALUES FOR CQS
730 K = 1
740 BB = CQ(J,K) - CQS
750 IF BB > = 0 THEN 785
760 K = K + 1
770 IF K > KK THEN 900
780 GOTO 740
785 IF K = 1 THEN 900
800 RT = BB / (CQ(J,K) - CQ(J,K - 1))
810 XT = CT(J,K) - RT * (CT(J,K) - CT(J,K - 1))
900 REM CONTINUE
1000 REM GET U VALUES
1020 K = 1
1030 BB = CT(J,K) - XT
1040 IF BB > = 0 THEN 1080
1050 K = K + 1
1060 IF K > KK THEN 1100
1070 GOTO 1030
1080 IF K = 1 THEN 1100
1085 RT = BB / (CT(J,K) - CT(J,K - 1))
1090 XU = .02 * (K - RT)
1100 REM CONTINUE
1120 CP = CQS * 2 * XSIG * (1 / (XU ^ 3))
1122 REM INSERT CP MULT HERE
1125 GOTO 1140
1130 PRINT "A=";XA;" LAH=";1 / XU;" CP=";CP;" CQ/S=";CQS;" CT/S=";XT
1140 X = INT (.5 + 12 * (1 / XU))
1150 Y = - 300 * CP + 160
1155 IF Y > 150 THEN HPLLOT X,159 TO X,161
1160 HPLLOT X,Y
1200 NEXT C
1210 GOTO 605
1230 INPUT " DO YOU WISH TO PRINT THIS ? (Y/N) ";OP$
1235 IF OP$ = "Y" THEN 500
1240 STOP
1500 REM SUBR TO PLOT AXIS
1510 HGR : HCOLOR= 3
1520 HPLLOT 0,0 TO 240,0 TO 240,160 TO 0,160 TO 0,0
1530 FOR L = 0 TO 237 STEP 237
1540 FOR M = 10 TO 145 STEP 15
```

```
1550 HPL0T L,M TO L + 3,M
1560 NEXT M: NEXT L
1570 FOR M = 0 TO 157 STEP 157
1580 FOR L = 24 TO 216 STEP 24
1590 HPL0T L,M TO L,M + 3
1595 NEXT L: NEXT M
1596 RETURN
```

APPENDIX 6.3

Derivation of Rotor Equations

I. The rotor coordinate system used in this derivation is shown in Figure 10 of the text. Note that u_c , v_c , and w_c are for blade number 1 in the rotating reference frame.

II. Write Velocities

From the Figure one can write the velocity for an elemental section of blade 1 in terms of the components

u_c , v_c and w_c as

$$u_c = \dot{\chi} \text{ (moment arm) (no wind or induced flow effects)}$$

$$u_c = \dot{\chi} \text{ (rotation term - flapping term)}$$

$$u_c = \dot{\chi} (S - r \tau \cos \delta_3) \cos \Psi \tag{3.1}$$

$$v_c = \Omega(r \cos \beta) - \dot{\chi}(S - \tau r \cos \delta_3) \sin \Psi$$

but for small flapping angle, β ,

$$\cos \beta = (1 - \frac{1}{2} \beta^2) = (1 - \frac{1}{2} \tau^2 \cos^2 \delta_3)$$

thus

$$v_c = \Omega r (1 - \frac{1}{2} \tau^2 \cos^2 \delta_3) - \dot{\chi} (S - \tau r \cos \delta_3) \sin \Psi \tag{3.2}$$

and

$$w_c = \text{flapping term} + \dot{\chi} \text{ (moment arm)}$$

$$w_c = \dot{\tau} r \cos \delta_3 + \dot{\chi} r \cos \Psi \tag{3.3}$$

III. Write Kinetic Energy, T

$$T = \frac{1}{2}m(\text{vel}^2) \quad (\text{elemental } T) \quad (3.4)$$

Note:

$$\circ \quad \text{vel}^2 = u_c^2 + v_c^2 + w_c^2 \quad (3.5)$$

$$\circ \quad M = \int_0^R m dr \quad (3.6)$$

$$\circ \quad I = r^2 \int_0^R m dr = Mr^2 \quad (3.7)$$

- o All equations are for Blade 1 only.
- o We will discard all terms of 3rd order or higher, i.e. $(\dot{\chi}^2 \tau)$, $(\dot{\chi}, \tau, \dot{\tau})$ etc. This is an approximation for simplicity.

$$\begin{aligned} u_c^2 &= (\dot{\chi} s - \dot{\chi} r \tau \cos \delta_3)^2 \cos^2 \psi \\ &= \dot{\chi}^2 s^2 \cos^2 \psi \\ &\quad - 2\dot{\chi}^2 \tau s r \cos^2 \psi \cos \delta_3 \geq 3\text{rd order} = 0 \\ &\quad + \dot{\chi}^2 \tau^2 r^2 \cos^2 \delta_3 \cos^2 \psi \geq 3\text{rd order} = 0 \end{aligned}$$

thus

$$u_c^2 = \dot{\chi}^2 S^2 \cos^2 \Psi \quad (3.8)$$

$$v_c^2 = (\Omega r - \frac{1}{2} \Omega r \tau^2 \cos^2 \delta_3 - \dot{\chi} S \sin \Psi + \dot{\chi} \tau r \cos \delta_3 \sin \Psi)^2$$

$$\begin{aligned} v_c^2 &= \Omega^2 r^2 \\ &- 2 \frac{1}{2} \Omega^2 r^2 \tau^2 \cos^2 \delta_3 \\ &- 2 \Omega r \dot{\chi} S \sin \Psi \\ &+ 2 \dot{\chi} \Omega r^2 \tau \cos \delta_3 \sin \Psi \\ &+ \frac{1}{4} \Omega^2 r^2 \tau^4 \cos^4 \delta_3 \geq 3\text{rd order} = 0 \\ &+ 2 \frac{1}{2} \Omega r \dot{\chi} S \tau^2 \cos^2 \delta_3 \sin \Psi \geq 3\text{rd order} = 0 \\ &- 2 \frac{1}{2} \Omega r^2 \dot{\chi} \tau^3 \cos^3 \delta_3 \sin \Psi \geq 3\text{rd order} = 0 \\ &+ \dot{\chi}^2 S^2 \sin^2 \Psi \\ &- 2 \dot{\chi}^2 S r \tau \cos \delta_3 \sin^2 \Psi \geq 3\text{rd order} = 0 \\ &+ \dot{\chi}^2 r \tau^2 \cos^2 \delta_3 \sin^2 \Psi \geq 3\text{rd order} = 0 \end{aligned}$$

$$v_c^2 = \Omega^2 r^2 \quad (3.9)$$

$$\begin{aligned} &- \Omega^2 r^2 \tau^2 \cos^2 \delta_3 \\ &- 2 \Omega r \dot{\chi} S \sin \Psi \\ &+ 2 \Omega r^2 \dot{\chi} \tau \cos \delta_3 \sin \Psi \\ &+ \dot{\chi}^2 S^2 \sin^2 \Psi \end{aligned}$$

$$w_c^2 = (\dot{t} r \cos\delta_3 + \dot{\chi} r \cos\psi)^2$$

$$\begin{aligned} w_c^2 &= \dot{t}^2 r^2 \cos^2\delta_3 \\ &+ 2 \dot{t} \dot{\chi} r^2 \cos\delta_3 \cos\psi \\ &+ \dot{\chi}^2 r^2 \cos^2\psi \end{aligned} \tag{3.10}$$

thus; from definitions of T, M, and I

$$T = \frac{1}{2} M \dot{\chi}^2 S^2 \cos^2\psi \quad \left. \begin{array}{l} \text{From} \\ (3.8) \end{array} \right\} \tag{3.11}$$

$$\left. \begin{aligned} &+ \frac{1}{2} I \Omega^2 \\ &- \frac{1}{2} I \Omega^2 \tau^2 \cos^2\delta_3 \\ &- M \Omega r \dot{\chi} S \sin\psi \\ &+ I \dot{\chi} \Omega \tau \cos\delta_3 \sin\psi \\ &+ \frac{1}{2} M \dot{\chi}^2 S^2 \sin^2\psi \end{aligned} \right\} \tag{3.9}$$

$$\left. \begin{aligned} &+ \frac{1}{2} I \dot{t}^2 \cos^2\delta_3 \\ &+ I \dot{t} \dot{\chi} \cos\delta_3 \cos\psi \\ &+ \frac{1}{2} I \dot{\chi}^2 \cos^2\psi \end{aligned} \right\} \tag{3.10}$$

IV. Since there are no potential energy terms (i.e. vacuum)

$$\text{Lagrangian, } L = T - V = T$$

Thus; equations of motion are:

$$\frac{d}{dt} \left(\frac{\partial T}{\partial \dot{t}} \right) - \frac{\partial T}{\partial t} = 0 \tag{3.12a}$$

$$\frac{d}{dt} \left(\frac{\partial T}{\partial \dot{\chi}} \right) - \frac{\partial T}{\partial \chi} = 0 \quad (3.12b)$$

V. Write Equations of Motion from Lagrangian:

(Note: $\dot{\psi} = \Omega$)

$$\begin{aligned} \frac{d}{dt} \left(\frac{\partial T}{\partial \dot{\tau}} \right) &= \frac{d}{dt} \left[\frac{1}{2} I \cos^2 \delta_3 (2\dot{\tau}) + I \dot{\chi} \cos \delta_3 \cos \psi \right] \\ &= I \cos^2 \delta_3 \ddot{\tau} \\ &\quad + I \cos \delta_3 (-\dot{\chi} \Omega \sin \psi + \ddot{\chi} \cos \psi) \end{aligned}$$

or

$$= I \cos \delta_3 (\cos \delta_3 \ddot{\tau} - \dot{\chi} \Omega \sin \psi + \ddot{\chi} \cos \psi)$$

$$\begin{aligned} \frac{d T}{d \tau} &= -\frac{1}{2} I \Omega^2 (2\tau) \cos^2 \delta_3 + I \dot{\chi} \Omega \cos \delta_3 \sin \psi \\ &= I \cos \delta_3 (-\tau \Omega^2 \cos \delta_3 + \dot{\chi} \Omega \sin \psi) \end{aligned}$$

Now the first equation is:

$$\begin{aligned} I \cos \delta_3 (\ddot{\tau} \cos \delta_3 + \tau \Omega^2 \cos \delta_3 \\ - 2 \dot{\chi} \Omega \sin \psi + \ddot{\chi} \cos \psi) = 0 \end{aligned} \quad (3.13a)$$

$$\frac{d}{dt} \frac{\partial T}{\partial \dot{\chi}} = \frac{d}{dt} \left[\begin{array}{l} + \frac{1}{2} M (2\dot{\chi}) S^2 \cos^2 \psi \\ - M \Omega r S \sin \psi \\ + I \Omega \tau \cos \delta_3 \sin \psi \\ + \frac{1}{2} M (2\dot{\chi}) S^2 \sin^2 \psi \\ + I \dot{\tau} \cos \delta_3 \cos \psi \\ + \frac{1}{2} I (2\dot{\chi}) \cos^2 \psi \end{array} \right]$$

$$\begin{aligned}
 &= M S^2 \left[\dot{\chi} (-2 \Omega \sin\psi \cos\psi) + \ddot{\chi} \cos^2\psi \right] \\
 &- M r S \Omega^2 \cos\psi \\
 &+ I \cos\delta_3 \Omega \left[\Omega \tau \cos\psi + \dot{\tau} \sin\psi \right] \\
 &+ M S^2 \left[\dot{\chi} (2 \Omega \sin\psi \cos\psi) + \ddot{\chi} \sin^2\psi \right] \\
 &+ I \cos\delta_3 \left[-\dot{\tau} \Omega \sin\psi + \ddot{\tau} \cos\psi \right] \\
 &+ I \left[\dot{\chi} (-2 \Omega \sin\psi \cos\psi) + \ddot{\chi} \cos^2\psi \right]
 \end{aligned}$$

$$\frac{\partial T}{\partial \chi} = 0$$

cancelling terms and noting

$$\cos^2\psi + \sin^2\psi = 1,$$

thus the second equation is:

$$\begin{aligned}
 &M S^2 \ddot{\chi} + I \cos^2\psi \ddot{\chi} + I \cos\delta_3 \cos\psi \ddot{\tau} && (3.13b) \\
 &- 2 I \Omega \sin\psi \cos\psi \dot{\chi} \\
 &+ I \cos\delta_3 \Omega^2 \cos\psi \tau \\
 &- M r S \Omega^2 \cos\psi = 0
 \end{aligned}$$

VI. Combine equations in matrix form:

Mass Matrix:

$$+ \begin{bmatrix} (I \cos^2\delta_3) & (I \cos\delta_3 \cos\psi) \\ (I \cos\delta_3 \cos\psi) & (M S^2 + I \cos^2\psi) \end{bmatrix} \begin{bmatrix} \ddot{\tau} \\ \ddot{\chi} \end{bmatrix} \quad (3.14)$$

Gyroscopic Matrix:

$$+ \begin{bmatrix} (0) & (-2 I \Omega \sin\Psi \cos\delta_3) \\ (0) & (-2 I \Omega \sin\Psi \cos\Psi) \end{bmatrix} \begin{bmatrix} \dot{\tau} \\ \dot{\chi} \end{bmatrix}$$

Stiffness Matrix:

$$+ \begin{bmatrix} (I \Omega^2 \cos^2\delta_3) & (0) \\ (I \Omega^2 \cos\delta_3 \cos\Psi) & (0) \end{bmatrix} \begin{bmatrix} \tau \\ \chi \end{bmatrix}$$

$$+ \begin{bmatrix} (0) \\ -(M r S \Omega^2 \cos\Psi) \end{bmatrix} = 0$$

(FOR BLADE 1 ONLY)

VII. Write Kinetic Energy for Second Blade

For second blade

τ becomes $-\tau$

and

χ becomes $-\chi$

From the equation for kinetic energy of Blade 1, the only term affected by the sign change is the term:

$$(-M \Omega r \dot{\chi} S \sin\Psi) \text{ (From } v_c^2)$$

it will become (+) due to the $\dot{\chi}$ sign change.

In the equations of motion, then, for the second blade the terms are all the same, except the forcing term which for both blades are added then the final equations of motion

will be the sum and will also include the moment of inertia of the nacelle in the $\ddot{\chi}$ term

I_N = Nacelle moment of inertia

Mass = M

$$2 \begin{bmatrix} (I \cos^2 \delta_3) & (I \cos \delta_3 \cos \Psi) \\ (I \cos \delta_3 \cos \Psi) & (I_N + M S^2 + I \cos^2 \Psi) \end{bmatrix} \begin{bmatrix} \ddot{\tau} \\ \ddot{\chi} \end{bmatrix} \quad (3.15a)$$

(Gyroscopic) = G

$$+2 \begin{bmatrix} (0) & (-2 I \Omega \sin \Psi \cos \delta_3) \\ (0) & (-2 I \Omega \sin \Psi \cos \Psi) \end{bmatrix} \begin{bmatrix} \dot{\tau} \\ \dot{\chi} \end{bmatrix}$$

(Stiffness = K)

$$+2 \begin{bmatrix} (I \Omega^2 \cos^2 \delta_3) & (0) \\ (I \Omega^2 \cos \delta_3 \cos \Psi) & (0) \end{bmatrix} \begin{bmatrix} \tau \\ \chi \end{bmatrix}$$

= {F}

VIII. Next, one must consider the aerodynamic forces and include these on the right side of the equation. Using definitions of MB, MQ, TQ and TB the forcing vector, F, becomes

$$\begin{aligned}
 (F) = & \left[\begin{array}{l}
 + (M\beta(1) - M\beta(2)) \cos\delta_3 \\
 + (MQ(1) \sin\beta(1) - MQ(2) \sin\beta(2)) \sin\delta_3 \\
 + S (TQ(2) - TQ(1)) \sin\Psi \\
 + S (T\beta(2) \sin\beta(2) - T\beta(1) \sin\beta(1)) \cos\Psi \\
 + (M\beta(1) - M\beta(2)) \cos\Psi \\
 + (MQ(1) \sin\beta(1) - MQ(2) \sin\beta(2)) \sin\Psi \\
 + \text{Yaw moment}
 \end{array} \right] \quad (3.15b)
 \end{aligned}$$

IX. Solving for $\ddot{\tau}$ and $\ddot{\chi}$

One now has:

$$\begin{aligned}
 2(M) \begin{pmatrix} \ddot{\tau} \\ \ddot{\chi} \end{pmatrix} + 2(G) \begin{pmatrix} \dot{\tau} \\ \dot{\chi} \end{pmatrix} + 2(K) \begin{pmatrix} \tau \\ \chi \end{pmatrix} &= (F) \\
 (M) \begin{pmatrix} \ddot{\tau} \\ \ddot{\chi} \end{pmatrix} &= \frac{1}{2}(F) - (G) \begin{pmatrix} \dot{\tau} \\ \dot{\chi} \end{pmatrix} - (K) \begin{pmatrix} \tau \\ \chi \end{pmatrix}
 \end{aligned}$$

Next; multiply G and K times τ and χ vectors,

Then; calculate $(M)^{-1}$,

Then; premultiply all terms by M^{-1} to decouple equations.

Now:

$$\begin{aligned}
 (I) \begin{pmatrix} \ddot{\tau} \\ \ddot{\chi} \end{pmatrix} &= - (M)^{-1} (G) \begin{pmatrix} \dot{\tau} \\ \dot{\chi} \end{pmatrix} - (M)^{-1} \\
 (K) \begin{pmatrix} \tau \\ \chi \end{pmatrix} &+ (M)^{-1} \frac{1}{2} (F)
 \end{aligned} \quad (3.16)$$

Where I is the identity matrix.

Equations for $\ddot{\eta}$ and $\ddot{\chi}$ can now be found by matrix manipulation.

X. Matrix Manipulations

Notation used:

$$(M) = \begin{bmatrix} M_{11} & M_{12} \\ M_{21} & M_{22} \end{bmatrix}$$

and

$$(M)^{-1} = \begin{bmatrix} \bar{M}_{11} & \bar{M}_{12} \\ \bar{M}_{21} & \bar{M}_{22} \end{bmatrix}$$

By definition:

$$\det M = M_{11} * M_{22} - (M_{12})^2 \text{ (symmetric)}$$

and

$$\bar{M}_{11} = M_{22}/\det M$$

$$\bar{M}_{12} = -M_{12} \det M = \bar{M}_{21} \text{ (symmetric)}$$

$$\bar{M}_{22} = M_{11}/\det M$$

Identifying the matrix terms from equation (3.15), one has:

$$M_{11} = I \cos^2 \delta_3 \tag{3.17}$$

$$M_{12} = I \cos \delta_3 \cos \Psi$$

$$M_{21} = I \cos \delta_3 \cos \Psi$$

$$M_{22} = I_N + M S^2 + I \cos^2 \Psi$$

$$G_{11} = 0$$

$$G_{12} = -2 I \Omega \sin \Psi \cos \delta_3$$

$$G_{21} = 0$$

$$G_{22} = -2 I \Omega \sin \Psi \cos \Psi$$

$$K_{11} = I \Omega^2 \cos^2 \delta_3$$

$$K_{12} = 0$$

$$K_{21} = I \Omega^2 \cos \delta_3 \cos \Psi$$

$$K_{22} = 0$$

$$F_1 = (MB(1) - MB(2)) \cos \delta_3 \\ + (MQ(1) \sin \beta(1) - MQ(2) \sin \beta(2)) \sin \delta_3$$

$$F_2 = S (TQ(2) - TQ(1)) \sin \Psi \\ + S (TB(2) \sin \beta(2) - TB(1) \sin \beta(1)) \cos \Psi \\ + (MB(1) - MB(2)) \cos \Psi \\ + (MQ(1) \sin \beta(1) - MQ(2) \sin \beta(2)) \sin \Psi \\ + \text{Yaw moment}$$

Thus carrying out the matrix multiplications and finding $(M)^{-1}$ one obtains:

$$\ddot{\tau} = \frac{1}{2} (\bar{M}_{11} * F_1 + \bar{M}_{22} * F_2) \tag{3.18} \\ - (\bar{M}_{11} * G_{12} \dot{\chi} + \bar{M}_{12} * G_{22} \dot{\chi}) \\ - (\bar{M}_{11} * K_{11} \tau + \bar{M}_{22} * K_{21} \tau)$$

$$\ddot{\chi} = \frac{1}{2} (\bar{M}_{21} * F_1 + \bar{M}_{22} * F_2) \tag{3.19} \\ - (\bar{M}_{21} * G_{12} \dot{\chi} + \bar{M}_{22} * G_{22} \dot{\chi}) \\ - (\bar{M}_{21} * K_{11} \tau + \bar{M}_{22} * K_{21} \tau)$$

These calculations are easily carried out in the computer by identifying the matrix terms from equation (3.17) and calculating the mass inverse matrix terms.

XI. Constant Yaw Rate Only

If simulations are limited to constant yaw rates only, then the $\ddot{\chi}$ equation is unnecessary and since $\dot{\chi} = 0$, one can simplify the matrix equations, since they decouple.

Thus

$$(M) \begin{pmatrix} \ddot{\tau} \\ \ddot{\chi} \end{pmatrix} = -(G) \begin{pmatrix} \dot{\tau} \\ \dot{\chi} \end{pmatrix} - (K) \begin{pmatrix} \tau \\ \chi \end{pmatrix} + \frac{1}{2} \begin{pmatrix} F1 \\ F2 \end{pmatrix} \quad (3.20)$$

can be written for constant yaw rate:

$$M11 \ddot{\tau} = -(G12 \dot{\chi}) - (K11 \tau) + \frac{1}{2} F1$$

(Since $G11 = K12 = 0$ for this case)

and

$$\ddot{\tau} = \frac{1}{M11} \left[-G12 \dot{\chi} - K11 \tau + \frac{1}{2} F1 \right] \quad (3.21)$$

APPENDIX 6.4

Documentation for Constant Yaw
Dynamics and Revplot Programs

A \$	Date and Notes for Simulation Run.
AA	Angle-of-attack (degrees).
APITCH	Aerodynamic Pitch Angle.
B	Total Blade Flap Angle (radians).
BD	Total Blade Flap Rate.
BR	Tip Loss Factor.
BØ	Precone (radians).
CD	Drag Coefficient.
CL	Lift Coefficient.
CNT	Azimuth Iteration Limit = INT ($2\pi/DPSI$).
CO	Azimuth Angle Counter.
CR	Blade Pitch Correction (degrees).
CW	Chord Width (m).
C3	Cos (δ_3).
DLT	Time Increment (seconds).
DPSI	Azimuth Increment (radians).
DR	Blade Span Element (m).
DTHETA	Local Total Blade Pitch (degrees).
DY	State Variable Derivative.
D3	Delta Three Angle (radians).
EL or ELAPSED	Elapse Time (seconds).
EY	Predictor-corrector Error Limit.

EZ State Variable Error After Each Revolution.
E1 Present Predictor-corrector Error.
FFLAG Maximum Iteration Limit for Predictor-corrector.
F1, F2 Scale Factors for Plotting.
G \$ Autorotation Flag.
H H Force (N).
H1 Total CT Counter for Averages.
H2 Total CQ Counter for Averages.
H3 Total NU Counter for Averages.
H4 Maximum Value Over Revolution of Array Variable S1.
H5 Minimum Value Over One Revolution of Array Variable S1.
H6 Maximum Over Revolution of Array Variable S2.
H7 Minimum Over Revolution of Array Variable S2.
I Loop Variable.
KT, KZ Revolution Limit Counters.
L Blade Counter (1 or 2).
MB Total Blade Thrust Moment (Nm).
MI Blade Moment of Inertia (kg m^2).
MQ Total Blade Driving Torque (Nm).
MZ Blade Mass (kg).
N Number of State Variables.
NI Nacelle Moment of Inertia (kg m^2).
NR Number of Blade Divisions.
P-\$ Print Flags.
PHI Inflow Angle (radians).

PI π

PSI Azimuth Angle (radians).

QF Scaling Factor for Plotting.

QP Option Select Flag.

R Local Blade Position of Element (m).

RADIUS Wind Turbine Blade Radius (m).

REV Revolution Counter.

REV.DAT.X File Name to Save Angle of attack, Cyclic Pitch, and Induced Flow Data from Previous Revolution.

RHO Air Density.

RY Reynolds Number.

R4 Dummy Variable = $\rho \pi R^4$.

R5 Dummy Variable = $\rho \pi R^5$.

S Distance from Yaw Axis to Rotor (m).

SD3 $\sin(\delta_3)$.

SL Solidity Ratio.

S1 Array Variable Saved for Printout. Usually Cyclic Pitch, Y(1), (radians).

S2 Array Variable Saved for Printout. Usually H Force, H(N), or Induced Flow, Y(5).

S3 Array Variable Saved for Printout. Usually Local Angle-of-attack, AA (degrees).

S4 Array Variable Saved for Printout. Usually Local Induced Flow, $(Z3 = V_i \text{ (m/s)})$.

TB Total Thrust Force Per Blade (N).

THETA Pitch Angle (radians).

TQ Total In-plane Force Per Blade (N).

TØ Blade Twist (degrees).

U Resultant Blade Element Velocity (m/s).
UP Normal Blade Element Velocity (m/s).
UT Tangential Blade Element Velocity (m/s).
VX In-plane Wind Velocity Component (m/s).
VZ Axial Wind Velocity Component (m/s).
WIND Wind Velocity (m/s).
WB, W1 Blade Frequency Coefficients (rad/s).
XY, ZY Dummy Variable to Save Previous State Variables.
XDY Dummy Variable to Save Previous State Variable Derivatives.
Y State Variables (see List in Text).
YØ Variable to Save Present State Variables as New Ones are Calculated in Predictor-corrector.
Z3 Dimensional Local Induced Velocity (m/s).

LIST

```
1 REM CONSTANT YAW DYNAMICS
2 REM REVISION 2/6/81
3 REM CONSTANT YAW RATES ONLY
4 REM SEE SUBR. 1400 FOR DYNAMIC YAW RATE CHANGES
5 D$ = CHR$(4)
20 DIM X(9),YX(9),VX(9),E1(9),DYX(9),XDYX(9),ZY(9),EZ(9),TB(2),MB(2),TK(2),MK(2),
    B(2),BD(2)
21 DIM S1(36),S2(36)
22 DIM S3(36,10),S4(36,10)
24 HOME : UTAB 5
25 PRINT "      NOTES": PRINT "1. 'CNTRL Z' STOPS PROGRAM ON EVEN REVOLUTION."
26 PRINT "2. UNITS ARE SI"
27 PRINT "3. PRESENTLY FOR CONSTANT YAW RATES ONLY. SEE SUBR. 1400."
28 INPUT "PRESS RETURN TO CONT.":H$
29 HOME
30 INPUT "ENTER DATE AND NOTES FOR THIS RUN, IF ANY > ":A$
31 PRINT
35 INPUT "IS THIS RUN FOR AUTOROTATION ? (Y/N) ":B$
36 PRINT
40 INPUT "INPUT DELTA AZIMUTH VALUE IN DEG ? ":DPSI
41 PRINT
45 INPUT "INPUT ERROR TOLERANCE FOR PRED. CORREC. ROUTINES ? ":EY
46 PRINT
50 INPUT "INPUT MAXIMUM NUMBER OF ITERATIONS FOR PRED. CORREC. ROUTINES
    ? ":FFLAG
51 PRINT
60 INPUT "INPUT NUMBER OF BLADE DIVISIONS FOR CALCULATIONS ?":NR
61 PRINT
65 INPUT "ENTER WIND SPEED (M/S) > ":WIND
66 HOME : UTAB 5
70 PRINT "WHICH PRINT ROUTINES DO YOU WANT? "
71 PRINT
72 PRINT " ANSWER (Y/N) ": PRINT : PRINT : PRINT
73 INPUT "DATE, INITIAL VALUES AND INPUT DATA? ":P0$
75 INPUT "DETAILED BLADE DATA? ":P1$
80 INPUT "CURRENT NON-DIH. DATA? ":P2$
85 INPUT "DIH. DATA? ":P3$
90 INPUT "CURRENT X(I) VALUES AND ERRORS? ":P4$
91 INPUT "AVERAGE VALUES AT END OF REV. PRINTED ? (Y/N) ":P5$
93 INPUT " OUTPUT TO PRINTER FOR X(I) VALUES AT EACH PSI (Y/N) ? ":PY$
95 REM INITIALIZE Y VALUES AND DATA
96 HOME
100 PRINT "ENTER INITIAL X(I) VALUES : "
102 N = 8: REM NUMBER OF STATE VARIABLES
105 FOR I = 1 TO N
107 PRINT " Y":I;
108 INPUT X(I)
110 NEXT I
115 FOR I = 1 TO N:ZY(I) = X(I): NEXT I
116 SL = .032: REM SOLIDITY RATIO
117 APITCH = -.5: REM AERODYN. PITCH ANGLE IN DEG.
118 CR = APITCH + 2.22: REM THIST CORRECTION
119 HZ = 15:NI = 51.6:S = .61
120 PI = 3.14159:BO = 0 * PI / 180:D3 = 67 * PI / 180:C3 = COS (D3):T3 =
    TAN (D3):MI = 40.7:RADIUS = 3.81:RHO = 1.23:S03 = SIN (D3)
121 MB = 7.46 * 2 * PI:MI = .1765 * 2 * PI:DR = (RADIUS - 1.016) / NR
122 R4 = RHO * PI * RADIUS ^ 4
```

```
123 R5 = R4 * RADIUS
125 IF P0$ = "Y" THEN GOSUB 2000
126 KT = 1:KZ = 0
127 PSI = 0:REV = 0:CO = 0
128 ELAPSED = 0
134 CNT = INT (362 / DPSI)
135 DPSI = DPSI * PI / 180
140 HOME
145 UTAB 19: HTAB 1: PRINT "WAIT"
150 REM LOOPS FOR ITERATIONS
160 IF CO = CNT THEN KZ = KZ + 1
161 IF CO = CNT THEN REV = REV + 1
180 GOSUB 800
181 S2(CO) = (TQ(2) - TQ(1)) * SIN (PSI)
182 REM S2 IS THE YAWING IMPLANE FORCE
195 IF P3$ = "Y" THEN GOSUB 2300
210 IF P2$ = "Y" THEN GOSUB 2200
220 IF KZ = KT THEN GOSUB 3000
225 IF CO = CNT THEN GOSUB 700
230 GOSUB 1000: REM CALL PRED CORREC.
235 EL = EL + DLT:CO = CO + 1
238 UTAB 24: PRINT CNT;": ";CO;": REV=";REV;": AZM="; INT (.5 + PSI * 180
/ PI);": TIME=";.01 * INT (100 * EL + .5);: UTAB 19
240 IF P4$ = "Y" THEN GOSUB 8500
250 IF P5$ = "Y" THEN GOSUB 8000
270 S1(CO) = Y(1)
400 GOTO 160
700 REM SUBR TO RESET ZY(I) AND CO
710 CO = 0
720 FOR I = 1 TO N
730 ZY(I) = Y(I)
740 NEXT I
750 RETURN
800 REM SUBR. BLADE FORCES
801 Z2 = SQRT ((1 - COS (Y(7))) / (1 + COS (Y(7))))
803 FOR L = 1 TO 2:TB(L) = 0:MB(L) = 0:TQ(L) = 0:MX(L) = 0
804 NEXT L
805 UX = WIND * SIN (Y(7))
807 UZ = WIND * COS (Y(7))
808 FOR L = 1 TO 2
809 IF L = 2 THEN PSI = PSI + PI
810 BK(L) = B0 + Y(3) + (- 1 ^ (L + 1)) * Y(1) * C3
812 BK(L) = Y(4) + (- 1 ^ (L + 1)) * Y(2) * C3
814 BR = RADIUS
818 FOR IR = 1 TO NR
820 R = 1.016 + IR * DR - .5 * DR
840 T0 = -.7107 * R ^ 3 + 6.834 * R ^ 2 - 23.359 * R + 28.85 + CR
845 IF R < 1.27 THEN T0 = 8.75 + CR
850 DTHETA = T0 + ((- 1 ^ (L + 1)) * Y(1) * SD3 * 180 / PI)
860 THETA = DTHETA * PI / 180
870 CH = -.075 * R + .392
880 IF R < 1.27 THEN CH = .8 * R - .7112
890 UT = Y(6) * R + (UX - Y(8) * S) * SIN (PSI)
895 Z3 = Y(6) * Y(5) * R * (1.33 + (15 * PI / 64)) * Z2 * COS (PSI)
900 UP = UZ - Z3 - R * BK(L) - (BK(L) * UX + Y(8) * R) * COS (PSI)
910 U2 = UT ^ 2 + UP ^ 2
915 RY = SQRT (U2) * CH * 1000 / .01394
920 PHI = ATN (UP / UT)
930 AA = (PHI - THETA) * 180 / PI
932 IF L < > 1 THEN 940
933 IF FLAG < > 0 THEN 940
```

```
934 S3(CO,IR) = AA:94(CO,IR) = Z3
940 GOSUB 6000: REM GET CL AND CD
942 IF IR = NR THEN 945: REM TIP LOSS CORRECTION
944 GOTO 950
945 BR = RADIUS * .96
946 IF G$ = "Y" THEN BR = RADIUS * .98: REM AUTOROTATION
948 CL = CL * (1 - (3.81 - BR) / DR)
950 Z1 = .5 * RHO * CM * U2 * DR
955 TR = Z1 * (CL * COS (PHI) + CD * SIN (PHI))
960 QR = Z1 * (CL * SIN (PHI) - CD * COS (PHI))
965 TB(L) = TB(L) + TR:MB(L) = MB(L) + (TR * R)
970 TQ(L) = TQ(L) + QR:MQ(L) = MQ(L) + (QR * R)
976 IF P1$ = "Y" THEN GOSUB 2100
980 NEXT IR: NEXT L
983 PSI = PSI - PI
985 RETURN
1000 REM SUBR. TO CALC YI AT TIME T +DLT
1010 GOSUB 1400: REM GET OYS
1020 FOR I = 1 TO N
1030 Y0(I) = Y(I)
1040 X0Y(I) = DY(I)
1050 NEXT I
1055 DLT = DPSI / Y0(6)
1060 FOR I = 1 TO N
1070 Y(I) = Y0(I) + DLT * (DY(I))
1080 XY(I) = Y(I)
1090 NEXT I
1094 PSI = PSI + DPSI
1095 FLAG = 1
1096 IF PSI > = (2 * PI) THEN PSI = PSI - 2 * PI
1100 GOSUB 800
1105 GOSUB 1400
1107 DLT = 2 * DPSI / (Y0(6) + Y(6))
1110 FOR I = 1 TO N
1120 Y(I) = Y0(I) + .5 * DLT * (X0Y(I) + DY(I))
1125 IF Y(I) = 0 THEN 1140
1130 E1(I) = ABS (Y(I) - XY(I)) / ABS (Y(I))
1140 NEXT I
1142 UTAB 18: HTAB 1: PRINT "
1143 PRINT "
1144 UTAB 18: HTAB 1: PRINT "ER%: ";
1146 FOR I = 1 TO N: PRINT INT (100 * E1(I) + .5);": ";
1148 NEXT I
1149 UTAB 19: HTAB 1: PRINT " FLAG= ";FLAG
1150 IF FLAG = FFLAG THEN 1250
1160 FOR I = 1 TO N
1170 IF E1(I) > EY THEN 1200
1180 NEXT I
1190 GOTO 1260
1200 FOR I = 1 TO N
1210 XY(I) = Y(I)
1230 NEXT I
1235 FLAG = FLAG + 1
1240 GOTO 1100
1250 UTAB 19: HTAB 1: PRINT "
```

```

1252 UTAB 19: PRINT " FLAG=" ;FLAG;" STOP ITERATION"
1260 REM LATEST Y(I) SAVED.CONTINUE
1265 DLT = 2 * DPSI / (Y(6) + Y(6))
1267 FLAG = 0
1275 RETURN
1400 REM SUBR TO CALC Y(I) DERIV.
1410 REM CALC MATRICIES
1415 CI = COS (PSI):SI = SIN (PSI):NI = 51.6 + 1.65 * Y(7)
1420 M1 = MI * (C3 ^ 2):M2 = MI * C3 * CI:M4 = NI + M2 * S ^ 2 + MI * (CI
    ^ 2)
1421 REM M2=M3
1430 G2 = - 2 * MI * Y(6) * C3 * SI:G4 = - 2 * MI * Y(6) * SI * CI
1440 K1 = MI * (Y(6) ^ 2) * C3 ^ 2:K3 = MI * (Y(6) ^ 2) * C3 * CI
1450 A1 = (MB(1) - MB(2)) * C3:B1 = (MX(1) * SIN (BX(1)) - MX(2) * SIN (BX(2)))
    * S03
1451 F1 = A1 + B1
1455 GOTO 1500: REM CONSTANT YAWRATE ONLY
1460 O1 = S * (TX(2) - TX(1)) * SI
1461 O2 = S * (TB(2) * SIN (BX(2)) - TB(1) * SIN (BX(1))) * CI
1462 O3 = (MB(1) - MB(2)) * CI
1463 O4 = (MX(1) * SIN (BX(1)) - MX(2) * SIN (BX(2))) * SI
1468 REM ADD YAW MOMENT TO 1470
1470 F2 = O1 + O2 + O3 + O4
1480 DM = (M1 * M4) - M2 ^ 2
1490 I1 = M4 / DM:I2 = - M2 / DM:I4 = M1 / DM
1491 REM I2=I3
1500 DY(1) = Y(2)
1505 GOTO 1525: REM CONSTANT YAWRATE ONLY
1510 O1 = .5 * (I1 * F1 + I2 * F2)
1511 O2 = - (I1 * G2 * Y(8) + I2 * G4 * Y(8))
1512 O3 = - (I1 * K1 * Y(1) + I2 * K3 * Y(1))
1520 DY(2) = O1 + O2 + O3
1524 REM 1525 NOT TRUE FOR DYNAMIC YAWRATE..DELETE
1525 DY(2) = (1 / M1) * (- G2 * Y(8) - K1 * Y(1) + .5 * F1)
1530 DY(3) = Y(4)
1535 A2 = (MB(1) + MB(2)) / (2 * MI)
1540 DY(4) = - 1 * (MB ^ 2 + (Y(6) ^ 2) * M1 ^ 2) * Y(3) + A2
1550 GOSUB 7000
1560 UW = SQRT ((MU ^ 2) + (INFLOW ^ 2))
1570 TT = (64 / (75 * PI)) / UW
1580 DY(5) = (Y(6) / TT) * ((.5 * CT / UW) - Y(5))
1600 IF 6$ = "Y" THEN G0 = 3.2E - 05 * R5 * Y(6) ^ 2
1605 REM AUTOROTATIONAL SHAFT TORQUE IS CG/S=.001 FROM TEST DATA
1610 IF 6$ = "N" THEN G0 = 2.56E - 04 * R5 * Y(6) ^ 2
1620 REM SHAFT TORQUE IS CG/S=.000 FROM TEST DATA
1630 DY(6) = (1 / (2 * MI)) * (MX(1) + MX(2) - G0)
1631 REM APPROX. IGNORES EFFECT OF FLAP ON TORQUE
1640 DY(7) = Y(8)
1645 REM FOR CONSTANT YAWRATE ONLY
1646 DY(8) = 0
1647 GOTO 1700
1650 O1 = .5 * (I3 * F1 + I4 * F2)
1651 O2 = - (I3 * G2 * Y(8) + I4 * G4 * Y(8))
1652 O3 = - (I3 * K1 * Y(1) + I4 * K3 * Y(1))
1660 DY(8) = O1 + O2 + O3
1700 RETURN
2000 REM SUBR. PRINTS INPUT DATA (P0$)
2002 HOME : UTAB 10: PRINT "READY TO PRINT THE INITIAL DATA SET."
2003 PRINT : INPUT "DO YOU WANT THE PRINTER ON? (Y/N) > " ;O$
2004 IF O$ = "Y" THEN PRINT D$;"PR#1"

```

```
2005 HOME : PRINT : PRINT "INITIALIZED DATA SET": PRINT : PRINT A$
2010 PRINT : PRINT "DELTA 3 (DEG)= ";D3 * 180 / PI
2011 PRINT "PRECONE ANGLE (DEG)= ";B0 * 180 / PI
2012 PRINT "BLADE I (KG M^2)= ";MI
2014 PRINT "BLADE NTL.FREQ (HZ)= ";HB / (2 * PI)
2016 PRINT "BLADE FREQ COEFF.(HZ)= ";HI / (2 * PI)
2018 PRINT "RADIUS (M)= ";RADIUS
2020 PRINT "AIR DENSITY (KG/M^3)= ";RHO
2022 PRINT "AERO DYN. PITCH AT .7R (DEG)= ";APITCH
2024 PRINT "DR (M)= ";DR
2035 GOSUB 2050
2040 RETURN
2050 PRINT : PRINT "OP. IN AUTOROT.?" ;G$
2052 PRINT " DELTA AZHTH.(DEG)= ";DPSI
2054 PRINT "# BLADE ELEM. = ";NR
2056 PRINT "PRED.CORR. ERROR LMT= ";EY
2058 PRINT "PRED.CORR. ITER. LMT= ";FFLAG
2060 PRINT "BLADE MASS (KG)= ";M2
2061 PRINT "MACELLE MOM.OF INERTIA (KG M^2)= ";MI;" FOR ZERO YAW ANGLE
    ONLY"
2062 PRINT "YAW MOM. ARM (M)= ";S
2065 PRINT "SOLIDITY RATIO= ";SL
2070 PRINT "WIND SPEED (M/S)= ";WIND
2080 PRINT : FOR I = 1 TO N
2082 PRINT " Y";I;" = ";Y(I)
2084 NEXT I
2085 INPUT " PRESS RETURN TO CONT." ;H$
2087 IF G$ = "Y" THEN PRINT D$;"PR#0"
2090 RETURN
2100 REM SUBR. TO PRINT CURRENT BLADE DATA. (P1$)
2102 HOME
2103 INPUT " PRINTER ON (Y/N) ? " ;PP$
2104 IF PP$ = "Y" THEN PRINT D$;"PR#1"
2105 PRINT " ELEMENTAL BLADE DATA"
2108 PRINT "STEP", "R", "AZM"
2110 PRINT IR,R,PSI * 180 / PI
2112 PRINT "TOTAL BETA VAL.(DEG)= ";B(L) * 180 / PI
2114 PRINT "TOTAL BETA DOT VAL(DEG/S)= ";B(L) * 180 / PI
2116 PRINT "CHORD (M)= ";CH
2118 PRINT "UT (M/S)= ";UT
2120 PRINT "UP (M/S)= ";UP
2122 PRINT "PITCH-TWST (DEG)= ";T0
2124 PRINT "TOTAL PITCH(DEG)= ";DTHETA
2126 PRINT "INFLOW ANGLE(DEG)= ";PHI * 180 / PI
2128 PRINT " ANGLE OF ATTACK(DEG)= ";AA
2130 PRINT "TIP LOSS FACTOR= ";(RADIUS - BR) / RADIUS
2132 PRINT "REYNOLD'S NUMBER= ";RV
2133 PRINT " LOCAL INDUCED FLOW (M/S)= ";Z3
2134 PRINT "CL= ";CL
2136 PRINT "CD= ";CD
2138 PRINT "ELEM. THRUST (N)= ";TR;" BL#";L
2140 PRINT "TOT. THRUST (N)= ";TB(L);" BL#";L
2142 PRINT "TOT. THR.MOM (NM)= ";MB(L);" BL#";L
2144 PRINT " ELEM. IN-PL FOR.(N)= ";OR;" BL#";L
2146 PRINT "TOT. IN-PL FOR.(N)= ";TB(L);" BL#";L
2148 PRINT "TORQUE (NM)= ";MB(L);" BL#";L
2155 IF PP$ = "Y" THEN PRINT D$;"PR#0"
2156 PP$ = "N"
2160 INPUT " PRESS RETURN TO CONT." ;H$
2165 HOME
2175 RETURN
```

```
2200 REM SUBR TO PRINT NON-DIM DATA
2201 HOME
2202 INPUT " PRINTER ON (Y/N) ? ";PP$
2203 IF PP$ = "Y" THEN PRINT D$;"PR#1"
2204 PRINT : PRINT "NON DIMENSIONAL DATA"
2205 PRINT : PRINT "AZIMUTH (DEG)= ";PSI * 180 / PI
2207 GOSUB 7000
2208 PRINT "U= ";U
2210 PRINT "TSR=1/U = ";1 / U
2220 PRINT "CT= ";CT
2225 PRINT "CQ= ";CQ
2230 PRINT "CP= ";CP
2235 PRINT "INFLOW= ";INFLOW
2240 PRINT "ADU RATIO= ";MU
2245 PRINT "INDUCED FLOW= ";NU
2246 INPUT " PRESS RETURN TO CONT.";H$
2247 HOME
2248 IF PP$ = "Y" THEN PRINT D$;"PR#0"
2249 PP$ = "N"
2250 RETURN
2300 REM SUBR TO PRINT DIM DATA
2301 HOME
2302 INPUT "PRINTER ON ? ";PP$
2303 IF PP$ = "Y" THEN PRINT D$;"PR#1"
2304 PRINT "AZIMUTH = "; INT (.5 + PSI * 180 / PI);" THR / THR MOM / IN-PL
  / TORQ / POWER "
2308 FOR L = 1 TO 2: PRINT "BLADE= ";L;: HTAB 11
2310 PRINT INT (.5 + TB(L));": "; INT (.5 + MB(L));": "; INT (.5 + TQ(L));":
  "; INT (.5 + MQ(L));": "; INT (.5 + MQ(L) * Y(6))
2312 NEXT L
2314 PRINT "TOTALS=";: HTAB 11
2316 PRINT INT (.5 + TB(1) + TB(2));": "; INT (.5 + MB(1) + MB(2));": ";
  INT (.5 + TQ(1) + TQ(2));": "; INT (.5 + MQ(1) + MQ(2));": "; INT
  (.5 + (MQ(1) + MQ(2)) * Y(6))
2330 IF PP$ = "Y" THEN PRINT D$;"PR#0"
2334 INPUT " PRESS RETURN TO CONT.";H$
2335 PP$ = "N"
2337 HOME
2340 RETURN
3000 REM SUBR. TO CALC ERRORS ON EACH REVOLUTION
3001 REM CNTRL Z STOPS PROGRAM IN THIS SUBR.
3003 KZ = 0
3004 HOME : UTAB 3: HTAB 5
3005 PRINT "AFTER ";REV;" ROTOR REVOLUTIONS THE Y(I) ERRORS ARE:"
3020 FOR I = 1 TO N
3029 IF ZY(I) = 0 THEN 3055
3030 EZ = ABS (Y(I) - ZY(I)) / ABS (ZY(I))
3054 GOTO 3060
3055 EZ = 0
3060 PRINT " Y";I;" = ";Y(I)
3061 PRINT " ERR";I;" = ";EZ
3100 NEXT I
3700 REM PRINT AVERAGES
3710 PRINT D$;"PR#1"
3720 PRINT "REV=";REV;" TIME=";.01 * INT (EL * 100 + .5);" YAM="; INT
  (Y(7) * 180 / PI + .5);" RPM="; INT (Y(6) / .105 + .5);" MU=";MU
3730 PRINT "AUGS: CT/S=";H1 / (CNT * .032);" CQ/S=";H2 / (CNT * .032);"
  MU=";H3 / CNT
3740 H1 = 0:H2 = 0:H3 = 0
3745 H5 = 10:H7 = 10
3746 H4 = 0:H6 = 0
```

```

3750 FOR I = 1 TO CNT
3760 IF S1(I) < H5 THEN H5 = S1(I)
3770 IF S2(I) < H7 THEN H7 = S2(I)
3780 IF S1(I) > H4 THEN H4 = S1(I)
3790 IF S2(I) > H6 THEN H6 = S2(I)
3800 NEXT I
3810 PRINT "MAX TAU=";.1 * INT (H4 * 1800 / PI + .5);" MIN TAU=";.1 *
      INT (H5 * 1800 / PI + .5);" MAX H =";H6;" MIN H =";H7
3820 PRINT D$;"PR#0"
3905 REM STOP OPTIONS
3915 XX = PEEK ( - 16384)
3916 POKE - 16368,0
3919 REM PRESS CNTRL Z TO STOP
3920 IF XX < > (128 + 26) THEN 4097
3925 PRINT : INPUT "PRESS RETURN TO CONT.";H$
3926 HOME : UTAB 5: HTAB 5
3950 PRINT "SELECT OPTION": PRINT , "1 CONTINUE": PRINT , "2 CHANGE PRINTOUT
      OPTION": PRINT , "3 CHANGE INPUT VALUES": PRINT , "4 STOP"
3951 PRINT , "5 CHANGE ITER. COUNTER": PRINT , "6 OUTPUT TO DISK"
3952 PRINT , "7 PRINT S2 VALUES"
3960 INPUT Z9
3961 ON Z9 GOTO 4097,3980,3983,3962,3972,4065,3965
3962 STOP
3965 PRINT D$;"PR#1"
3966 FOR I = 0 TO CNT - 1
3967 PRINT "AZ= ";I * (360 / CNT);" H FORCE (N)= ";S2(I);HF = S2(I) + HF:
      NEXT I
3968 PRINT "H FORCE TOTAL(N)= ";HF;HF = 0
3970 PRINT D$;"PR#0"
3971 GOTO 3926
3972 HOME : UTAB 5
3973 PRINT " CURRENT AZIMUTH ITERATION COUNTER, KT= ";KT
3975 PRINT : INPUT " INPUT NEW KT VALUE ";KT
3976 HOME : UTAB 10: HTAB 3: PRINT " NEW KT VALUE = ";KT
3977 INPUT " PRESS RETURN TO CONT.";H$
3978 GOTO 3926
3980 HOME
3981 INPUT "INPUT PRINT OPTIONS (Y/N), INITIAL DATA, BLADES, NON-DIM, DIM,
      X(I): INPUT ALL FIVE AS Y OR N ? ";P0$,P1$,P2$,P3$,P4$
3982 PRINT : INPUT "PRINTER ON FOR X(I) AT EACH PSI VALUE (Y/N) ? ";PY$:
      GOTO 3926
3983 HOME
3984 DPSI = DPSI * 180 / PI: PRINT : PRINT "CURRENT DELTA AZIMUTH (DEG)=
      ";DPSI: INPUT " CHANGE VALUE ? ";Z$
3985 IF Z$ = "Y" THEN INPUT "NEW DPSI-DEG? ";DPSI
3986 PRINT : PRINT "CURRENT PR. COR. ERROR AND ITERATIONS= ";EY,FFLAG: INPUT
      "CHANGE VALUES?(Y/N) ";Z$
3987 IF Z$ = "Y" THEN INPUT "NEW EY AND FFLAG? ";EY,FFLAG
3991 PRINT : PRINT "CURRENT AUTOROT. FLAG = ";8$
3992 INPUT " CHANGE VALUE ? ";Z$
3993 IF Z$ = "Y" THEN INPUT " NEW AUTOR. FLAG (Y/N)= ";6$
3994 PRINT : PRINT " CURRENT WIND VALUE= ";WIND
3995 INPUT " CHANGE VALUES ? ";Z$
3996 IF Z$ = "Y" THEN INPUT "NEW WIND VALUE > ";WIND
3997 PRINT : PRINT " CURRENT BLADE STEPS = ";NR: INPUT " CHANGE VALUE ?
      ";Z$: IF Z$ = "Y" THEN INPUT " NEW BLADE STEP NUMBER ? ";NR
4000 PRINT : PRINT "CURRENT YAWRATE= ";Y(8): REM FOR CONSTANT YAWRATE ONLY
4002 INPUT "CHANGE VALUE ?(Y/N) ";Z$
4004 IF Z$ = "Y" THEN INPUT " ENTER NEW YAWRATE VALUE > ";Y(8)
4018 HOME : PRINT " CORRECTED INPUT VALUES ARE:": GOSUB 2050
4020 CNT = INT (362 / DPSI)

```

```
4030 DPSI = DPSI * PI / 180
4040 DR = (RADIUS - 1.016) / NR
4060 GOTO 3926
4065 REM DISK OUTPUT
4066 PRINT D$;"MON C.I,0"
4067 PRINT D$;"OPEN REV.DAT. ";REV
4068 PRINT D$;"DELETE REV.DAT. ";REV
4069 PRINT D$;"OPEN REV.DAT. ";REV
4070 PRINT D$;"WRITE REV.DAT. ";REV
4071 PRINT REV: PRINT CNT: PRINT DLT: PRINT NR
4072 PRINT (Y(6) * RADIUS)
4075 FOR I = 1 TO CNT
4076 PRINT S1(I): PRINT S2(I): NEXT I
4077 PRINT 99999
4078 FOR I = 1 TO CNT
4079 FOR J = 1 TO NR
4080 PRINT S3(I,J)
4081 PRINT S4(I,J)
4082 NEXT J: NEXT I
4083 PRINT D$;"CLOSE REV.DAT. ";REV
4090 GOTO 3926
4097 GOSUB 700
4098 HOME
4100 RETURN
6000 REM SUBR TO GET CD AND CL
6010 IF R < 1.55 THEN CL = .075 * AA + .2
6020 IF R >= 1.55 AND R < 2.5 THEN CL = .0875 * AA + .3
6030 IF R >= 2.5 THEN CL = .1 * AA + .4
6040 AK = AA: IF AA < 0 THEN AK = - AA
6050 IF AK > 90 THEN AK = 180 - AK
6060 CD = .01 + (.5 * ((AK * PI / 180) ^ 2))
6065 IF ABS(AK) > 20 THEN 6067
6066 GOTO 6100
6067 IF FLAG < > 0 THEN 6100
6068 UTAB 19: HTAB 1: PRINT "
"; UTAB 19: HTAB 1
6070 PRINT D$;"PR#1"
6080 PRINT "BL=";L;" STEP=";IR;" AZH="; INT (.5 + PSI * 180 / PI);" AA=";AK;"
DEG";"REV=";REV
6090 PRINT D$;"PR#0"
6100 RETURN
7000 REM SUBR TO CALC NON-DIM DATA
7005 CT = (TB(1) + TB(2)) / (R4 * Y(6) ^ 2)
7010 CQ = (MQ(1) + MQ(2)) / (R5 * Y(6) ^ 2)
7015 U = WIND / (RADIUS * Y(6))
7020 CP = 2 * CQ / (U ^ 3)
7025 INFLOW = (UZ / (Y(6) * RADIUS)) - Y(5)
7030 MU = UX / (Y(6) * RADIUS)
7035 NU = Y(5)
7050 RETURN
8000 REM CALC AVERAGES
8005 IF P4$ = "N" THEN GOSUB 7000
8010 H1 = CT + H1
8020 H2 = CQ + H2
8030 H3 = Y(5) + H3
8050 RETURN
8500 REM SUBROUTINE PRINT Y(I),CT,ETC
8505 GOSUB 7000
8510 IF PY$ = "Y" THEN PRINT D$;"PR#1"
8520 FOR I = 1 TO N: UTAB I: HTAB 9: PRINT "
"; UTAB I: HTAB
5
```

```
8530 PRINT "Y";I;" = ".0001 * INT (10000 * Y(I) + .5): NEXT I
8535 PRINT D$;"PR#0"
8540 HTAB 14: PRINT "           "; HTAB 10: PRINT "DY5=";DY<5>
8550 HTAB 14: PRINT "           "; HTAB 10: PRINT "DY6=";DY<6>
      )
8560 HTAB 7: PRINT "           "; HTAB 2: PRINT "CT/S=";CT / SL
8570 HTAB 7: PRINT "           "; HTAB 2: PRINT "CQ/S=";CQ / SL
8580 HTAB 7: PRINT "           "; HTAB 3: PRINT "LAM=";1 / U
8590 HTAB 7: PRINT "           "; HTAB 1: PRINT "FLAP1="; INT (B<1> *
      180 / PI + .5)
8610 RETURN
```

JLOAD REUPLOT.
JLIST

```
10 REM REUPLOT PROGRAM
15 REM REVISION 1/23/81
20 D$ = CHR$(4)
30 DIM S1(36),S2(36)
31 DIM S3(24,5),S4(24,5)
35 HOME : UTAB 5
40 INPUT "ENTER NAME OF FILE > ";Z$
45 PRINT
50 PRINT D$;"MON C,I,0"
60 PRINT D$;"OPEN ";Z$
70 PRINT D$;"READ ";Z$
75 INPUT REV: INPUT CNT: INPUT DLT: INPUT NR: INPUT RV6
77 FOR I = 1 TO CNT
79 INPUT S1(I): INPUT S2(I): NEXT I
80 INPUT O0
81 IF O0 < > 99999 THEN STOP
85 FOR I = 1 TO CNT: FOR J = 1 TO NR
87 INPUT S3(I,J): INPUT S4(I,J): NEXT J,I
112 PRINT D$;"CLOSE ";Z$
114 HOME : UTAB 10
115 PRINT "SELECT PLOT:"
116 PRINT "1 TAU"
117 PRINT "2 S2"
118 PRINT "3 AA"
119 PRINT "4 NU"
125 PRINT : INPUT " ENTER SELECTION > ";QP
130 HGR : HCOLOR= 3
135 ON QP GOTO 140,140,600,600
140 HPLOT 0,0 TO 240,0 TO 240,160 TO 0,160 TO 0,0
150 FOR J = 0 TO 237 STEP 237
160 FOR K = 20 TO 140 STEP 20
170 HPLOT J,K TO J + 3,K
180 NEXT K: NEXT J
190 HPLOT 0,80 TO 240,80
200 FOR J = 20 TO 220 STEP 20
210 HPLOT J,78 TO J,82
220 NEXT J
230 ON QP GOTO 250,500
250 REM PLOT POINTS
254 UTAB 24
255 INPUT "ENTER TAU SCALING FACTOR > ";F1
260 FOR I = 1 TO CNT
270 X = INT (.5 + 240 * I / CNT)
280 Y = 80 - (S1(I) * (180 / 3.14159) * 20 / F1)
290 HPLOT X,Y
300 NEXT I
```

```
310 INPUT " DO YOU WISH TO PRINT THIS? (Y/N) ";P$
315 TEXT
320 IF P$ = "N" THEN 114
340 INPUT "ENTER GRAPH TITLE > ";U$
345 INPUT "ENTER DATE > ";C$
350 PRINT D$;"PR#1"
360 PRINT : PRINT "TITLE: ";U$
370 PRINT : PRINT "DATE: ";C$
380 PRINT : PRINT "TIME FOR ONE REV.= ";CNT * DLT;" SECONDS"
385 PRINT "REVOLUTION NUMBER=" ;REV
386 IF QP = 1 THEN QF = F1
387 IF QP = 2 THEN QF = F2
390 PRINT "SCALE: ONE UNIT=" ;QF
395 PRINT D$;"PR#0"
400 CALL - 16046
410 GOTO 114
500 REM CT ROUTINE
502 UTAB 24
505 INPUT "ENTER S2 SCALING FACTOR > ";F2
510 FOR I = 1 TO CNT
520 X = INT (.5 + 240 * I / CNT)
530 Y = 80 - (S2(I) * 20 / F2)
540 H$PLOT X,Y
550 NEXT I
560 GOTO 310
600 REM PLOT CIRCLE
605 PI = 3.14159;RAD = 3.81;CO = 1.016
610 DR = (RAD - CO) / NR;AZ = 2 * PI / CNT
612 H$PLOT 140.96 TO 165.96
614 H$PLOT 165.93 TO 235.93 TO 235.99 TO 165.99 TO 165.93
615 FOR I = 0 TO 360 STEP 2
618 THETA = 2 * PI - I * PI / 180
620 X = INT (140.5 + 95 * COS (THETA))
625 Y = INT (96.5 - 95 * SIN (THETA))
630 H$PLOT X,Y
655 NEXT I
675 ON QP GOTO 114,114,700,800
700 REM AA PLOT
704 UTAB 24: HTAB 1
705 INPUT " ENTER AA (99=EXIT) > ";AK
710 IF AK = 99 THEN 310
725 FOR I = 1 TO CNT
730 FOR J = 1 TO 4
735 IF AK > = S3(I,J) AND AK < S3(I,J + 1) THEN 760
740 IF AK < S3(I,J) AND AK > = S3(I,J + 1) THEN 760
745 GOTO 767
760 D = (S3(I,J + 1) - AK) / (S3(I,J + 1) - S3(I,J))
765 GOSUB 900
767 NEXT J
770 NEXT I
775 GOTO 705
795 GOTO 310
800 REM NU PLOT
837 UTAB 24: HTAB 1
840 INPUT " ENTER NU (99=EXIT) > ";NU
843 IF NU = 99 THEN 310
844 NU = NU * RYS
845 FOR I = 1 TO CNT
850 FOR J = 1 TO 4
855 IF NU > = S4(I,J) AND NU < S4(I,J + 1) THEN 880
856 IF NU < S4(I,J) AND NU > = S4(I,J + 1) THEN 880
```

```
860 GOTO 887
880 D = (S4(I,J + 1) - NU) / (S4(I,J + 1) - S4(I,J))
885 GOSUB 900
887 NEXT J
890 NEXT I
892 GOTO 840
895 GOTO 310
900 REM SUBROUTINE
905 PR = (CO + (J + 1 - D) * DR - .5 * DR) / RAD
910 IF PR > 1 OR PR < (CO / RAD) THEN 950
915 THETA = 2 * PI - AZ * I
920 X = INT (140.5 + PR * 95 * COS (THETA))
925 Y = INT (96.5 - PR * 95 * SIN (THETA))
930 HPL0T X,Y
950 RETURN
1000 END
```

APPENDIX 6.5

Data Analysis Software

Introduction

Nine computer programs were developed in order to evaluate and analyze the performance of the experimental wind turbine. Brief Logical Descriptions along with the program listing are presented here.

1. The "Wind-2" Program

1.1 Program Logic

1. Type operator instructions
2. Check variable conversion constants and desired values of cyclic pitch amplitude limits and furl angle
3. Calculate required furl set angle to account for rotor tilt and display result
4. Read clock - store start time
5. Sample wind speed and RPM twice consecutively and calculate mean value
6. Sample furl angle
7. Calculate current value of average RPM during test
8. Test RPM preset value to avoid operation in starting regime. If test fails go to #16
9. Test furl angle in limits. If test fails go to #15

10. Sample cyclic pitch position 47 times (approximately 1 second), store the values, then calculate the amplitude of the signal and store the value
11. Test cyclic pitch within limits; if test fails, print warning on screen, toggle speaker and continue
12. Calculate bin number based on sampled wind speed and 0.5 m/s bin width
13. For each bin array, RPM and cyclic pitch amplitude update the following values at the current bin number. Maximum value in the bin, minimum value, number of samples, mean value, and standard deviation
14. Go to #17
15. Print furl angle out of limits, pause and go to #17
16. Print RPM out of limits and pause
17. Test wind \neq 0, if test fails, go to #20
18. Calculate current wind speed, RPM, cyclic pitch amplitude and tip to wind speed ratio and print out these values on the monitor
19. Go to #21
20. Print wind is calm

- 21 Test to see if operator wishes to pause or stop sampling program. If pause is desired, to to pause subroutine; if neither, go to #5 and repeat sampling
22. Read clock, calculate elapsed time of test and total rotor revolutions using current average RPM value
23. Print out bin arrays
24. Store bin array data on disk along with other pertinent test data.
25. End

Documentation for
Sampling Programs
Wind 2, Wind 6, RPM 6, Wind 2 Fast,
Yawrate, and Binplot Programs

AR Average Rotor Speed.
B% Bin Number (integer).
CB Boom Calibration, Per Volt.
CC Cyclic Pitch Calibration, Per Volt.
CF Flap Bending Calibration, Per Volt.
COLLECT 5
OBJECT Assembly Language Sampling Program.
CR RPM Calibration, Per Volt.
CT Torque Calibration, Per Volt.
CV Generator Volts Calibration, Per Volt.
CW Wind Calibration, Per Volt.
CY Yaw Post Bending Calibration, Per Volt.
DAT.BINS File Name for Bin Data or Disk.
D1 Ambient Temperature ($^{\circ}\text{C}$).
D2 Ambient Pressure (atm).
D3 Wind Direction (degrees).
D4 Generator Load (ohms).
D5 Gear Ratio, Rotor to Generator.
D6 Furl Angle, (degrees) Desired.
FC Density Correction Factor
 $\rho(\text{standard}) * \frac{1}{\text{FC}} = \rho(\text{corrected})$

FS	Furl Set Angle Correcting for Rotor Tilt.
FV	Fast Variable Address Counter for Getting Sampled Data. See Collect 5 Program.
I	Sampled Variable Number.
J	Bin Number Counter.
K	Channel Number Counter.
K- $\$$	Channel Names.
MAX	Maximum Value in Bin.
MEAN	Mean Value in Bin.
MN	Minimum Value in Bin.
N	Number of Samples in Bin.
NR	Number of RPM Samples for Average.
OS	Furl Voltage for Controlling Data Collection at Proper Furl Angle.
PM	Maximum Cyclic Pitch Voltage (0-255).
PN	Minimum Cyclic Pitch Voltage (0-255).
REV	Revolution Counter.
RPM	Rotor RPM.
S	Sampled Variable for Bin Data.
SBAR	Dummy Variable for Bin Data.
SE	Standard Deviation in Bin.
SLW	Slow Variable Address Counter (See Collect 5 Program).
ST	Number of Data Sets Counter.
TABLE	Pointer for Collect 5 Program.
TIME	Elapsed Time.
TSR	Tip Speed Ratio, $\Omega R/v$.
T- $\$$	Clock Variables.

V1 Number of Digital Units Equivalent to One Volt
 for Analog Board.

WIND Wind Speed (m/s).

Z\$ Data File Name.

FOR WIND 2 ONLY

BP Desired Furl Angle.

CCYCP Same as CC.

CRPM Same as CR.

CWIND Same as CW.

F1 Sampled Furl Angle.

XS Sampled Cyclic Pitch.

VF Same as OS.

FOR YAWRATE ONLY

CDYN Dynamic Channel Number

CYAW Yaw Position Channel Number.

DH Maximum Dynamic Value Sampled.

DL Minimum Dynamic Value Sampled.

ET Elapsed Time.

FURL Furl Angle.

HS Maximum RPM for Test.

LS Minimum RPM for Test.

QP Yaw Direction 0 = CCW, 1 = CW.

Y1P 1st Yaw Position.

Y2P 2nd Yaw Position.

Y% Yaw Rate Bin (integer).

LIST

```
5 REM THE WIND2 PROGRAM
6 REM *****
10 D$ = CHR$(4)
20 PRINT D$;"MON C.I.0"
30 PRINT D$;"OPEN DAT.W2"
40 PRINT D$;"DELETE DAT.W2"
50 PRINT D$;"OPEN DAT.W2"
60 PRINT D$;"CLOSE DAT.W2"
61 REM FILE DAT.W2 ON DISK IS CYCLIC PITCH DATA FILE.
65 HOME : UTAB 5: PRINT "THERE ARE 4 CONTROL INSTRUCTIONS:"
66 PRINT "1. '0' PUTS CYCLIC PITCH DATA ON DISK": PRINT " ANY KEY RECOVERS":
PRINT "2. 'CNTRL W' IS A WAIT ROUTINE": PRINT "3. 'CNTRL S' RECOVERS FOR DATA SA
AMPLING": PRINT "4. 'CNTRL Z' STOPS PROG. AND STORES DATA"
67 PRINT : PRINT : INPUT " PRESS RETURN TO CONT.":H$
71 U1 = 54
72 HOME : UTAB 5: PRINT " CHANNEL ASSIGNMENTS": PRINT ,"0 = WIND": PRINT ,"1 =
RPM": PRINT ,"2 = CYCLIC PITCH": PRINT : PRINT
73 PRINT ,"3=BOOM POTENT.": PRINT : PRINT
75 PRINT " PRESENTLY ONE VOLT = ";U1
76 PRINT " CHANGE LINE 71 IF DESIRED"
77 PRINT : PRINT "CHECK VARIABLE CALIBRATION CONSTANTS IN LINE 85 IF REQUIRED
BEFORE RUNNING PROGRAM."
78 PRINT : INPUT " PRESS RETURN TO CONT.":H$
79 HOME : UTAB 5
80 INPUT "INPUT MAX AND MIN CYCLIC PITCH CONTROL NUMBERS.. NORMAL VALUES ARE- 2
45 AND 4 ? ":PM,PN
85 CWIND = 6.705:CRPM = 60.0:CCYCP = 5
90 XR = CRPM / U1:NR = 0:AR = 0
100 DIM S(3),MAX(56,2),MNK(56,2),HEANK(56,2),NK(56,2),SE(56,2),SBAR(56,2)
110 DIM XS(50)
115 PRINT : PRINT : INPUT " ENTER FURL ANGLE INCLUDING ROTOR TILT > ":BP
117 XZ = ( COS (BP * 3.14159 / 180)) / ( COS (.14))
118 FS = - ATN (XZ / SQRT (- XZ * XZ + 1)) + 1.5708
119 PRINT : PRINT "FURL SET ANGLE IS ";FS * 180 / 3.14159;" DEGREES": PRINT
120 UF = FS * 6 * U1 * .95 / 3.14159
125 PRINT : PRINT : INPUT " PRESS RETURN TO CONT.":H$
131 HOME : UTAB 12: INPUT " PRESS RETURN TO START DATA SAMPLING":H$
132 GOSUB 2000:H$ = T$:T1$ = T$
140 FOR J = 1 TO 56: FOR K = 0 TO 2
150 MN(J,K) = 255
160 NEXT K
170 NEXT J
180 LL = 47
190 FOR I = 0 TO 1: REM SAMPLE WIND AND RPM
200 POKE - 15871,1
202 P1 = PEEK (- 15872)
204 POKE - 15871,1
206 P2 = PEEK (- 15872)
210 S(I) = .5 * (P1 + P2)
220 NEXT I
225 POKE - 15871,3
226 F1 = PEEK (- 15872)
230 NR = NR + 1
240 AR = S(1) * XR / NR + (NR - 1) * AR / NR
245 IF S(1) < 15 THEN 660
246 IF F1 > (UF + 7) THEN 656
247 IF F1 < (UF - 4) THEN 656
250 REM SAMPLE CYCLIC PITCH
260 FOR L = 1 TO LL
270 POKE - 15871,2
280 XS(L) = PEEK (- 15872)
290 NEXT L
300 REM CALC CYC.PIT AMP.
```

```
310 MM = 0
320 XN = 255
330 FOR L = 1 TO LL
340 IF XS(L) > MM THEN MM = XS(L)
350 IF XS(L) < XN THEN XN = XS(L)
360 NEXT L
370 IF MM > PM OR XN < PN THEN GOTO 390
380 GOTO 430
390 PRINT "CYCLIC PITCH OUT OF LIMITS!"
400 FOR B = 1 TO 140
410 S = PEEK ( - 16336)
420 NEXT B
430 S(2) = .5 * (MM - XN): REM S(2)=HALF TOTAL AMPL.
450 REM BIN CALC. 56 BINS, .090 U/BIN
460 B% = (2.015 + S(0)) / 4.0268
470 REM UPDATE BIN ARRAYS
480 FOR I = 1 TO 2
490 IF S(I) > MAX(B%,I) THEN MAX(B%,I) = S(I)
500 IF S(I) < MIN(B%,I) THEN MIN(B%,I) = S(I)
510 N(B%,I) = N(B%,I) + 1
520 MEAN(B%,I) = (S(I) + ((N(B%,I) - 1) * MEAN(B%,I))) / N(B%,I)
530 SBAR(B%,I) = (SBAR(B%,I) * (N(B%,I) - 1) + S(I) ^ 2) / N(B%,I)
540 SE(B%,I) = SQR (SBAR(B%,I) - MEAN(B%,I) ^ 2)
550 NEXT I
560 HW = PEEK ( - 16384)
570 IF HW < > (128 + 68) THEN GOTO 675
580 REM PUSHING THE D KEY CAUSES THE
590 REM CYCLIC PITCH DATA TO BE STORED ON DISK. PUSH ANY OTHER KEY TO STOP.
600 PRINT D$;"APPEND DAT.W2"
610 PRINT D$;"WRITE DAT.W2"
620 FOR MM = 1 TO LL
630 PRINT XS(MM)
640 NEXT MM
650 PRINT D$;"CLOSE DAT.W2"
655 GOTO 675
656 PRINT : PRINT "FURL ANGLE OUT OF LIMITS - RESET"
657 PRINT : PRINT " BIN DATA NOT UPDATED"
658 FOR IH = 1 TO 1200: NEXT IH
659 GOTO 675
660 PRINT : PRINT : PRINT "RPM TOO LOW"
665 PRINT : PRINT : PRINT "BIN DATA NOT UPDATED"
666 PRINT : PRINT
670 FOR HQ = 1 TO 1000: NEXT HQ
675 IF S(0) = 0 THEN GOTO 760
680 WIND = CWIND * S(0) / U1:RPM = CRPM * S(1) / U1:CYP = CCYP * S(2) / U1
690 TSR = .4 * RPM / WIND
700 TSR = .1 * INT (TSR * 10 + .5)
710 RPM = INT (RPM + .5):CYP = .1 * INT (10 * CYP + .5)
720 PRINT "TIP SPEED R","RPM","CYC PTCH"
730 PRINT TSR,RPM,CYP
740 WIND = .1 * INT (WIND * 10 + .5): PRINT : PRINT "WIND,M/S": PRINT WIND: PRINT
750 GOTO 770
760 PRINT "WIND IS CALM"
770 REM
780 REM LOGIC FOR STOPPING PROGRAM
785 REM WAIT SUBR..PRESS CNTRL W
786 Q6 = PEEK ( - 16384)
787 IF Q6 = 151 THEN GOSUB 1500
790 REM TO STOP SAMPLING PRESS CNTRL Z
800 XX = PEEK ( - 16384)
810 IF XX < > (128 + 26) THEN 190
```

```
811 GOSUB 2000
812 HOME : UTAB 5
814 GOSUB 3000:M2 = STD
816 T$ = T1$: GOSUB 3000:H1 = STD
818 TIME = (M2 - H1) / 3600
820 ST = 0: FOR K = 1 TO 2: FOR J = 1 TO 56
830 IF N(J,K) = 0 THEN 850
840 ST = ST + 1
850 NEXT J: NEXT K
860 PRINT "TIME OF TEST START WAS:" : PRINT : PRINT H$
870 PRINT " ELAPSED TIME OF TEST WAS": PRINT ,TIME;" HOURS"
880 REV = INT (AR * 60 * TIME + .5)
885 PRINT : PRINT "TOTAL ROTOR REV.= ";REV;" REVS."
886 PRINT : PRINT " INSERT DATA DISK IF DESIRED"
887 PRINT : INPUT "PRESS RETURN TO CONT.":H$
890 PRINT D$;"OPEN DAT.BINS"
900 PRINT D$;"DELETE DAT.BINS"
910 PRINT D$;"OPEN DAT.BINS"
920 PRINT D$;"WRITE DAT.BINS"
925 PRINT U1: PRINT CHIND: PRINT CRPM: PRINT CCYCP
930 PRINT ST: PRINT H$
940 PRINT TIME
950 PRINT BP: PRINT REV
960 FOR K = 1 TO 2: FOR J = 1 TO 56
970 IF N(J,K) = 0 THEN 1060
980 PRINT K
990 PRINT J
1000 PRINT N(J,K)
1010 PRINT MAX(J,K)
1020 PRINT MEAN(J,K)
1030 PRINT MN(J,K)
1040 PRINT SE(J,K)
1050 PRINT SBAR(J,K)
1060 NEXT J
1070 NEXT K
1080 PRINT D$;"CLOSE DAT.BINS"
1090 PRINT D$;"PR#1"
1100 PRINT "START TIME= ";H$
1110 PRINT "ELAPSED TIME= ";TIME;" HOURS": PRINT
1120 PRINT "FURL ANGLE = ";BP;" DEGREES"
1130 PRINT "ROTOR REV.(CALC.)= ";REV: PRINT : PRINT
1150 PRINT "CH#/BIN#/NH#/MEAN/STD.DEV/MAX/MIN"
1160 PRINT
1170 FOR K = 1 TO 2: FOR J = 1 TO 56
1180 IF N(J,K) = 0 THEN 1220
1190 PRINT K;" ";J;" ";N(J,K);" ";MEAN(J,K);" ";SE(J,K);" ";MAX(J,K);" ";
MN(J,K)
1220 NEXT J
1230 NEXT K
1240 PRINT D$;"PR#0"
1250 HOME : UTAB 5: PRINT "DONT FORGET TO RENAME DAT.BINS. DATA IS DELETED WHEN
PROGRAM IS RUN AGAIN,!!!!!"
1260 END
1500 REM SUBR WAIT. CNTRL G RETURNS TO PROGRAM
1510 POKE - 16368,0
1517 S2 = - 16336
1520 FOR Q2 = 1 TO 90:AZ = PEEK (S2): NEXT Q2
1530 Q7 = PEEK ( - 16384)
1540 IF Q7 < > (135) THEN 1520
1545 POKE - 16368,0
1550 RETURN
2000 REM
2005 REM *** SUBR - GET THE TIME
```

```
2010 REM *** THESE NEED TO BE CHANGED IF DISK IS NOT USED
2025 REM FOR SLOT 4 CLOCK ONLY ***
2030 PRINT D$;"IN#4"
2040 PRINT D$;"PR#4"
2050 INPUT " ";T$
2060 PRINT D$;"IN#0"
2070 PRINT D$;"PR#0"
2080 RETURN
3000 REM
3001 REM FOR LEAP YEAR***:L=1
3005 REM SUBR - STD
3006 REM
3010 REM CALCULATE SECONDS TO DATE FOR EACH TIME (STD)
3020 REM THIS IS THE NUMBER OF SECONDS SINCE JANUARY 1
3030 REM DO THIS FOR STRING TIME T$
3040 REM RETURN A NUMBER - STD
3050 REM
3060 REM FIND #'S FOR DATE AND TIME
3070 MT = VAL ( MID$ (T$,1,2))
3080 D = VAL ( MID$ (T$,4,2))
3090 H = VAL ( MID$ (T$,7,2))
3100 M = VAL ( MID$ (T$,10,2))
3110 S = VAL ( MID$ (T$,13,6))
3130 REM CALCULATE DAYS TO DATE - DTD
3135 RESTORE
3140 DTD = 0
3150 FOR I = 1 TO MT
3160 READ J
3170 DTD = DTD + J
3180 NEXT I
3200 DATA 0,31,28,31,30,31,30,31,31,30,31,30,31
3205 REM ADD IN DAYS AND LEAP YEAR DAY
3210 DTD = DTD + D
3230 IF MT > 2 AND L = 1 THEN DTD = DTD + 1
3240 REM FIND SECONDS TO DATE - STD
3250 STD = DTD * 86400 + H * 3600 + M * 60 + S
3300 RETURN
```

2. The "Collect 5" Subroutine by Micro Systems Development

Note:

The following narrative and flow chart describe the task accomplished by the machine language program developed by Micro Systems Development Company. They are designed to give an overview and a logical description of the program. They do not describe the actual sequence of events which was optimized for CPU/memory efficiency.

Upon call, the machine language program performs some initialization and bookkeeping functions, sets flags, etc. It then checks for user interrupts, and services them on a first in first out basis. Then the A/D board fast channels are processed and the local data table updated. This process is repeated until a set (128 values for each variable) is collected at which point the less rapidly changing variables are read once.

If the rotor speed is below a preset value data are not desired, and control is returned to the calling program; otherwise, a test for critical loads is conducted. Next the global data bank is updated and mean and axial amplitude values are calculated completing the task of a single call.

When an unacceptable load condition is confirmed, the data buffers are transferred to random access memory, and rapid read/dump-to-disk cycle initiated. This will result in each of the fast variable values being written to disk at

a rate of approximately 128 values/second until the disk is filled, which should give extremely detailed time histories for about 2 minutes following detection of a critical load.

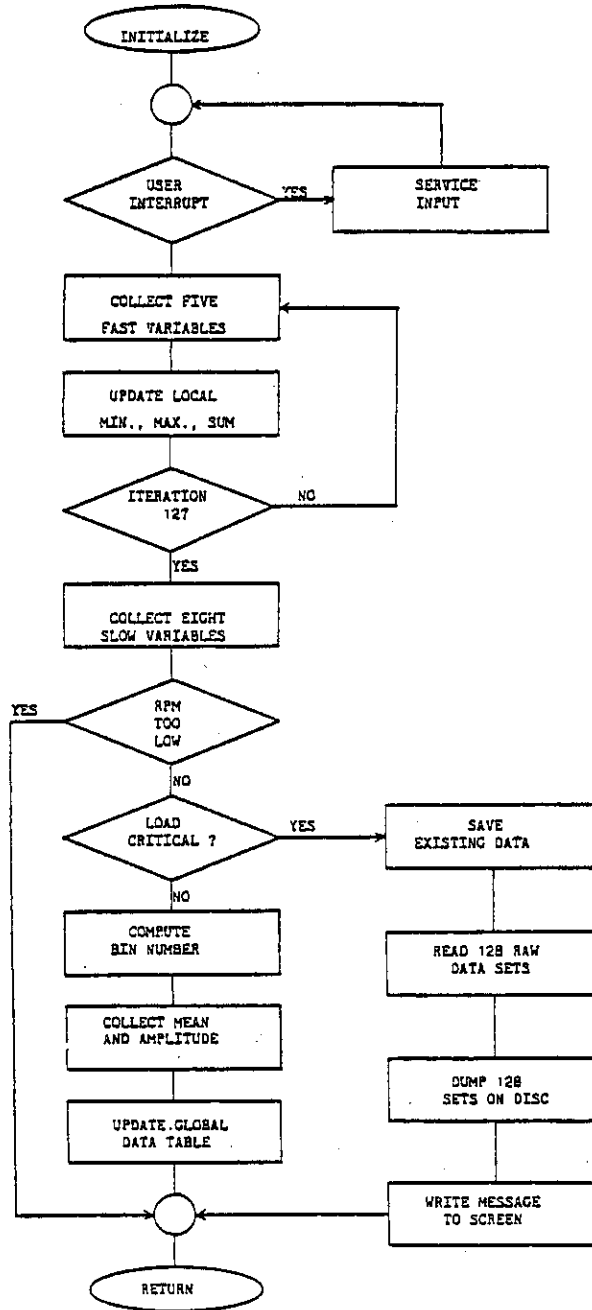


Figure 6.5.1. COLLECT 5 SUBROUTINE FLOW CHART

:ASM

```
1000 * DATA COLLECTION
1010 * MICRO SYS DEV CO
1020 * 5/24/80
1030 *
1040 * COLLECTS SOURCE
1050 *
1060 * REVISION 8/30/80
1070 *
1080 * ORIGIN = 9000
1090 * PROGRAM SPACE = 768 BYTES
1100 * $9000 - $92FF
1110 * GLOBAL DATA TABLE = 768 BYTES
1120 * $9300 - $95FF
1130 * DOS SPACE = 10752 BYTES
1140 * $9600 - $BFFF
1150 * DISK APLSFT SPACE = 10243 BYTES
1160 * $0800 - $3003
1170 * HARDWARE SPACE = 2047 BYTES
1180 * $0000 - $07FF
1190 *
1200 * SPACE REMAINING = 25341 BYTES
1210 *
1220 * INDIRECT INDEX POINTERS
1230 * $FC/$FD - GLOBAL "BTBL"
1240 * $FE/$FF - DATA "DPNT"
1250 *
1260 .OR $9000
1270 .TA $0800
1280 *
1290 * DATA TABLE BASE ADDRESS
1300 * HIGH BYTE ONLY LOW = $00
1310 DPNT .EQ $00FE
1320 BTBL .EQ $00FC
1330 LTBL .EQ $02A2
1340 BUFR .EQ $0200
1350 *
1360 CHNL .EQ $C201 A-D PORTS
1370 STDH .EQ $C202
1380 INTM .EQ $C203
1390 DATA .EQ $C200
1400 EOCF .EQ $C202
1410 INTF .EQ $C203
1420 *
1430 SPCK .EQ $C0C6 CLOCK PORTS
1440 STCK .EQ $C0C5
1450 TME1 .EQ $C0C4
1460 TME2 .EQ $C0C3
1470 TME3 .EQ $C0C2
1480 TME4 .EQ $C0C1
1490 TME5 .EQ $C0C0
1500 *
1510 RWTS .EQ $03D9 FIRMWARE
1520 KYBD .EQ $C000 SUBROUTINES
1530 STRB .EQ $C010
1540 SPKR .EQ $FBDD
1550 YAWN .EQ $FCA8
1560 IORS .EQ $FF3F
1570 IOSV .EQ $FF4A
1580 *
```

```
1590 *
1600 *
9000- 20 4A FF 1610 WJTA JSR IOSV    SAVE REGISTERS
9003- 20 0A 90 1620      JSR MODE  PROGRAM
9006- 20 3F FF 1630      JSR IORS  RESTORE REG'S
9009- 60      1640      RTS
1650 *
900A- AD EC 92 1660 MODE LDA CRIT  CRITICAL?
900D- F0 0E 1670      BEQ MOD2  NO!
900F- AD CE 92 1680      LDA CMND
9012- C9 02 1690      CMP #02  CMND=WRITE?
9014- D0 03 1700      BNE MOD1  NO!
9016- 4C 4F 92 1710      JMP CRIT
9019- 9D EC 92 1720 MOD1 STA CRIT  THEN CMND=3
901C- 60      1730      RTS
1740 *
901D- AD CE 92 1750 MOD2 LDA CMND  INITIALIZE
9020- D0 03 1760      BNE MOD3  PROGRAM?
9022- 4C 09 92 1770      JMP INIT
1780 *
9025- C9 04 1790 MOD3 CMP #04  INITIALIZE
9027- D0 09 1800      BNE STRT  DISK?
9029- 20 BA 92 1810      JSR DISK
902C- A9 02 1820      LDA #02  SET CMND
902E- 8D CE 92 1830      STA CMND  TO WRITE
9031- 60      1840      RTS
1850 *
9032- AD 00 C0 1860 STRT LDA KYBD  TEST FOR
9035- 10 18 1870      BPL ENTR  USER
9037- 2C 10 C0 1880      BIT STRB  INTERRUPT
903A- C9 DA 1890      CMP #218  + 128
903C- D0 06 1900      BNE ENT0
903E- A9 02 1910      LDA #02
9040- 8D F6 92 1920      STA ABRT
9043- 60      1930      RTS
1940 *
9044- 20 D0 FB 1950 ENT0 JSR SPKR  HALT PROGRAM
9047- 2C 00 C0 1960      BIT KYBD
904A- 10 F8 1970      BPL ENT0
904C- 2C 10 C0 1980      BIT STRB
1990 *
904F- AE E8 92 2000 ENTR LDX FVAR  INITIALIZE
9052- 90 00 2010      LDY #00  LOCAL DATA
9054- 98 2020      TYA  TABLE
9055- 99 A2 02 2030 ENT3 STA LTBL,Y
9058- C8 2040      INY
9059- A9 FF 2050      LDA #FF
905B- 99 A2 02 2060      STA LTBL,Y
905E- C8 2070      INY
905F- A9 00 2080      LDA #00
9061- 99 A2 02 2090      STA LTBL,Y
9064- C8 2100      INY
9065- 99 A2 02 2110      STA LTBL,Y
9068- C8 2120      INY
9069- 99 A2 02 2130      STA LTBL,Y
906C- C8 2140      INY
```

```

906D- CA      2150      DEX
906E- D0 E5    2160      BNE ENT3
9070- AD EA 92 2170      LDA ASET
9073- CD E7 92 2171      CMP MSET
9076- D0 0C    2172      BNE ENT4
9078- A9 00    2173      LDA #00
907A- 8D EA 92 2174      STA ASET
907D- 85 FE    2175      STA DPNT
907F- AD CB 92 2176      LDA BUFL+1
9082- 85 FF    2177      STA DPNT+1
9084- 20 D9 90 2180 ENT4 JSR PNTB
9087- 20 8D 90 2190      JSR FAST
908A- 4C E6 90 2200      JMP NEXT
          2210 *
908D- 20 A3 90 2220 FAST JSR FAS1      FAST VARIABLES
9090- AD EC 92 2230      LDA CRIT
9093- D0 03    2240      BNE FAS0
9095- 20 65 91 2250      JSR MXMN
9098- C8      2260 FAS0 INY
9099- C0 80    2270      CPY #128
909B- F0 26    2280      BEQ SLOW
909D- 20 B5 90 2290      JSR FAS2
90A0- 4C 8D 90 2300      JMP FAST
          2310 *
90A3- 20 49 91 2340 FAS1 JSR GET
90A6- 9D 00 02 2350      STA BUFR.X
90A9- A9 80    2355      LDA #128
90AB- 20 5B 91 2356      JSR UPAD
90AE- E8      2360      INX
90AF- EC E8 92 2370      CPX FVAR
90B2- D0 EF    2380      BNE FAS1
90B4- 60      2390      RTS
          2400 *
90B5- A2 00    2410 FAS2 LDX #00
90B7- 20 0E 91 2420      JSR NEX1
90BA- AD EB 92 2440      LDA DLY1
90BD- F0 03    2450      BEQ FAS3
90BF- 20 A8 FC 2460      JSR YAWN
90C2- 60      2470 FAS3 RTS
          2480 *
90C3- A0 00    2490 SLOW LDY #00      SLOW VARIABLES
90C5- A0 00    2510      LDY #00
90C7- 20 49 91 2520 SLO1 JSR GET
90CA- 99 00 02 2530      STA BUFR.Y
90CD- E8      2540      INX
90CE- C8      2550      INY
90CF- CC E9 92 2560      CPY SUAR
90D2- D0 F3    2570      BNE SLO1
90D4- 98      2575      TYA
90D5- 20 5B 91 2577      JSR UPAD      PLUS 8
90D8- 60      2580      RTS      TO INDIR ADDRESS
          2590 *
90D9- A0 00    2600 PNTB LDY #00
90DB- A5 FE    2610      LDA DPNT      SET
90DD- 8D EF 92 2620      STA PBSE      BASE
90E0- A5 FF    2630      LDA DPNT+1    POINTER
90E2- 8D F0 92 2640      STA PBSE+1
90E5- 60      2650      RTS

```

		3320	*				
9165-	98	3330	MXMN	TYA		LOCAL DATA MAX	
9166-	48	3340		PHA		MIN MEAN TEST	
9167-	8A	3345		TXA			
9168-	48	3347		PHA			
9169-	A2 00	3350		LDX #00			
916B-	A0 00	3360		LDY #00			
916D-	B9 00 02	3370	MXM1	LDA BUFR,Y			
9170-	DD A2 02	3380		CMP LTBL,X			
9173-	90 1F	3390		BCC MXM5			
9175-	F0 03	3400		BEQ MXM2			
9177-	9D A2 02	3410		STA LTBL,X			
917A-	E8	3420	MXM2	INX			
917B-	E8	3430	MXM3	INX			
917C-	E8	3435		INX			
917D-	18	3440		CLC			
917E-	7D A2 02	3450		ADC LTBL,X			
9181-	9D A2 02	3460		STA LTBL,X			
9184-	90 1A	3470		BCC MXM7			
9186-	E8	3480		INX			
9187-	FE A2 02	3490		INC LTBL,X			
918A-	C8	3500	MXM4	INX			
918B-	CC E8 92	3510		CPY FUAR			
918E-	F0 14	3520		BEQ MXM8			
9190-	E8	3530		INX			
9191-	4C 6D 91	3540		JMP MXM1			
9194-	E8	3550	MXM5	INX			
9195-	DD A2 02	3560		CMP LTBL,X			
9198-	B0 03	3570		BCS MXM6			
919A-	9D A2 02	3580		STA LTBL,X			
919D-	4C 7B 91	3590	MXM6	JMP MXM3			
91A0-	E8	3600	MXM7	INX			
91A1-	4C 8A 91	3610		JMP MXM4			
91A4-	68	3620	MXM8	PLA			
91A5-	AA	3625		TAX			
91A6-	68	3627		PLA			
91A7-	A8	3630		TAY			
91A8-	AD F8 92	3640		LDA CRIV			
91AB-	CD 00 02	3650		CMP BUFR			
91AE-	B0 05	3660		BCS MXM9			
91B0-	A9 01	3670		LDA #01			
91B2-	8D FA 92	3680		STA TCRI			
91B5-	60	3690	MXM9	RTS			
		3700	*				
91B6-	A2 00	3710	MEAN	LDX #00		COMPUTE MEAN &	
91B8-	BD A2 02	3720	MEAR1	LDA LTBL,X		UPDATE GLOBAL	
91B9-	48	3730		PHA		MAX/MIN	
91BC-	D1 FC	3740		CMP (BTBL),Y			
91BE-	90 07	3750		BCC MEAR2			
91C0-	91 FC	3760		STA (BTBL),Y		GLOBAL MAX	
91C2-	C8	3770		INX			
91C3-	E8	3780		INX			
91C4-	4C 02 91	3790		JMP MEAR3			
91C7-	C8	3800	MEAR2	INX			
91C8-	E8	3810		INX			
91C9-	B0 A2 02	3820		LDA LTBL,X			
91CC-	D1 FC	3830		CMP (BTBL),Y			
91CE-	B0 02	3840		BCS MEAR3			
91D0-	91 FC	3850		STA (BTBL),Y		GLOBAL MIN	
91D2-	C8	3860	MEAR3	INX			
91D3-	68	3870		PLA			

```

2660 *
90E6- AD FA 92 2670 NEXT LDA TCRI
90E9- 8D EC 92 2680 STA CRIT
90EC- A2 00 2690 LDX #00
90EE- A0 00 2700 LDY #00
90F0- BD 00 02 2710 LDA BUFR,X COMPUTE BIN #
90F3- 29 FC 2720 AND #FC
90F5- 8D ED 92 2730 STA WIND
90F8- 4A 2740 LSR
90F9- 4A 2750 LSR
90FA- 8D EE 92 2760 STA BINN
90FD- 20 F1 91 2770 JSR GBIN
9100- E8 2780 INX
9101- BD 00 02 2790 LDA BUFR,X
9104- CD F9 92 2800 CMP LRPM RPM TEST
9107- B0 10 2810 BCS LAS0
9109- A9 01 2820 LDA #01 SET FLAG & RET
910B- 8D F6 92 2830 STA ABRT IF TOO SLOW
910E- AD EF 92 2831 NEX1 LDA PBSE
9111- 85 FE 2832 STA DPNT
9113- AD F0 92 2833 LDA PBSE+1
9116- 85 FF 2834 STA DPNT+1
9118- 60 2840 RTS
9119- D1 FC 2850 LAS0 CMP (BTBL),Y
911B- 90 06 2860 BCC LAS1
911D- 91 FC 2870 STA (BTBL),Y MAX GLOBAL RPM
911F- C8 2880 INY
9120- 4C 2A 91 2890 JMP LAS2
9123- C8 2900 LAS1 INY
9124- D1 FC 2910 CMP (BTBL),Y
9126- B0 02 2920 BCS LAS2
9128- 91 FC 2930 STA (BTBL),Y MIN GLOBAL RPM
912A- E8 2940 LAS2 INX
912B- BD 00 02 2950 LDA BUFR,X
912E- CD F4 92 2960 CMP ALTH MAX ALT TEMP
9131- 90 06 2970 BCC LAS3
9133- 8D F4 92 2980 STA ALTH
9136- 4C 41 91 2990 JMP LAS4
9139- CD F5 92 3000 LAS3 CMP ALTL MIN ALT TEMP
913C- B0 03 3010 BCS LAS4
913E- 8D F5 92 3020 STA ALTL
9141- C8 3030 LAS4 INY
9142- 20 B6 91 3040 JSR MEAN
9145- EE EA 92 3130 INC ASET
9148- 60 3160 END RTS
3170 *
9149- BD D7 92 3180 GET LDA UCHN,X A-D ACCESS
914C- 8D 01 C2 3190 STA CHNL
914F- AD FB 92 3200 LDA DLY2
9152- 20 A0 FC 3210 JSR YAWN
9155- AD 00 C2 3220 LDA DATA
9158- 91 FE 3230 STA (DPNT),Y
915A- 60 3240 RTS
3250 *
915B- 18 3260 UPAD CLC UPDATE POINTER
915C- 65 FE 3270 ADC DPNT
915E- 85 FE 3280 STA DPNT
9160- 90 02 3290 BCC NOCY
9162- E6 FF 3300 INC DPNT+1
9164- 60 3310 NOCY RTS

```

```

91D4- 38          3890      SEC
91D5- FD A2 02 3890      SBC LTBL,X
91D8- 4A          3900      LSR
91D9- E8          3910      INX
91DA- 9D A2 02 3920      STA LTBL,X      LOCAL
91DD- E8          3930      INX      AMPLITUDE
91DE- 1E A2 02 3940      ASL LTBL,X
91E1- E8          3950      INX
91E2- 3E A2 02 3960      ROL LTBL,X      MEAN-INTEGERS
91E5- CA          3970      DEX
91E6- 5E A2 02 3980      LSR LTBL,X      MEAN-REMAINDER
91E9- E8          3990      INX
91EA- E8          4000      INX
91EB- CC F1 92 4010      CPY FVR1
91EE- D0 C8      4020      BNE MEA1
91F0- 60          4030      RTS
          4040 *
          4050 * COMPUTE GLOBAL BIN ADDRESS
          4060 *
91F1- AD F3 92 4070 GBIN LDA GTBL
91F4- 85 FD          4080      STA BTBL+1
91F6- AD ED 92 4090      LDA WIND      BIN # X 4
91F9- 48          4100      PHA
91FA- 0A          4110      ASL      BIN # X 8
91FB- 20 02 92 4120      JSR GBI1
91FE- 68          4130      PLA
91FF- 18          4140      CLC
9200- 65 FC          4150      ADC BTBL      (X 4) + (X 8)
9202- 85 FC          4160 GBI1 STA BTBL
9204- 90 02          4170      BCC GBI2
9206- E6 FD          4180      INC BTBL+1
9208- 60          4190 GBI2 RTS
          4200 *
9209- AD F2 92 4210 INIT LDA BASE      INITIALIZE
920C- 8D CB 92 4220      STA SUFL+1
920F- 8D F0 92 4230      STA PBSE+1
9212- 85 FF          4240      STA DPNT+1
9214- A9 C2          4250      LDA #TBL0      VARIABLE
9216- 85 06          4260      STA #06      REFERENCE
9218- A9 92          4270      LDA /TBL0      ADDRESS
921A- 85 07          4280      STA #07
921C- A9 00          4290      LDA #00
921E- 85 FE          4300      STA DPNT
9220- 85 FC          4310      STA BTBL
9222- AD F3 92 4320      LDA GTBL
9225- 85 FD          4330      STA BTBL+1
9227- A2 03          4340      LDX #03      INITIALIZE
9229- A0 00          4350      LDY #00      GLOBAL DATA
922B- A9 00          4360 INI1 LDA #00      TABLE
922D- 91 FC          4370      STA (BTBL),Y
922F- C8          4380      INY
9230- A9 FF          4390      LDA #$FF
9232- 91 FC          4400      STA (BTBL),Y
9234- C8          4410      INY
9235- D0 F4          4420      BNE INI1
9237- CA          4430      DEX
9238- F0 05          4440      BEQ INI2
923A- E6 FD          4450      INC BTBL+1
923C- 4C 2B 92 4460      JMP INI1

```

```
923F- A9 03 4470 INI2 LDA #03
9241- 8D CE 92 4480 STA CMND
9244- AD E8 92 4490 LDA FUAR
9247- 0A 4500 ASL
9248- 18 4505 CLC
9249- 69 02 4507 ADC #02
924B- 8D F1 92 4510 STA FUR1
924E- 60 4520 RTS
          4530 *
924F- AD F7 92 4540 CRI0 LDA CRIL
9252- 8D E7 92 4550 STA MSET
9255- AD EA 92 4560 LDA ASET
9258- 8D 00 02 4600 STA BUFR
925B- AD 01 02 4610 LDA BUFR+1
925E- 8D CB 92 4620 STA BUFL+1
9261- 20 BA 92 4630 JSR DISK
9264- 20 96 92 4640 JSR RITE
9267- A9 00 4650 CRI1 LDA #00
9269- 85 FE 4660 STA DPNT
926B- AD F2 92 4670 LDA BASE
926E- 85 FF 4680 STA DPNT+1
9270- A9 20 4690 LDA #32
9272- 8D EA 92 4700 STA ASET
9275- 20 D9 90 4710 CRI2 JSR PNTB
9278- A2 00 4720 LDX #00
927A- 20 8D 90 4730 CRI3 JSR FAST
927D- CE EA 92 4750 DEC ASET
9280- AD EA 92 4760 LDA ASET
9283- D0 F0 4770 BNE CRI2
9285- 20 96 92 4780 JSR RITE
9288- CE E7 92 4790 DEC MSET
928B- AD E7 92 4800 LDA MSET
928E- D0 D7 4810 BNE CRI1
9290- A9 02 4820 LDA #02
9292- 8D EC 92 4830 STA CRIT
9295- 60 4840 RTS
          4850 *
9296- AD F2 92 4860 RITE LDA BASE
9299- 8D CB 92 4870 STA BUFL+1
929C- A2 51 4880 LDX #81
929E- EE C7 92 4890 CRI4 INC SECT
92A1- AD C7 92 4900 LDA SECT
92A4- C9 0D 4910 CMP #13
92A6- D0 08 4920 BNE CRI5
92A8- A9 00 4930 LDA #00
92AA- 8D C7 92 4940 STA SECT
92AD- EE C6 92 4950 INC TRAK
92B0- 20 BA 92 4960 CRI5 JSR DISK
92B3- EE CB 92 4970 INC BUFL+1
92B6- CA 4980 DEX
92B7- D0 E5 4990 BNE CRI4
92B9- 60 5000 RTS
          5010 *
          5020 *
92BA- A0 C2 5030 DISK LDY #TBL0
92BC- A9 92 5040 LDA /TBL0
92BE- 20 D9 03 5050 JSR RNTS
92C1- 60 5060 DONE RTS
          5070 *
          5080 *
          5090 *
```

CRITICAL
PROCESSING
ROUTINE

SAVE INP BUFR
SAVE PRE DATA

SET BASE ADDR

GET 32

DISK BUFFER
= RAW DATA TBL

SAVE DATA TABL

```
92C2- 01 60 01
92C5- 00      5100 TBL0 .HS 01600100
92C6- 00      5110 TRAK .DA #00
92C7- 00      5120 SECT .DA #00
92C8- 03      5130 DCTL .DA #DCTA
92C9- 92      5140 DCTH .DA /DCTA
92CA- 00 3F   5150 BUFL .DA $3F00
92CC- 00 00   5160 TBL1 .HS 0000
92CE- 00      5170 CMND .DA #00
92CF- 00 00 60
92D2- 01      5180 TBL2 .HS 00006001
92D3- 00 01 EF
92D6- 08      5190 DCTA .HS 0001EFD8
          5200 *
          5210 * CHANNEL ASSIGNMENT-SEQUENCE
          5220 *

92D7- 00 01 02
92DA- 03      5230 UCHN .HS 00010203
92DB- 04 05 06
92DE- 07      5240      .HS 04050607
92DF- 08 09 0A
92E2- 0B      5250      .HS 08090A0B
92E3- 0C 0D 0E
92E6- 0F      5260      .HS 0C0D0E0F
          5270 *

92E7- 20      5280 MSET .DA #32      VARIABLES &
92E8- 05      5290 FUAR .DA #05      CONSTANTS
92E9- 08      5300 SVAR .DA #08
92EA- 00      5310 ASET .DA #00
92EB- 2E      5320 DLY1 .DA #46
92EC- 00      5330 CRIT .DA #00
92ED- 00      5340 WIND .DA #00
92EE- 00      5350 BINN .DA #00 -
92EF- 00 3F   5360 PBSE .DA $3F00
92F1- 00      5370 FUR1 .DA #00
92F2- 3F      5380 BASE .DA #$3F
92F3- 93      5390 GTBL .DA #$93
92F4- 00      5400 ALTH .DA #00
92F5- FF      5410 ALTL .DA #$FF
92F6- 00      5420 ABRT .DA #00      0-OK $FF-SLOW
92F7- 04      5430 CRIL .DA #04
92F8- E6      5440 CRIV .DA #230
92F9- 00      5450 LAPH .DA #00
92FA- 00      5460 TCRI .DA #00
92FB- 09      5465 DLY2 .DA #09
          5470 *
          5480 *
          5490 * LOCAL DATA TABLE ADDRESSES
          5500 *
          5510 * $02A2 FU1 MAX
          5520 * $02A3 FU1 MIN
          5530 * $02A4 FU1 AMPLITUDE
          5540 * $02A5 FU1 MEAN-REMAINDER
          5550 * $02A6 FU1 MEAN-INTEGERS
          5560 *
          5570 * $02A7 FU2 MAX
          5580 * $02A8 FU2 MIN
          5590 * $02A9 FU2 AMPLITUDE
          5600 * $02AA FU2 MEAN-REMAINDER
          5610 * $02AB FU2 MEAN-INTEGERS
```

5620 *
5630 * \$02AC FU3 MAX
5640 * \$02AD FU3 MIN
5650 * \$02AE FU3 AMPLITUDE
5660 * \$02AF FU3 MEAN-REMAINDER
5670 * \$02B0 FU3 MEAN-INTEGER
5680 *
5690 * \$02B1 FU4 MAX
5700 * \$02B2 FU4 MIN
5710 * \$02B3 FU4 AMPLITUDE
5720 * \$02B4 FU4 MEAN-REMAINDER
5730 * \$02B5 FU4 MEAN-INTEGER
5740 *
5750 * \$02B6 FU5 MAX
5760 * \$02B7 FU5 MIN
5770 * \$02B8 FU5 AMPLITUDE
5780 * \$02B9 FU5 MEAN-REMAINDER
5790 * \$02BA FU5 MEAN-INTEGER
5800 *
5810 *
5820 * CHANNEL SEQUENCE / VARIABLE
5830 *
5840 * 1 CYCLIC PITCH
5850 * 2 DYNAMIC VARIABLE
5860 * 3 DYNAMIC VARIABLE
5870 * 4 DYNAMIC VARIABLE
5880 * 5 DYNAMIC VARIABLE
5890 *
5900 * 6 WIND SPEED
5910 * 7 RPM
5920 * 8 ALTERNATOR TEMP
5930 *
5940 * 9 SLOW VARIABLE
5950 * 10 SLOW VARIABLE
5960 * 11 SLOW VARIABLE
5970 * 12 SLOW VARIABLE
5980 * 13 SLOW VARIABLE

SYMBOL TABLE

DPNT	00FE	BTBL	00FC	LTBL	02A2
BUFR	0200	CHNL	C201	STDM	C202
INTM	C203	DATA	C200	EOCF	C202
INTF	C203	SPCK	C0C6	STCK	C0C5
TME1	C0C4	TME2	C0C3	TME3	C0C2
TME4	C0C1	TME5	C0C0	RWTS	03D9
KYBD	C000	STRB	C010	SPKR	FBDD
YAHN	FC08	IORS	FF3F	IOSU	FF4A
WUTA	9000	MODE	900A	MOD1	9019
MOD2	901D	MOD3	9025	STRT	9032
ENT0	9044	ENTR	904F	ENT3	9055
ENT4	9064	FAST	908D	FAS0	9098
FAS1	90A3	FAS2	90B5	FAS3	90C2
SLOW	90C3	SLO1	90C7	FNTB	90D9
NEXT	90E6	NEX1	910E	LAS0	9119
LAS1	9123	LAS2	912A	LAS3	9139
LAS4	9141	END	9148	GET	9149
UPAD	915B	NOCY	9164	MXMN	9165
MXM1	916D	MXM2	917A	MXM3	917B
MXM4	918A	MXM5	9194	MXM6	919D
MXM7	91A0	MXM8	91A4	MXM9	91B5
MEAN	91B6	MEAR	91B8	MEAR	91C7
MEAR	91D2	GBIN	91F1	GBI1	9202
GBI2	9208	INIT	9209	INI1	922B
INI2	923F	CRIO	924F	CR11	9267
CR12	9275	CR13	927A	RITE	9296
CR14	929E	CR15	92B0	DISK	92BA
DONE	92C1	TBL0	92C2	TRAK	92C6
SECT	92C7	DCTL	92C8	DCTH	92C9
BUFL	92CA	TBL1	92CC	CHND	92CE
TBL2	92CF	DCTA	92D3	UCHN	92D7
MSET	92E7	FUAR	92E8	SUAR	92E9
ASET	92EA	DLY1	92EB	CRIT	92EC
HIND	92ED	BINN	92EE	PBSE	92EF
FUR1	92F1	BASE	92F2	GTBL	92F3
ALTH	92F4	ALTL	92F5	ABRT	92F6
CRIL	92F7	CRIV	92F8	LRPM	92F9
TCRI	92FA	DLY2	92FB		

3. The "Wind 6" Program

3.1 Program Logic

1. List operating instructions and initialize data
2. Calculate correction to standard atmosphere based on pressure and temperature
3. Enter desired yaw angle for test
4. Calculate furl set angle based on desired yaw angle and 8 degree rotor tilt
5. Calculate offset for yaw post signal based on furl set angle. This compensates for the changing boom gravity loads at various furl angles.
6. Load "Collect 5" subroutine and initialize
7. Calculate base data addresses and name data channel variables
8. Disable critical dump and abort feature of the subroutine
9. Call "Collect 5" subroutine and sample data for 1 second
10. Calculate current values of the six performance variables and furl angle based on the data stored from the "Collect 5" subroutine
11. Update average RPM value
12. Test RPM. If below limit go to #21
13. Test cyclic pitch amplitude. If out of limits then go to #16

14. Test furl angle. If out of limits then go to #20
15. Skip to #17
16. Toggle speaker and print cyclic pitch warning on screen
17. Read bin number, and check within limits
18. Update 6 bin arrays based on current bin number and variable value. Update maximum, minimum, mean, standard deviation, and number of samples
19. Skip to #22
20. Print furl angle out of limits warning, then go to #22
21. Print RPM out of limits warning, pause, then go to #22
22. Test for zero wind speed. If zero then go to #25
23. Print wind speed, RPM, cyclic pitch amplitude, and tip to wind speed ratio
24. Skip to #26
25. Print "Wind is Calm"
26. Check for operator signal to stop data sampling. If no stop signal then go to #9 and repeat sampling
27. Print test time and rotor revolutions of test based on average RPM and elapsed time

28. Store bin data and test parameters on disk
29. Print out bin data and test parameters on printer
30. End

JPR#0
JLIST

```
5 REM THE WINDS PROGRAM
6 REM *****
10 D$ = CHR$(4)
11 PRINT D$;"MON C,I,0"
12 HIMEH: 16127
15 HOME : UTAB 1: PRINT " DYNAMIC SAMPLING PROGRAM-WIND5"
16 PRINT : PRINT : PRINT
17 PRINT : PRINT "CHANNEL ASSIGNMENTS"
18 PRINT ,"0.CYCLIC PITCH": PRINT ,"1.TORQUE"
19 PRINT ,"2.FLAP": PRINT ,"3.YAWPOST BENDING"
20 PRINT ,"4.OPTIONAL FAST VARIABLE"
21 PRINT ,"5.WIND SPEED": PRINT ,"6.RPM"
22 PRINT ,"7.ALT.TEMP.": PRINT ,"8.ALT.VOLTS"
23 PRINT ,"9.BOOM POTENT."
24 PRINT ,"10,11,12.OPT."
25 PRINT : INPUT "PRESS RETURN TO CONT.":H$
27 READ U1,CH,CR,CC,CT,CF,CY,CU
28 DATA 54,6.705,60,5.94,2,355,1428,100
30 HOME : UTAB 5: PRINT "PRESENT CALIBRATION FACTORS ARE-": PRINT ,"ONE VOLT=";
U1
31 PRINT ,"WIND=";CH: PRINT ,"RPM=";CR
32 PRINT ,"CYCLIC PITCH=";CC: PRINT ,"TORQUE=";CT
33 PRINT ,"FLAP=";CF: PRINT ,"YAWPOST=";CY
34 PRINT ,"ALT.VOLTS=";CU
35 PRINT "GO TO LINE 28 FOR CHANGES IF REQUIRED": INPUT " PRESS RETURN TO CONT
.";H$
36 HOME : UTAB 2: PRINT " TEST PARAMETERS": PRINT : PRINT "INPUT WEATHER VARI
ABLES"
37 PRINT : INPUT "ENTER AMB.TEMP.(C) > ";D1: INPUT " AMB.PRESSURE (ATM) >
";D2: INPUT " WIND DIRECTION (DEG) > ";D3
38 FC = ((D1 + 273) / 288) * (1 / D2)
39 PRINT : PRINT : PRINT " CORRECTION FACTOR=";FC: PRINT : INPUT " PRESS RET
URN TO CONT.":H$
40 HOME : UTAB 10: INPUT "ENTER TOTAL GEN. LOAD (OHMS) > ";D4: INPUT " GEA
R RATIO (IE 25 FOR 25:1) > ";D5
41 PM = 245;PN = 4: HOME : UTAB 10
42 PRINT : PRINT : PRINT "MAX AND MIN CYCLIC PITCH CONTROL NUMBERS ARE ";PM;"
AND ";PN: PRINT "CHANGE LINE 41 IF REQUIRED"
43 PRINT : PRINT : INPUT " PRESS RETURN TO CONT.":H$
45 HOME : UTAB 10: PRINT "ENTER FURL ANGLE INCLUDING ROTOR TILT.": PRINT : PRIN
T
46 INPUT " ENTER FURL (DEG) > ";D6
47 XZ = ( COS (D6 * 6.283 / 360)) / ( COS (.14)):FS = - ATN (XZ / SQR ( - XZ
* XZ + 1)) + 1.5708
48 PRINT : PRINT " FURL SET ANGLE IS ";FS * 180 / 3.14159;" DEGREES":UF = FS *
6 * .95 * 54 / 3.14159
49 OS = U1 * (2.95 - (FS * 4.5 / 3.14159))
50 INPUT "PRESS RETURN TO CONT. ":H$: HOME : UTAB 5: PRINT " CONTROL FUNCTION
S"
51 PRINT : PRINT "ANY KEY PUTS PROGRAM IN TEMP. HOLD...ANY KEY RECOVERS"
52 PRINT : PRINT "CNTRL Z STOPS PROGRAM AND SENDS DATA TO PRINTER AND DISK"
53 PRINT : PRINT : INPUT " PRESS RETURN TO CONT.":H$
90 XR = CRPM / U1:NR = 0:AR = 0
145 HOME : HTAB 4: UTAB 12: PRINT "PROGRAM LOADING INTO MEMORY"
150 PRG = 36864
152 PRINT D$;"BLOAD COLLECTS OBJECT,A$9000"
154 CALL PRG
155 PRINT : PRINT : PRINT " PROGRAM INITIALIZED"
156 DIM S(10),MEAN(35,6),K(35,6),SE(35,6),SBAR(35,6),MAX(35,6),MIN(35,6)
157 FOR K = 1 TO 6: FOR J = 1 TO 35
158 M(K,J,K) = 255 ^ 2
159 NEXT J: NEXT K
160 TABLE = (256 * PEEK (7)) + PEEK (6)
165 FU = 673:SLW = 16768: REM FIRST SLOW VBL
166 GBL = 37632: REM FIRST GLOBAL DATA
170 IX = 0:NR = 0:AR = 0
172 ACRT = TABLE + 42:ABRT = TABLE + 52
173 BIN = TABLE + 44
175 K1$ = "CH.1=RPM":K2$ = "CH.2=GEN.VOLTS"
```

```
176 K3$ = "CH.3=CYCLIC PITCH AMPL.":K4$ = "CH.4=ROTOR POWER"
177 K5$ = "CH.5=EFF.":K6$ = "CH.6=THRUST(N)"
178 HOME : UTAB 12: INPUT " PRESS RETURN TO START DATA SAMPLING":H$
179 PRINT : PRINT : INPUT " ENTER START TIME AND DATE > ":H$
180 POKE ACRT,0: POKE AABRT,0
185 CALL PRG
187 JX = IX * 648
190 S(0) = PEEK (SLW + JX): REM WIND
191 S(1) = PEEK (SLW + 1 + JX): REM RPM
192 S(2) = PEEK (SLW + 3 + JX):S(2) = S(2) ^ 2: REM GEN. POWER
193 S(3) = PEEK (FU + 3): REM CY.P.AMPL.
194 S(4) = S(1) * PEEK (FU + 10): REM ROTOR POWER
204 IF S(4) = 0 THEN 210
205 S(5) = S(2) / S(4): REM EFFICIENCY
208 GOTO 215
210 S(5) = 0
215 REM CONTINUE
217 S(6) = PEEK (FU + 20)
218 S(6) = S(6) - 05
219 S(7) = PEEK (SLW + 4 + JX): REM FURL ANGLE
220 IX = IX + 1
225 IF INT (IX / 32) > 0 THEN IX = 0
230 NR = NR + 1
240 AR = S(1) * XR / NR + (NR - 1) * AR / NR
245 IF S(1) < 14 THEN 660
370 IF S(3) > (PM - PN) THEN 390
375 IF S(7) > (UF + 7) THEN 656
376 IF S(7) < (UF - 4) THEN 656
380 GOTO 450
390 PRINT "CYCLIC PITCH OUT OF LIMITS!"
400 FOR B = 1 TO 140
410 BZ = PEEK ( - 16336)
420 NEXT B
450 B% = PEEK (BIN)
451 PRINT "BIN= ":B%
452 IF B% > 35 THEN B% = 0
490 FOR I = 1 TO 6
490 IF S(I) > MAX(B%,I) THEN MAX(B%,I) = S(I)
500 IF S(I) < MIN(B%,I) THEN MIN(B%,I) = S(I)
510 NK(B%,I) = NK(B%,I) + 1
520 MEAN(B%,I) = (S(I) + ((NK(B%,I) - 1) * MEAN(B%,I))) / NK(B%,I)
530 SBAR(B%,I) = (SBAR(B%,I) * (NK(B%,I) - 1) + S(I) ^ 2) / NK(B%,I)
540 SE(B%,I) = SQR (SBAR(B%,I) - MEAN(B%,I) ^ 2)
550 NEXT I
655 GOTO 675
656 PRINT : PRINT "FURL ANGLE OUT OF LIMITS - RESET"
657 PRINT : PRINT "BIN DATA NOT UPDATED"
658 GOTO 675
660 PRINT : PRINT : PRINT "RPM TOO LOW"
665 PRINT : PRINT : PRINT "BIN DATA NOT UPDATED"
666 PRINT : PRINT
670 FOR HQ = 1 TO 1000: NEXT HQ
675 IF S(0) = 0 THEN GOTO 760
680 WIND = CWIND * S(0) / U1:RPM = CRPM * S(1) / U1:PTH = CC * S(3) / U1
690 TSR = .4 * RPM / WIND
700 TSR = .1 * INT (TSR * 10 + .5)
710 RPM = INT (RPM + .5):PTH = .1 * INT (10 * PTH + .5)
720 PRINT "TIP SPEED R","RPM","CYC PITCH"
730 PRINT TSR,RPM,PTH
740 WIND = .1 * INT (WIND * 10 + .5): PRINT : PRINT "WIND,H/S": PRINT WIND: PRI
NT : PRINT : PRINT : PRINT
750 GOTO 800
```

```
760 PRINT "WIND IS CALM"
790 REM TO STOP SAMPLING PRESS CNTRL Z
800 XX = PEEK ( - 16384)
810 IF XX < > (154) THEN 180
811 HOME : UTAB 5: PRINT " START TIME WAS ";H$
814 PRINT : PRINT : INPUT "ENTER ELAPSED TIME IN HRS. > ";TIME
816 HOME : UTAB 3
820 ST = 0: FOR K = 1 TO 6: FOR J = 1 TO 35
830 IF N(J,K) = 0 THEN 850
840 ST = ST + 1
850 NEXT J: NEXT K
860 PRINT "TIME OF TEST START WAS:" : PRINT : PRINT H$
870 PRINT " ELAPSED TIME OF TEST WAS": PRINT ,TIME;" HOURS"
880 REV = INT (AR * 60 * TIME + .5)
885 PRINT : PRINT "TOTAL ROTOR REV.= ";REV;" REUS."
886 PRINT : PRINT " INSERT DATA DISK IF DESIRED"
887 PRINT : INPUT "PRESS RETURN TO CONT.";H$
889 D$ = CHR$(4)
890 PRINT D$;"OPEN DAT.BINS"
900 PRINT D$;"DELETE DAT.BINS"
910 PRINT D$;"OPEN DAT.BINS"
920 PRINT D$;"WRITE DAT.BINS"
924 REM 1 VOLT, CWIND, CRPH, CCYCP
925 PRINT U1: PRINT CH: PRINT CR: PRINT CC
926 REM CTORQUE(NM), CFLAP, CYAMPPOST, CGEN.VOLTS
927 PRINT CT: PRINT CF: PRINT CY: PRINT CU
928 REM ANB.TEMP,PRESS,WIND DIR., GEN LOAD
930 PRINT D1: PRINT D2: PRINT D3: PRINT D4
931 REM GEAR RATIO, FURL ANGLE, CORREC. FACTOR
933 PRINT D5: PRINT D6: PRINT FC
934 REM CHANNEL TITLES FOR BIN DATA
935 PRINT K1$: PRINT K2$: PRINT K3$: PRINT K4$: PRINT K5$: PRINT K6$
936 REM SETS, START TIME, ET, REV
940 PRINT ST: PRINT H$: PRINT TIME: PRINT REV
960 FOR K = 1 TO 6: FOR J = 1 TO 35
970 IF N(J,K) = 0 THEN 1060
980 PRINT K
990 PRINT J
1000 PRINT N(J,K)
1010 PRINT MAX(J,K)
1020 PRINT MEAN(J,K)
1030 PRINT M(K,J,K)
1040 PRINT SE(J,K)
1050 PRINT SBARK(J,K)
1060 NEXT J
1070 NEXT K
1080 PRINT D$;"CLOSE DAT.BINS"
1085 HOME : UTAB 10: INPUT " ENTER NAME OF TEST > ";N1$
1090 PRINT D$;"PR#1"
1095 PRINT : PRINT "TEST NAME IS ";N1$
1100 PRINT "START TIME= ";H$
1110 PRINT "ELAPSED TIME= ";TIME;" HOURS"
1130 PRINT "ROTOR REV.(CALC.) = ";REV
1132 PRINT "CALIBRATIONS AND TEST PARAMETERS"
1133 PRINT "FURL ANGLE (INCL. TILT) = ";D6
1134 PRINT "ONE VOLT=";U1;" CWIND=";CH;" CRPH=";CR;" CCYPTCH=";CC
1135 PRINT "CTORQUE=";CT;" CFLAP=";CF;" CYAMPPOST=";CY;" CGEN.U=";CU
1136 PRINT "TEMP(DEG C)=";D1;" PRESS(ATM)=";D2;" CORR.FAC.=";FC;" WIND DIR="
;D3
1137 PRINT "GEN LOAD(OHMS)=";D4;" GEAR RATIO = ";D5;" TO 1"
1140 PRINT K1$;" ";K2$;" ";K3$
1141 PRINT K4$;" ";K5$;" ";K6$
```

```
1145 PRINT
1150 PRINT "CH#/BIN#/N#/MEAN/S.DEV/MAX/MIN"
1170 FOR K = 1 TO 6: FOR J = 1 TO 35
1180 IF N(J,K) = 0 THEN 1220
1190 PRINT K; " " ; J; " " ; N(J,K); " " ; MEAN(J,K); " " ; SE(J,K); " " ; MAX(J,K); " " ;
MN(J,K)
1220 NEXT J
1230 NEXT K
1240 PRINT 0; "PR#0"
1250 HOME : UTAB 5: PRINT "DONT FORGET TO RENAME DAT.BINS. DATA IS DELETED WHEN
PROGRAM IS RUN AGAIN.!!!!!"
1260 END
```

4. "Wind-2, Fast"

4.1 Program Logic

- 1 to 9. The first 9 steps are identical to the "Wind 6" program logic 10.
10. Read data for two "fast" variables at appropriate addresses
11. Update average RPM value
12. Read bin number at appropriate address
13. Print current variable values to screen
14. Test bin number in limits
15. Update bin arrays for the two variables as in the "Wind 6" program
16. Test for stop sampling signal. If none, then go to #9 and repeat sampling
- 17,18,19. Same as steps 27, 28, 29 for "Wind 6" program
20. End

1PR#0
1L151

```
5 REM THE WIND2.FAST PROGRAM
6 REM *****
7 REM APPROXIMATELY 1.4 SECONDS PER SAMPLE
10 D$ = CHR$(4)
11 PRINT D$;"MON C,1,0"
12 HIMEM: 16127
15 HOME : UTAB 1: PRINT " DYNAMIC SAMPLING PROGRAM -WIND2.FAST"
16 PRINT : PRINT : PRINT
17 PRINT : PRINT "CHANNEL ASSIGNMENTS"
18 PRINT ,"1.TORQUE": PRINT ,"2.RPM"
19 PRINT ,"5.WIND SPEED"
24 PRINT ,"10,11,12.OPT."
25 PRINT : INPUT "PRESS RETURN TO CONT.":H$
27 READ V1,CW,CR,CT
28 DATA 54,6.705,60,94.2
29 ZR = CR / U1:ZT = .105 * CR * CT / (U1 ^ 2)
30 HOME : UTAB 5: PRINT "PRESENT CALIBRATION FACTORS ARE-": PRINT ,"ONE VOLT=":
U1
31 PRINT ,"WIND=":CW: PRINT ,"RPM=":CR
32 PRINT ,"TORQUE=":CT
35 PRINT "GO TO LINE 28 FOR CHANGES IF REQUIRED": INPUT " PRESS RETURN TO CONT
":H$
36 HOME : UTAB 2: PRINT " TEST PARAMETERS": PRINT : PRINT "INPUT WEATHER VARI
ABLES"
37 PRINT : INPUT "ENTER AMB.TEMP.(C) > ":D1: INPUT " AMB.PRESSURE (ATM) >
":D2: INPUT " WIND DIRECTION (DEG) > ":D3
38 FC = ((D1 + 273) / 288) * (1 / D2)
39 PRINT : PRINT : PRINT " CORRECTION FACTOR=" :FC: PRINT : INPUT " PRESS RET
URN TO CONT.":H$
40 HOME : UTAB 10: INPUT "ENTER TOTAL GEN. LOAD (OHMS) > ":D4: INPUT " GEA
R RATIO (IE 25 FOR 25:1) > ":D5
43 PRINT : PRINT : INPUT " PRESS RETURN TO CONT.":H$
45 HOME : UTAB 10: PRINT "ENTER FURL ANGLE INCLUDING ROTOR TILT.": PRINT : PRIN
T
46 INPUT " ENTER FURL (DEG) > ":D6
47 XZ = ( COS (D6 * 6.283 / 360)) / ( COS (.14)):FS = - ATN (XZ / SQRT ( - XZ
* XZ + 1)) + 1.5708
48 PRINT : PRINT " FURL SET ANGLE IS ":FS * 180 / 3.14159," DEGREES":UF = FS *
6 * .95 * 54 / 3.14159
50 INPUT "PRESS RETURN TO CONT. ":H$: HOME : UTAB 5: PRINT " CONTROL FUNCTION
S"
51 PRINT : PRINT "ANY KEY PUTS PROGRAM IN TEMP. HOLD...ANY KEY RECOVERS"
52 PRINT : PRINT "CNTRL Z STOPS PROGRAM AND SENDS DATA TO PRINTER AND DISK"
53 PRINT : PRINT : INPUT " PRESS RETURN TO CONT.":H$
90 XR = CRPM / U1:NR = 0:AR = 0
145 HOME : HTAB 4: UTAB 12: PRINT "PROGRAM LOADING INTO MEMORY"
150 PRG = 36864
152 PRINT D$;"BLOAD COLLECT5 OBJECT,A$9000"
154 CALL PRG
155 PRINT : PRINT : PRINT " PROGRAM INITIALIZED"
156 DIM SX(10),MEAN(35,2),MK(35,2),SE(35,2),SBAR(35,2),MAX(35,2),MN(35,2)
157 FOR K = 1 TO 2: FOR J = 1 TO 35
158 MN(J,K) = 255 ^ 2
159 NEXT J: NEXT K
160 TABLE = (256 * PEEK (7)) + PEEK (8)
165 FU = 673:SLW = 16768: REM FIRST SLOW VBL
166 GBL = 37632: REM FIRST GLOBAL DATA
170 IX = 0:NR = 0:AR = 0
172 ACRT = TABLE + 42:ABRT = TABLE + 52
173 BIN = TABLE + 44
175 K1$ = "CH.1=RPM":K2$ = "CH.2=ROTOR POWER"
178 HOME : UTAB 12: INPUT " PRESS RETURN TO START DATA SAMPLING":H$
179 PRINT : PRINT : INPUT " ENTER START TIME AND DATE > ":H$
180 POKE ACRT,0: POKE ABRT,0
185 CALL PRG
191 S(1) = PEEK (FU + 15)
192 S(2) = S(1) * PEEK (FU + 10)
230 NR = NR + 1
```

```
240 AR = S(1) * XR / NR + (NR - 1) * AR / NR
440 B% = PEEK (BIN):R% = S(1) * ZR:K% = S(2) * ZT
445 PRINT "BIN=";B%;" RPM=";R%;" R.PWR=";H%
452 IF B% > 35 THEN B% = 0
480 FOR I = 1 TO 2
490 IF S(I) > MAX(B%,I) THEN MAX(B%,I) = S(I)
500 IF S(I) < MIN(B%,I) THEN MIN(B%,I) = S(I)
510 N(B%,I) = N(B%,I) + 1
520 MEAN(B%,I) = (S(I) + ((N(B%,I) - 1) * MEAN(B%,I))) / N(B%,I)
530 SBAR(B%,I) = (SBAR(B%,I) * (N(B%,I) - 1) + S(I) ^ 2) / N(B%,I)
540 SE(B%,I) = SQR (SBAR(B%,I) - MEAN(B%,I) ^ 2)
550 NEXT I
800 XX = PEEK ( - 16384)
810 IF XX < > (154) THEN 180
811 HOME : UTAB 5: PRINT " START TIME WAS ";H%
814 PRINT : PRINT " ENTER ELAPSED TIME IN HRS. > ";TIME
816 HOME : UTAB 3
820 ST = 0: FOR K = 1 TO 2: FOR J = 1 TO 35
830 IF N(J,K) = 0 THEN 850
840 ST = ST + 1
850 NEXT J: NEXT K
860 PRINT "TIME OF TEST START WAS:" : PRINT : PRINT H%
870 PRINT " ELAPSED TIME OF TEST WAS:" : PRINT ,TIME;" HOURS"
880 REV = INT (AR * 60 * TIME + .5)
885 PRINT : PRINT "TOTAL ROTOR REV. = ";REV;" REVS."
886 PRINT : PRINT " INSERT DATA DISK IF DESIRED"
887 PRINT : INPUT "PRESS RETURN TO CONT. ";H%
889 D$ = CHR$(4)
890 PRINT D$;"OPEN DAT.BINS"
900 PRINT D$;"DELETE DAT.BINS"
910 PRINT D$;"OPEN DAT.BINS"
920 PRINT D$;"WRITE DAT.BINS"
924 REM 1 VOLT,CHIND,CAPH,CCYCP
925 PRINT V1: PRINT CW: PRINT CR: PRINT CC
926 REM CTORQUE(NM),CFLAP,CYANPOST,CSEN,UOLTS
927 PRINT CT: PRINT CF: PRINT CY: PRINT CU
928 REM ANB.TEMP,PRESS,WIND DIR,.6EN LOAD
930 PRINT D1: PRINT D2: PRINT D3: PRINT D4
931 REM GEAR RATIO, FURL ANGLE, CORREC. FACTOR
933 PRINT D5: PRINT D6: PRINT FC
934 REM CHANNEL TITLES FOR BIN DATA
935 PRINT K1$: PRINT K2$: PRINT K3$: PRINT K4$: PRINT K5$: PRINT K6$
936 REM SETS, START TIME, ET, REV
940 PRINT ST: PRINT H$: PRINT TIME: PRINT REV
960 FOR K = 1 TO 2: FOR J = 1 TO 35
970 IF N(J,K) = 0 THEN 1060
980 PRINT K
990 PRINT J
1000 PRINT N(J,K)
1010 PRINT MAX(J,K)
1020 PRINT MEAN(J,K)
1030 PRINT MIN(J,K)
1040 PRINT SE(J,K)
1050 PRINT SBAR(J,K)
1060 NEXT J
1070 NEXT K
1080 PRINT D$;"CLOSE DAT.BINS"
1085 HOME : UTAB 10: INPUT " ENTER NAME OF TEST > ";N1$
1090 PRINT D$;"PR#1"
1095 PRINT : PRINT "TEST NAME IS ";N1$
1100 PRINT "START TIME= ";H%
```

```
1110 PRINT "ELAPSED TIME=" ;TIME;" HOURS"
1130 PRINT "ROTOR REV.(CALC.)=" ;REV
1132 PRINT "CALIBRATIONS AND TEST PARAMETERS"
1133 PRINT "FURL ANGLE (INCL. TILT)=" ;D6
1134 PRINT "ONE VOLT=" ;U1;" CHIND=" ;CH;" CRPM=" ;CR;" CCYPTCH=" ;CC
1135 PRINT "CTORQUE=" ;CT;" CFLAP=" ;CF;" CYANPOST=" ;CY;" CGEN.U=" ;CU
1136 PRINT "TEMP(DEG C)=" ;D1;" PRESS(ATM)=" ;D2;" CORR.FAC.=" ;FC;" WIND DIR="
;D3
1137 PRINT "GEN LOAD(OHMS)=" ;D4;" GEAR RATIO = " ;D5;" TO 1"
1140 PRINT K1$;" " ;K2$;" " ;K3$
1141 PRINT K4$;" " ;K5$;" " ;K6$
1145 PRINT
1150 PRINT "CH#/BIN#/N#/MEAN/S.DEV/MAX/MIN"
1170 FOR K = 1 TO 2: FOR J = 1 TO 35
1180 IF N(J,K) = 0 THEN 1220
1190 PRINT K;" " ;J;" " ;N(J,K);" " ;MEAN(J,K);" " ;SE(J,K);" " ;MAX(J,K);" " ;
MN(J,K)
1220 NEXT J
1230 NEXT K
1240 PRINT D$;"PR#0"
1250 HOME : UTAB 5: PRINT "DONT FORGET TO RENAME DAT.BINS. DATA IS DELETED WHEN
PROGRAM IS RUN AGAIN,!!!!!"
1260 END
```

5. "RPM-6"

5.1 Program Logic

The program logic for the "RPM-6" program is identical to that of the "Wind 6" program. Channel assignments and conversion constants are changed so that desired variables are related to RPM bins rather than wind speed bins, but the logic remains the same.

JPR#0
JLIST

```
5 REM THE RPM6 PROGRAM
6 REM *****
10 D$ = CHR$(4)
11 PRINT D$;"MON C.I.0"
12 HIMEM: 16127
15 HOME : UTAB 1: PRINT " DYNAMIC SAMPLING PROGRAM-RPM6"
16 PRINT : PRINT : PRINT
17 PRINT : PRINT "CHANNEL ASSIGNMENTS"
18 PRINT ,"0.CYCLIC PITCH": PRINT ,"1.TORQUE"
19 PRINT ,"2.FLAP": PRINT ,"3.YAMPOST BENDING"
20 PRINT ,"4.VERTICAL BOOM"
21 PRINT ,"5.RPM"
22 PRINT ,"6.7.8.OPEN"
23 PRINT ,"9.BOOM POTENT."
24 PRINT ,"10.11.12.OPT."
25 PRINT : INPUT "PRESS RETURN TO CONT.":H$
27 READ U1,CB,CR,CC,CT,CF,CY,CU
28 DATA 54,290,60,5,94.2,355,1428,100
30 HOME : UTAB 5: PRINT "PRESENT CALIBRATION FACTORS ARE-": PRINT ,"ONE VOLT=";
U1
31 PRINT ,"BOOM=";CB: PRINT ,"RPM=";CR
32 PRINT ,"CYCLIC PITCH=";CC: PRINT ,"TORQUE=";CT
33 PRINT ,"FLAP=";CF: PRINT ,"YAMPOST=";CY
34 PRINT ,"ALT.VOLTS=";CU
35 PRINT "GO TO LINE 28 FOR CHANGES IF REQUIRED": INPUT " PRESS RETURN TO CONT
." :H$
36 HOME : UTAB 2: PRINT " TEST PARAMETERS": PRINT : PRINT "INPUT WEATHER VARI
ABLES"
37 PRINT : INPUT "ENTER AMB.TEMP.(C) > ";D1: INPUT " AMB.PRESSURE (ATM) >
";D2: INPUT " WIND DIRECTION (DEG) > ";D3
38 FC = ((D1 + 273) / 288) * (1 / D2)
39 PRINT : PRINT : PRINT " CORRECTION FACTOR=";FC: PRINT : INPUT " PRESS RET
URN TO CONT.":H$
40 HOME : UTAB 10: INPUT "ENTER TOTAL GEN. LOAD (OHMS) > ";D4: INPUT " GEA
R RATIO (IE 25 FOR 25:1) > ";D5
41 PM = 245:PN = 4: HOME : UTAB 10
42 PRINT : PRINT : PRINT "MAX AND MIN CYCLIC PITCH CONTROL NUMBERS ARE ";PM;"
AND ";PN: PRINT "CHANGE LINE 41 IF REQUIRED"
43 PRINT : PRINT : INPUT " PRESS RETURN TO CONT.":H$
45 HOME : UTAB 10: PRINT "ENTER FURL ANGLE INCLUDING ROTOR TILT.": PRINT : PRIN
T
46 INPUT " ENTER FURL (DEG) > ";D6
47 XZ = ( COS (D6 * 6.283 / 360)) / ( COS (.14)):FS = - ATN (XZ / SQRT ( - XZ
* XZ + 1)) + 1.5708
48 PRINT : PRINT " FURL SET ANGLE IS ";FS * 180 / 3.14159;" DEGREES":UF = FS *
6 * .95 * 54 / 3.14159
49 OS = U1 * (2.95 - (FS * 4.5 / 3.14159)): PRINT : PRINT "YAMPOST OFFSET=";OS
/ U1;" VOLTS"
50 INPUT "PRESS RETURN TO CONT. ":H$: HOME : UTAB 5: PRINT " CONTROL FUNCTION
S"
51 PRINT : PRINT "ANY KEY PUTS PROGRAM IN TEMP. HOLD...ANY KEY RECOVERS"
52 PRINT : PRINT "CNTRL Z STOPS PROGRAM AND SENDS DATA TO PRINTER AND DISK"
53 PRINT : PRINT : INPUT " PRESS RETURN TO CONT.":H$
90 XR = CRPM / U1:NR = 0:AR = 0
145 HOME : HTAB 4: UTAB 12: PRINT "PROGRAM LOADING INTO MEMORY"
150 PRG = 36864
152 PRINT D$;"BLOAD COLLECT5 OBJECT,A$9000"
154 CALL PRG
155 PRINT : PRINT : PRINT " PROGRAM INITIALIZED"
156 DIM SX(10),MEAN(35,6),NK(35,6),SE(35,6),SBR(35,6),MAX(35,6),MN(35,6)
157 FOR K = 1 TO 6: FOR J = 1 TO 35
158 MN(J,K) = 255 ^ 2
159 NEXT J: NEXT K
160 TABLE = (256 * PEEK (7)) + PEEK (6)
165 FU = 673:SLW = 16768: REM FIRST SLOW UBL
166 GBL = 37632: REM FIRST GLOBAL DATA
170 IX = 0:NR = 0:AR = 0
172 ACRIT = TABLE + 42:ABART = TABLE + 52
173 BIN = TABLE + 44
175 K1$ = "CH.1=MEAN FLAP":K2$ = "CH.2=FLAP AMPL."
```

```
176 K3$ = "CH.3=YAWPOST AMPL.(THRUST)":K4$ = "CH.4=TORQUE AMPL."
177 K5$ = "CH.5=U.Boom AMPL.":K6$ = "CH.6=CYCLIC PITCH AMPL."
178 HOME : UTAB 12: INPUT " PRESS RETURN TO START DATA SAMPLING":H$
179 PRINT : PRINT : INPUT " ENTER START TIME AND DATE > ":H$
180 POKE ACRIT.0: POKE AABRT.0
185 CALL PRG
187 JX = IX * 648
190 S(0) = PEEK (SLH + JX): REM RPM
191 S(1) = PEEK (FU + 15): REM MEAN FLAP
192 S(2) = PEEK (FU + 13): REM FLAP AMPL.
193 S(3) = PEEK (FU + 18): REM YAWPOST AMPL.
195 S(4) = PEEK (FU + 8): REM TORQUE AMPL.
196 S(5) = PEEK (FU + 23): REM U. BOOM AMPL.
197 S(6) = PEEK (FU + 3): REM CYCLIC PITCH AMPL.
219 S(7) = PEEK (SLH + 4 + JX): REM FURL ANGLE
220 IX = IX + 1
225 IF INT (IX / 32) > 0 THEN IX = 0
230 NR = NR + 1
240 AR = S(1) * XR / NR + (NR - 1) * AR / NR
245 IF S(0) < 14 THEN 660
370 IF S(6) > (PM - PN) THEN 390
375 IF S(7) > (UF + 7) THEN 656
376 IF S(7) < (UF - 4) THEN 656
380 GOTO 450
390 PRINT "CYCLIC PITCH OUT OF LIMITS!"
400 FOR B = 1 TO 140
410 BZ = PEEK ( - 16336)
420 NEXT B
450 B% = .5 * PEEK (BIN)
451 PRINT "BIN= ";B%
452 IF B% > 35 THEN B% = 0
480 FOR I = 1 TO 6
490 IF S(I) > MAX(B%,I) THEN MAX(B%,I) = S(I)
500 IF S(I) < MIN(B%,I) THEN MIN(B%,I) = S(I)
510 N(B%,I) = N(B%,I) + 1
520 MEAN(B%,I) = (S(I) + ((N(B%,I) - 1) * MEAN(B%,I))) / N(B%,I)
530 SBAR(B%,I) = (SBAR(B%,I) * (N(B%,I) - 1) + S(I) ^ 2) / N(B%,I)
540 SE(B%,I) = SQR (SBAR(B%,I) - MEAN(B%,I) ^ 2)
550 NEXT I
655 GOTO 675
656 PRINT : PRINT "FURL ANGLE OUT OF LIMITS - RESET"
657 PRINT : PRINT "BIN DATA NOT UPDATED"
658 GOTO 675
660 PRINT : PRINT : PRINT ",RPM TOO LOW"
665 PRINT : PRINT : PRINT ",BIN DATA NOT UPDATED"
666 PRINT : PRINT
670 FOR HQ = 1 TO 1000: NEXT HQ
675 PRINT : PRINT : PRINT ",RPM = ";60 * S(0) / U1: PRINT
790 REM TO STOP SAMPLING PRESS CNTRL Z
800 XX = PEEK ( - 16384)
810 IF XX < > (154) THEN 180
811 HOME : UTAB 5: PRINT " START TIME WAS ";H$
814 PRINT : PRINT : INPUT "ENTER ELAPSED TIME IN HRS. > ":TIME
816 HOME : UTAB 3
820 ST = 0: FOR K = 1 TO 6: FOR J = 1 TO 35
830 IF N(J,K) = 0 THEN 850
840 ST = ST + 1
850 NEXT J: NEXT K
860 PRINT "TIME OF TEST START WAS:": PRINT : PRINT H$
870 PRINT " ELAPSED TIME OF TEST WAS:": PRINT :PRINT ",TIME;" " HOURS"
880 REV = INT (AR * 60 * TIME + .5)
```

```
885 PRINT : PRINT "TOTAL ROTOR REV.= ";REV;" REVS."
886 PRINT : PRINT " INSERT DATA DISK IF DESIRED"
887 PRINT : INPUT "PRESS RETURN TO CONT.";H$
889 D$ = CHR$(4)
890 PRINT D$;"OPEN DAT.BINS"
900 PRINT D$;"DELETE DAT.BINS"
910 PRINT D$;"OPEN DAT.BINS"
920 PRINT D$;"WRITE DAT.BINS"
924 REM 1 VOLT,CBOOM,CRPM,CCYCP
925 PRINT U1: PRINT CB: PRINT CR: PRINT CC
926 REM CTORQUE(NM),CFLAP,CYANPOST,CGEN.VOLTS
927 PRINT CT: PRINT CF: PRINT CY: PRINT CU
928 REM AMB.TEMP,PRESS,WIND DIR.,GEN LOAD
930 PRINT D1: PRINT D2: PRINT D3: PRINT D4
931 REM GEAR RATIO, FURL ANGLE, CORREC. FACTOR
933 PRINT D5: PRINT D6: PRINT FC
934 REM CHANNEL TITLES FOR BIN DATA
935 PRINT K1$: PRINT K2$: PRINT K3$: PRINT K4$: PRINT K5$: PRINT K6$
936 REM SETS, START TIME, ET, REV
940 PRINT ST: PRINT H$: PRINT TIME: PRINT REV
960 FOR K = 1 TO 6: FOR J = 1 TO 35
970 IF NK(J,K) = 0 THEN 1060
980 PRINT K
990 PRINT J
1000 PRINT NK(J,K)
1010 PRINT MAX(J,K)
1020 PRINT MEAN(J,K)
1030 PRINT MN(J,K)
1040 PRINT SE(J,K)
1050 PRINT SBARX(J,K)
1060 NEXT J
1070 NEXT K
1080 PRINT D$;"CLOSE DAT.BINS"
1085 HOME : UTAB 10: INPUT " ENTER NAME OF TEST > ";N1$
1090 PRINT D$;"PR#1"
1095 PRINT : PRINT "TEST NAME IS ";N1$
1100 PRINT "START TIME= ";H$
1110 PRINT "ELAPSED TIME= ";TIME;" HOURS"
1130 PRINT "ROTOR REV.(CALC.)= ";REV
1132 PRINT "CALIBRATIONS AND TEST PARAMETERS"
1133 PRINT "FURL ANGLE (INCL. TILT)= ";D6
1134 PRINT "ONE VOLT=";U1;" CBOOM=";CB;" CRPM=";CR;" CCYPTCH=";CC
1135 PRINT "CTORQUE=";CT;" CFLAP=";CF;" CYANPOST=";CY;" CGEN.U=";CU
1136 PRINT "TEMP(DEG C)=";D1;" PRESS(ATM)=";D2;" CORR.FAC.=";FC;" WIND DIR="
;D3
1137 PRINT "GEN LOAD(OHMS)=";D4;" GEAR RATIO = ";D5;" TO 1"
1140 PRINT K1$;" ";K2$;" ";K3$
1141 PRINT K4$;" ";K5$;" ";K6$
1145 PRINT
1150 PRINT "CH#/BIN#/N#/MEAN/S.DEV/MAX/MIN"
1170 FOR K = 1 TO 6: FOR J = 1 TO 35
1180 IF NK(J,K) = 0 THEN 1220
1190 PRINT K;" ";J;" ";NK(J,K);" ";MEAN(J,K);" ";SE(J,K);" ";MAX(J,K);" ";
MN(J,K)
1220 NEXT J
1230 NEXT K
1240 PRINT D$;"PR#0"
1250 HOME : UTAB 5: PRINT "DONT FORGET TO RENAME DAT.BINS. DATA IS DELETED WHEN
PROGRAM IS RUN AGAIN,!!!!!"
1260 END
```

6. "Yaw Rate" Program

6.1 Program Logic

1. Provide operator instructions and initialize data
2. Define directional code (i.e. clockwise or counter clockwise yaw rates)
3. Read clock for test start time
4. Sample yaw position
5. Sample clock
6. Sample dynamic variable, usually cyclic pitch, for 0.5 seconds (24 samples)
7. Sample yaw position
8. Sample clock
9. Calculate elapsed time
10. Calculate yaw rate
11. Check yaw rate within limits. If not then go to #13
12. Skip to #14
13. Print yaw rate out of limits. Go to #17
14. Calculate amplitude of dynamic signal
15. Calculate yaw rate bin
16. Update bin array with current value to include maximum, minimum, mean, standard deviation and number of samples
17. Sample and test RPM in limits. If not, pause and test again until within limits

18. Check for operator stop signal. If none, then go to #4 and repeat sampling
19. Output bin array data to disk and printer
20. End

```
JPR#0
JLIST

5 REM THE YAWRATE CORRELATION PROGRAM
6 REM *****
10 REM THIS PROGRAM IS USED TO CALCULATE A YAW RATE AND CORRELATE IT TO A DYNAMIC VARIABLE
12 REM *** CLOCK IN SLOT 4
14 REM *** PRINTER IN SLOT 1
16 REM *** LEAP YEAR (L=1)
17 HOME : UTAB 2: PRINT " DO NOT TEST WITH NORTHERLY WINDS ": PRINT : PRINT : PRINT
18 REM FOLLOWING TESTS LIMITS OF TEST
19 PRINT " THIS PROGRAM CORRELATES YAW": PRINT " RATES TO A DYNAMIC VARIABLE":
PRINT " YAW RATE BIN # IS 1 DEG PER SEC": PRINT " MAX VALUE IS 35 DEG PER SEC."
20 PRINT : INPUT " INPUT LOW AND HIGH RPM VALUES FOR TEST ? ";LS,HS
21 PRINT : PRINT : INPUT " INPUT 1 VOLT=? AND CRPM=? ";U1,CRPM
22 INPUT " INPUT TEST FURL ANGLE ? ";FURL
23 HOME : UTAB 2: PRINT "RPM IS CHANNEL 1": PRINT : PRINT
30 PRINT : PRINT "DIRECTION OF ROTATION FOR TEST"
35 PRINT " ENTER A '1' FOR CLOCKWISE"
36 PRINT " ENTER A '0' FOR COUNTERCLOCKWISE"
37 PRINT : INPUT " ENTER > ";OP
50 INPUT " INPUT YAW POSITION CHANNEL ?";CYAW
51 INPUT " INPUT DYNAMIC POSITION CHANNEL ? ";CDYN
60 REM 24 POINTS ARE SAMPLED AND SAMPLE TIME IS APPROXIMATELY 0.5 SEC.
80 D$ = CHR$(4): REM SETS CNTRL D
81 PRINT D$;"NOHON C,I,0"
82 INPUT "INPUT NAME OF DYN VARIABLE ? ";U$
83 PRINT D$;"PR#1"
84 PRINT " CORRELATION OF YAW RATE US ";U$: PRINT : PRINT D$;"PR#0"
85 GOSUB 2000: GOSUB 3000:BEGIN = STD
90 DIM DY(47),MAX(35),MNK(35),NK(35),SBAR(35),MEAN(35),SE(35)
95 FOR I = 0 TO 35:MNK(I) = 255: NEXT I
100 POKE - 15871,CYAW
110 Y1P = PEEK ( - 15872)
120 GOSUB 2000: REM GET TIME AS T$
130 FOR I = 1 TO 24: POKE - 15871,CDYN:DY(I) = PEEK ( - 15872): NEXT I
140 POKE - 15871,CYAW
150 Y2P = PEEK ( - 15872)
160 T1$ = T$: GOSUB 2000
170 REM GET ELAPSED TIME
180 GOSUB 3000:S2 = STD
190 T$ = T1$: GOSUB 3000:S1 = STD
200 ET = S2 - S1
220 REM CONVERT YAWRATE TO DEG PER SEC.
221 YQ = Y2P - Y1P
222 IF OP = 1 AND YQ < 0 THEN 100
223 IF OP = 0 AND YQ > 0 THEN 100
224 YQ = ABS (YQ)
230 Y% = (YQ) * (100 / U1) * (1 / ET) + .5
236 IF Y% > 35 THEN 238
237 GOTO 240
238 PRINT " YAW RATE OUT OF RANGE": PRINT " YAW RATE = ";Y%
239 GOTO 100
240 REM CALC DYN VARIABLE
245 DH = 0:DL = 255
250 FOR I = 1 TO 24
260 IF DY(I) > DH THEN DH = DY(I)
270 IF DY(I) < DL THEN DL = DY(I)
280 NEXT I
290 AMPL = (DH - DL) / 2
291 PRINT : PRINT "YAW RATE= ";Y%,"AMPL= ";AMPL
300 REM UPDATE BINS
```

```
310 IF AMPL > MAX(Y%) THEN MAX(Y%) = AMPL
320 IF AMPL < MIN(Y%) THEN MIN(Y%) = AMPL
330 NK(Y%) = NK(Y%) + 1
340 MEAN(Y%) = (AMPL + ((NK(Y%) - 1) * MEAN(Y%))) / NK(Y%)
350 SBAR(Y%) = (SBAR(Y%) * (NK(Y%) - 1) + AMPL ^ 2) / NK(Y%)
358 QQ = ABS (SBAR(Y%) - MEAN(Y%) ^ 2)
360 SE(Y%) = SQRT (QQ)
370 REM RPM TEST
375 POKE - 15871,1
377 RPM = (CRPH / U1) * PEEK (- 15872)
380 IF RPM < LS OR RPM > HS THEN 382
381 GOTO 390
382 PRINT : PRINT "RPM OUT OF LIMITS": PRINT : PRINT " BIN DATA NOT UPDATED"
383 FOR WZ = 1 TO 2000: NEXT WZ
384 GOTO 375
390 REM STOP****PRESS CNTRL Z
392 XX = PEEK (- 16384)
393 IF XX < > (128 + 26) THEN 100
400 REM PRINT OUTS
402 HOME : UTAB 12: INPUT "INPUT CONVERSION FACTOR FOR DYNAMIC VARIABLE. I.E. C
ONVERTS DIGITAL DATA TO DESIRED VALUE ? (USE 1 IF DIGITAL DATA DESIRED) ? ";CG
405 REM GET DATE AND TIME OF TEST
406 GOSUB 5000: PRINT
407 GOSUB 4000
408 PRINT D$;"PR#1"
409 PRINT "RPM FOR TEST WAS BETWEEN ";LS;" AND ";HS: PRINT "FURL ANGLE FOR TEST
WAS ";FURL;" DEG"
410 IF QP = 1 THEN PRINT "ROTATION WAS CLOCKWISE"
411 IF QP = 0 THEN PRINT "ROTATION WAS COUNTERCLOCKWISE"
412 PRINT
415 FOR I = 0 TO 35
420 IF N(I) = 0 THEN 450
430 PRINT " YAWRATE (DEG/S) = ";I
435 PRINT "N= ";N(I);" MAX=";CG * MAX(I);" MIN=";CG * MIN(I);" MEAN=";CG * MEAN
(I);" STD DEV=";CG * SE(I)
440 PRINT
450 NEXT I
455 PRINT D$;"PR#0"
460 END
2000 REM
2005 REM *** SUBR - GET THE TIME
2010 REM *** THESE NEED TO BE CHANGED IF DISK IS NOT USED
2024 SLOT = 4
2025 REM FOR SLOT 4 ONLY***
2030 PRINT D$;"IN#";SLOT
2040 PRINT D$;"PR#";SLOT
2050 INPUT " ";T$
2060 PRINT D$;"IN#0"
2070 PRINT D$;"PR#0"
2080 RETURN
3000 REM
3001 REM FOR LEAP YEAR***L=1
3005 REM SUBR - STD
3006 REM
3010 REM CALCULATE SECONDS TO DATE FOR EACH TIME (STD)
3020 REM THIS IS THE NUMBER OF SECONDS SINCE JANUARY 1
3030 REM DO THIS FOR STRING TIME T$
3040 REM RETURN A NUMBER - STD
3050 REM
3060 REM FIND #'S FOR DATE AND TIME
3070 MT = VAL ( MID$ ( T$,1,2))
3080 D = VAL ( MID$ ( T$,4,2))
3090 H = VAL ( MID$ ( T$,7,2))
3100 M = VAL ( MID$ ( T$,10,2))
```

```
3110 S = VAL ( MID$ ( T$, 13, 6 ) )
3130 REM CALCULATE DAYS TO DATE - DTD
3135 RESTORE
3140 DTD = 0
3150 FOR I = 1 TO MT
3160 READ J
3170 DTD = DTD + J
3180 NEXT I
3200 DATA 0,31,28,31,30,31,30,31,31,30,31,30,31
3205 REM ADD IN DAYS AND LEAP YEAR DAY
3210 DTD = DTD + D
3230 IF MT > 2 AND L = 1 THEN DTD = DTD + 1
3240 REM FIND SECONDS TO DATE - STD
3250 STD = DTD * 86400 + H * 3600 + M * 60 + S
3300 RETURN
4000 REM
4010 REM SUBR - PUT SECONDS INTO DAYS, HOURS, MINUTES, SECONDS
4020 REM GIVEN ET IN SECONDS
4025 PRINT D$;"PR#1"
4030 ET = STD + ET - BEGIN
4040 D = INT ( ET / 86400 )
4050 ET = ET - D * 86400
4060 H = INT ( ET / 3600 )
4070 ET = ET - H * 3600
4080 M = INT ( ET / 60 )
4090 S = ET - M * 60
4091 PRINT : PRINT : PRINT "ELAPSED TIME OF TEST WAS: " : PRINT
4092 PRINT ,D;" DAYS"
4093 PRINT ,H;" HOURS"
4094 PRINT ,M;" MINUTES"
4095 PRINT ,S;" SECONDS"
4096 PRINT : PRINT : PRINT
4097 PRINT D$;"PR#0"
4100 RETURN
5000 REM SUBROUTINE FOR DATE AND TIME
5001 REM WILL PRINT TO SCREEN OR PRINTER
5010 REM *** APPLESOFT DATE AND TIME ***
5020 REM
5030 REM ***** BY SHERI MUHONEN *****
5040 REM
5050 REM
5060 D$ = CHR$ ( 4 )
5070 PRINT D$;"NOHON I,O,C": REM PREVENT DISK COMMANDS FROM PRINTING ON SCREEN
5080 SLOT = 4: REM FOR CLOCK IN SLOT 4***
5090 YEAR$ = "1980"
5120 REM READ THE TIME
5130 REM
5140 PRINT D$;"IN#";SLOT: REM SET INPUT TO CLOCK
5150 PRINT D$;"PR#";SLOT: REM SET OUPUT TO CLOCK
5170 INPUT " ";T$: REM OBTAIN TIME
5180 PRINT D$;"IN#0": REM RESTORE INPUT TO KEYBOARD
5190 PRINT D$;"PR#0": REM RESTORE OUTPUT TO CRT
5200 REM
5210 REM OBTAIN MONTH, DAY, HOUR,...ECT
5220 REM
5230 MTH$ = LEFT$ ( T$, 2 )
5240 DAY$ = MID$ ( T$, 4, 2 )
5250 HOUR$ = MID$ ( T$, 7, 2 )
5260 MINUTE$ = MID$ ( T$, 10, 2 )
5270 SEC$ = MID$ ( T$, 13, 2 )
5280 FRAC$ = RIGHT$ ( T$, 3 )
```

```
5290 REM
5300 REM OBTAIN MONTH (JANUARY, FEBRUARY...)
5310 REM
5320 MTH = UAL (MTH$): REM FIND DECIMAL # FOR MONTH
5330 RESTORE : FOR I = 0 TO 12: READ DD: NEXT I
5340 FOR I = 1 TO MTH
5350 READ MTH$: REM FIND NAME OF MONTH
5360 NEXT I
5370 DATA "JANUARY","FEBRUARY","MARCH","APRIL","MAY","JUNE"
5380 DATA "JULY","AUGUST","SEPTEMBER","OCTOBER","NOVEMBER","DECEMBER"
5390 REM
5400 REM OUTPUT DATE AND TIME
5410 REM
5420 PRINT D$;"PR#1"
5430 PRINT "DATE: ";MTH$;" ";DAY$;" ",;YEAR$
5450 PRINT "TIME: ";HOUR$;" ":";MINUTE$;" ":";SEC$;" ";FRAC$
5455 PRINT D$;"PR#0"
5460 RETURN
```

7. "Bin Plot" Programs

7.1 Program Logic

1. Provide operator instructions
2. Name data test file to be plotted
3. Display menu
4. Select plot
5. Read data

Note: Steps 4 and 5 may be reversed depending on the plotting program

6. Calculate "X" position based on bin number
7. Calculate "Y" position based on scaling factor and bin data, to include maximum, minimum, mean, standard deviation and number of samples as desired
8. Plot data on axis scale which was previously loaded in graphics memory
9. Go to #4 and repeat
10. End

JPR#
JLIST

```
3 REM THE BINPLOT.WIND2 PROGRAM
4 REM *****
5 DIM N(35,2),MAX(35,2),MEAN(35,2),MN(35,2),SE(35,2)
7 HOME : UTAB 5
8 PRINT : PRINT " TYPE -CONT- AFTER PLOT IS DRAWN": PRINT : INPUT " PRESS RET
URN TO CONT.";H$
9 HOME : UTAB 5
10 D$ = CHR$(4)
20 INPUT "NAME TEXT FILE FOR PLOTTING? ";Z$
21 PRINT : INPUT " INPUT DATA DISK";H$
22 PRINT D$;"MON C,I,0"
24 PRINT D$;"OPEN ";Z$: PRINT D$;"READ ";Z$
40 INPUT U1,CHIND,CRPM,CCYCP
50 INPUT SETS,H$,TIME,BP,REV
80 FOR S = 1 TO SETS
90 INPUT K,J,N(J,K),MAX(J,K),MEAN(J,K),MN(J,K),SE(J,K),SBAR
100 NEXT S
105 PRINT D$;"CLOSE ";Z$
107 PRINT : INPUT " INPUT BINPLOT DISK";H$
110 HOME : UTAB 5: PRINT " SELECT PLOT": PRINT
111 PRINT ,"RPM=1": PRINT ,"CYCLIC PITCH=2": PRINT ,"SAMPLE FREQUENCY=3"
112 PRINT ,"PRINT GRAPH=4"
114 PRINT : INPUT " ENTER SELECTION > ";QP
115 ON QP GOTO 120,300,1000,7000
120 K = 1
124 HGR
125 POKE - 16302,0
126 HCOLOR= 3
127 PRINT D$;"BLOAD AXIS-RPM"
128 CR = CRPM / U1
130 FOR J = 1 TO 35
140 IF N(J,K) < 10 THEN 250
145 X = 42 + J * 7
170 R = MEAN(J,K) * CR
180 GOSUB 500
210 R = MEAN(J,K) * CR + SE(J,K) * CR: GOSUB 500
215 R1 = R
220 R = MEAN(J,K) * CR - SE(J,K) * CR: GOSUB 500
225 R2 = R
226 Y1 = INT ( - .4677 * R1 + 156.5)
227 Y2 = INT ( - .4677 * R2 + 156.5)
230 IF Y2 > 156 THEN Y2 = 156
232 HPLOT X,Y1 TO X,Y2
250 NEXT J
260 STOP
270 TEXT
280 GOTO 110
300 K = 2
310 HGR : HCOLOR= 3
315 POKE - 16302,0
320 PRINT D$;"BLOAD AXIS-TAU"
330 CC = CCYCP / U1
340 FOR J = 1 TO 35
350 IF N(J,K) = 0 THEN 470
360 X = 42 + J * 7
370 C = MAX(J,K) * CC: GOSUB 600
380 C = MEAN(J,K) * CC: GOSUB 600
390 C = MN(J,K) * CC: GOSUB 600
400 C = MEAN(J,K) * CC + SE(J,K) * CC: GOSUB 600
```

Short Title: Yawed Flow On Wind Turbine Rotors Swift, D.Sc. 1981

```
410 C1 = C
420 C = MEAN(J,K) * CC - SE(J,K) * CC: GOSUB 600
430 C2 = C
440 Y1 = INT ( - 12.000 * C1 + 156.5)
450 Y2 = INT ( - 12.000 * C2 + 156.5)
455 IF Y2 > 156 THEN Y2 = 156
460 HPLOT X,Y1 TO X,Y2
470 NEXT J
480 STOP
485 TEXT
490 GOTO 110
500 Y = INT ( - .4677 * R + 156.5)
505 IF Y > 156 THEN Y = 156
506 IF Y < 4 THEN Y = 0
510 HPLOT X - 2,Y TO X + 2,Y
520 RETURN
600 Y = INT ( - 12.000 * C + 156.5)
605 IF Y > 156 THEN Y = 156
606 IF Y < 4 THEN Y = 0
610 HPLOT X - 2,Y TO X + 2,Y
620 RETURN
700 PRINT D$;"PR#1"
705 PRINT : PRINT
707 PRINT "NAME OF TEST FILE IS ";Z$
710 PRINT "START TIME= ";H$
715 PRINT " (MTH/DY HR;MIN;SEC.FRAC)"
716 PRINT
720 PRINT "ELAPSED TIME= ";TIME;" HOURS": PRINT
730 PRINT "YAW ANGLE= ";BP;" DEGREES": PRINT
735 PRINT " AUTOROTATION DATA"
740 PRINT " ROTOR REV.(CALC)= ";REV;" REV.
750 PRINT : PRINT : PRINT
755 PRINT D$;"PR#0"
760 RETURN
1000 REM SUBR FOR SAMPLES PLOT
1010 GOSUB 700
1020 HGR : HCOLOR= 3: POKE - 16302,0
1030 PRINT D$;"BLOAD AXIS-SAMPLES"
1040 K = 1
1050 FOR J = 1 TO 35
1055 IF N(J,K) = 0 THEN 1240
1060 X = 42 + J * 7
1100 REM CALC LOG N
1110 I1 = 1
1120 E1 = 10 ^ I1
1130 IF (N(J,K) - E1) < 0 THEN 1170
1140 I1 = I1 + 1
1145 IF I1 > 6 THEN STOP
1150 GOTO 1120
1170 I2 = 1
1180 E2 = 10 ^ ((I1 - 1) + (I2 / 24))
1190 IF (N(J,K) - E2) < 0 THEN 1220
1200 I2 = I2 + 1
1205 IF I2 > 24 THEN STOP
1210 GOTO 1180
1220 Y = 156 - (24 * (I1 - 1) + (I2 - 1))
1230 HPLOT X,Y
1240 NEXT J
1250 STOP
1260 TEXT
1270 GOTO 110
```

```
7000 REM PRINT SUBROUTINE
7010 HOME : UTAB 10
7020 PRINT "LARGE OR SMALL PLOT (L/S)"
7030 INPUT " ENTER > ":ANS$
7040 IF ANS$ = "S" THEN 7500
7050 REM PRINTS LARGE PICTURE
7055 REM PRINTER IN SLOT 1
7060 POKE 1272,0
7061 POKE 1144,32
7063 POKE 1400,1
7064 POKE 1528,128
7065 POKE 1656,1
7066 CALL - 16000
7080 GOTO 110
7500 CALL - 16046
7510 GOTO 110
```

JPR#0
JLVS#

```

3 REM THE BINPLOT.WIND6 PROGRAM
4 REM *****
5 DIM N(35),MAX(35),MEAN(35),MNK(35),SE(35),SBARK(35)
6 HOME : UTAB 5
7 PRINT " RESET HIMEM IF REQUIRED": PRINT : PRINT
8 PRINT : PRINT " TYPE -CONT- AFTER PLOT IS DRAWN": PRINT : INPUT " PRESS RET
URN TO CONT.";H$
9 HOME : UTAB 5
10 D$ = CHR$(4)
15 PRINT D$;"MON C,I,0"
17 RZ% = 0
20 INPUT "NAME TEXT FILE FOR PLOTTING? ";Z$
25 HOME : UTAB 5: PRINT "SELECT PLOT": PRINT " ALWAYS SELECT TITLE FIRST": PRI
NT
26 PRINT "0.PRINT GRAPH (SMALL)": PRINT "1.TITLE PAGE": PRINT "2.SAMPLE FREQ
UENCY": PRINT "3.RPM": PRINT "4.CYCLIC PITCH AMPLE."
27 PRINT "5.GEN. POWER": PRINT "6.ROTOR POWER": PRINT "7.EFFICIENCY": PRINT
"8.THRUST": PRINT : INPUT " ENTER SELECTION > ";QP
28 IF QP = 1 THEN 55
29 IF QP = 8 THEN K = 6
30 IF QP = 2 THEN K = 1
31 IF QP = 3 THEN K = 1
32 IF QP = 4 THEN K = 3
33 IF QP = 5 THEN K = 2
34 IF QP = 6 THEN K = 4
35 IF QP = 7 THEN K = 5
36 IF QP = 0 THEN 7000
39 PRINT "SETS= ";ST
40 RZ% = 25 + (K - 1) * (ST / 5) * 8
41 PRINT "RZ= ";RZ%
55 PRINT : INPUT " INPUT DATA DISK";H$: PRINT D$;"OPEN ";Z$
56 PRINT D$;"POSITION ";Z$;"R ";RZ%
57 PRINT D$;"READ ";Z$
58 IF RZ% > 0 THEN 80
60 INPUT U1,UH,UR,UC,UT,UF,UY,UW
65 INPUT D1,D2,D3,D4,D5,D6,FC
70 INPUT K1$,K2$,K3$,K4$,K5$,K6$
75 INPUT ST,H$,TIME,REV
76 IF RZ% = 0 THEN 105
80 FOR S = 1 TO ST
81 ONERR GOTO 105
82 INPUT KT
85 IF KT > K THEN 105
86 IF KT < > K THEN STOP
90 INPUT J,NK(J),MAX(J),MEAN(J),MNK(J),SE(J),SBARK(J)
100 NEXT S
105 PRINT D$;"CLOSE ";Z$
106 INPUT " INPUT BINPLOT DISK";H$
107 ON QP GOTO 700,1000,120,300,2000,3000,4000,5000
120 REM RPM
124 HGR
125 POKE - 16302,0
126 HCOLOR= 3
127 PRINT D$;"BLOAD AXIS-RPM"
128 CR = UR / U1
130 FOR J = 1 TO 32
140 IF NK(J) = 0 THEN 250
145 X = 42 + J * 7
170 R = MEAN(J) * CR
180 GOSUB 500
210 R = MEAN(J) * CR + SE(J) * CR: GOSUB 500
215 R1 = R

```

```
220 R = MEAN(J) * CR - SE(J) * CC: GOSUB 500
225 R2 = R
226 Y1 = INT ( - .4677 * R1 + 156.5)
227 Y2 = INT ( - .4677 * R2 + 156.5)
230 IF Y2 > 156 THEN Y2 = 156
232 H PLOT X,Y1 TO X,Y2
250 NEXT J
260 STOP
270 TEXT
280 GOTO 25
300 REM PLOT ROUTINE
310 HGR : HCOLOR= 3
315 POKE -16302,0
320 PRINT D$;"BLORD AXIS-TAU"
330 CC = UC / U1
340 FOR J = 1 TO 32
350 IF N(J) = 0 THEN 470
360 X = 42 + J * 7
370 C = MAX(J) * CC: GOSUB 600
380 C = MEAN(J) * CC: GOSUB 600
390 C = MIN(J) * CC: GOSUB 600
400 C = MEAN(J) * CC + SE(J) * CC: GOSUB 600
410 C1 = C
420 C = MEAN(J) * CC - SE(J) * CC: GOSUB 600
430 C2 = C
440 Y1 = INT ( - 12.000 * C1 + 156.5)
445 IF Y1 < 4 THEN Y1 = 4
450 Y2 = INT ( - 12.000 * C2 + 156.5)
455 IF Y2 > 156 THEN Y2 = 156
460 H PLOT X,Y1 TO X,Y2
470 NEXT J
480 STOP
485 TEXT
490 GOTO 25
500 Y = INT ( - .4677 * R + 156.5)
505 IF Y > 156 THEN Y = 156
506 IF Y < 4 THEN Y = 0
510 H PLOT X - 2,Y TO X + 2,Y
520 RETURN
600 Y = INT ( - 12.000 * C + 156.5)
605 IF Y > 156 THEN Y = 156
606 IF Y < 4 THEN Y = 0
610 H PLOT X - 2,Y TO X + 2,Y
620 RETURN
700 PRINT D$;"PR#1"
705 PRINT
707 PRINT "FILE NAME IS ";Z$
710 PRINT "START TIME= ";H$
720 PRINT "ELAPSED TIME= ";TIME;" HOURS"
730 PRINT "FURL ANGLE(INCL. TILT OF ROTOR) =";D6;" DEG"
740 PRINT " ROTOR REV.(CALC) = ";REV;" REV."
750 PRINT "ONE VOLT=";U1;" CHIND=";UH;" CRPH=";UR;" CCYPTCH=";UC
760 PRINT "CTORQUE=";UT;" CFLAP=";UF;" CYANPOST=";UY;" CGEN.VOLTS=";UU
770 PRINT "TEMP (DEG C)=";D1;" PRESS(ATM)=";D2;" CORR.FAC.=";FC;" WIND DIR="
;D3
780 PRINT "GEN. LOAD (OHMS)=";D4;" GEAR RATIO=";D5;" TO 1"
790 PRINT K1$;" ";K2$;" ";K3$
800 PRINT K4$;" ";K5$;" ";K6$
810 PRINT
820 PRINT D$;"PR#0"
830 GOTO 25
1000 REM SUBR FOR SAMPLES PLOT
```

```
1020 HGR : HCOLOR= 3: POKE - 16302,0
1030 PRINT D$:"BLOAD AXIS-SAMPLES"
1050 FOR J = 1 TO 32
1055 IF (NKJ) = 0 THEN 1240
1060 X = 42 + J * 7
1100 REM CALC LOG N
1110 I1 = 1
1120 E1 = 10 ^ I1
1130 IF (NKJ) - E1 < 0 THEN 1170
1140 I1 = I1 + 1
1145 IF I1 > 6 THEN STOP
1150 GOTO 1120
1170 I2 = 1
1180 E2 = 10 ^ ((I1 - 1) + (I2 / 24))
1190 IF (NKJ) - E2 < 0 THEN 1220
1200 I2 = I2 + 1
1205 IF I2 > 24 THEN STOP
1210 GOTO 1180
1220 Y = 156 - (24 * (I1 - 1) + (I2 - 1))
1230 HPLOT X,Y
1240 NEXT J
1250 STOP
1260 TEXT
1270 GOTO 25
2000 REM GEN POWER PLOT
2010 HGR : HCOLOR= 3: POKE - 16302,0
2020 PRINT D$:"BLOAD AXIS-6.PHR"
2022 FOR J = 1 TO 32
2024 MAX(J) = 0:MNK(J) = 0
2025 NEXT J
2030 CC = (((UU * 1.03) / U1) ^ 2) / D4
2035 CC = CC / 1000
2040 GOTO 340
3000 REM ROTOR POWER
3010 HGR : HCOLOR= 3: POKE - 16302,0
3020 PRINT D$:"BLOAD AXIS-R.PHR"
3022 FOR J = 1 TO 32
3024 MAX(J) = 0:MNK(J) = 0
3025 NEXT J
3030 CC = (UT * UR * .105) / (U1 ^ 2)
3035 CC = CC / 1000
3040 GOTO 340
4000 REM EFFICIENCY
4010 HGR : HCOLOR= 3: POKE - 16302,0
4020 PRINT D$:"BLOAD AXIS-EFF."
4022 FOR J = 1 TO 32
4024 MAX(J) = 0:MNK(J) = 0
4025 NEXT J
4030 CC = ((UU * 1.03) ^ 2) / (UT * UR * .105 * D4)
4035 CC = CC * 10
4040 GOTO 340
5000 REM THRUST
5010 HGR : HCOLOR= 3: POKE - 16302,0
5020 PRINT D$:"BLOAD AXIS-THRUST"
5030 CC = UY / U1
5035 CC = CC / 150
5040 GOTO 340
7000 REM PLOT SUBROUTINE
7010 HOME : UTAB 10
7020 PRINT "LARGE OR SMALL (L/S)"
7030 INPUT " ENTER > ";ANS$
```

```
7040 IF ANS# = "S" THEN 7500
7050 REM PRINT LARGE PICTURE
7055 REM PRINTER IN SLOT 1
7060 POKE 1272,0
7061 POKE 1144,32
7062 POKE 1400,1
7063 POKE 1528,128
7064 POKE 1656,1
7065 CALL - 16000
7080 GOTO 25
7500 CALL - 16046
7510 GOTO 25
```

JPR#0
JLIST

```
3 REM THE BINPLOT.WIND2.FAST PROGRAM
4 REM *****
5 DIM N(35),MAX(35),MEAN(35),MNK(35),SE(35),SBAR(35)
6 HOME : UTAB 5
7 PRINT " RESET HIMEM IF REQUIRED": PRINT : PRINT
8 PRINT : PRINT " TYPE -CONT- AFTER PLOT IS DRAWN": PRINT : INPUT " PRESS RET
URN TO CONT.":H$
9 HOME : UTAB 5
10 D$ = CHR$(4)
15 PRINT D$:"MON C,I,0"
17 RZ% = 0
20 INPUT "NAME TEXT FILE FOR PLOTTING? ":Z$
25 HOME : UTAB 5: PRINT "SELECT PLOT": PRINT " ALWAYS SELECT TITLE FIRST": PRI
NT
26 PRINT "0.PRINT GRAPH (SMALL)": PRINT "1.TITLE PAGE": PRINT "2.SAMPLE FREQ
UENCY": PRINT "3.RPM": PRINT "4.ROTOR POWER"
27 PRINT : INPUT " ENTER SELECTION > ":QP
28 IF QP = 1 THEN 55
30 IF QP = 2 THEN K = 1
31 IF QP = 3 THEN K = 1
32 IF QP = 4 THEN K = 2
36 IF QP = 0 THEN 7000
39 PRINT "SETS=" ;ST
40 RZ% = 25 + (K - 1) * (ST / 2) * 8
41 PRINT "RZ=" ;RZ%
55 PRINT : INPUT " INPUT DATA DISK":H$: PRINT D$:"OPEN ":Z$
56 PRINT D$:"POSITION ":Z$;"R ":R ;RZ%
57 PRINT D$:"READ ":Z$
58 IF RZ% > 0 THEN 80
60 INPUT U1,UW,UR,UC,UT,UF,UY,UU
65 INPUT D1,D2,D3,D4,D5,D6,FC
70 INPUT K1$,K2$,K3$,K4$,K5$,K6$
75 INPUT ST,H$,TIME,REV
76 IF RZ% = 0 THEN 105
80 FOR S = 1 TO ST
81 ONERR GOTO 105
82 INPUT KT
85 IF KT > K THEN 105
86 IF KT < > K THEN STOP
90 INPUT J,N(J),MAX(J),MEAN(J),MNK(J),SE(J),SBAR(J)
100 NEXT S
105 PRINT D$:"CLOSE ":Z$
106 INPUT " INPUT BINPLOT DISK":H$
107 ON QP GOTO 700,1000,120,3000
120 REM RPM
124 HGR
125 POKE - 16302,0
126 HCOLOR= 3
127 PRINT D$:"BLOAD AXIS-RPM"
128 CR = UR / U1
130 FOR J = 1 TO 32
140 IF N(J) = 0 THEN 250
145 X = 42 + J * 7
170 R = MEAN(J) * CR
180 GOSUB 500
210 R = MEAN(J) * CR + SE(J) * CR: GOSUB 500
215 R1 = R
220 R = MEAN(J) * CR - SE(J) * CR: GOSUB 500
225 R2 = R
226 Y1 = INT ( -.4677 * R1 + 156.5)
227 Y2 = INT ( -.4677 * R2 + 156.5)
```

```
230 IF Y2 > 156 THEN Y2 = 156
232 H$PLOT X,Y1 TO X,Y2
250 NEXT J
260 STOP
270 TEXT
280 GOTO 25
300 REM PLOT ROUTINE
310 HGR : HCOLOR= 3
315 POKE - 16302,0
320 PRINT D$;"BLORD AXIS-TAU"
330 CC = UC / U1
340 FOR J = 1 TO 32
350 IF NK(J) = 0 THEN 470
360 X = 42 + J * 7
370 C = MAX(J) * CC: GOSUB 600
380 C = MEAN(J) * CC: GOSUB 600
390 C = MIN(J) * CC: GOSUB 600
400 C = MEAN(J) * CC + SE(J) * CC: GOSUB 600
410 C1 = C
420 C = MEAN(J) * CC - SE(J) * CC: GOSUB 600
430 C2 = C
440 Y1 = INT ( - 12.000 * C1 + 156.5)
445 IF Y1 < 4 THEN Y1 = 4
450 Y2 = INT ( - 12.000 * C2 + 156.5)
455 IF Y2 > 156 THEN Y2 = 156
460 H$PLOT X,Y1 TO X,Y2
470 NEXT J
480 STOP
485 TEXT
490 GOTO 25
500 Y = INT ( - .4677 * R + 156.5)
505 IF Y > 156 THEN Y = 156
506 IF Y < 4 THEN Y = 0
510 H$PLOT X - 2,Y TO X + 2,Y
520 RETURN
600 Y = INT ( - 12.000 * C + 156.5)
605 IF Y > 156 THEN Y = 156
606 IF Y < 4 THEN Y = 0
610 H$PLOT X - 2,Y TO X + 2,Y
620 RETURN
700 PRINT D$;"PR#1"
705 PRINT
707 PRINT "FILE NAME IS ";Z$
710 PRINT "START TIME= ";H$
720 PRINT "ELAPSED TIME= ";TIME;" HOURS"
730 PRINT "FURL ANGLE(INCL. TILT OF ROTOR) =";D6;" DEG"
740 PRINT " ROTOR REV.(CALC) = ";REV;" REV."
750 PRINT "ONE VOLT=";U1;" CHIND=";UH;" CRPM=";UR;" CCYPTCH=";UC
760 PRINT "CTORQUE=";UT;" CFLAP=";UF;" CYAWPOST=";UY;" CGEN.VOLTS=";UU
770 PRINT "TEMP (DEG C)=";D1;" PRESS(ATM)=";D2;" CORR.FAC.=";FC;" WIND DIR="
;D3
780 PRINT "GEN. LOAD (OHMS)=";D4;" GEAR RATIO=";D5;" TO 1"
790 PRINT K1$;" ";K2$;" ";K3$
800 PRINT K4$;" ";K5$;" ";K6$
810 PRINT
820 PRINT D$;"PR#0"
830 GOTO 25
1000 REM SUBR FOR SAMPLES PLOT
1020 HGR : HCOLOR= 3: POKE - 16302,0
1030 PRINT D$;"BLORD AXIS-SAMPLES"
1050 FOR J = 1 TO 32
1055 IF NK(J) = 0 THEN 1240
```

```
1060 X = 42 + J * 7
1100 REM CALC LOG N
1110 I1 = 1
1120 E1 = 10 ^ I1
1130 IF (NKJ) - E1 < 0 THEN 1170
1140 I1 = I1 + 1
1145 IF I1 > 6 THEN STOP
1150 GOTO 1120
1170 I2 = 1
1180 E2 = 10 ^ ((I1 - 1) + (I2 / 24))
1190 IF (NKJ) - E2 < 0 THEN 1220
1200 I2 = I2 + 1
1205 IF I2 > 24 THEN STOP
1210 GOTO 1180
1220 Y = 156 - (24 * (I1 - 1) + (I2 - 1))
1230 HPLLOT X,Y
1240 NEXT J
1250 STOP
1260 TEXT
1270 GOTO 25
2000 REM GEN POWER PLOT
2010 HGR : HCOLOR= 3: POKE - 16382,0
2020 PRINT D$:"BLOAD AXIS-G.PWR"
2022 FOR J = 1 TO 32
2024 MAX(J) = 0:MIN(J) = 0
2025 NEXT J
2030 CC = (((UU * 1.03) / U1) ^ 2) / D4
2035 CC = CC / 1000
2040 GOTO 340
3000 REM ROTOR POWER
3010 HGR : HCOLOR= 3: POKE - 16382,0
3020 PRINT D$:"BLOAD AXIS-R.PWR"
3022 FOR J = 1 TO 32
3024 MAX(J) = 0:MIN(J) = 0
3025 NEXT J
3030 CC = (UT * UR * .105) / (U1 ^ 2)
3035 CC = CC / 1000
3040 GOTO 340
4000 REM EFFICIENCY
4010 HGR : HCOLOR= 3: POKE - 16382,0
4020 PRINT D$:"BLOAD AXIS-EFF."
4022 FOR J = 1 TO 32
4024 MAX(J) = 0:MIN(J) = 0
4025 NEXT J
4030 CC = ((UU * 1.03) ^ 2) / (UT * UR * .105 * D4)
4035 CC = CC * 10
4040 GOTO 340
5000 REM THRUST
5010 HGR : HCOLOR= 3: POKE - 16382,0
5020 PRINT D$:"BLOAD AXIS-THRUST"
5030 CC = UV / U1
5035 CC = CC / 150
5040 GOTO 340
7000 REM PLOT PICTURE
7010 HOME : UTAB 10
7020 PRINT "LARGE OR SMALL (L/S)"
7030 INPUT " ENTER > ":ANS$
7040 IF ANS$ = "S" THEN 7500
7050 REM PRINT LARGE PICTURE
7055 REM PRINTER IN SLOT 1
7060 POKE 1272,0
```

```
7061 POKE 1144,32
7062 POKE 1400,1
7063 POKE 1528,128
7064 POKE 1656,1
7065 CALL - 16000
7080 GOTO 25
7500 CALL - 16046
7510 GOTO 25
```

!LOADR#0
JLIST

```
3 REM THE BINPLOT.RPM6 PROGRAM
4 REM *****
5 DIM NK(35),MAX(35),MEAN(35),MNK(35),SE(35),SBARK(35)
6 HOME : UTAB 5
7 PRINT " RESET HIGH IF REQUIRED": PRINT : PRINT
8 PRINT : PRINT " TYPE -CONT- AFTER PLOT IS DRAWN": PRINT : INPUT " PRESS RET
URN TO CONT.":H$
9 HOME : UTAB 5
10 D$ = CHR$(4)
15 PRINT D$:"MON C,I,0"
17 RZ% = 0
20 INPUT "NAME TEXT FILE FOR PLOTTING? ":Z$
25 HOME : UTAB 5: PRINT "SELECT PLOT": PRINT " ALWAYS SELECT TITLE FIRST": PRI
NT
26 PRINT "0.PRINT GRAPH (SMALL)": PRINT "1.TITLE PAGE": PRINT "2.SAMPLE FREQ
UENCY": PRINT "3.MEAN FLAP": PRINT "4.FLAP AMPL."
27 PRINT "5.FRONT ACCEL. ": PRINT "6.IN PLANE AMPL.": PRINT "7.U. BOOM AMPL.
": PRINT "8.CYCLIC PITCH AMPL.": PRINT : INPUT " ENTER SELECTION > ":QP
28 IF QP = 1 THEN 55
29 IF QP = 8 THEN K = 6
30 IF QP = 2 THEN K = 1
31 IF QP = 3 THEN K = 1
32 IF QP = 4 THEN K = 2
33 IF QP = 5 THEN K = 3
34 IF QP = 6 THEN K = 4
35 IF QP = 7 THEN K = 5
36 IF QP = 8 THEN 7000
39 PRINT "SETS= ":ST
40 RZ% = 25 + (K - 1) * (ST / 6) * 8
41 PRINT "RZ= ":RZ%
55 PRINT : INPUT " INPUT DATA DISK":H$: PRINT D$:"OPEN ":Z$
56 PRINT D$:"POSITION ":Z$:"R ":RZ%
57 PRINT D$:"READ ":Z$
58 IF RZ% > 0 THEN 80
60 INPUT U1,UB,UR,UC,UT,UF,UY,UU
65 INPUT D1,D2,D3,D4,D5,D6,FC
70 INPUT K1$,K2$,K3$,K4$,K5$,K6$
75 INPUT ST,H$,TIME,REV
76 IF RZ% = 0 THEN 105
80 FOR S = 1 TO ST
81 ONERR GOTO 105
82 INPUT KT
85 IF KT > K THEN 105
86 IF KT < > K THEN STOP
90 INPUT J,MK(J),MAX(J),MEAN(J),MNK(J),SE(J),SBARK(J)
100 NEXT S
105 PRINT D$:"CLOSE ":Z$
106 PRINT : INPUT " INPUT BINPLOT DISK":H$
107 ON QP GOTO 700,1000,2000,3000,4000,5000,6000,3000
300 REM PLOT ROUTINE
310 HGR : HCOLOR= 3
315 POKE - 16302,0
320 PRINT D$:"PR#1"
322 PRINT " PLOT OF CYCLIC PITCH AMPLITUDE US RPM FOLLOWS"
324 PRINT " ONE VOLT = ":UC:" DEGREES"
325 PRINT D$:"PR#0"
327 PRINT D$:"BLOAD AXIS-VOLTS/RPM"
330 CC = 2 / U1
340 FOR J = 1 TO 32
350 IF MK(J) = 0 THEN 470
360 X = 42 + J * 7
370 C = MAX(J) * CC: GOSUB 600
```

```
380 C = MEAN(J) * CC: GOSUB 600
390 C = MNK(J) * CC: GOSUB 600
400 C = MEAN(J) * CC + SE(J) * CC: GOSUB 600
410 C1 = C
420 C = MEAN(J) * CC - SE(J) * CC: GOSUB 600
430 C2 = C
440 Y1 = INT ( - 12.000 * C1 + 156.5)
450 Y2 = INT ( - 12.000 * C2 + 156.5)
455 IF Y2 > 156 THEN Y2 = 156
460 HPLOT X,Y1 TO X,Y2
470 NEXT J
480 STOP
485 TEXT
490 GOTO 25
500 Y = INT ( - .4677 * R + 156.5)
505 IF Y > 156 THEN Y = 156
506 IF Y < 4 THEN Y = 0
510 HPLOT X - 2,Y TO X + 2,Y
520 RETURN
600 Y = INT ( - 12.000 * C + 156.5)
605 IF Y > 156 THEN Y = 156
606 IF Y < 4 THEN Y = 0
610 HPLOT X - 2,Y TO X + 2,Y
620 RETURN
700 PRINT D$;"PR#1"
705 PRINT
707 PRINT "FILE NAME IS ";Z$
710 PRINT "START TIME= ";H$
720 PRINT "ELAPSED TIME= ";TIME;" HOURS"
730 PRINT "FURL ANGLE(INCL. TILT OF ROTOR) =";D6;" DEG"
740 PRINT " ROTOR REV.(CALC) = ";REV;" REV.
750 PRINT "ONE VOLT=";U1;" CBOOM=";UB;" CCYLCPTCH=";UC
760 PRINT "CINPLNE=";UT;" CFLAP=";UF;" CF.ACCEL=";UY
770 PRINT "TEMP (DEG C)=";D1;" PRESS(ATM)=";D2;" CORR.FAC.=";FC;" WIND DIR="
;D3
780 PRINT "GEN. LOAD (OHMS)=";D4;" GEAR RATIO=";D5;" TO 1"
790 PRINT K1$;" ";K2$;" ";K3$
800 PRINT K4$;" ";K5$;" ";K6$
810 PRINT
820 PRINT D$;"PR#0"
830 GOTO 25
1000 REM SUBR FOR SAMPLES PLOT
1020 HGR : HCOLOR= 3: POKE - 16302,0
1030 PRINT D$;"BLOOD AXIS-SAMPLES/RPM"
1050 FOR J = 1 TO 32
1055 IF N(J) = 0 THEN 1240
1060 X = 42 + J * 7
1100 REM CALC LOG N
1110 I1 = 1
1120 E1 = 10 ^ I1
1130 IF (N(J) - E1) < 0 THEN 1170
1140 I1 = I1 + 1
1145 IF I1 > 6 THEN STOP
1150 GOTO 1120
1170 I2 = 1
1180 E2 = 10 ^ ((I1 - 1) + (I2 / 24))
1190 IF (N(J) - E2) < 0 THEN 1220
1200 I2 = I2 + 1
1205 IF I2 > 24 THEN STOP
1210 GOTO 1180
1220 Y = 156 - (24 * (I1 - 1) + (I2 - 1))
1230 HPLOT X,Y
```

```
1240 NEXT J
1250 STOP
1260 TEXT
1270 GOTO 25
2000 REM MEAN FLAP
2010 HGR : HCOLOR= 3: POKE - 16302,0
2025 PRINT D$;"PR#1"
2026 PRINT " PLOT OF MEAN FLAP VS RPM FOLLOWS"
2027 PRINT " ONE VOLT = ";UF;" MM FLAP BENDING"
2030 CC = 2 / U1
2035 PRINT D$;"PR#0"
2038 PRINT D$;"BLOAD AXIS-VOLTS/RPM"
2040 GOTO 340
3000 REM FLAP AMPL.
3010 HGR : HCOLOR= 3: POKE - 16302,0
3020 PRINT D$;"PR#1"
3022 PRINT " PLOT OF FLAP AMPLITUDE VS RPM FOLLOWS"
3024 PRINT " ONE VOLT = ";UF;" MM FLAP BENDING"
3025 PRINT D$;"PR#0"
3030 CC = 2 / U1
3035 PRINT D$;"BLOAD AXIS-VOLTS/RPM"
3040 GOTO 340
4000 REM YAWPOST AMPL.
4010 HGR : HCOLOR= 3: POKE - 16302,0
4020 PRINT D$;"PR#1"
4022 PRINT " PLOT OF FRONT ACCELEROMETER AMPLITUDE VS RPM FOLLOWS"
4025 PRINT " ONE VOLT = ";UY;" .2 G"
4028 PRINT D$;"PR#0"
4030 CC = 2 / U1
4035 PRINT D$;"BLOAD AXIS-VOLTS/RPM"
4040 GOTO 340
5000 REM TORQUE AMPL.
5010 HGR : HCOLOR= 3: POKE - 16302,0
5020 PRINT D$;"PR#1"
5022 PRINT " PLOT OF IN PLANE AMPLITUDE VS RPM FOLLOWS"
5024 PRINT " ONE VOLT = ";UT;" MM IN PLANE BENDING"
5028 PRINT D$;"PR#0"
5030 CC = 2 / U1
5035 PRINT D$;"BLOAD AXIS-VOLTS/RPM"
5040 GOTO 340
6000 REM U. BOOM AMPL.
6010 HGR : HCOLOR= 3: POKE - 16302,0
6020 PRINT D$;"PR#1"
6022 PRINT " PLOT OF VERTICAL BOOM BENDING AMPLITUDE VS RPM FOLLOWS"
6024 PRINT " ONE VOLT = ";UB;" MM BOOM BENDING"
6028 PRINT D$;"PR#0"
6030 CC = 2 / U1
6035 PRINT D$;"BLOAD AXIS-VOLTS/RPM"
6040 GOTO 340
7000 REM PLOT SUBROUTINE
7010 HOME : UTAB 10
7020 PRINT "LARGE OR SMALL (L/S)"
7030 INPUT " ENTER > ";ANS$
7040 IF ANS$ = "S" THEN 7500
7050 REM PRINT LARGE PICTURE
7055 REM PRINTER IN SLOT 1
7060 POKE 1272,0
7061 POKE 1144,32
7062 POKE 1400,1
7063 POKE 1528,128
7064 POKE 1656,1
```

7065 CALL - 16000
7080 GOTO 25
7500 CALL - 16046
7510 GOTO 25

JPR#0
JLIST

```
3 REM THE BINPLOT.YAWRATE PROGRAM
4 REM *****
5 DIM N(35,2),MAX(35,2),MEAN(35,2),MN(35,2),SE(35,2)
7 HOME : UTAB 5
8 PRINT : PRINT " TYPE -CONT- AFTER PLOT IS DRAWN": PRINT : INPUT " PRESS RET
URN TO CONT.";H$
9 HOME : UTAB 5
10 D$ = CHR$(4)
20 INPUT "NAME TEXT FILE FOR PLOTTING? ";Z$
21 PRINT : INPUT " INPUT DATA DISK";H$
22 PRINT D$;"MON C,I,0"
24 PRINT D$;"OPEN ";Z$: PRINT D$;"READ ";Z$
40 INPUT SETS,FURL,CG,U1,NA$,FL$,LS,HS
50 INPUT MTH$,DAY$,YEAR$,HOURS$,MINUTE$
60 INPUT SEC$,H,M,S
65 SD = S
80 FOR S = 1 TO SETS
90 INPUT K,J,N(J,K),MAX(J,K),MEAN(J,K),MN(J,K),SE(J,K),SBAR
100 NEXT S
105 PRINT D$;"CLOSE ";Z$
107 PRINT : INPUT " INPUT BINPLOT DISK";H$
110 HOME : UTAB 5: PRINT " SELECT PLOT": PRINT
111 PRINT "0.PRINT GRAPH": PRINT "1.TITLE": PRINT "2.CCH SAMPLES": PRINT "3
.CH SAMPLES": PRINT "4.CCH": PRINT "5.CH"
112 PRINT : INPUT " ENTER SELECTION > ";QP
114 IF QP = 0 THEN 1500
115 ON QP GOTO 700,1000,1000,300,300
300 IF QP = 4 THEN K = 1
301 IF QP = 5 THEN K = 2
310 HGR : HCOLOR= 3
315 POKE - 16302,0
320 PRINT D$;"BLOAD AXIS-YAWRATE"
330 CC = CG / U1
340 FOR J = 1 TO 32
350 IF N(J,K) < 5 THEN 470
360 X = 42 + J * 7
380 C = MEAN(J,K) * CC: GOSUB 600
400 C = MEAN(J,K) * CC + SE(J,K) * CC: GOSUB 600
410 C1 = C
420 C = MEAN(J,K) * CC - SE(J,K) * CC: GOSUB 600
430 C2 = C
440 Y1 = INT ( - 12.000 * C1 + 156.5)
450 Y2 = INT ( - 12.000 * C2 + 156.5)
455 IF Y2 > 156 THEN Y2 = 156
456 IF Y1 < 4 THEN Y1 = 4
460 HPLOT X,Y1 TO X,Y2
470 NEXT J
480 STOP
485 TEXT
490 GOTO 110
600 Y = INT ( - 12.000 * C + 156.5)
605 IF Y > 156 THEN Y = 156
606 IF Y < 4 THEN Y = 0
610 HPLOT X - 2,Y TO X + 2,Y
620 RETURN
700 PRINT D$;"PR#1"
705 PRINT : PRINT
707 PRINT "NAME OF TEST FILE IS ";FL$
708 PRINT "NAME OF TEST IS ";NA$
710 PRINT : PRINT "START TIME WAS ";MTH$;" ";DAY$;" ";YEAR$
```

```
715 PRINT ,HOUR$;":":;MINUTE$;" HOURS"
720 PRINT "ELAPSED TIME="
721 PRINT ,H;" HOURS"
722 PRINT ,M;" MINUTES"
723 PRINT ,S;" SECONDS"
730 PRINT "FURL ANGLE= ";FURL;" DEGREES"
740 PRINT "CALIBRATION CONSTANTS : CS=";CS;" ONE VOLT=";U1
750 PRINT : PRINT : PRINT
755 PRINT D$;"PR#0"
760 GOTO 110
1000 REM SUBR FOR SAMPLES PLOT
1010 IF QP = 2 THEN K = 1
1011 IF QP = 3 THEN K = 2
1020 HGR : HCOLOR= 3: POKE - 16382,0
1030 PRINT D$;"BLOOD AXIS-SAMPLES/YARRATE"
1050 FOR J = 1 TO 32
1055 IF NKJ,K) = 0 THEN 1240
1060 X = 42 + J * 7
1100 REM CALC LOG N
1110 I1 = 1
1120 E1 = 10 ^ I1
1130 IF (NKJ,K) - E1) < 0 THEN 1170
1140 I1 = I1 + 1
1145 IF I1 > 6 THEN STOP
1150 GOTO 1120
1170 I2 = 1
1180 E2 = 10 ^ ((I1 - 1) + (I2 / 24))
1190 IF (NKJ,K) - E2) < 0 THEN 1220
1200 I2 = I2 + 1
1205 IF I2 > 24 THEN STOP
1210 GOTO 1180
1220 Y = 156 - (24 * (I1 - 1) + (I2 - 1))
1230 HPLLOT X,Y
1240 NEXT J
1250 STOP
1260 TEXT
1270 GOTO 110
1500 REM PRINTER
1510 CALL - 16046
1520 GOTO 110
```

8. Coefficient of Performance Analysis; "CP" Program

8.1 Program Logic

1. Provide user instructions
2. Determine data source
3. Read data (i.e. rotor power and number of samples vs. bin number)
4. Enter bin limits for analysis
5. Calculate total data points in all bins
6. Calculate mean wind speed
7. Calculate mean wind power and speed at which it occurs based on air density corrected for pressure and temperature
8. Calculate average CP using mean rotor power over all bins and corrected air density
9. Print results
10. Calculate CP by bin number with mean rotor power and corrected air density
11. Print results
12. Load CP axis vs. bin number
13. Plot CP vs. bin number, if desired
14. Plot rotor power vs. bin number if desired
15. End

Documentation for
CP Program

I1	Rotor Power Per Bin.
I2	Wind Power Per Bin.
I3	Rotor Performance Coefficient Per Bin.
JL	Lower Bin Used for Analysis.
JU	Upper Bin Used for Analysis.
MP	Mean Wind Power Over All Bins.
MR	Mean Rotor Power Over All Bins.
M3	Average Cube of Wind Speed or Wind Speed at Mean Wind Power.
PC	Rotor Coefficient of Performance, C_p .
QP	File Selector.
RZ%	Position Selector on Disk.
SB	Array of C_p Values Per Bin.
SUM	Number of Sample Points, Total.
SW	Average Wind Speed for Test.
Z\$	Bin Plot Data File Name.

IPR##
JLIST

```
3 REM THE CP PROGRAM
4 REM *****
5 DIM NK(35),MAX(35),MEANK(35),HNK(35),SE(35),SBARK(35)
6 HOME : UTAB 5
7 PRINT " RESET HIMEM IF REQUIRED": PRINT : PRINT
8 PRINT : PRINT " TYPE -CONT- AFTER PLOT IS DRAWN": PRINT : INPUT " PRESS RET
URN TO CONT.":H$
9 HOME : UTAB 5
10 D$ = CHR$(4)
15 PRINT D$;"MON C,I,0"
17 RZ% = 0
20 INPUT "NAME TEXT FILE FOR PLOTTING? ";Z$
25 HOME : UTAB 5: PRINT "IS THIS A WINDS OR WIND2.FAST PROGRAM ?": PRINT : PRIN
T "WINDS = 1": PRINT "WIND2.FAST = 2"
27 PRINT : INPUT " ENTER SELECTION > ";QP
28 IF QP = 1 THEN K = 4
29 IF QP = 1 THEN OP = 6
30 IF QP = 2 THEN K = 2
31 IF QP = 2 THEN OP = 2
35 GOTO 55
38 PRINT D$;"CLOSE ";Z$
39 PRINT "SETS=";ST
40 RZ% = 25 + (K - 1) * (ST / OP) * 8
41 PRINT "RZ=";RZ%
55 PRINT : INPUT " INPUT DATA DISK";H$: PRINT D$;"OPEN ";Z$
56 PRINT D$;"POSITION ";Z$;"R ";RZ%
57 PRINT D$;"READ ";Z$
58 IF RZ% > 0 THEN 80
60 INPUT U1,UH,UR,UC,UT,UF,UY,UW
65 INPUT D1,D2,D3,D4,D5,D6,FC
70 INPUT K1$,K2$,K3$,K4$,K5$,K6$
75 INPUT ST,H$,TIME,REV
76 GOTO 38
80 FOR S = 1 TO ST
81 ONERR GOTO 105
82 INPUT KT
85 IF KT > K THEN 105
86 IF KT < > K THEN STOP
90 INPUT J,NK(J),MAX(J),MEANK(J),HNK(J),SE(J),SBARK(J)
100 NEXT S
105 PRINT D$;"CLOSE ";Z$
106 INPUT " INPUT BINPLOT DISK";H$
107 GOSUB 700
140 INPUT "ENTER LOWER AND UPPER BIN LIMITS FOR CALCULATIONS > ";JL,JU
150 REM SUM POINTS
160 FOR J = JL TO JU
170 SUM = SUM + NK(J)
175 NEXT J
180 REM FIND MEAN WIND SPEED
185 FOR J = JL TO JU
190 SH = SH + J * NK(J) * .5
195 NEXT J
200 SH = SH / SUM
210 REM MEAN WIND^3
215 FOR J = JL TO JU
220 M3 = M3 + NK(J) * (J / 2) ^ 3
230 NEXT J
235 M3 = M3 / SUM
236 HP = M3 * .5 * 1.23 * 3.14159 * (3.81 ^ 2) / FC
240 M3 = M3 ^ .3333
```

```
245 FOR J = JL TO JU
246 HR = HR + MEAN(J) * NK(J)
247 NEXT J
248 HR = HR / SUM
249 MR = HR * (UT * UR * .105 / (U1 ^ 2))
250 PC = MR / MP
251 PRINT D$;"PR#1"
252 PRINT " DATA ANALYSIS FOR FILE ";Z$
253 PRINT
255 PRINT "MEAN WIND SPEED(M/S)=";SH
256 PRINT "MEAN WIND PWR (WATTS)=";HP
257 PRINT "SPEED AT MEAN WIND POWER=";M3
258 PRINT "MEAN ROTOR POWER(WATTS)=";MR
259 PRINT "AVERAGE CP=";PC
260 PRINT "TOTAL SAMPLES=";SUM
262 FOR J = JL TO JU
264 I1 = MEAN(J) * (UT * UR * .105) / (U1 ^ 2)
266 I2 = 1.23 * 3.14159 * (3.81 ^ 2) * ((J / 2) ^ 3) / (2 * FC)
268 I3 = I1 / I2
270 PRINT "WIND SPEED (M/S)=";J / 2;" CP=";I3
272 SB(J) = I3
273 NEXT J
275 PRINT D$;"PR#0"
276 INPUT "DO YOU WISH TO PLOT CP VS WIND SPEED (Y/N)";H$
278 IF H$ = "N" THEN STOP
279 HGR :HCOLR = 3: POKE - 16302,0
282 PRINT D$;"BLOAD AXIS-CP"
284 FOR J = JL TO JU
286 X = 42 + J * 7
288 C = SB(J) * 10
290 Y = INT ( - 12 * C + 156.5)
292 IF Y > 156 THEN Y = 156
293 IF Y < 4 THEN Y = 0
294 H$PLOT X,Y
295 NEXT J
296 STOP
298 TEXT
300 INPUT "DO YOU WANT TO PRINT GRAPH?";H$
302 IF H$ = "Y" THEN CALL - 16046
304 INPUT "DO YOU WANT TO PLOT ROTOR POWER BINPLOT? (Y/N)";H$
306 IF H$ = "Y" THEN GOTO 3000
308 STOP
330 REM PLOT ROUTINE
340 FOR J = 1 TO 32
350 IF NK(J) = 0 THEN 470
360 X = 42 + J * 7
370 C = MAX(J) * CC: GOSUB 600
380 C = MEAN(J) * CC: GOSUB 600
390 C = MIN(J) * CC: GOSUB 600
400 C = MEAN(J) * CC + SE(J) * CC: GOSUB 600
410 C1 = C
420 C = MEAN(J) * CC - SE(J) * CC: GOSUB 600
430 C2 = C
440 Y1 = INT ( - 12.000 * C1 + 156.5)
445 IF Y1 < 4 THEN Y1 = 4
450 Y2 = INT ( - 12.000 * C2 + 156.5)
455 IF Y2 > 156 THEN Y2 = 156
460 H$PLOT X,Y1 TO X,Y2
470 NEXT J
480 STOP
485 TEXT
```

```
486 INPUT " DO YOU WISH TO PRINT GRAPH?";M$
487 IF M$ = "Y" THEN CALL - 16046
490 END
600 Y = INT ( - 12.000 * C + 156.5)
605 IF Y > 156 THEN Y = 156
606 IF Y < 4 THEN Y = 0
610 HPLOT X - 2,Y TO X + 2,Y
620 RETURN
700 PRINT D$;"PR#1"
705 PRINT
707 PRINT "FILE NAME IS ";Z$
710 PRINT "START TIME= ";H$
720 PRINT "ELAPSED TIME= ";TIME;" HOURS"
730 PRINT "FURL ANGLE(INCL. TILT OF ROTOR) =";D6;" DEG"
740 PRINT " ROTOR REV.(CALC)= ";REV;" REV."
750 PRINT "ONE VOLT=";U1;" CHIND=";UH;" CAPM=";UR;" CCYPTCH=";UC
760 PRINT "CTORQUE=";UT;" CFLAP=";UF;" CYAWPOST=";UY;" CGEN.VOLTS=";UU
770 PRINT "TEMP (DEG C)=";D1;" PRESS(ATM)=";D2;" CORR.FAC.=";FC;" WIND DIR="
;D3
780 PRINT "GEN. LOAD (OHMS)=";D4;" GEAR RATIO=";D5;" TO 1"
790 PRINT K1$;" ";K2$;" ";K3$
800 PRINT K4$;" ";K5$;" ";K6$
810 PRINT
820 PRINT D$;"PR#0"
830 RETURN
3000 REM ROTOR POWER
3010 HGR : HCOLOR= 3: POKE - 16382,0
3020 PRINT D$;"BLDAD AXIS-R.PWR"
3022 FOR J = 1 TO 32
3024 MAX(J) = 0;MNX(J) = 0
3025 NEXT J
3030 CC = (UT * UR * .105) / (U1 ^ 2)
3035 CC = CC / 1000
3040 GOTO 340
```

9. Axis Plotting Routines

All axis plots are based on these programs with minor changes in axis labelling or scaling.

9.1 Program Logic

1. Load graphics character generator
2. Print vertical scale
3. Print horizontal scale
4. Draw axis lines
5. Print vertical label
6. Print horizontal label
7. Print grid scale lines
8. Plot constant tip speed ratio lines (RPM only)
9. Save Axis as a binary file
10. End

```
5 REM THE RPM AXIS PLOT PROGRAM
6 REM *****
10 D$ = CHR$(4)
15 HGR : HCOLOR= 3
20 PRINT D$;"BRUN HI-RES CHARACTER GENERATOR"
26 PRINT D$;"BLOAD GREEK LETTERS"
40 FOR I = 1 TO 7:: HTAB 3: UTAB 3 * I - 1: PRINT 350 - 50 * I: NEXT I
60 FOR I = 1 TO 3: UTAB 21: HTAB 6 + 10 * I: PRINT 5 * I: NEXT I
70 HPLOT 42,4 TO 266,4 TO 266,156 TO 42,156 TO 42,4
80 FOR I = 1 TO 3: HTAB 1: UTAB 6 + I
81 IF I = 1 THEN PRINT "R"
82 IF I = 2 THEN PRINT "P"
83 IF I = 3 THEN PRINT "M"
84 NEXT I
90 UTAB 24: HTAB 8: PRINT "RPM US WIND SPEED (M/S)"
100 FOR Y = 4 TO 153 STEP 149: FOR X = 77 TO 266 STEP 35
110 HPLOT X,Y + 1 TO X,Y + 3
120 NEXT X: NEXT Y
130 FOR X = 42 TO 263 STEP 221: FOR Y = 12 TO 132 STEP 24
140 HPLOT X + 1,Y TO X + 3,Y
150 NEXT Y: NEXT X
160 FOR LAM = 5 TO 20 STEP 5: FOR X = 46 TO 266 STEP 4
170 Y = 156 - .086 * (X - 42) * LAM
175 IF Y < 4 THEN Y = 4
180 HPLOT X,Y
190 NEXT X: NEXT LAM
200 UTAB 10: HTAB 35: PRINT "%=5"
210 UTAB 2: HTAB 30: PRINT "10"
220 UTAB 2: HTAB 22: PRINT "15"
230 UTAB 2: HTAB 18: PRINT "20"
240 PRINT D$;"BSAVE AXIS-RPM.A#2000.L#2000"
250 END
```

```
ILoad TAU:
JPR#0
JLIST
```

```
5 REM THE TAU AXIS PLOT PROGRAM
6 REM *****
10 D$ = CHR$(4)
15 HGR : HCOLOR= 3
17 POKE - 16302,0
20 PRINT D$;"BRUN HI-RES CHARACTER GENERATOR"
26 PRINT D$;"BLOAD GREEK LETTERS"
40 FOR I = 1 TO 7:: HTAB 3: UTAB 3 * I - 1: PRINT 14 - 2 * I: NEXT I
60 FOR I = 1 TO 3: UTAB 21: HTAB 6 + 10 * I: PRINT 5 * I: NEXT I
70 HPLOT 42,4 TO 266,4 TO 266,156 TO 42,156 TO 42,4
80 FOR I = 1 TO 5: HTAB 1: UTAB 6 + I
81 IF I = 1 THEN PRINT "*"
82 IF I = 2 THEN PRINT " "
83 IF I = 3 THEN PRINT "D"
84 IF I = 4 THEN PRINT "E"
85 IF I = 5 THEN PRINT "6"
86 NEXT I
90 UTAB 24: HTAB 5: PRINT "CYCLIC PITCH US WIND SPEED (M/S)"
100 FOR Y = 4 TO 153 STEP 149: FOR X = 77 TO 266 STEP 35
110 HPLOT X,Y + 1 TO X,Y + 3
120 NEXT X: NEXT Y
130 FOR X = 42 TO 263 STEP 221: FOR Y = 12 TO 132 STEP 24
140 HPLOT X + 1,Y TO X + 3,Y
150 NEXT Y: NEXT X
240 END
```

```
5 REM THE VOLTS AXIS PLOT PROGRAM
6 REM *****
10 O$ = CHR$(4)
15 HGR : HCOLOR= 3
17 POKE - 16382,0
20 PRINT O$;"BRUN HI-RES CHARACTER GENERATOR"
26 PRINT O$;"BLOAD GREEK LETTERS"
40 FOR I = 1 TO 7:: HTAB 3: UTAB 3 * I - 1: PRINT 7 - I: NEXT I
60 FOR I = 1 TO 4: UTAB 21: HTAB 6 + 8 * I: PRINT 75 * I: NEXT I
70 HPLOT 42,4 TO 266,4 TO 266,156 TO 42,156 TO 42,4
80 FOR I = 1 TO 5: HTAB 1: UTAB 6 + I
81 IF I = 1 THEN PRINT "U"
82 IF I = 2 THEN PRINT "O"
83 IF I = 3 THEN PRINT "L"
84 IF I = 4 THEN PRINT "T"
85 IF I = 5 THEN PRINT "S"
86 NEXT I
90 UTAB 24: HTAB 12: PRINT " VOLTS VS RPM"
100 FOR Y = 4 TO 153 STEP 149: FOR X = 98 TO 266 STEP 56
110 HPLOT X,Y + 1 TO X,Y + 3
120 NEXT X: NEXT Y
130 FOR X = 42 TO 263 STEP 221: FOR Y = 12 TO 132 STEP 24
140 HPLOT X + 1,Y TO X + 3,Y
150 NEXT Y: NEXT X
160 PRINT O$;"BSAVE AXIS-VOLTS/RPM,A$2000,L$2000"
240 END
```

```
ILoad SAMPLPR#
JLIST
```

```
5 REM THE SAMPLES AXIS PLOT PROGRAM
6 REM *****
10 O$ = CHR$(4)
12 PRINT O$;"NOHON C,I,O"
15 HGR : HCOLOR= 3
16 POKE - 16382,0
20 PRINT O$;"BRUN HI-RES CHARACTER GENERATOR"
26 PRINT O$;"BLOAD GREEK LETTERS"
40 FOR I = 1 TO 7:: HTAB 4: UTAB 3 * I - 1: PRINT 7 - I: NEXT I
60 FOR I = 1 TO 3: UTAB 21: HTAB 6 + 10 * I: PRINT 5 * I: NEXT I
70 HPLOT 42,4 TO 266,4 TO 266,156 TO 42,156 TO 42,4
80 FOR I = 1 TO 5: HTAB 1: UTAB 6 + I
81 IF I = 1 THEN PRINT "L"
82 IF I = 2 THEN PRINT "O"
83 IF I = 3 THEN PRINT "G"
84 IF I = 4 THEN PRINT " "
85 IF I = 5 THEN PRINT "N"
86 NEXT I
90 UTAB 24: HTAB 3: PRINT "LOG SAMPLES (N) VS WIND SPEED (M/S)"
100 FOR Y = 4 TO 153 STEP 149: FOR X = 77 TO 266 STEP 35
110 HPLOT X,Y + 1 TO X,Y + 3
120 NEXT X: NEXT Y
130 FOR X = 42 TO 263 STEP 221: FOR Y = 12 TO 132 STEP 24
140 HPLOT X + 1,Y TO X + 3,Y
150 NEXT Y: NEXT X
160 FOR X = 42 TO 263 STEP 221: FOR Y = 19 TO 139 STEP 24
170 HPLOT X + 1,Y TO X + 2,Y
180 NEXT Y: NEXT X
200 PRINT O$;"BSAVE AXIS-SAMPLES,A$2000,L$2000"
240 END
```

7. BIBLIOGRAPHY

1. DeMontbrial, T., "Energy: The Countdown, A Report to the Club of Rome", Pergamon Press, Great Britian, 1979.
2. Hohenemser, K. H., "Some Alternative Dynamic Design Configurations for Large Horizontal Axis WECS", Wind Turbine Structural Dynamics Workshop, NASA-Lewis, Cleveland, Ohio, November, 1977.
3. Wilson, R. E., and Lissaman, P. B. S., "Applied Aerodynamics of Wind Power Machines", Oregon State University, May, 1974.
4. Wilson, R. E., and Patton, E. M., "Design Analysis of Performance and Aerodynamic Loading of Non-Flexible Horizontal Axis Wind Turbines", Draft Report, DOE Contract No. EY-76-S-06-2227, Oregon State University, August, 1978.
5. Castles, W., and DeLeeuw, J. H., "The Normal Component of Induced Velocity in the Vicinity of a Lifting Rotor and Some Examples of its Application", NACA TR 1184, 1954.
6. Carta, F. O. et al, "Investigation of Airfoil Dynamic Stall and its Influence on Helicopter Control Loads", United Aircraft Corporation Research Laboratories, U.S. Army Air Mobility Research and Development Laboratory Technical Report 72-51, East Hartford, Connecticut, September, 1972.
7. Hoffman, J., "Users Manual for MOSTAB-HFA", Paragon Pacific Report PP-1013-1, September, 1975.
8. Kaza, Janetzke, Sullivan, "Evaluation of MOSTAS Computer Code for Prediction of Dynamic Loads in Two-Bladed Wind Turbines", NASA TM-79101, June, 1979, NTIS No. DOE/NASA/1038-79/2.
9. Stoddard, F., Perkins, F., and Cromack, D., "Wind Tunnel Tests for Fixed-Pitch Start-up and Yaw Characteristics", Technical Report UM-WT-TR-78-1, NASA-Lewis, Cleveland, Ohio, June, 1978.
10. Wheatley, J. B., and Bioletti, C., "Wind Tunnel Tests of 10 foot Diameter Autogiro Rotors", NACA Report No. 552, October, 1935.

11. Hohenemser, K., "A Theory of Blade Pitch Control for Helicopters", translation by Bertram Kelley of Bell Aircraft Co., AMC Wrightfield Translation No. F-TS-1008-RE, September, 1946. (The 1939 DVL model tests were never published. However, many of the test results are in the above cited translation of a report written in 1944.)
12. Stoddard, F. S., "Structural Dynamics, Stability and Control of High Aspect Ratio Wind Turbines", University of Massachusetts, for Rockwell International Energy Systems Group, Subcontract PF67025F, December, 1978.
13. Stoddard, F. S., "Dynamic Rotor Loads of a Wind Turbine via Hand-Held Calculators", proceedings of American Institute of Aeronautics and Astronautics, Solar Energy Research Institute, Wind Energy Conference, Boulder, Colorado, April, 1980.
14. Gessow, A., and Myers, G. D., Jr., "Aerodynamics of the Helicopter", MacMillan Co., New York, 1952.
15. Norton, J. H., "The Development and Testing of a Variable Axis Rotor Control System with a 5 Meter Rotor and Direct-Drive Alternator", proceedings of the Small Wind Turbine Systems Conference, February 27 to March 1, 1979, Boulder, Colorado.
16. Durand, W. F., (Editor in Chief), "Aerodynamic Theory", Volume IV, Division L, Chapter X, Section 5; Julius Springer, Berlin Germany, 1935.
17. Pitt, D. M., and Peters, D. A., "Theoretical Prediction of Dynamic-Inflow Derivatives", proceedings of the Sixth European Rotorcraft and Powered Lift Aircraft Forum, Bristol, England, September, 1980.
18. Conte, S., D., and de Boor, C., "Elementary Numerical Analysis, An Algorithmic Approach", McGraw-Hill, 1972.
19. Glauert, H., "A General Theory of the Autogiro", Aeronautical Research Council, Report and Memorandum No. 1111, 1926.
20. Abbott, I. A., and von Doenhoff, H. E., "Theory of Wing Sections", Dover Publications, Inc., New York, 1959.
21. Sissingh, G. J., "Dynamics of Rotors Operating at High Advance Ratios", Journal of The American Helicopter Society, 13, No. 3, July, 1968.

22. Hohenemser, K. H., Swift, A. H. P., Jr., and Peters, D. A., "The Yawing of Wind Turbines With Blade Cyclic Pitch Variation", Solar Energy Research Institute TR-8085-14, Draft Final Report - Unpublished at this date.
23. Hohenemser, K. H., and Swift, A. H. P., Jr., "Dynamics of an Experimental Two-Bladed Horizontal Axis Wind Turbine With Blade Cyclic Pitch Variation", proceedings of the Second DOE/NASA Wind Turbine Dynamics Workshop, Cleveland, Ohio, February, 1981.
24. Hohenemser, K. H., and Swift, A. H. P., Jr., "The Yawing of Wind Turbines With Blade Cyclic Pitch Variation", proceedings of the Second Wind Energy Innovative Systems Conference, Colorado Springs, Colorado, December, 1980.
25. Jacobs, E. N., and Sherman, A., "Airfoil Section Characteristics as Affected by Variations of the Reynolds Number", Report No. 586, 1937 NACA Reports.
26. Kirchoff, R. H., "Measurements of the Wind Field Interaction With the UMASS 25 kW Wind Turbine", proceedings of the Small Wind Turbine Systems 1979 Workshop coordinated by Rockwell International and held at Boulder, Colorado, February/March, 1979, Vol. 1, pp. 179-188.
27. Glasgow, J. C., and Miller, D. R., "Teetered, Tip-controlled Rotor: Preliminary Test Results from MOD-0 100 kW Experimental Wind Turbine", proceedings of the American Institute of Aeronautics and Astronautics/Solar Energy Research Institute, Wind Energy Conference, Boulder, Colorado, April, 1980.
28. Hajek, T. J., and Fejer, A. A., "A New Approach to Rotor Blade Stall Analysis", Paper Number 11, 4th European Rotorcraft and Powered Lift Aircraft Forum, Stresa, Italy, September, 1978.

8.0 VITA

Biographical items on the author of the thesis, Mr. Andrew H. P. Swift, Jr.

- 1) Born January 21, 1946, Troy, New York.
- 2) Attended Union College, Schenectady, New York from September 1963 to June 1968. Received a degree of Bachelor of Science in Mechanical Engineering and a degree of Bachelor of Science in Mathematics.
- 3) Commissioned as a Second Lieutenant in the United States Air Force in 1968 and served as an Air Force pilot until separation as a Captain in 1974.
- 4) Attended Sever Insitute, Washington University, St. Louis Missouri from January, 1975 to present. Received a Master of Science Degree in May, 1977 in Mechanical Engineering, and presently enrolled in the Dr. of Science Degree Program in Mechanical Engineering. Expected completion date is May, 1981.
- 5) Experience:

Research assistant and consultant on a part-time basis from 1976 to the present, in the area of alternative energy system design and analysis, to include:

A. Government Sponsored Projects:

1. Co-designer of a solar hot water heating system for a 112 unit apartment building in St. Louis for the Housing and Urban Development Solar Heating and Cooling Demonstration Program.
2. Participation in computer simulation work for a study of Low Temperature Applications of Solar Energy for the State of Illinois.
3. Co-investigator in a generic study of the sailing and its application to wind energy conversion systems for the Solar Energy Research Institute, Golden, Colorado.

4. Research assistant and Co-investigator in the design, construction and testing of a full scale, yaw controlled wind turbine with passive cyclic pitch. The project was funded by the Innovative Systems Program, Solar Energy Research Institute Golden, Colorado.
5. Principal investigator for a Department of Energy, Appropriate Technology Project for the design and construction of a combined wind-solar energy conversion system.

B. Other Projects:

1. Research on the use of computer aided design of solar and wind energy conversion systems. This work was partially funded by a Grant-in-Aid from the American Society of Heating, Refrigeration and Air-Conditioning Engineers.
2. Co-designer and builder of a Solar Testing Facility for the Department of Mechanical Engineering, Washington University, St. Louis, Missouri.
3. Consultant on an innovative Solar Energy Availability Reporting Program in the St. Louis Area for KMOX, TV, St. Louis, Missouri.
4. Assisted in research on the optimal design of passive solar homes using computer simulation and optimization techniques.

6) Membership in Professional and Honor Societies:

American Society of Mechanical Engineers
American Society of Heating, Refrigerating and Air-
Conditioning Engineers
Sigma Xi Research Society
Pi Tau Sigma Engineering Society
Missouri Solar Energy Association
International Solar Energy Society

7) Publications:

Masters Thesis: "Computer Aided Design of a Solar Wind Energy System", Washington University, St. Louis, Missouri, May, 1977.

Doctoral Dissertation: "The Effects of Yawed Flow on Wind Turbine Generators", Washington University, St. Louis, Missouri, May, 1981 (expected completion date).

Swift, A., "Computer Aided Design of a Continuous Duty Energy System", Second Annual UMR-MEC Energy Conference, University of Missouri, Rolla, Missouri, October, 1976.

Hohenemser, K., Swift, A., and Peters, D., "A Definitive Generic Study for Sailing Wind Energy Systems", Final Report, Solar Energy Research Institute, Technical Report TR-8003-2, October, 1979.

Myers, K., Icerman, L., and Swift, A., "Simulation and Optimization Techniques for Determining Energy Efficient and Cost Effective Passive Home Design", Proceedings of the 4th National Passive Solar Conference, Kansas City, Missouri, October, 1979.

Icerman, L., Myers, K., and Swift, A., "The Potential of Combined Wind-Solar Energy Conversion Systems for Electric Utility Capacity Displacement", Proceedings of the 6th Annual University of Missouri, Rolla, Department of Natural Resources Conference, Rolla, Missouri, October, 1979.

Swift, A., "The Effect of Yaw Angles on the Performance of Wind Turbines", a paper presented to the St. Louis Section of the American Helicopter Society for consideration of the Robert Lichten Award, February, 1980.

Cargal, W., Icerman, L., and Swift, A., "Demonstration and Analysis of a Combined Wind Solar Energy Conversion System", Proceedings of the American Institute of Aeronautics and Astronautics/Solar Energy Research Institute Wind Energy Conference, Boulder, Colorado, April 1980.

Hohenemser, K., and Swift, A., "The Yawing of Wind Turbines with Blade Cyclic Pitch Variation", Proceedings of the Second Wind Energy Innovative Systems Conference, sponsored by the Solar Energy Research Institute, Colorado Springs, Colorado, December, 1980.

Hohenemser, K., and Swift, A., "Dynamics of an Experimental Two-Bladed Horizontal Axis Wind Turbine with Blade Cyclic Pitch Variation", Proceedings of the Second DOE/NASA Wind Turbine Dynamics Workshop, Cleveland, Ohio, February, 1981.